Efficient Polyester Resin Synthesis using Microwave Heating with Scale-up from 50 mL to 5 L



George William Hargreaves, MSci (Hons)

Thesis submitted to the University of Nottingham

for the degree of Doctor of Philosophy

April 2017

Declaration

Except where specific reference has been made to other sources, the work presented within this thesis is the original work of the author. It has not been submitted, in whole, or in part, for any other degree of qualification.

Signed…….. Date……..

George William Hargreaves

Acknowledgements

Firstly I'd like to thank my supervisor Professor Derek Irvine for his persistent guidance throughout the project. His wealth of knowledge and experience has been instrumental to help me complete my research as a PhD student. His constant insults were gratefully received, much like his endless tales of ICI, which were strangely just the same couple repeated every few months.

Thank you to the Microwave Process Engineering research group in the Chemical and Environmental Engineering department for their expert microwave advice. Specifically; Dr Chris Dodds, Dr Adam Buttress and Dr Angelique Sklavounou whose help with the scale-up vessel was instrumental to its completion.

I would like to thank AkzoNobel for the project funding as well as the expert advice from Dr Pierre Martin-Tanchereau and Dr Matthew Unthank.

I'd like to say thanks to Professor Steve Howdle who allowed me to occupy space in his lab in Chemistry which allowed me to perform my research. As such, thanks to everyone in lab B10 for keeping my time during my PhD enjoyable and for not getting too annoyed at me for my constant ramblings of absolute nonsense.

Thanks to my mum and dad for their constant support throughout the years, I'm sure you're just happy that I'm finally finishing school and getting a "proper job"!

Finally, and most importantly, thanks with all my heart to Bex. You're amazing and I feel so lucky to have you in my life. You mean everything to me and I can't wait to start the rest of my life with you. Go Beaves!

Thesis Abstract

Polyesters are a vital part of modern day life, with a plethora of different uses such as clothing, coatings, biomedical engineers, drug encapsulation and much more. This means that the synthesis of these products from the raw materials is vital and investigating a way to increase the synthesis efficiency is an important topic of research. The work discussed within this thesis aims to assess in depth the impact which microwave energy has on a melt polycondensation system, suggesting that implementing a microwave heating into the polycondensation, there is potential to reduce production times and potentially increase product molecular weights. This is explained through a discussion about catalytic mechanisms and selective microwave heating. This led to the design and commissioning of a 5 L scale-up vessel with hybrid conventional and microwave heating capabilities to show that these technologies can be scaled to an industrially meaningful scale.

Chapter 1 introduces the background to polymers and polymer chemistry, with a detailed assessment of polyester synthesis routes and properties. Powder coatings are presented with the different types and application methods discussed. Microwave theory is then presented with the challenges and potential benefits toward scale-up outlined. Finally, a literature review is completed on polyester synthesis using microwave heating as well as recent developments in large scale microwave reactions.

Chapter 2 discusses the specific microwave equipment used throughout this thesis. The materials used and synthesis methods are then discussed. There is also a brief discussion about the characterisation techniques implemented.

Chapter 3 focusses on the polymerisation of adipic acid and 1,6-hexanediol using both conventional and microwave heating. A detailed investigation into catalyst effects on the polymerisation are discussed. This focusses on mechanistic differences between the catalysts and heating methods.

Chapter 4 furthers the catalyst investigation from chapter 3 but with an industrially used monomer system. This focusses on the importance of catalyst selection for the polymerisation and outlines how microwaves can be used to efficiently produce product within reduced reaction times. There is also a brief examination into whether microwaves increase product qualities.

Chapter 5 discusses the impact of using a high powered pulse on a polyesterification compared to a lower powered, continuous pulse. This is discussed for both previously investigated polymerisations and outlines if continued high power application is better than a more intermitted use. Finally, the scale-up process is discussed and initial reactions using the vessel are detailed. Again, differences in product quality are investigated.

Lastly, Chapter 6 provides the overall conclusions from the body of work with potential future work detailed for each section.

Abbreviations

^1H	Proton
AA	Adipic Acid
AV	Acid Value
b.p.	Boiling Point
Bi triflate	Bismuth(III) trifluoromethanesulfonate
$CDCl_3$	Deuterated Chloroform
CH	Conventional Heating
COOH	Carboxyl
CW	Continuous Wave
Đ	Polydispersity
DHB	2,5-Dihydroxybenzoic acid
DHBTC	Dihydroxybutyl tinchloride
DMSO-d_6	Deuterated Dimethyl Sulfoxide
DNA	Deoxyribonucleic acid
DP	Degree of Polymerisation
d_p	Penetration Depth
DSC	Differential Scanning Calorimetry
E_a	Activation Energy
EF	Electric Field
EFBC	Electrostatic Fluidized Bed Coating
EM	Electromagnetic
FBC	Fluidized Bed Coating
FDA	Food and Drug Administration
FO	Fibre Optic
GPC	Gel Permeation Chromatography
GS	Gardner Scale
HD	1,6-Hexanediol
HPLC	High-Pressure Liquid Chromatography
IPA	Isophthalic Acid
IR	Infrared
KHP	Hydrogen Potassium Phthalate
KOH	Potassium Hydroxide
m.p.	Melting Point
MALDI-TOF MS	Matrix Assisted Laser Desorption/Ionisation-Time of Flight Mass Spectrometry
MeoD	Deuterated Methanol
MF	Magnetic Field
M_n	Number Average Molecular Weight
M_p	Molecular Weight of Highest Peak
M_w	Weight Average Molecular Weight
MWH	Microwave Heating

MWt	Molecular Weight
NMR	Nuclear Magnetic Resonance
NPG	Neopentyl Glycol
OH	Hydroxyl
OHV	Hydroxyl Value
PA	Phosphoric Acid
P_{av}	Average Power
PET	Poly(Ethylene Terephthalate)
PET	Poly(Ethylene)
PLA	Poly(Lactic Acid)
P_{max}	Maximum Power
P_{min}	Minimum Power
PPA	Pyrophosphoric Acid
PTFE	Poly(Tetrafluoroethylene)
pTSA	p-Toluenesulfonic Acid
PVC	Poly(Vinyl Chloride)
PVF	Poly(Vinyl Fluoride)
RI	Refractive Index
ROP	Ring Opening Polymerisation
RT	Room Temperature
SEC	Size Exclusion Chromatography
$Sn(Oct)_2$	Tin(II) 2-ethylhexanoate
tanδ	Loss Tangent
T_g	Glass Transition Temperature
TGIC	1,3,5-Triglycidyl Isocyanurate
THF	Tetrahydrofuran
T_m	Melting Transition Temperature
TMP	Trimethylolpropane
UoN	University of Nottingham
Zinc triflate	Zinc(II) trifluoromethanesulfonate
ZrDC	Bis(cyclopentadienyl)zirconium(IV) dichloride
ε'	Dielectric Constant
ε''	Dielectric Loss
τ	Relaxation Time

Contents

Declaration i

Acknowledgements iii

Thesis Abstract v

Abbreviations vii

Contents ix

List of Figures xiv

List of Tables xxvi

List of Equations xxx

1 Introduction 1-1

1.1 Overview 1-1

1.2 Introduction to polymers 1-1

1.2.1 Types of Polymer and Polymer Structures 1-2

1.2.2 Types of Polymerisation 1-6

1.2.3 Polyesters 1-8

1.3 Microwaves 1-22

1.3.1 Microwave Fundamentals 1-22

1.3.2 Microwave/Dielectric Heating Mechanisms 1-23

1.3.3 Dielectric Properties 1-24

1.3.4 Penetration depth 1-27

1.3.5 Microwave Heating Effects 1-28

1.3.6 Temperature Monitoring of a Microwave System 1-30

1.3.7 Literature for Microwave Heating of Polymers and Specifically Polyesters 1-31

1.3.8 Scale-up of Microwave Reactions 1-34

1.4 References 1-37

2 Experimental and Equipment 2-1

2.1 Overview 2-1

2.2 Processing Methods and Equipment Overview 2-1

2.2.1 Conventional Heating Equipment and Set-up 2-1

2.2.2 Small scale microwave heating equipment and set-up 2-3

2.2.3 5 L 2 kW Hybrid Batch Reactor 2-7

2.3 Reaction Methods 2-12

2.3.1 Materials 2-12

2.3.2 Reaction Methods 2-13

2.4 Analytical Techniques 2-22

2.4.1 Proton (^{1}H) Nuclear Magnetic Resonance (NMR) 2-22

2.4.2 Differential Scanning Calorimetry (DSC) 2-25

2.4.3 Titration 2-26

2.4.4 Gel Permeation Chromatography (GPC) 2-30

2.4.5 Matrix-Assisted Laser Desorption/Ionisation Time-of-Flight Mass Spectrometry (MALDI-ToF MS) 2-31

2.4.6 Determination of Product Discolouration – Gardner Scale Colorimetry 2-32

2.4.7 Dielectric Property Analysis - Cavity Perturbation Technique 2-34

2.5 References 2-36

3 Adipic Acid, 1,6-Hexanediol Polycondensation Reaction 3-1

3.1 Overview 3-1

3.2 Initial Evaluation of Process Cycle Time 3-2

3.3 Investigation into Comparing Tin Catalyst Reactivity Between Conventional and Microwave Heated Reactions 3-4

3.3.1 Mass Transfer Studies to Assess the Dominant Factor Within the Polycondensation 3-5

3.3.2 Conventional versus Microwave Heating of Polycondensations using Tin Catalysts Conducted at 185 °C 3-13

3.3.3 Temperature Effects on the Reaction Rates of the Adipic Acid, Hexanediol System – a Comparison of Conventional and Microwave Heating at Lower Temperatures 3-22

3.4 Differing Catalyst Studies 3-25

3.4.1 Organometallic Catalysts Investigation 3-25

3.4.2 Investigation into Differences in Non-Organometallic Catalyst Activity for the Adipic acid, Hexanediol Polycondensation 3-80

3.5 Conclusions 3-98

3.5.1 Summary of Conclusions from Observations 3-98

3.5.2 Mechanistic Conclusion 3-103

3.6 References 3-107

4 Polymerisation of Isophthalic acid (IPA), Neopentyl glycol (NPG) and Trimethylolpropane (TMP) – Working Towards an Industrial Resin Process 4-1

4.1 Overview 4-1

4.2 Results and Discussion 4-3

4.2.1 Isophthalic Acid, Neopentyl Glycol Polycondensation 4-3

4.2.2 Industrial Resin Process 4-46

4.3 Conclusions 4-53

4.4 References 4-60

5 Pulsed Microwave and Scale-up Experiments 5-1

5.1 Overview.....5-1

5.2 Results and Discussion.....5-3

5.2.1 Pulsed Microwaves 5-3

5.2.2 5 L Scale-Up Hybrid Heating Rig 5-20

5.3 Conclusions 5-49

5.4 References 5-54

6 Conclusions and Future Work.....6-1

6.1 Overview.....6-1

6.2 Chapter 3: Adipic Acid, 1,6-Hexanediol Polycondensation Reaction 6-1

6.2.1 Conclusions 6-1

6.2.2 Future Work.....6-4

6.3 Chapter 4: Crystalline Polymerisation of Isophthalic acid (IPA), Neopentyl glycol (NPG) and Trimethylolpropane (TMP) – Working Towards an Industrial Resin Process 6-5

6.3.1 Conclusions 6-5

6.3.2 Future Work.....6-8

6.4 Chapter 5: Pulsed Microwave and Scale-up Experiments.....6-10

6.4.1 Conclusions 6-10

6.4.2 Future Work 6-12

6.5 References 6-14

List of Figures

Figure 1-1. Example of different polymer types. A = Homopolymer, B = Statistical copolymer, C = Alternating copolymer, D - Block copolymer and E = Graft/Comb copolymer. 1-3

Figure 1-2. Simple ball representation of possible polymer architectures. A = Star, B = Hyperbranched, C = Dendrimer. 1-5

Figure 1-3. Representation of step-growth polymerisation. 1-7

Figure 1-4. Comparison of molecular weight build with increasing conversion. 1-8

Figure 1-5. Example of a polyester repeating unit. 1-9

Figure 1-6. Scheme for the synthesis of ethylene glycol with terephthalic acid to create polyethylene terephthalate (PET). 1-9

Figure 1-7. Reaction schemes for the different methods of polyester manufacture. 1-11

Figure 1-8. Formation of a diepoxy, 1 = diol, 2 = organochlorine compound containing an epoxy, 3a = first synthesised diepoxy, 3b = diepoxy after reaction with monoepoxy. 1-14

Figure 1-9. Schematic representation of a partially fluorinated polymer and a perfluoropolymer. 1-15

Figure 1-10. Example of the different types of bed powder coating. a) Fluidized Bed Coating, b) Electrostatic Fluidized Bed Coating with plate/grid below the porous plate. 1-17

Figure 1-11. Gun nozzles for electrospray powder coating applications. a) Corona and b) Tribo. 1-20

Figure 1-12. Heating mechanisms found in MWH, a) dipolar polarisation and b) ionic conduction, as described by Kappe et al. [109] 1-23

Figure 1-13. Temperature gradient 1 minute after heat application to ethanol under microwave energy and open vessel oil bath. Kappe et al. [122] 1-28

Figure 1-14. Representation of an FO probe containing a GaAs crystal..... 1-31

Figure 1-15. Diagram of the microwave heating components used in the 20 L scale-up polycondensation of lactic acid by Nakamura et al. [162]..... 1-36

Figure 2-1. Picture of a standard adipic acid, hexanediol reaction set-up using the Drysyn® heating mantle and a long necked round bottomed flask..... 2-2

Figure 2-2. Picture of the Sairem Miniflow ss200 system with annotations. . 2-4

Figure 2-3. 2 kW pulse rig schematic. 2-6

Figure 2-4. Example of an EM simulation of the 5 L hybrid rig. The scale shows the intensity of the magnetic field in V/m with the red areas signalling high intensities and the blue low. 2-7

Figure 2-5. Technical drawing of 5 L hybrid rig. 2-9

Figure 2-6. Calibration plot for the voltage output of circuit breaker. 2-11

Figure 2-7. Picture of Dean-Stark like set-up. 2-12

Figure 2-8. ETS-Lingren HI-1600 Microwave Oven Survey Meter consisting of microwave detector, A, and the readout, B. 2-14

Figure 2-9. NMR spectra for a standard adipic acid, hexanediol polycondensation reaction indicating the relevant peaks needing to be intergrated for the conversion calculation. A = diol peaks and B = ester peaks. 2-24

Figure 2-10. Representation of terminating groups in a linear polyester..... 2-26

Figure 2-11. Reaction scheme for the hydroxyl value process of a polyester. a) Acylation of hydroxyl groups. “A” moles of hydroxyl group are acetylated with “C” moles of acetic anhydride producing “A” moles of acetic acid and “(C – A)” moles of acetic anhydride. b) Conversion of remaining acetic anhydride to acetic acid via hydrolysis. “(C - A)” moles of acetic anhydride hydrolysed to form

"2A" moles acetic acid. c) Titration of all acidic groups. "A" moles of remaining acetic acid groups and "B" moles of acid groups from the original sample. 2-29

Figure 2-12. Representation of polyester backbone for MALDI analysis. A can consist of a hydrogen or diol unit, B can be a hydroxyl group or a diacid....2-32

Figure 2-13. Gardner scale colour calibration examples for the Lovibond colorometer. [18] 2-33

Figure 2-14. Schematic representation of the dielectric cavity used in cavity perturbation.....2-35

Figure 3-1. Plot of kinetic analysis of reaction conversion with time for a 5 hour adipic acid, hexanediol polyesterification conducted at 185 °C using CH and an $Sn(Oct)_2$ catalyst and no mass transfer methods applied. 3-3

Figure 3-2. Chemical structures of the different tin catalysts used.....3-5

Figure 3-3. Pictorial representation of reagent and product movement through the different phases within a polycondensation reaction.....3-6

Figure 3-4. Comparison of the effect of stirring rates upon the conversion versus time for adipic acid, hexanediol polycondensation using a dihydroxybutyl tinchloride catalyst conducted at 150 °C using CH and with no mass transfer applied. 3-8

Figure 3-5. Plot of conversion versus time for adipic acid, hexanediol polycondensations using a dihydroxybutyl tinchloride catalyst using CH conducted at 150 °C with varying levels of vacuum applied. 3-11

Figure 3-6. A plot of the variation in tanδ with temperature for $Sn(Oct)_2$ and DHBTC, performed using cavity perturbation technique at 2.45 GHz. 3-14

Figure 3-7. Plot of conversion versus time for adipic acid, hexanediol polyesterifications using different tin catalysts and varying the heating method used at 185 °C with no mass transfer applied. 3-16

Figure 3-8. Comparison of CH and MWH heating profiles for an adipic acid, hexanediol polycondensation conducted at 185 °C using $Sn(Oct)_2$ with circles depicting when the internal temperature achieved reaction temperature.... 3-17

Figure 3-9. Proposed mechanisms for the tin catalysed reactions. a = $Sn(Oct)_2$ via carboxyl coordination, b = $Sn(Oct)_2$ insertion mechanism and c = DHBTC Lewis acid..... 3-20

Figure 3-10. Comparison of conversion rate versus time for adipic acid, hexanediol polycondensations at 150 °C using different tin catalysts with no mass transfer applied. 3-23

Figure 3-11. Chemical structures of the new organometallic catalysts investigated further. 3-26

Figure 3-12. Ziegler-Natta polyolefin synthesis mechanism using bis(cyclopentadienyl)zirconium(IV) dichloride. 3-27

Figure 3-13. Proposed mechanism for the polyesterification based upon a Ziegler-Natta like bis(cyclopentadienyl)zirconium(IV) dichloride..... 3-28

Figure 3-14. Protic esterification mechanism suggested by Buzin et al for triflate catalysts. [41] 3-29

Figure 3-15. Complexation of carboxyl group esterification mechanism for triflate proposed by Garaleh et al. [47] 3-29

Figure 3-16. Plots of conversion versus time for adipic acid, hexanediol CH polyesterifications at 185 °C using differing metal catalysts with no mass transfer applied..... 3-31

Figure 3-17. Plots of conversion versus time for adipic acid, hexanediol MWH polyesterifications at 185 °C using differing metal catalysts with no mass transfer applied..... 3-32

Figure 3-18. Dielectric properties of all catalysts in respect to temperature, calculated using cavity perturbation technique performed at 2.45 GHz after drying of samples in a 120 °C oven..... 3-36

Figure 3-19. Typical GPC trace for a polyester. Sample shown is a polyester synthesised using $Sn(Oct)_2$ catalyst and MWH. 3-38

Figure 3-20. Plot of the relationship between tanδ value at reaction temperature and GS number for an adipic acid, hexanediol polycondensation at 185 °C using MWH. Green line indicates the line of best fit. 3-43

Figure 3-21. Plot of the relationship between tanδ value at reaction temperature and GS number for an adipic acid, hexanediol polycondensation at 185 °C using MWH with DHBTC omitted. 3-44

Figure 3-22. Picture of three polyester samples produced under CH using different catalysts. A = $Sn(Oct)_2$, B = Zinc triflate, C = ZrDC. 3-45

Figure 3-23. Solubility of $Sn(Oct)_2$ in THF, left, compared to pure THF, right..3-45

Figure 3-24. GS number versus conversion trend for AA, HD polycondensations using different catalysts and heating methods. X-axis plot starts from 75 % conversion. Note. The CH Bi triflate catalysed reaction has been omitted due to having a too high GS number to analyse.....3-46

Figure 3-25. Repeating unit of AA, HD polymer in MALDI analysis with exact mass. 3-47

Figure 3-26. Standard MALDI spectra for a synthesised adipic acid, hexanediol polyester, showing the 228.14 repeating unit gap. The spectra shown is from polymer produced using the zirconium catalyst and CH. 3-48

Figure 3-27. Zinc triflate catalysed AA, HD polyester, showing a different primary series to the other catalysts. 3-49

Figure 3-28. Plot of conversion versus acid value of adipic acid, hexanediol polycondensations using the studied organometallic catalysts at 185 °C. Red crosses = zinc triflate catalysed samples. Blue crosses = $Sn(Oct)_2$, DHBTC, ZrDC and no catalysed samples. 3-51

Figure 3-29. A typical DSC trace. Example shown is for DHBTC using CH. ..3-55

Figure 3-30. Graphical comparison of adipic acid, hexanediol polyesters synthesised at 185 °C of a) final conversion versus Tm compared to b) M_n^{GPC} versus T_m with CH and MWH in different colours for each graph. Blue = CH, red = MWH, ■ = Final conversion versus T_m and ◊ = M_n^{GPC} versus T_m. Note: for both plots the x-axis starts from 30 °C and for plot "a)" the y-axis from 60 % for clarity. 3-56

Figure 3-31. Plot of conversion versus time for adipic acid, hexanediol polyesterifications at 150 °C with CH using differing metal catalysts and with no mass transfer applied. 3-59

Figure 3-32. Plot of conversion versus time for adipic acid, hexanediol polyesterifications at 150 °C MWH using differing metal catalysts with no mass transfer applied. 3-60

Figure 3-33. Dielectric properties of the organometallic catalysts used at 150 °C. 3-63

Figure 3-34. A typical heating profile for an adipic acid, hexanediol reaction to 150 °C using MWH. The catalyst used was zinc triflate and only the first hour is plotted.....3-66

Figure 3-35.Plots of MnGPC against level of conversion for the adipic acid, hexanediol polycondensations at 150 °C (blue) and 185 °C (red) using organometallic catalysts. For 185 °C Bi triflate has been omitted due to the depolymerisation/degradation. Line of best fit added as the theoretical M_n values based on Carothers equation. [56] 3-69

Figure 3-36. Representation of relationship between highest tanδ catalyst and highest GS number catalyst for a AA, HD polycondensation at 150 °C. 3-73

Figure 3-37. Representation of relationship between highest tanδ catalyst and highest GS number catalyst for a AA, HD polycondensation at 150 °C with the $Sn(Oct)_2$ catalysed product data omitted. 3-74

Figure 3-38. Comparison of final conversion percentage versus AV for AA, HD polyesterifications at 150 and 185 °C using organometallic catalysts, independent of heating method. ■ = 150 °C, ♦ = 185 °C NOTE: for the 185 °C data set, the zinc triflate data has been omitted as it was shown to skew the data.....3-77

Figure 3-39. Graphical comparison of adipic acid, hexanediol polyesters synthesised at 150 °C of a) final conversion versus Tm compared to b) Mn versus Tm with CH and MWH in different colours for each graph. Blue = CH, red = MWH, ■ = Final conversion versus T_m and ◊ = M_n versus T_m. Note: the x-axis starts at 25 °C and for graph "a" the y-axis begins at 60 %. 3-79

Figure 3-40. Fischer esterification mechanism.[75].....3-82

Figure 3-41. Plot of conversion % versus time for AA, HD polycondensation at 185 °C using different heating methods, non-organometallic catalysts and an industrially used DHBTC tin catalyst for comparison and with no mass transfer application.....3-83

Figure 3-42. Dielectric properties of all non-organometallic catalysts with DHBTC for reference with respect to temperature, calculated using cavity perturbation technique at 910 MHz. Note: as the b.p. of PA is 153 °C the dielectric analysis was stopped at 150 °C due to safety concerns.....3-87

Figure 3-43. Plot of conversion % versus time for AA, HD polycondensation at 150 °C using different heating methods, non-organometallic catalysts and an industrially used DHBTC tin catalyst for comparison and with no mass transfer application.....3-92

Figure 3-44. M_n^{GPC} versus Tm values for the AA, HD polyesters synthesised using DHBTC and non-organometallic catalysts independent of heating method. 3-97

Figure 4-1. Scheme of an IPA, NPG polycondensation. 4-3

Figure 4-2. Conversion versus time for an IPA, NPG polycondensation at 200 °C showing the difference between catalysts and heating methods. 4-6

Figure 4-3. Dielectric properties of the catalysts used in the IPA, NPG polycondensation at 910 MHz. 4-8

Figure 4-4. Initial heating profiles for IPA, NPG polycondensation at 200 °C using different catalysts. a) DHBTC, b) Sn(Oct)2, c) PA and d) PPA. With a black dotted line indicating 200 °C 4-10

Figure 4-5. Dielectric properties of monomers and catalysts used in the IPA, NPG polycondensation at 910 MHz. 4-12

Figure 4-6. GPC traces of the polyester products from the reaction between isophthalic acid and neopentyl glycol at 200 C with differing catalysts. Blue line = tin octanoate catalyst, red = DHBTC catalyst, purple = PA catalyst, black = PPA catalyst. 4-16

Figure 4-7. Pre-heating of diol trials for NPG, IPA polycondensation, a) CH, b) MWH 4-19

Figure 4-8. Reflected power comparison between pre-heated diol/water and non-pre-heated diol/water reactions. 4-20

Figure 4-9. Comparison of heating methods in terms of conversion versus time for DHBTC catalysed polycondensation of NPG and IPA at 200 °C. 4-22

Figure 4-10. GPC traces for the polyester products synthesised at 200 °C using DHBTC catalyst with differing heating methods.. 4-23

Figure 4-11. Dielectrics of IPA and NPG monomers with increasing temperatures. 4-28

Figure 4-12. Conversion versus time for an IPA, NPG polycondensation using an increased stoichiometry of NPG for CH and MWH. 4-29

Figure 4-13. Comparison of CH and MWH for NPG, IPA polycondensation at 225 °C with diol/water pre-heat. 4-33

Figure 4-14. Heat-up times to 225 °C reaction temperature for isophthalic acid, neopentyl glycol polycondensation reaction. 4-34

Figure 4-15. GPC trace comparison between heating methods used for the synthesis of an isophthalic acid, neopentyl glycol polyester at 225 °C after normalisation of traces. 4-35

Figure 4-16. Conversion versus. time plot for isophthalic acid, neopentyl glycol polycondensation at 225 °C with 400 mbar vacuum addition after 120 mins in CH and 60 mins in MWH. 4-39

Figure 4-17. Heat-up times of isophthalic acid, neopentyl glycol polycondensation to 225 °C reaction temperature. Lines have been added to show at what point the 400 mbar vacuum was added. 4-40

Figure 4-18. GPC traces for an isophthalic acid, neopentyl glycol polycondensation at 225 °C using different heating methods and vacuum addition. 4-41

Figure 4-19. Structure of trimethylolpropane. 4-46

Figure 4-20. Plot of conversion versus time for a CH and MWH reaction for an industrially synthesised polyester resin. 4-47

Figure 4-21. Heat-up times of industrial polyester resin process to 225 °C reaction temperature using CH and MWH with indication of vacuum application. 4-48

Figure 4-22. GPC traces of an isophthalic acid, neopentyl glycol, trimethylolpropane polycondensation at 225 °C implementing different heating methods. 4-49

Figure 5-1. Schematic of pulse frequency. 5-3

Figure 5-2. Comparison between pulsed microwave at differing frequencies and continuous wave microwave heating for an adipic acid, hexanediol polycondensation at 185 °C. 5-6

Figure 5-3. Initial heating profile comparison for an adipic acid, hexanediol polycondensation between a CW and pulsed microwave reactions at 50 Hz for 10 % and 1,000 Hz for 14 % of the time to achieve an average absorbed power of 150 W. 5-7

Figure 5-4. Averaged absorbed power for CW and Pulsed microwave application reactions. Note. The CW data is time averaged and therefore cannot start from time = 0 minutes. 5-8

Figure 5-5. GPC traces for the adipic acid, hexanediol polyesterification using CW and pulsed microwave power input. 5-10

Figure 5-6. Conversion versus time for a neopentyl glycol, isophthalic acid polycondensation at 200 °C reaction using pulsed microwaves at 50 Hz with 1,500 W at 10 % of the time compared to a CW reaction. 5-13

Figure 5-7. Absorbed power and temperature profile for an isophthalic acid, neopentyl glycol polycondensation at 200 °C using 1,500 W of pulsed microwaves 10 % of the time 5-14

Figure 5-8. Time averaged absorbed power for pulsed isophthalic acid, neopentyl glycol polyesterification at 200 °C using a 10 % duty cycle and with P_{max} = 1,500 W. 5-15

Figure 5-9. Conversion versus time for a polycondensation of isophthalic acid with neopentyl glycol using pulsed microwaves at P_{max} = 1,500 W and pulse frequency = 50 Hz with duty cycle matching to an internal temperature of 200 °C. 5-16

Figure 5-10. Absorbed power and temperature profiles for the polycondensation of isophthalic acid with neopentyl glycol using pulsed microwave power at a maximum powers of 1,500 W, matching duty cycle to an internal temperature of 200 °C. a) Experiment 1, b) Experiment 2. 5-17

Figure 5-11. GPC traces of isophthalic acid, neopentyl glycol polyesters synthesised using continuous microwave pulsing and matching the temperature to pulse duration at 200 °C. 5-19

Figure 5-12. Schematic of 5 L vessel. 5-23

Figure 5-13. Comparison of heating method conversion over time for a 5 L scale adipic acid, hexanediol polycondensation at 185 °C. 5-24

Figure 5-14. Temperature profiles for the CH and MWH reaction of adipic acid, hexanediol at a 5 L scale at 185 °C. 5-26

Figure 5-15. Absorbed power for the heat-up period of the adipic acid, hexanediol polycondensation at 185 °C. 5-27

Figure 5-16. GPC traces for the AA, HD polyesterification using DHBTC catalyst at 185 °C at 5 L scale. 5-28

Figure 5-17. Flow chart for industrial resin production. 5-32

Figure 5-18. Bulk and stillhead temperature profiles for an industrial polyester resin synthesis at 5 L scale implementing CH. 5-34

Figure 5-19. GPC traces for the samples and final product of the industrial polyester resin using conventional heating at a 5 L scale. 5-39

Figure 5-20. Comparison of bulk and stillhead temperature profiles for an industrial polyester resin synthesis at 5 L scale implementing CH and MWH. 5-41

Figure 5-21. Time averaged absorbed power for the 5 L microwave polycondensation of an industrial resin system. 5-43

Figure 5-22. GPC traces for the samples and final product of the industrial polyester resin using microwave heating at a 5 L scale. 5-46

Figure 6-1. Designs for 50 mL vessel to allow mechanical stirring in current microwave cavities..... 6-9

Figure 6-2. Chemical structures of proposed lower b.p. polyesterification catalysts. 6-9

List of Tables

Table 2-1. Table of 5 L hybrid reactor system components and ID tags. 2-8

Table 2-2. Internal temperature set points, maximum power inputs and power application duration for the ramp to temperature in the industrial polyester synthesis. 2-22

Table 2-3. Values of atoms nuclear spin in relation to mass number and atomic number.....2-23

Table 3-1. Final conversion percentages for AA, HD polycondensations conducted at 150 °C using the dihydroxybutyl tinchloride catalyst with varying levels of vacuum. 3-12

Table 3-2. Final conversion percentages and their MWt values for the polyesters synthesised in the vacuum level study. 3-13

Table 3-3. Polyester conversions after 15 minutes of reaction time for each catalyst system using CH. 3-33

Table 3-4. Order at which catalysts enabled the polyesterification to reach 90 % conversion for both CH and MWH.....3-34

Table 3-5. pH of triflate catalysts. 3-35

Table 3-6. GPC data for AA HD reactions at 185 °C using different metal catalysts. 3-39

Table 3-7. Gardner scale analysis of AA HD polyester synthesised at 185 °C using different catalysts and heating methods. 3-41

Table 3-8. Comparison of zinc triflate AV's compared to polyesters using different catalysts with similar M_n^{GPC} values. 3-53

Table 3-9. Correlation between tan of organometallic catalysts and T_m of the polyesters synthesised at 185 °C. 3-57

Table 3-10. Comparison of time to 90 % conversion between tin at 185 °C and triflate catalysts at 150 °C when using CH. 3-61

Table 3-11. GPC data for AA HD reactions at 150 °C using different metal catalysts. 3-67

Table 3-12. Gardner scale analysis of AA HD polyester synthesised at 150 °C using different catalysts and heating methods. 3-71

Table 3-13. GPC data for adipic acid, hexanediol reactions at 185 °C using non-organometallic catalysts compared to an industrially used tin catalyst. 3-85

Table 3-14. GS colour analysis of AA HD polyester synthesised at 185 °C using non-organometallic catalysts and industrially used DHBTC tin catalysts with different heating methods. 3-88

Table 3-15. DSC results for an AA HD polyester processed at 185 °C for the non-organometallic catalysed reactions compared to industrially used DHBTC. MWt data has been added for comparison 3-90

Table 3-16. GPC analysis of non-organometallic catalysed adipic acid, hexanediol polycondensations compared to industrially used DHBTC polyester. 3-94

Table 3-17. GS colour analysis of AA HD polyester synthesised at 150 °C using non-organometallic catalysts and industrially used DHBTC tin catalysts with different heating methods. 3-95

Table 3-18. DSC results for an AA HD polyester processed at 150 °C for the non-organometallic catalysed reactions compared DHBTC. 3-97

Table 4-1. Heat-up times to 200 °C reaction temperature for an isophthalic acid, neopentyl glycol polycondensation. 4-11

Table 4-2. Penetration depth of catalysts at 910 MHz and 200 °C used in the epolycondensation of isophthalic acid and neopentyl glycol..... 4-13

Table 4-3. Comparison of GPC analysis for the different catalysts used in an IPA, NPG polycondensation at 200 °C. 4-15

Table 4-4. Comparison of molecular weight data between CH and MWH for the repeated reactions of IPA and NPG polycondensation at 200 °C. 4-24

Table 4-5 Comparison of average T_g data between CH and MWH for the repeated reactions of IPA and NPG polycondensation at 200 °C. 4-25

Table 4-6. Reaction times to 80 % conversion in IPA, NPG polycondensation with increased NPG stoichiometry.....4-30

Table 4-7. GPC and DSC analysis on the neopentyl glycol, isophthalic acid polyesters using increasing stoichiometries of neopentyl glycol monomer. 4-31

Table 4-8. Comparison of molecular weight data between CH and MWH for the IPA and NPG polycondensation at 225 °C. 4-35

Table 4-9. Comparison of polyester molecular weight after processing at different temperatures. 4-36

Table 4-10. Comparison of polyester thermal properties after processing at different temperatures. 4-37

Table 4-11. Thermal properties of isophthalic acid, neopentyl glycol polyester with addition of mono/di/trimeric kinetic sample.....4-38

Table 4-12. GPC data for isophthalic acid, neopentyl glycol polycondensation with addition of 400 mbar vacuum. 4-41

Table 4-13. MWt comparison between isophthalic acid, neopentyl glycol polycondensation with and without addition of vacuum. 4-42

Table 4-14. GPC and DSC data for the industrial polyester resin synthesis at 225 °C using CH and MWH. 4-49

Table 4-15. DSC data for industrial polyester resin processed at 225 °C using CH and MWH and maximum vacuum settings. 4-52

Table 5-1. Example of different experiments to input identical average powers but changing how the microwave power is applied. 5-4

Table 5-2. MWt data for the adipic acid, hexanediol polyesterifications conducted on the pulse microwave rig. 5-9

Table 5-3. Average power percentage and therefore overall average absorbed power for the power matching pulse reactions. 5-18

Table 5-4. Molecular weight and thermal properties of isophthalic acid, neopentyl glycol polyesters synthesised using continuous microwave pulsing and matching the temperature to pulse duration at 200 °C..... 5-19

Table 5-5. Molecular weight and thermal properties data for the 5 L scale adipic acid, hexanediol polycondensations at 185 °C. 5-29

Table 5-6. Targeted acid and hydroxyl values for an isophthalic acid, trimethylolpropane, neopentyl glycol and adipic acid industrial resin to meet industrial specification..... 5-33

Table 5-7. Evolution of acid and hydroxyl value over time in an industrial polyester resin synthesis using CH. 5-35

Table 5-8. Molecular weight and thermal properties data for the samples taken throughout the industrial resin polyesterification using CH. 5-37

Table 5-9. Evolution of acid and hydroxyl value over time in an industrial polyester resin synthesis using MWH. 5-44

Table 5-10. Molecular weight and thermal properties data for the samples taken throughout the industrial resin polyesterification using MWH. 5-47

Table 5-11. Comparison of the final product between implementing CH and MWH at 5 L scale for an industrial resin synthesis. 5-48

List of Equations

Equation 1-1 1-4

Equation 1-2 1-23

Equation 1-3 1-25

Equation 1-4 1-26

Equation 1-5 1-26

Equation 1-6 1-26

Equation 1-7 1-27

Equation 1-8 1-27

Equation 2-1 2-24

Equation 2-2 2-27

Equation 2-3 2-27

Equation 2-4 2-28

Equation 2-5 2-30

Equation 2-6 2-34

Equation 4-1 4-13

Equation 5-1 5-31

Equation 5-2 5-31

Equation 5-3 5-31

1 Introduction

1.1 Overview

This chapter aims to introduce the general concepts of polymer chemistry used throughout this thesis. Polymer structures and architectures are discussed and how they can affect the final properties of the polymer. Polyesters are then discussed in detail with the general reaction schemes outlined and the strategies used in industrial polyester synthesis. Powder coatings are then focused on with a brief description of the different types and how they are used/applied to a surface. This is focussed on due to it being the final use of the polyesters synthesised in this thesis. An introduction to microwaves is then covered, with the basic theory into how microwaves are used in chemical reactions and what needs to be considered when implementing microwave heating in a synthesis. Finally, the literature relevant to this thesis is discussed. This includes the use of microwaves in polymerisations, specifically step-growth polymerisations. An assessment of the literature on the catalysts investigated in this thesis in terms of melt polycondensations and, in the case of some catalysts, ring opening polymerisations (ROP). Scale-up processes are also considered when implementing microwave heating, with previous work outlined and the challenges in scaling-up discussed.

1.2 Introduction to polymers

As defined by IUPAC (International Union of Pure and Applied Chemistry) a polymer is:

“A molecule of high relative molecular mass, the structure of which essentially comprises the multiple repetition of units derived, actually or conceptually, from molecules of low relative molecular mass.” [1]

Put simply, a polymer is a long-chained molecule compromising of repeating units, known as a monomers.

Polymers can be found both in nature (DNA, protein, lignin) and are synthetically produced on a mass scale [nylon, poly(ethylene terephthalate) (PET), Kevlar, poly(vinyl chloride) (PVC)]. The chemical/thermal/physical properties which a polymer possesses can be tailored for a specific use thanks to there being many contributing factors, such as; monomer choice, sequencing, molecular weight (MWt). As such, there are many everyday uses for polymers which include; consumer goods (clothing, packaging, cosmetics), biomedical applications (drug delivery, implants, dentistry), and many more.[2-10]

1.2.1 Types of Polymer and Polymer Structures

In a polymer the monomeric units can be arranged in a variety of ways, shown in Figure 1-1 . This orientation/architecture effects the polymer properties which include; thermal stability, rigidity, solubility and viscosity.[11-13]

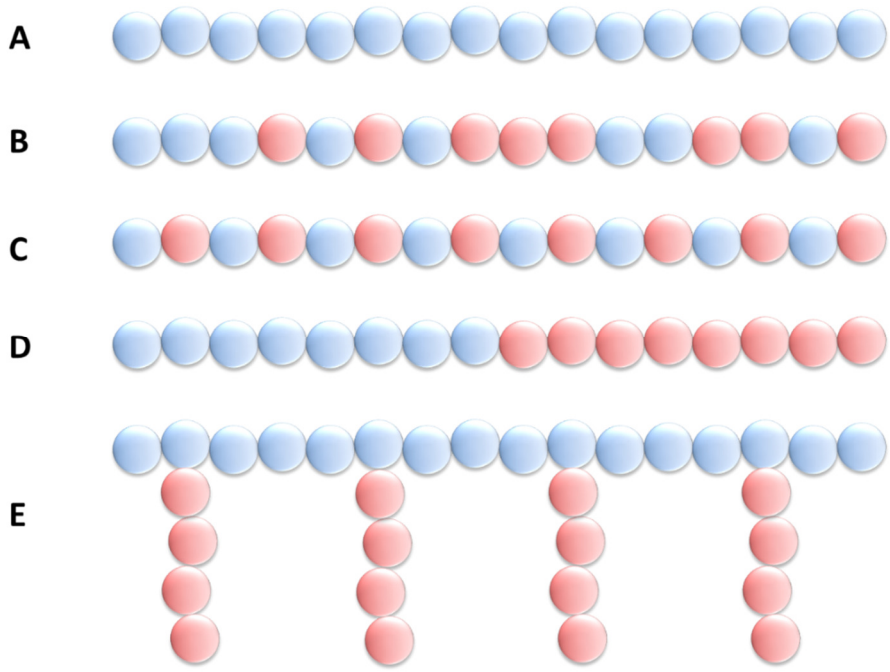


Figure 1-1. Example of different polymer types. A = Homopolymer, B = Statistical copolymer, C = Alternating copolymer, D - Block copolymer and E = Graft/Comb copolymer.

The simplest type of polymer is known as a homopolymer (Figure 1-1, A). This is when one monomer is reacted with itself to form a polymeric chain, e.g. poly(ethylene) (PE). When a second monomer is incorporated into the polymerisation the polymeric orientation can become complicated. The orientation which is produced by multiple monomers is mainly dependent on the stoichiometric mixture and reactivity of monomers and/or processing conditions implemented. When the distribution of monomers within the polymer backbone is random a statistical copolymer is formed (Figure 1-1, B). When monomers have an affinity to react with one another and not themselves this forms an alternating set of monomers in a polymer backbone, known as an alternating copolymer (Figure 1-1, C). The properties of statistical and random copolymers synthesised are a blend of the ratio of monomers used [14,15] and properties such as glass transition temperature (T_g) can be calculated using the Fox equation, Equation 1-1. [16]

$$\frac{1}{T_g} = \frac{w_1}{T_{g,1}} + \frac{w_2}{T_{g,2}} \qquad \text{Equation 1-1}$$

Where T_g is the glass transition temperature of the overall blend, $T_{g,1}$ and $T_{g,2}$ are the glass transition temperatures of the two influencing homopolymers and w_1 and w_2 are the weight fractions of homopolymers 1 and 2 respectively.

When one monomer is reacted to form a homopolymer and then another monomer is sequentially added onto the reactive end site to form another homopolymer, a block copolymer is formed (Figure 1-1, D). If a homopolymer is formed with reactive pendant group sites along the backbone, another monomer can be sequentially added at these sites to form homopolymer arms and a graft copolymer is created (Figure 1-1, E). [17,18] Because these two types of copolymer are formed by growing homopolymer chains off others, the polymers produced can keep the properties of each polymer chain simultaneously. The uses of graft polymer include; creating core shell particles[19] and microphase separation, [20] however these are not the only examples.

Another important factor in polymer synthesis is branching. This occurs when considering a multifunctional monomer with multiple reactive sites. From these sites other polymer chains can be grown, similar to the graft polymer structure. Branched polymers can exhibit interesting properties when compared to linear polymers, such as; reduced stability at similar MWt's due to a decrease in intramolecular forces and hydrodynamic radius. [21,22] The different types of branching polymer architectures are described in Figure 1-2.

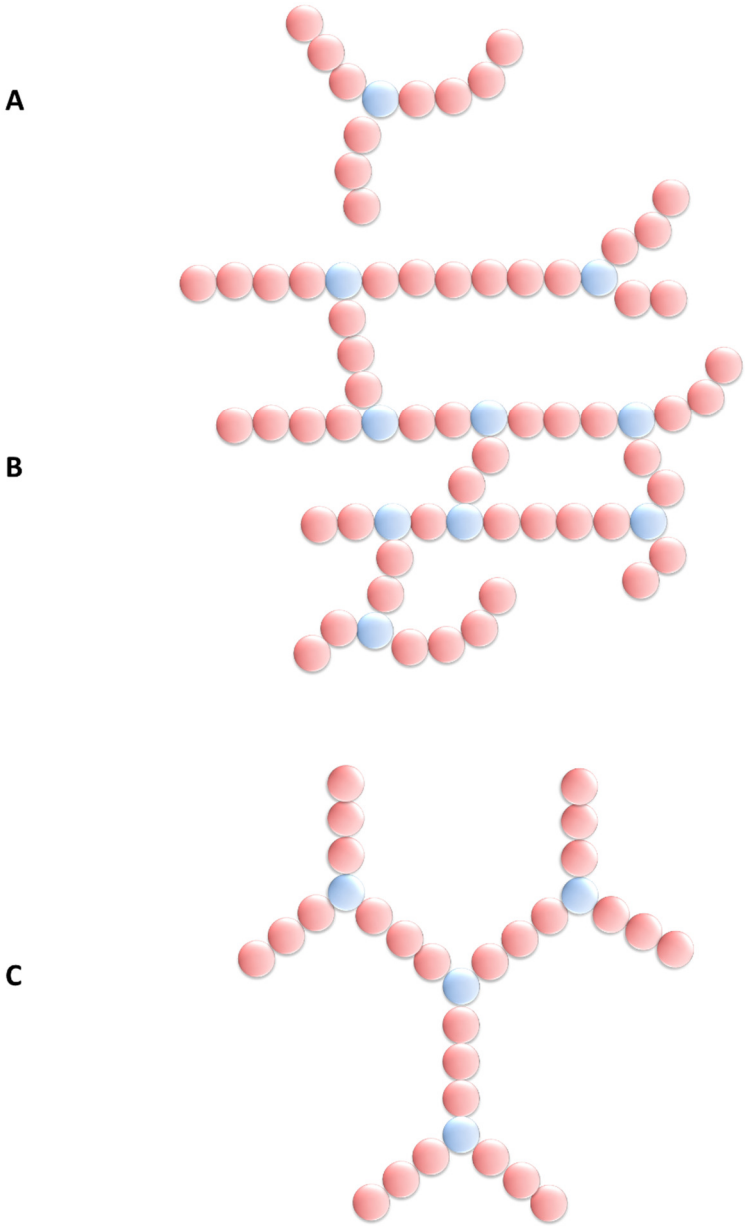


Figure 1-2. Simple ball representation of possible polymer architectures. A = Star, B = Hyperbranched, C = Dendrimer.

A star polymer (Figure 1-2, A) consists of a multi-functional (usually 3 or more) reactive centre/initiator which allows for polymer chain growth to start from this site. [23] They are highly investigated because of their useful structures and properties such as high densities of functional groups being available on the end of the stars arms. This can lead to many applications such as drug encapsulation and antifouling coatings. [24,25]

A hyperbranched polymer (Figure 1-2, B) is described as a polymer containing a high number of branching groups which are inter connected to form a 3-dimensional macromolecule. [26,27] Hyperbranched polymers come in many different types including; polyesters, polyamides, polyphenylenes and polycarbonates to name a few and are usually synthesised *via* a one-pot synthesis route. [28-31] This leads to relatively short reaction timescales. Hyperbranched materials contain a large number of functional groups, intramolecular cavities and have been found to have relatively low viscosities with high solubility. This leads to many potential applications which include viscosity modifiers, drug carries, resins, coatings and many more. [32-34]

A sub-section of hyperbranched polymers is a dendrimer (Figure 1-2, C). A dendrimer is a branched polymer which contains perfectly ordered arms and is therefore symmetric around the core. [35] Dendrimers are synthesised by two routes, divergent (growth from a functional core) [36,37] and convergent (small molecule addition) [38] and are well known for being difficult to synthesise due to long reaction times (sometimes weeks in a multi-layered step process). [39]

1.2.2 Types of Polymerisation

There are two main types of polymerisations; chain-growth and step-growth polymerisation.[40] The differences are discussed below.

1.2.2.1 Chain-growth Polymerisation

Chain growth polymerisation occurs much like adding extra links to a chain. The monomer adds onto the reactive site of the growing polymer chain. This creates

a new reactive site at the end of the added monomer. This type of polymerisation leads to a rapid increase in MWt at very low conversions. [41,42] However, for this thesis this type of polymerisation mechanism is not discussed.

1.2.2.2 Step-growth Polymerisation

Step-growth polymerisation proceeds *via* individual reactions of multi-functional monomer units with others, usually with the loss of a small molecule, hence it is commonly referred to as condensation polymerisation. A monomer unit reacts with another to form a dimer. This dimer can then react with another dimer or a monomer and so on (Figure 1-3). This reaction sequence then propagates until full conversion or until the reaction has subsided.

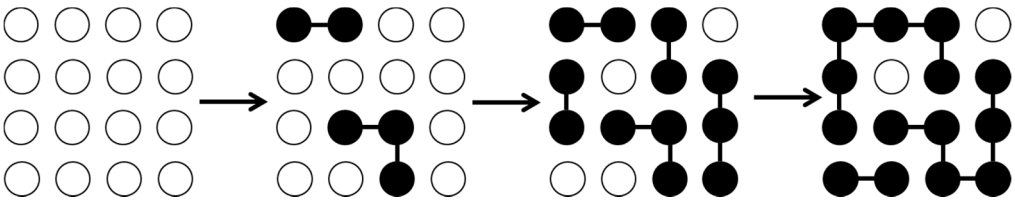


Figure 1-3. Representation of step-growth polymerisation.

Using this method creates polymers with a low MWt until high conversion (~ 95 %), at which point a drastic increase in MWt occurs as the large polymer chains combine. [43]

The difference between the two polymerisation methods is demonstrated by plotting the two techniques together in terms of MWt against conversion, shown in Figure 1-4.

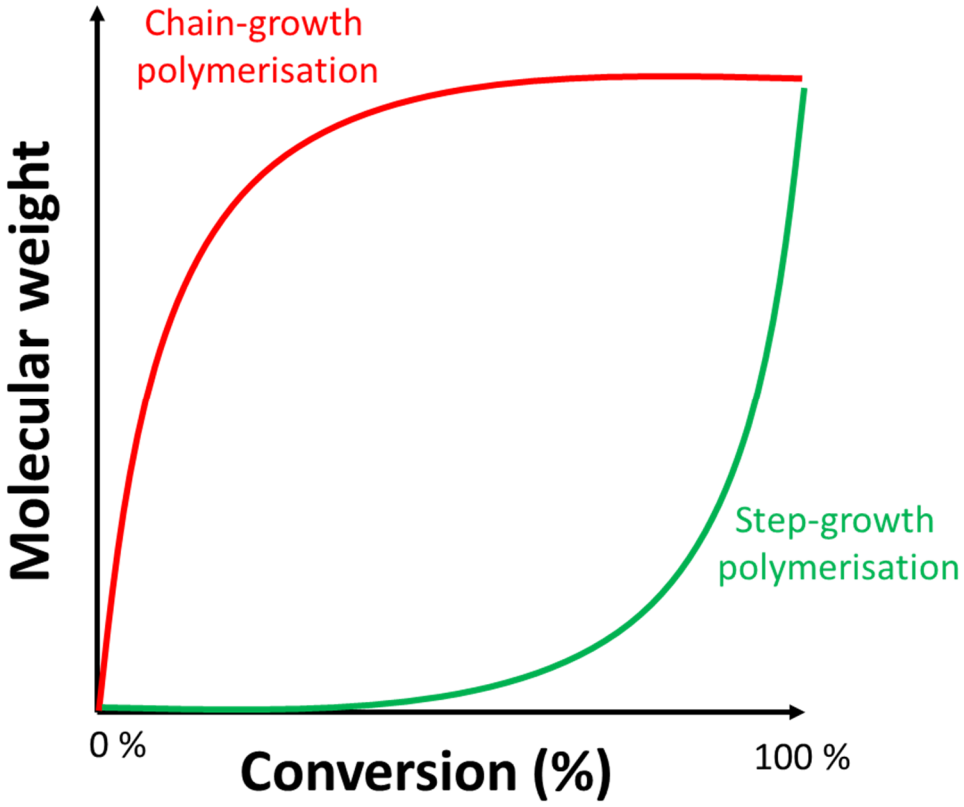


Figure 1-4. Comparison of molecular weight build with increasing conversion.

Figure 1-4 demonstrates the large differences in polymer growth between the two polymerisation mechanisms. It highlights the need to process step-growth polymers to high conversions to achieve large MWt's, which is a key factor in this thesis.

1.2.3 Polyesters

Polyesters are a group of polymers which consist of a backbone which contains an ester linkage, shown in Figure 1-5.

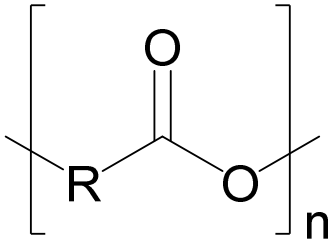


Figure 1-5. Example of a polyester repeating unit.

Linear polyesters were first synthesised by W. Carothers in 1932 at DuPont *via* heating a carboxylic acid and diol together in a melt polycondensation, but his research was halted after the discovery of Nylon. [44] Therefore, further research on polyesters was not achieved until Whinfield and Dickson filed for a patent in 1941 for the polyesterification of ethylene glycol and terephthalic acid to form a high melting, fibrous product, the scheme for which is described below in Figure 1-6. [45,46]

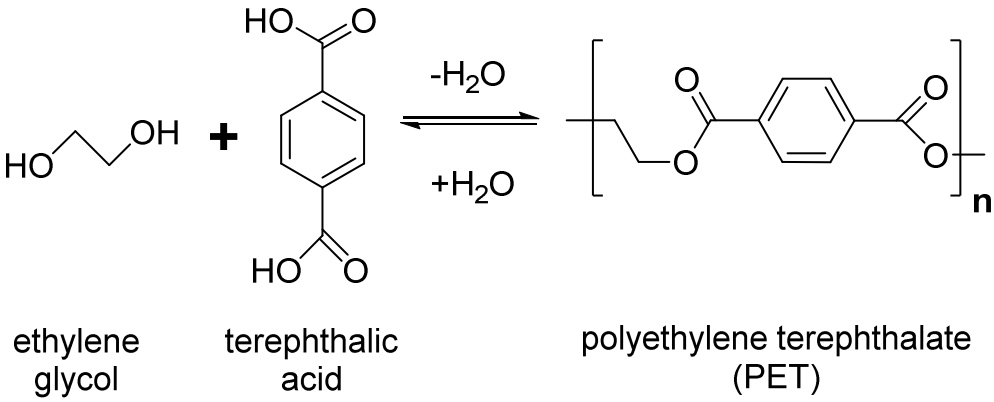


Figure 1-6. Scheme for the synthesis of ethylene glycol with terephthalic acid to create polyethylene terephthalate (PET).

Once the initial work had been completed by these pioneers, many different polyesters were discovered and it was deduced that they fit into two distinct groups:

1. Thermoplastics.
2. Thermosets.

Thermoplastics are polymeric materials which become rubbery and mouldable at high temperatures and solid once cooled.[47] These polyesters can then be re-heated once cooled and moulded again, making the heating of the polyester a reversible transition. Some widely used thermoplastics include Nylon and poly(lactic acid) (PLA).

Thermosets (often known as prepolymers) are soft/rubbery polymers that, once heated, undergo an irreversible reaction to create an insoluble, brittle network.[48] This heating process is commonly known as curing and usually involves the cross-linking of polymeric chains and is a vital stage in processing thermosets to achieve the required end properties.

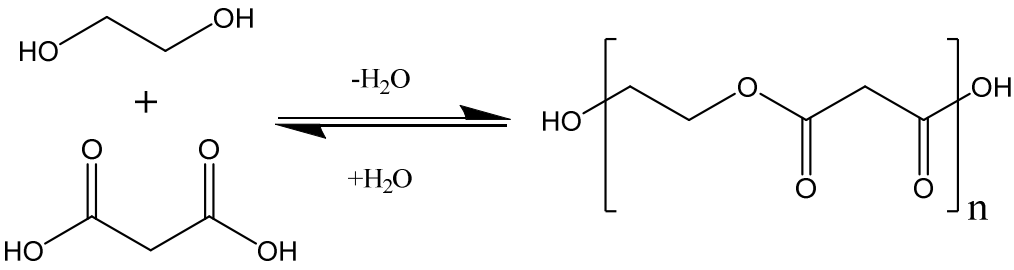
These differing properties of polyesters lead to their use in a plethora of aspects of everyday life. With large parts of industry dedicated to the production of many different uses of polyesters. These uses include; fabrics for clothes/furnishing,[49,50] PET for plastic bottles,[51,52] coatings [53,54] and many more.

When synthesising a polyester there are a number of different synthesis routes which must be considered. These routes are detailed below:

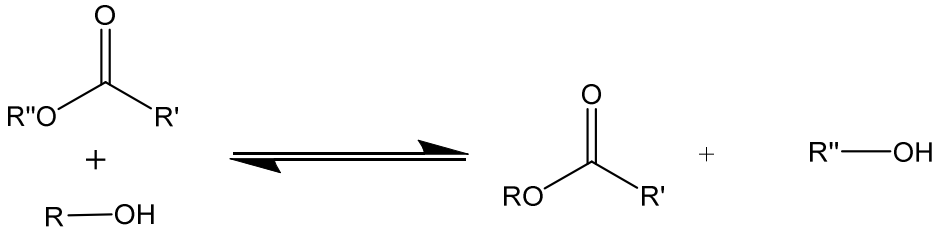
1) Melt polycondensation reactions. Usually involving the reaction between a diol and a diacid at high temperatures and long processing times. This reaction creates a water by-product. [55]
2) Transesterification. When an alcohol-terminated polymer condenses with an ester-terminated polymer to form an ester link, emitting an alcohol. [56,57]
3) Ring-opening polymerisation. Polyesters are assembled by the ring-opening of lactones under catalytic conditions. [58-60]

Schematic representations of these routes is detailed below in Figure 1-7.

1) Melt Polycondensation



2) Transesterification



3) Ring-opening polymerisation

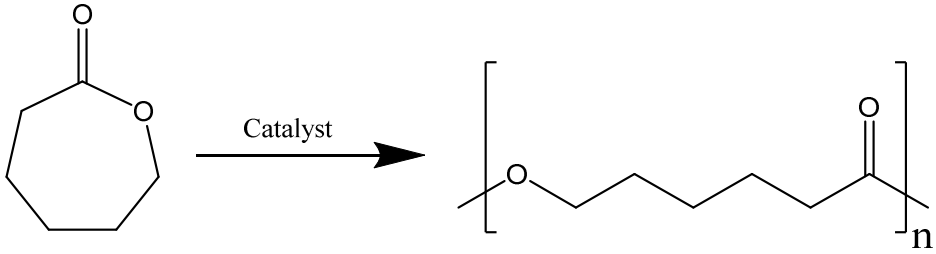


Figure 1-7. Reaction schemes for the different methods of polyester manufacture.

Figure 1-7 demonstrates that melt polycondensations and transesterification routes are reversible/in equilibrium and therefore are dictated by Le Chatilier's principle. This principle states that when a system is in equilibrium, a change in concentration, temperature, volume or pressure will be counteracted by changing the production of one product/reagent to nullify the change. [61]

In this thesis it is the melt polycondensations reaction scheme which is focussed on. During this process, the back reaction of water with polyester to make the starting materials represents a major challenge due to the fact that it decreases the reaction rate substantially towards the end of the reaction. This

factor, when added to the slow MWt building of step-growth polymerisations, described in Figure 1-4, is why it is crucial to employ a mass transfer strategy. These strategies include; processing at very high temperatures (+240 °C), [62,63] addition of vacuum to the head space, [64,65] sparging (bubbling inert gas through the system), [66,67] azeotropic solvent evaporation, [68,69] and stirring. [70]

In this thesis, the end products will be used in the powder coating industry. Therefore, powder coatings are discussed in detail below.

1.2.3.1 Powder Coatings

Powder coatings are becoming increasingly common when a protective and decorative layer is being applied to an end-user product. They are known to be more environmentally friendly than the liquid-based coatings because:

i. No Volatile Organic Compounds (VOC's) are emitted during the application process.
ii. They can produce much thicker coatings than liquid-based coatings without any run.
iii. Any overspray (particles that miss the intended surface) can be recycled and used again. This leads to >95% of the powder particles being applied to a surface.
iv. No prior mixing, thinning or stirring is required before application, which is required when using a liquid-based coating.
v. Extended product use due to the high mechanical, chemical and heat resistance of powder coatings.

These advantages have led to a market value estimation of $8.3 billion in 2013 and a projected compound annual growth rate of 6.54 % until 2019 to an

estimated value of $12.1 billion. [71] Therefore, there is large scope for research in this field and there are many companies interested in improving powder coatings performance and synthesis.

1.2.3.1.1 Types of Powder Coatings

In general, there are 4 main types of powder coatings widely used in industry; polyester, acrylic, epoxy, and fluoropolymer. These are all described in detail below.

Typically, polyesters for powder coatings are thermosets and include an aromatic diacid (to increase viscosity and T_g) and aliphatic diols (to plasticize the coating, lowering the T_g). The targeted T_g range of these coatings is usually found to be between 50 – 80 °C to allow ease of curing whilst keeping relatively good heat protection. [72] Depending on monomer loading ratios and end-use factors, the polyesters are processed to be either hydroxyl (excess diol) [73,74] or carboxyl (excess diacid) terminated. [75,76] These chain ends are then cross-linked using an agent [common cross-linkers include styrene and 1,3,5-triglycidyl Isocyanurate (TGIC)][72,77] to form a large polyester network with enhanced properties. Polyester powder coatings are usually used to coat buildings due their high colour/gloss retention and stability to UV light.

Acrylic powder coatings are ones which contain a backbone of (meth)acrylate groups *e.g* methacrylic acid and methyl methacrylate. Acrylics are considered very strong, durable and chemically resistant coatings and are commonly used in the automotive industry. [78,79] The T_g's are wide ranging from -65 °C in a 2-ethylhexyl acrylate polymer to 112 °C in a methyl methacrylate polymer. [80] Therefore, there are many different applications for an acrylic powder coating.

Epoxy resins were first discovered in 1909 by Prileschajew [81] and are defined as low MWt prepolymers containing an epoxy group. They are widely used in many fields such as adhesives and coatings. This is due to their high resistance to environmental degradation and good mechanical properties. [82] Epoxy resins are typically synthesised by creating a diepoxy and then curing it, usually using a diamine, alkali or anhydride (all curing agents). The curing agent selected has a significant impact on the final properties of the epoxy resin. [83] A diepoxy is made by the reaction of a diol with an organochlorine compound containing an epoxy under basic conditions. This diepoxy can then further react with more epoxy species *via* a ring opening mechanism to increase chain length, described in Figure 1-8.

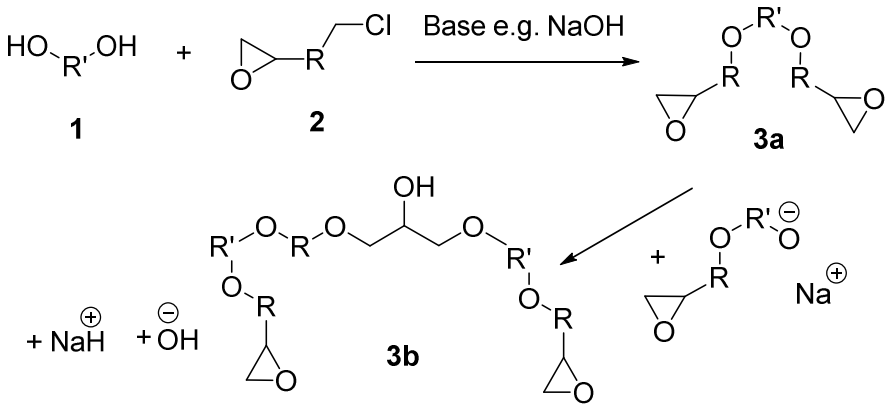


Figure 1-8. Formation of a diepoxy, 1 = diol, 2 = organochlorine compound containing an epoxy, 3a = first synthesised diepoxy, 3b = diepoxy after reaction with monoepoxy.

Flouropolymers are powder coatings which consist of a flourorcarbon backbone, with many strong hydrogen-fluoride bonds. These polymers come in two types; perfluoropolymers and partially fluorinated. Perfluoropolymers are polymers in which all the hydrogen atoms have been fully replaced by fluorides e.g. Polytetrafluoroethylene PTFE, discovered in 1938 by RJ Plunkett. [84] Partial fluorinated polymers on the other hand still contain some hydrogen atoms. [85] Figure 1-9 displays the difference between the two types of fluoropolymers.

Fluoropolymer coatings are very solvent, acid and base resistant, making them perfect for elongating the lifespan of the product which is coated.

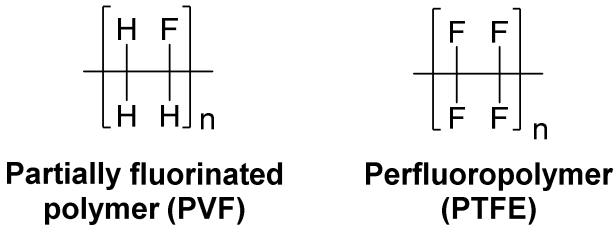


Figure 1-9. Schematic representation of a partially fluorinated polymer and a perfluoropolymer.

Therefore, when selecting a powder coating, careful consideration is needed to choose a polymer with the correct properties to fulfil the criteria selected by the end user.

1.2.3.1.2 Applying a Powder Coating

The first step in any coating application is to clean the surface to remove any unwanted particles *i.e.* dust and grease. After this, the application method is chosen. For powder coatings there are 3 main types of application processes:

1. Fluidized bed coating (FBC)
2. Electrostatic fluidized bed coating (EFBC)
3. Electrostatic spray process.

FBC is the simplest form of covering an article with a powder coating. It involves having an open top container consisting of a porous plate bottom with an air plenum, Figure 1-10 (a). The container holds the powder which is fluidized by passing air through the plenum and porous plate, making the powder resemble a boiling liquid. The article to be coated is then heated to just above the melting temperature of the powder and dipped into the powder. The powder then melts

and adheres to the surface, creating a continuous coat on the article. The product is then removed from the fluidized powder and left to cool. [72,86]

EFBC is similar to FBC but there is commonly no pre-heating of the article as a high DC voltage is applied to the fluidized powder particles. This voltage is usually applied by the mounting of the charging plate/grid below the powder and porous plate, Figure 1-10 (b). This grid charges the particles which are repelled by the grid as well as each other, forming a powder cloud above the bed. The article being coated is grounded and then passed over the powder cloud and the particles are attracted to the surface and stick. A larger film thickness can be applied by pre-heating of the article. [72,87]

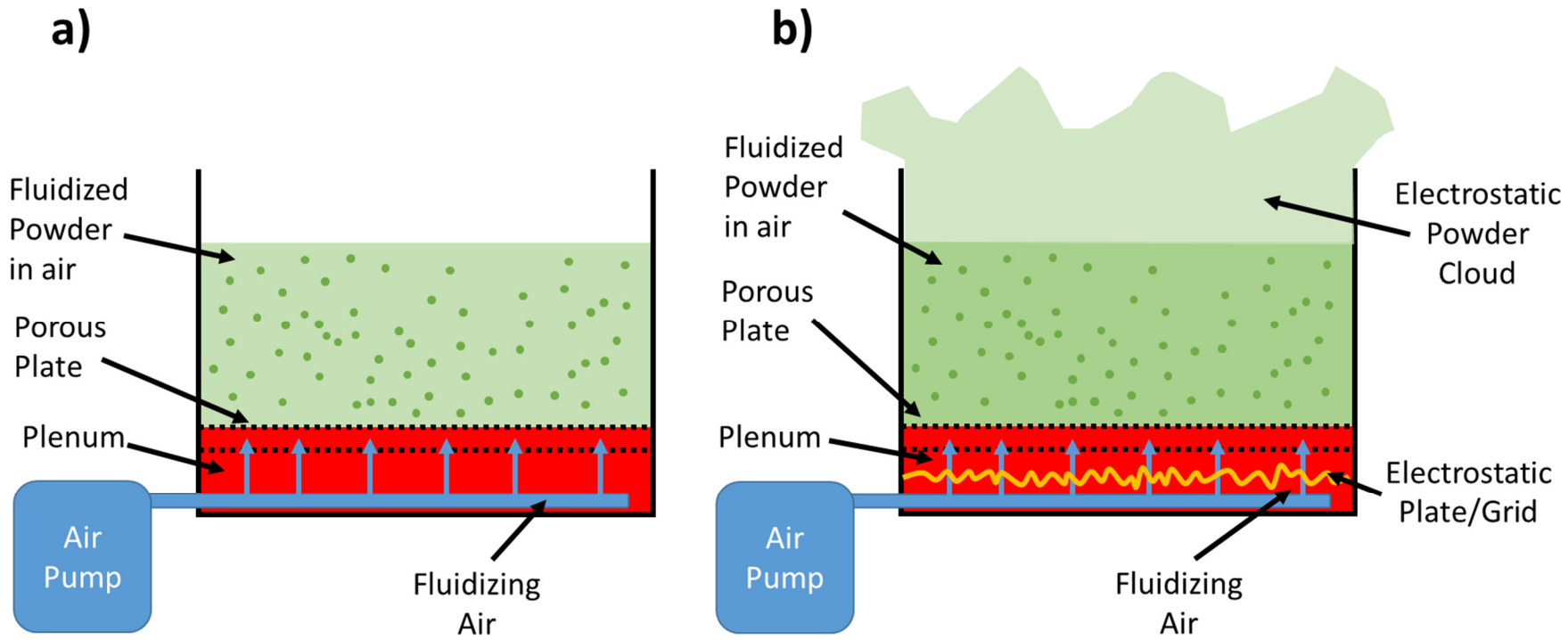


Figure 1-10. Example of the different types of bed powder coating. a) Fluidized Bed Coating, b) Electrostatic Fluidized Bed Coating with plate/grid below the porous plate.

The electrostatic spray process is the most commonly used process for applying a powder coating to an article. In general, the equipment needed consists of an electrospray gun, a feed hopper with the fluidized powder contained within, air compressor, power to supply DC voltage and a spray booth with recovery system. There are two major types of electrostatic spray charging processes/guns; Corona charging and Tribo charging.

Corona charging creates an electric field between the electrospray gun tip and the grounded object being sprayed. When the electric field is sufficiently high to surpass the breakdown voltage of air (3×10^6 V/m), [88] a corona discharge is created (electric field between the gun and article being coated). This makes the powder particles travelling through the tip negatively charged and allows them to follow the electric field and air flow towards the grounded object. Once the powders are close to the object, coulombic interactions attract the particles onto the surface and they stick. [72,89] For this spraying method flat surfaces are preferred as complicated shape architectures can create a “Faraday cage” effect and become difficult to coat. A Faraday cage effect is a phenomenon which occurs with charged powder spraying where the field lines will line up with the closest surfaces of the artefact being coated. Therefore, if a cavity, corner or hole is present the field lines will not enter these architectures. As the powder being sprayed will mostly follow these field lines these parts will not be coated, creating a Faraday cage. A representation of a Corona gun tip with powder trajectories and electric field is shown in Figure 1-11, (a).

Tribo charging creates the charged particles within the gun chamber. This is created by the frictional charge between the flowing powder and the electron accepting coating inside the gun (*e.g.* PTFE). This creates positively charged particles and free electrons, which are released through a grounded electron discharge meter. The particles are then fired at the grounded object by a jet of

compressed air. This lack of electric field means that the “Faraday cage” effect is negligible in a Tribo system. This leads to smoother and thicker finishes when applied. [90] A representation of a Tribo gun tip with powder trajectories is shown in Figure 1-11, (b).

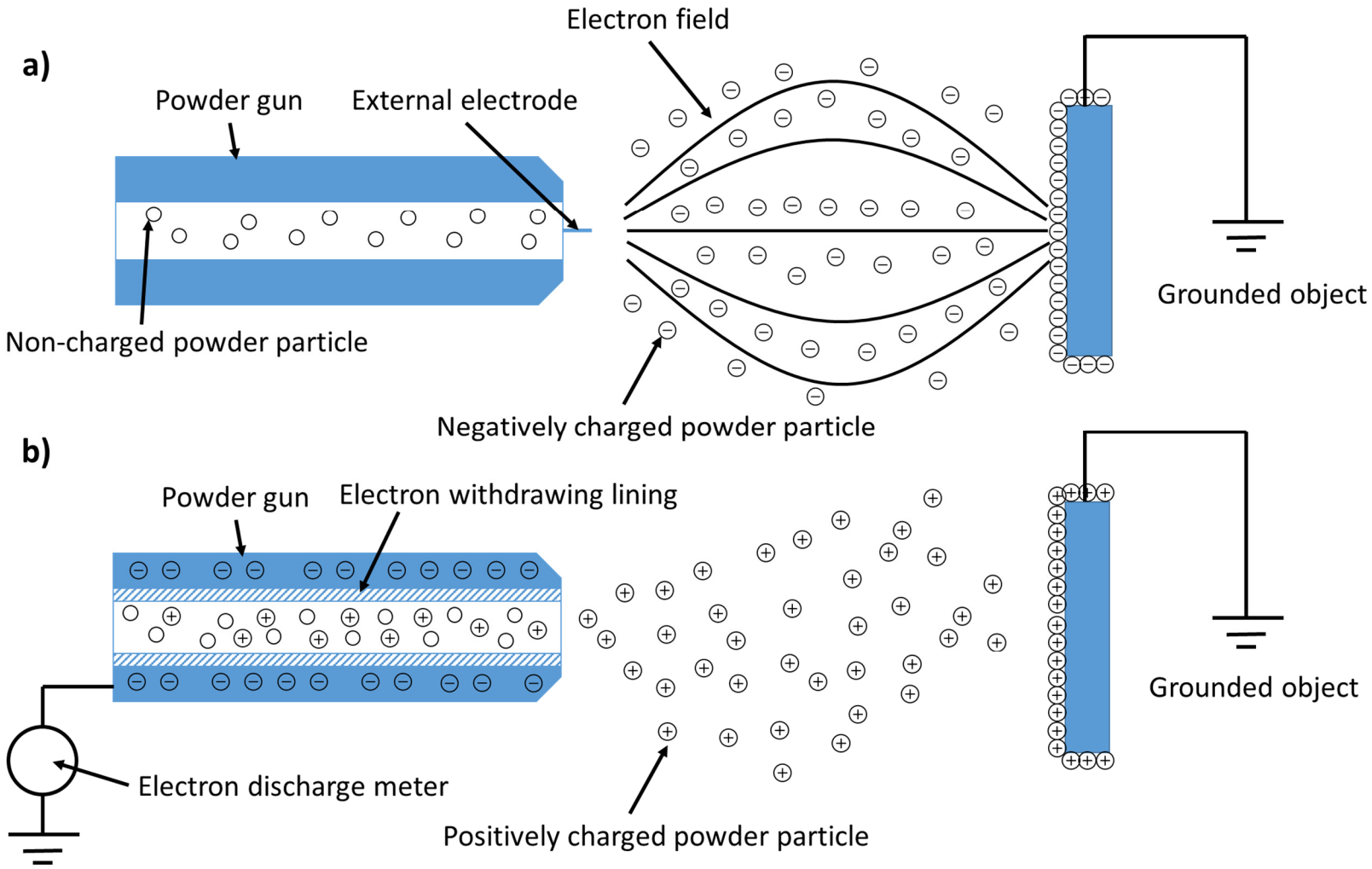


Figure 1-11. Gun nozzles for electrospray powder coating applications. a) Corona and b) Tribo.

1.2.3.1.3 Curing of powder coatings

The curing of powder coatings is an important part of the coating process. It is important to understand this process as the type of powder will affect the cure temperature as well as the coating thickness. Also, the difference must be noted between the two types of powder coatings; thermoplastic and thermoset. When a thermoplastic is cured, the plastic is softened and this creates a smooth surface on top of the object. Once cooled the coating can then be re-heated to form a soft/liquid state and therefore the cure is reversible. Conversely, thermosets undergo a chemical reaction (cross-linking) when cured and therefore cannot be re-melted when heat is applied after cooling. [91,92] In general, there are two types of curing; convection oven and infra-red curing.

Convection oven curing is the most commonly used type of curing and involves cycling hot air throughout an oven in which the powder coated object is suspended. This air is heated above the melt or cure temperature of the powder and heats the object through convection and conduction. Therefore, this heating method is slow and creates long lead times which can prove heavily energy intensive. Convection oven curing is an ideal technique for small, complex products as they will heat up efficiently/quickly and the air will flow around all types of architectures. Whereas, large objects will take longer to heat up to the cure temperature. When implementing convection curing, care must be taken not to blow unwanted dust/contaminants onto the objects surface as it may interfere with the cure or the final finish of the product. Therefore, the air is usually filtered before being circulated in the curing cavity. [93,94]

Infra-red curing involves emitting infra-red radiation directly onto the surface of the object being cured. The electromagnetic (EM) waves are transmitted onto the surface of the object and therefore do not need a medium to be transported

in as they will directly interact with the surface from the source. This means that only the specific part in which the infra-red radiation hits will be heated. Therefore, infra-red curing is much less energy intensive as convection curing due to the direct application of the heat to the object surface. But, this means that complex objects with multi-layered architectures are not ideally suited to this method whereas, a consistently shaped/smooth/flat product is ideal. [93,94]

1.3 Microwaves

1.3.1 Microwave Fundamentals

Throughout the history of chemical research traditional methods of heating reactions have been implemented, from Bunsen burners to oil baths and hot plates. However, after Giguere and Gedey first applied microwaves to organic reactions in 1986, [95,96] there has been an increased interest in using microwaves as a heating method. [97-104]

Microwaves are a form of EM energy with a frequency range between 0.3 and 300 GHz. [105] This puts them in the region between radio waves (larger wavelengths) and infra-red (smaller wavelengths) with wavelengths of 100 m to 1 mm. Microwaves are used in a plethora of different modern day applications including; radar, communications, home cooking and navigation systems. Therefore, when using a microwave reactor in the lab, there is a set of certain frequencies which are defined to allow safe lab use without interfering with any other applications. These frequencies are 896 MHz and 2.45 GHz and are known as the IMS (Industrial, Medical and Scientific) allowed frequencies. [106] An energy value for these frequencies can be calculated using Planck's equation, Equation 1-2.

$$E = hv$$

Equation 1-2

Where E is the energy, v is the frequency of the wave, and h is Planck's constant ($4.135667662 \times 10^{-15}$ eVs).

Therefore, at 2.45 GHz this creates an energy of 0.00001 eV which is significantly below the threshold for breaking covalent bonds (*e.g.* an I-I bond has an eV of ~1.6 eV and is considered weak). [107] Therefore, microwave energy is known as "non-ionising" and will only effect the movement of molecules. Therefore, any changes in heating mechanisms witnessed will be due to a selective heating effect or frictional heating and not bond breaking/making.

1.3.2 Microwave/Dielectric Heating Mechanisms

When considering microwave heating (MWH) there are two types of heating mechanisms to consider; dipolar polarisation and ionic conduction, shown in Figure 1-12. [108]

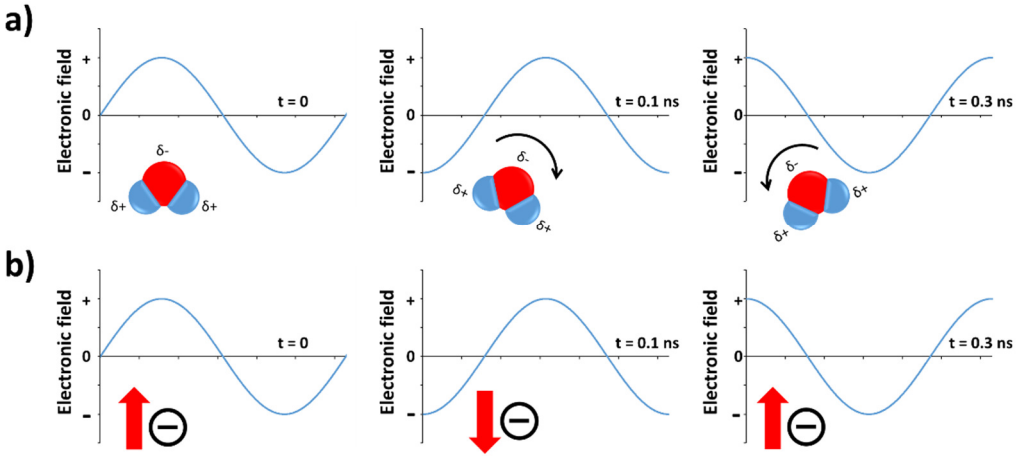


Figure 1-12. Heating mechanisms found in MWH, a) dipolar polarisation and b) ionic conduction, as described by Kappe et al. [109]

Dipolar polarisation occurs in molecules which have a dipole moment. This is an opposite, partial charge between neighbouring atoms which occurs due to differences in atom electronegativity. This dipole allows the molecule to align with the electric field. The sinusoidal nature of the electric field then causes the molecule to oscillate as it attempts to realign with the alternating field. This oscillation of the molecule creates kinetic energy in the form of heat. If the frequency of the microwave is too low, the molecules align with the electric field perfectly and no heating will occur. Conversely, if the frequency is too high, the molecules will not align with the rapidly oscillating field. Therefore, frequency of the wave is an important factor when heating *via* microwave energy. [110]

Ionic conduction occurs in molecules with formal positive and negative charges. The charged species move with the oscillating electric field. This movement causes the species to collide with others and it is these collisions which result in energy release and heating. Again, if the frequency of the wave is too high, the molecules will not align and therefore no movement will occur and no friction is created. If the wave frequency is too low, all molecules will be in phase with the field and no frictional energy will be created. [109]

The main heating mechanism focused on in this work is dipolar polarisation. However, as some of the catalysts under investigation have separate charges between metals and ligands, ionic conduction is also observed.

1.3.3 Dielectric Properties

When implementing MWH, it is imperative to evaluate how effectively the materials will heat under EM energy. To do this the material's dielectric properties are evaluated. The dielectric properties are defined as the ability of a

material to convert EM energy into heat. This ability is represented by a term called the loss tangent, (tan**δ**), and is calculated using Equation 1-3.

$$\tan\delta = \frac{\varepsilon''}{\varepsilon'} \qquad \textit{Equation 1-3}$$

Where ε' is the dielectric constant and represents the ability of the material to store electromagnetic energy and ε'' represents the dielectric loss which is the ability of the material to convert the stored electromagnetic energy into heat.[98,111,112]

Materials are generally considered to heat efficiently under MWH if their tan**δ** value is above 0.1. [109] However, this is a nominal value and if multiple molecules within the reaction possess a value above 0.1, it is those with the highest values which are considered the best heaters using MWH.

When considering dielectric properties for a chemical reaction, the dependency of these values on outside factors need to be considered. This is because the dielectric properties of a substance are dependent on temperature and the frequency of the wave. [113]

For low frequencies, dielectric constant (ε') will be at its highest value. This is due to the electron cloud being able to shift with the low frequency effectively, causing the largest dipole and polarisability. The polarisability of a material can be calculated for ε' and dielectric loss (ε'') using the Debey equations shown below in Equation 1-4 and Equation 1-5. [114]

$$\varepsilon' = \varepsilon_\infty \frac{\varepsilon_s - \varepsilon_\infty}{1 + (\omega\tau)^2}$$ Equation 1-4

$$\varepsilon'' = \frac{(\varepsilon_s - \varepsilon_\infty)\omega\tau}{1 + (\omega\tau)^2}$$ Equation 1-5

Where ε_∞ represents the dielectric constant at frequencies too high for molecular orientation, ε_s is the static dielectric constant, ω is the angular frequency (2πf) and τ is the relaxation time i.e. the time in seconds taken for the dipoles to revert back to the original, random orientation when the electric field is stopped.

Therefore, if the frequency is large, ε_∞ will also be large. This will decrease the value of both the dielectric constant and loss.

Dielectric properties are also affected by the temperature of the system. [109] This is dictated by the relaxation time of the molecules. Again, Debye proposed an equation to explain this relationship between relaxation time and temperature, described in Equation 1-6 below. [115,116]

$$\tau = \frac{4\pi r^3 \eta}{kT}$$ Equation 1-6

Where r is the radius of the molecule/molecules in question, η is the viscosity, k is the rate constant and T is the temperature.

Equation 1-6 demonstrates two important factors. Firstly, the larger polymeric chains will significantly affect the relaxation time due to the increases in r and η. Therefore, as molecules increase in size, the ability for individual dipoles to rotate and align with the field will be reduced due to the large/increased intermolecular forces. Secondly, with increased temperature there is a decrease in relaxation time. This is because as the temperature increases, the molecules return to a randomised state quicker due to the increased energy in the system.

1.3.4 Penetration depth

Penetration depth (how far/deep the microwave energy penetrates into the bulk) is an important value when considering microwave synthesis. It is defined as the depth at which the power density of the initial wave has decreased by 37%. [109] The penetration depth is calculated using Equation 1-7.

$$\mathbf{d_p} = \frac{\boldsymbol{\lambda_o}\sqrt{\boldsymbol{\varepsilon'}}}{\mathbf{2\pi\varepsilon''}} \qquad \textit{Equation 1-7}$$

Where d_p represents the penetration depth, λ_o is the wavelength of the microwave, ε' is the dielectric constant and ε'' is the dielectric loss.

At 2.45 GHz the wavelength of the microwave is 12.24 cm, which can be derived using Equation 1-8.

$$\boldsymbol{\lambda_o} = \frac{\mathbf{c}}{\mathbf{f}} \qquad \textit{Equation 1-8}$$

Where c represents the speed of light (299,792,458 m/s) and f represents the frequency of the wave.

An important characteristic of penetration depth is that it varies with temperature. [117] Therefore, it would be ideal to match the frequency with the desired penetration depth for the cavity of the microwave reactor and geometry of reaction vessel. However, most lab microwaves and literature have a processing frequency of 2.45 GHz. Therefore, the frequency would only be changed if an industrial system would benefit from using a different frequency (on a large scale this would usually be to 896 MHz as lowering the frequency will increase the d_p).

1.3.5 Microwave Heating Effects

When microwaves were first introduced into organic synthesis, there were many promising results in the field. Many researchers were boasting large reaction rate increases, altered products, higher yields and better control when compared to conventional heating (CH) methods at identical temperatures. [118-121] This was theorised to be the efficient nature of the MWH mechanism and potentially a special microwave heating effect on the molecules when compared to CH. These effects will be discussed below.

When CH methods are employed into a reaction, the heating mechanism occurs through conduction and convection currents. This heating process is usually very slow and inefficient, especially at larger scales. Therefore, reactor design, size and stirring capabilities affect the heating efficiency significantly. Utilising CH leads to the reactor walls being the hottest part of the vessel and can lead to a large temperature gradient from the outside in. In contrast, MWH is shown to penetrate through the outer vessel walls and heat the reaction mixtures from the inside, described by Kappe and Dallinger in Figure 1-13.[122] This is known as bulk heating and allows MWH to heat all the reacting materials simultaneously. This can lead to highly energy efficient heating, especially in larger scale reactions. [123]

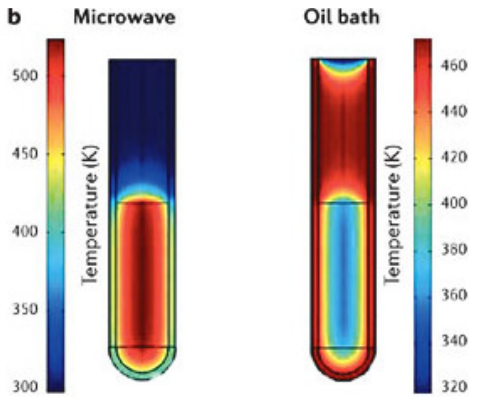


Figure 1-13. Temperature gradient 1 minute after heat application to ethanol under microwave energy and open vessel oil bath. Kappe et al. [122]

This bulk heating effect leads to increased heating efficiency of reactant mixtures when compared to CH and is widely cited as the main advantage of MWH. But, there are other specific microwave effects suggested by literature and it is a highly debated subject within the scientific community. These other effects are; specific microwave effects and non-thermal effects.

Specific microwave effects are suggested to arise due to the unique nature of the MWH mechanism, which cannot be achieved using CH. Specific microwave effects are defined as localised/in-core heating of specific functional groups and molecules. [124] This leads to all the energy being dissipated into the reaction sites which can therefore increase reaction rates when compared to CH. An example of this is the superheating of solvents at atmospheric pressure, where boiling points can be up to 40 K higher than CH methods, however this only occurs when the glassware is 100 % clean as this eliminated the coalescence points which are needed for boiling to occur. [125] If this heating mechanism exists then it could be substantially beneficial when wanting to heat specific reagents within a heterogeneous mixture, which is theorised to be possible due to the varying dielectric properties of materials.

Non-thermal microwave effects are considered the most controversial theory within the microwave community. They are described as when the microwave energy has a direct effect on the molecules without the energy transforming into heat. An example of this non-thermal effect is the lowering of the activation energy for a system. [109] This is notoriously difficult to prove due to the short lifetimes of the intermediate species involved. But, a review published by del la Hoz *et al.* has argued that there is evidence of this effect in certain circumstances. [99] Whereas, many other publications have disproved this theory, specifically in liquid systems where the energy redistribution between molecules is quicker than the oscillation of microwave energy. [126,127]

1.3.6 Temperature Monitoring of a Microwave System

When performing chemical reactions it is vitally important to have an accurate temperature monitoring and controlling system. It has been recently shown that when MWH was introduced into the literature, temperature readings were inaccurate. This was through a study named “Microwave Effects in Organic Synthesis: Myth or Reality?” by Kappe *et al.* who employed stringent temperature measuring conditions to assess claims of rate increases in organic reactions. [128] It was deduced that the large property and rate enhancements found when using MWH were down to increased temperatures in MWH reactions due to inaccuracies in the infra-red (IR) temperature measurement.

In general, microwave reactors control the input power *via* a temperature feedback loop which requires constant, precise measurement (even found in domestic ovens). [129,130] Commonly, the technique used for this measurement is an external IR sensor. These sensors are built to be within the microwave cavity and record the temperature of the vessel walls. But, as discussed previously, using MWH creates a bulk heating effect with an inverse temperature gradient. Therefore, an IR sensor will be recording the temperature for the coolest part of the reaction. This, along with studies which have shown that slight differences in internal temperature cannot be distinguished, [131] are reasons why IR is an inadequate method for measuring temperatures of MWH reactions.

As such, fibre optic (FO) technology has become the leading method of temperature measurement for MWH reactions. [132] Although expensive, FO probes are particularly attractive because they are dielectrically transparent and are not affected by the EM energy, therefore they do not need to be shielded within the reaction. A FO probe consists of a gallium arsenide (GaAs) semiconductor crystal mounted onto the tip of a FO (glass/quartz). Temperature

measurement is achieved by passing a beam of light down the FO from a light source. The light is then partially absorbed by the crystal with some being reflected, with a mini spectrometer providing a spectrum from this reflected light. The differences in temperature are detected by exploiting the temperature dependence on the crystal's band gap size. This follows as the differences in band gap size will dictate the level of light reflected. A rough representation of a FO probe is shown in Figure 1-14.

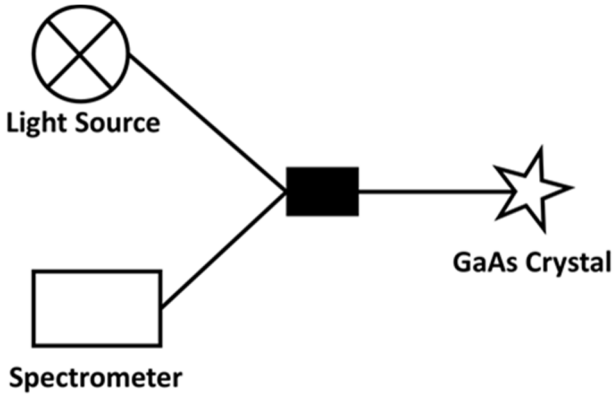


Figure 1-14. Representation of n FO probe containing a GaAs crystal.

1.3.7 Literature for Microwave Heating of Polymers and Specifically Polyesters

Microwave synthesis of polymers is a well-researched area. Many different researchers have investigated the subject and there have been a large amount of important reviews on the topic. [133-136] These reviews have helped highlight the notable work done towards understanding the use of microwaves in polymerisation reactions. For step-growth polymerisations, recent publications by Mallakpour and Raifee [124] and Komorowska-Durka *et al.* [137] have indicated the most recent advances. These microwave reactions include the synthesis of poly(amide)s, [138,139] poly(imide)s, [140,141] poly(ether)s, [142] and poly(urea)s. [143,144]

This emphasises the vast use of microwaves as an efficient heating source for step-growth polymerisations.

Tin catalysts are widely used as they have been shown to be excellent catalysts for polyesterification reactions with microwave reactions being of specific interest. $SnCl_2$ has been investigated in the adipic acid, neopentyl glycol melt polycondensation by Komorowska *et al.* [145] It was concluded that using MWH had a positive effect on the heat up times of the systems, (MWH ~3 times faster than CH) and the final product properties were not affected, with similar conversions and acid reactivities observed. Yamada *et al.* investigated the melt polycondensation of L-lactide using $SnCl_2$ and concluded that there are enhanced properties derived from use of MWH *i.e.* higher MWt. [146] Within this study it was discovered that using only the electric field (EF) positively affected the polymerisation and only using the magnetic field (MF) inhibited the polymerisation. This suggested that the type of EM energy applied to the system is an important factor in MWH polycondensations. Tin octanoate ($Sn(Oct)_2$) is a widely used esterification catalyst due to its availability, low impurities, stability at high temperatures and Food and Drug Administration (FDA) approval. [147] There has been much research into its use in ring opening polymerisations (ROPs) using MWH. Singla *et al.* demonstrated that implementing MWH instead of CH increased the ROP rate of lactide substantially. [148] This was further investigated by Nguyen *et al.* [59] on an ε- caprolactone system and it was shown that utilising MWH produces an acceleration in the pre-initiation period when compared to CH. This was proven by increasing the percentage of catalyst which decreased the heat-up period, emphasising the temperature overshoot within the reaction. These promising results, coupled with the fact that tin is widely used in industry as an esterification catalyst, [149-151] is the reason why it was investigated and focussed on in this thesis.

Triflate catalysts have been an interesting area of study for polycondensations. The theory behind using triflates is that they are considered more environmentally friendly than many organometallic alternatives and are very strong acids (acidic conditions catalyse esterifications). [152] Takasu *et al.* investigated the use of Sc, Yb and Y triflates using CH and an array of diacids and diols in a 1:1 molar ratio to assess if using a triflate catalyst was viable for polycondensations. [153] These catalysts were shown to efficiently catalyse polycondensations at low and high temperatures, with minimal side reactions (especially over 80 °C). Buzin *et al.* investigated linear aliphatic polycondensations, concentrating on bismuth triflate but also considering Na, Mg, Al, Zn Sn, Sc and Hf. [154] Bi triflate was shown to be the optimum triflate as the highest M_n's were achieved whilst using relatively mild conditions. Buzin *et al.* discovered that using a more acidic triflate resulted in a higher yield and therefore suggested a protic esterification mechanism. But Garaleh *et al.*[155] later tested this hypothesis and found that this series does not occur. Therefore, a carbonyl complexation mechanism was proposed due to the fact that metal carboxylates are more stable than metal alkoxides. These two mechanisms are discussed in detail in chapter 3.

Non-organometallic catalysts will also be considered in this thesis, specifically phosphoric acid (PA) and its dimer pyrophosphoric acid (PPA). This is because of the previous literature on condensation reactions using these catalysts by S. Göbölös *et al.* [156] implemented a PA catalyst supported on a substrate, to achieve high conversions of the condensation of allyl alcohol with ammonia. Nakato *et al.* [157] investigated the effects of PA on the bulk polycondensation of succinimide and established that employing this catalyst produced a polymer with high conversions (≥99 %) and satisfactory MWt's (23 $kg.mol^{-1}$). PPA was also considered due to research conducted by Adlington *et al.* [158] which

suggested that when implementing MWH conditions on polymerisations, it is the dimers and trimers of materials which have increased dielectric properties. This was because oligomeric structures are still small enough to have free dipole movement while exhibiting a greater viscosity which means that there is greater molecular friction created from this movement.

1.3.8 Scale-up of Microwave Reactions

An important section of this thesis is the investigation into the scale-up possibility of polymerisation reactions using MWH. Developing a large microwave reactor can present many problems with processing such as power density and d_p. It is also crucial to consider the safety aspects of introducing a high amount of microwave energy to a large amount of sample. Because of this, a brief literature search into the scale-up of general chemical reactions was conducted. From this it was deduced that there was two possible processing options when scaling-up; batch reactions and continuous flow reactions. In this thesis it is only a batch reactor system which is considered because the long reaction times and high viscosities of polyesterifications do not allow easy continuous flow processing.

With batch reactors there are two options to consider. These are sealed and open-top vessels. Both options will be discussed below with some current literature for each.

A sealed batch microwave reactor was reported by Dallinger *et al.* [159] utilising a masterwave BTR single mode microwave with a large cavity. A 1 L PTFE vessel was milled to fit the dimensions of the cavity with a PTFE paddle stirrer. Temperature was monitored through a pt100 thermocouple inserted into the bottom of the vessel. Using this vessel, many organic reactions were performed

including; Diels-Alder, heterocycle synthesis, aromatic substitution and many more. These examples were investigated for scalability with microwave application and it was identified that all these reactions scaled well in the microwave, with no change in the optimized conditions from small scale to large scale. Batch loads of up to 720 mL were achieved and the usual operating limits of small batch microwave reactors were matched (250 °C/30 bar). Similar to this work, Schmink *et al.* investigated the use of a 12 L sealed batch microwave reactor to assess large scale solvent heating and to process multi stage reactions. [160] Promisingly, no penetration depth issues were found when heating solvents in large quantities and no optimization from small scale was needed when scaling-up chemical reactions. These results showed promise for scale-up, but the vessel used was a sealed unit. This system would not be applicable for an esterification reaction as the condensate produced would not leave the reaction and therefore high conversions could not be achieved. Therefore, open top vessels were considered.

In the case of open-vessel esterifications, Amore et al. [161] employed a multimode RotoSynth Rotative Solid-Phase Microwave Reactor capable of processing up to 3 mol of propionic acid and 1-octanol, making ~0.5 kg of product. Reactions were performed using a 5 minute ramp to 120 °C with a H_2SO_4 catalyst and varying reaction times. Depending on the reaction time, yields of 75 – 87 % were achieved. Reactions using propanol and butanol at 100 °C were investigated and high yields of 94 and 82 % respectively were achieved. This reaction apparatus and geometry showed that microwave reactors can be used to facilitate condensate removal in condensation reactions in larger scale reactions.

The polycondensation of lactic acid to form PLA was investigated on a 70, 200 and 20,000 mL scale by Nakamura *et al.* [162] Different microwave reactors were

used for each scale of the process, with the 20 L reactor being pilot plant scale. The magnetron set-up for the 20 L experiments is detailed below in Figure 1-15 and will be the basis for the scale-up work in this thesis.

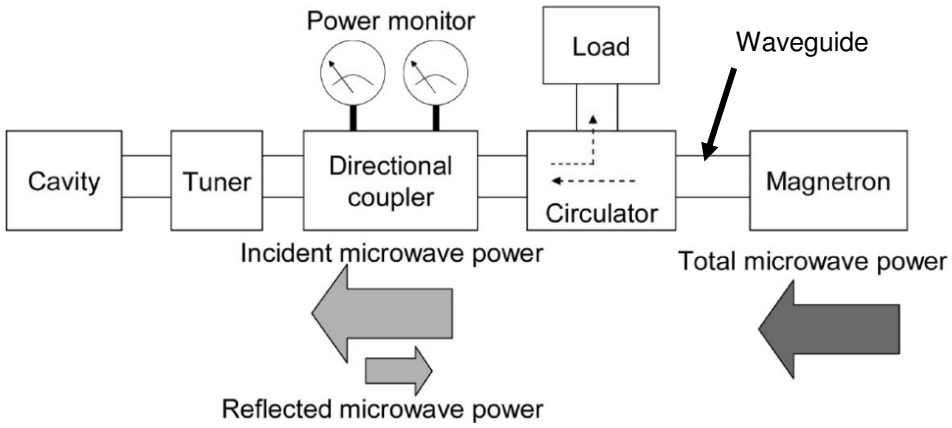


Figure 1-15. Diagram of the microwave heating components used in the 20 L scale-up polycondensation of lactic acid by Nakamura et al. [162]

From each scale, average molecular weights of ~10,000 $g.mol^{-1}$ were achieved. Deductions were made which suggested that as the reaction size increased, more of the incident microwaves were absorbed into the reaction bulk, increasing heating efficiency. This allowed the researchers to achieve a 94 % efficiency increase when scaling-up and a 70 % energy reduction when changing heating techniques from CH to MWH. This large efficiency increase when scaling-up highlights the potential of microwaves in large scale production.

Therefore, it has been shown that the scale-up of a microwave process is possible. This previous work was considered when designing a large rig for the polycondensations presented in this thesis, with emphasis of creating a hybrid rig which allowed concurrent CH and MWH. This allowed for direct comparisons between the two heating methods to be drawn (discussed in chapter 5).

1.4 References

1 IUPAC. *Pure and Applied Chemistry*. (1996).

2 Kohan, M. I. & Kohan, M. I. *Nylon Plastics Handbook*. (Hanser Publishers, 1995).

3 Hanle, J. E., Merz, E. H. & Mesrobian, R. B. Polymers in packaging. *Journal of Polymer Science Part C: Polymer Symposia* 12, 185-195, doi:10.1002/polc.5070120115 (1966).

4 Ammala, A. Biodegradable polymers as encapsulation materials for cosmetics and personal care markets. *International journal of cosmetic science* 35, 113-124, doi:10.1111/ics.12017 (2013).

5 Loh, X. J. *Polymers for Personal Care Products and Cosmetics*. (Royal Society of Chemistry, 2016).

6 Liechty, W. B., Kryscio, D. R., Slaughter, B. V. & Peppas, N. A. Polymers for Drug Delivery Systems. *Annual review of chemical and biomolecular engineering* 1, 149-173, doi:10.1146/annurev-chembioeng-073009-100847 (2010).

7 Lan, Z. Y. *et al.* Novel Biodegradable Drug-Eluting Stent Composed of Poly-L-Lactic Acid and Amorphous Calcium Phosphate Nanoparticles Demonstrates Improved Structural and Functional Performance for Coronary Artery Disease. *Journal of Biomedical Nanotechnology* 10, 1194-1204, doi:10.1166/jbn.2014.1868 (2014).

8 Priya James, H., John, R., Alex, A. & Anoop, K. R. Smart polymers for the controlled delivery of drugs – a concise overview. *Acta Pharmaceutica Sinica B* 4, 120-127, doi:http://dx.doi.org/10.1016/j.apsb.2014.02.005 (2014).

9 Teo, A. J. T. *et al.* Polymeric Biomaterials for Medical Implants and Devices. *ACS Biomaterials Science & Engineering* 2, 454-472, doi:10.1021/acsbiomaterials.5b00429 (2016).

10 Leprince, J. G., Palin, W. M., Hadis, M. A., Devaux, J. & Leloup, G. Progress in dimethacrylate-based dental composite technology and curing efficiency. *Dent. Mater.* 29, 139-156, doi:http://dx.doi.org/10.1016/j.dental.2012.11.005 (2013).

11 Flory, P. *Principles of Polymer Chemistry*. (Cornell University Press, 1953).

12 Krause, S. Polymer Chemistry: An Introduction, 3rd Edition (Stevens, Malcolm P.). *J. Chem. Educ.* 77, 35, doi:10.1021/ed077p35 (2000).

13 Mark, J. E. *Physical Properties of Polymers Handbook*. (Springer New York, 2007).

14 Bicerano, J. *Prediction of Polymer Properties*. (CRC Press, 2002).

15 Hiemenz, P. C. & Lodge, T. P. *Polymer Chemistry, Second Edition*. (CRC Press, 2007).

16 Fox, T. G. Influence of diluent and of copolymer composition on the glass temperature of a polymer system. *Am. Phys. Soc.*, 123-125 (1956).

17 Yousi, Z., Donghai, L., Lizong, D. & Jinghui, Z. Synthesis of graft copolymer by coupling reaction of living poly(methyl methacrylate) with bromomethylated polystyrene. *Polymer* 39, 2665-2668, doi:http://dx.doi.org/10.1016/S0032-3861(97)00572-7 (1998).

18 Hadjichristidis, N., Pispas, S., Pitsikalis, M., Iatrou, H. & Lohse, D. J. in *Encyclopedia of Polymer Science and Technology* (John Wiley & Sons, Inc., 2002).

19 Smulders, W. & Monteiro, M. J. Seeded Emulsion Polymerization of Block Copolymer Core–Shell Nanoparticles with Controlled Particle Size and

Molecular Weight Distribution Using Xanthate-Based RAFT Polymerization. *Macromolecules* 37, 4474-4483, doi:10.1021/ma049496l (2004).

20 Hülya, A. Block and Graft Copolymerization by Controlled/Living Radical Polymerization Methods. *InTech* (2012).

21 Yates, C. R. & Hayes, W. Synthesis and applications of hyperbranched polymers. *European Polymer Journal* 40, 1257-1281, doi:http://dx.doi.org/10.1016/j.eurpolymj.2004.02.007 (2004).

22 Zhu, X., Zhou, Y. & Yan, D. Influence of branching architecture on polymer properties. *Journal of Polymer Science Part B: Polymer Physics* 49, 1277-1286, doi:10.1002/polb.22320 (2011).

23 Wu, W., Wang, W. & Li, J. Star polymers: Advances in biomedical applications. *Progress in Polymer Science* 46, 55-85, doi:http://dx.doi.org/10.1016/j.progpolymsci.2015.02.002 (2015).

24 Liu, J., Duong, H., Whittaker, M. R., Davis, T. P. & Boyer, C. Synthesis of functional core, star polymers via RAFT polymerization for drug delivery applications. *Macromol Rapid Commun* 33, 760-766, doi:10.1002/marc.201200029 (2012).

25 Kim, D.-G., Kang, H., Choi, Y.-S., Han, S. & Lee, J.-C. Photo-cross-linkable star-shaped polymers with poly(ethylene glycol) and renewable cardanol side groups: synthesis, characterization, and application to antifouling coatings for filtration membranes. *Polymer Chemistry* 4, 5065-5073, doi:10.1039/C3PY00756A (2013).

26 Zheng, Y., Li, S., Weng, Z. & Gao, C. Hyperbranched polymers: advances from synthesis to applications. *Chemical Society Reviews* 44, 4091-4130, doi:10.1039/C4CS00528G (2015).

27 Caminade, A.-M., Yan, D. & Smith, D. K. Dendrimers and hyperbranched polymers. *Chemical Society Reviews* 44, 3870-3873, doi:10.1039/C5CS90049B (2015).

28 Kambouris, P. & Hawker, C. J. A versatile new method for structure determination in hyperbranched macromolecules. *Journal of the Chemical Society, Perkin Transactions 1*, 2717-2721, doi:10.1039/P19930002717 (1993).

29 Miller, T. M., Neenan, T. X., Kwock, E. W. & Stein, S. M. Dendritic analogs of engineering plastics: A general one-step synthesis of dendritic polyaryl ethers. *J. Am. Chem. Soc.* 115, 356-357, doi:10.1021/ja00054a057 (1993).

30 Kim, Y. H. & Webster, O. W. Hyperbranched polyphenylenes. *Macromolecules* 25, 5561-5572, doi:10.1021/ma00047a001 (1992).

31 Kricheldorf*, H. R. & Bolender, O. New Polymer Syntheses 98. Hyperbranched Poly(Ester-amide)s Derived from Naturally Occurring Monomers. *Journal of Macromolecular Science, Part A* 35, 903-918, doi:10.1080/10601329808002020 (1998).

32 Liu, B., Kazlauciunas, A., Guthrie, J. T. & Perrier, S. One-Pot Hyperbranched Polymer Synthesis Mediated by Reversible Addition Fragmentation Chain Transfer (RAFT) Polymerization. *Macromolecules* 38, 2131-2136, doi:10.1021/ma048035x (2005).

33 Boogh, L., Pettersson, B. & Månson, J.-A. E. Dendritic hyperbranched polymers as toughenners for epoxy resins. *Polymer* 40, 2249-2261, doi:http://dx.doi.org/10.1016/S0032-3861(98)00464-9 (1999).

34 Gurunathan, T., Mohanty, S. & Nayak, S. K. Hyperbranched Polymers for Coating Applications: A Review. *Polymer-Plastics Technology and Engineering* 55, 92-117, doi:10.1080/03602559.2015.1021482 (2016).

35 Sampathkumar, S.-G. & Yarema, K. J. in *Nanotechnologies for the Life Sciences* (Wiley-VCH Verlag GmbH & Co. KGaA, 2007).

36 Zhang, H. *et al.* Easy synthesis of dendrimer-like polymers through a divergent iterative "end-grafting" method. *Polymer Chemistry* 4, 830-839, doi:10.1039/C2PY20742G (2013).

37 Saldivar-Guerra, E. & Vivaldo-Lima, E. *Handbook of Polymer Synthesis, Characterization, and Processing*. (Wiley, 2013).

38 Hawker, C. J. & Frechet, J. M. J. Preparation of polymers with controlled molecular architecture. A new convergent approach to dendritic macromolecules. *J. Am. Chem. Soc.* 112, 7638-7647, doi:10.1021/ja00177a027 (1990).

39 Simanek, E. E. *et al.* The 8 year thicket of triazine dendrimers: strategies, targets and applications. *Proceedings of the Royal Society A: Mathematical, Physical and Engineering Science* 466, 1445-1468, doi:10.1098/rspa.2009.0108 (2010).

40 Teegarden, D. M. *Polymer Chemistry: Introduction to an Indispensable Science*. (NSTA Press, National Science Teachers Association, 2004).

41 McGrath, J. E. Chain reaction polymerization. *J. Chem. Educ.* 58, 844, doi:10.1021/ed058p844 (1981).

42 Young, R. J. & Lovell, P. A. *Introduction to Polymers, Second Edition*. (Taylor & Francis, 1991).

43 Stille, J. K. Step-growth polymerization. *J. Chem. Educ.* 58, 862, doi:10.1021/ed058p862 (1981).

44 Carothers W.H & Hill J.W. Linear Superpolyesters. *J Amer Chem Soc* 54, 1559-1566 (1932).

45 McIntyre, J. E. *Synthetic Fibres: Nylon, Polyester, Acrylic, Polyolefin*. (Elsevier Science, 2004).

46 Whinfield J.R. & J.T., D. Improvements relating to manufacture of highly polymeric substances. 578079 (June 1946).

47 Olabisi, O. & Adewale, K. *Handbook of Thermoplastics*. (Taylor & Francis, 1997).

48 Dodiuk, H. & Goodman, S. H. in *Handbook of Thermoset Plastics (Third Edition)* 1-12 (William Andrew Publishing, 2014).

49 Davis, S., Capjack, L., Kerr, N. & Fedosejevs, R. Clothing as protection from ultraviolet radiation: Which fabric is most effective? *Int. J. Dermatol.* 36, 374-379, doi:10.1046/j.1365-4362.1997.00046.x (1997).

50 Prahsarn, C., Barker, R. L. & Gupta, B. S. Moisture vapor transport behavior of polyester knit fabrics. *Textile Research Journal* 75, 346-351, doi:10.1177/0040517505053811 (2005).

51 Ki, H. C. & Park, O. O. Synthesis, characterization and biodegradability of the biodegradable aliphatic-aromatic random copolyesters. *Polymer* 42, 1849-1861, doi:10.1016/s0032-3861(00)00466-3 (2001).

52 Vaidya, U. R. & Nadkarni, V. M. Unsaturated polyester resins from poly(ethylene-terephthalate) waste .1. Synthesis and characterization. *Industrial & Engineering Chemistry Research* 26, 194-198, doi:10.1021/ie00062a003 (1987).

53 Xiong, J. S., Xia, L., Shentu, B. Q. & Weng, Z. X. Synthesis of Fluoroalkyl-Modified Polyester and Its Application in Improving the Hydrophobicity and Oleophobicity of Cured Polyester Coatings. *Journal of Applied Polymer Science* 131, doi:10.1002/app.39812 (2014).

54 Zouari, M., Kharrat, M. & Dammak, M. Wear and friction analysis of polyester coatings with solid lubricant. *Surface & Coatings Technology* 204, 2593-2599, doi:10.1016/j.surfcoat.2010.02.001 (2010).

55 Okada, M. Chemical syntheses of biodegradable polymers. *Progress in Polymer Science* 27, 87-133, doi:10.1016/s0079-6700(01)00039-9 (2002).

56 Park, O., Kim, D. & Dordick, J. Enzyme-catalyzed synthesis of sugar-containing monomers and linear polymers. *Biotechnology and bioengineering* 70, 208-216 (2000).

57 Varma, I. K., Albertsson, A. C., Rajkhowa, R. & Srivastava, R. K. Enzyme catalyzed synthesis of polyesters. *Progress in Polymer Science* 30, 949-981, doi:10.1016/j.progpolymsci.2005.06.010 (2005).

58 Albertsson, A. C. & Varma, I. K. Recent developments in ring opening polymerization of lactones for biomedical applications. *Biomacromolecules* 4, 1466-1486, doi:10.1021/bm034247a (2003).

59 Nguyen, N. T. *et al.* Understanding the acceleration in the ring-opening of lactones delivered by microwave heating. *Tetrahedron* 70, 996-1003, doi:10.1016/j.tet.2013.11.031 (2014).

60 Ruan, J. M., Xiao, A. G., Wu, H. W. & Yang, H. L. Review - recent development of ring-opening polymerization of cyclic esters using aluminum complexes. *Designed Monomers and Polymers* 17, 345-355, doi:10.1080/15685551.2013.840509 (2014).

61 Le Chatelier, H. L. A General Statement of the Laws of Chemical Equilibrium. *Comptes Rendus* 99, 786-789 (1884).

62 Kricheldorf, H. R. *Handbook of Polymer Synthesis*. (Taylor & Francis, 1991).

63 Sokolsky-Papkov, M., Langer, R. & Domb, A. J. Synthesis of aliphatic polyesters by polycondensation using inorganic acid as catalyst. *Polymers for advanced technologies* 22, 502-511 (2011).

64 Bhatia, K. K. Polyesters production process. US5599900A (1997).

65 Bacaloglu, R., Fisch, M. & Biesiada, K. Kinetics of polyesterification of adipic acid with 1,3-butanediol. *Polymer Engineering and Science* 38, 1014-1022, doi:10.1002/pen.10268 (1998).

66 Goodman, E. S. H. *Handbook Of Thermoset Plastics*. (Jaico Publishing House, 2005).

67 Appleby, D. B. *et al.* Polyol polyester synthesis. CA 2089170 C (2007).

68 Kaska, J. & Lešek, F. Processes and equipment for alkyd and unsaturated polyester resin manufacture. *Progress in Organic Coatings* 19, 283-331, doi:http://dx.doi.org/10.1016/0033-0655(91)80016-C (1991).

69 Ishii, M., Okazaki, M., Shibasaki, Y., Ueda, M. & Teranishi, T. Convenient Synthesis of Aliphatic Polyesters by Distannoxane-Catalyzed Polycondensation. *Biomacromolecules* 2, 1267-1270, doi:10.1021/bm015576a (2001).

70 Compton, R. G., Bamford, C. H. & Tipper†, C. F. H. *Non-Radical Polymerisation*. 517 (Elsevier Science, 1976).

71 MarketsandMarkets. Powder Coatings Market by Resin Type (Epoxy, Epoxy-Polyester Hybrid, Polyester, Acrylic, Polyurethane, & Others) and by End-User Industries (Architectural, Appliances, Automotive, General Industrial, Furniture & Others) - Global Forecast to 2019. (2014).

72 Malshe, V. C. *Basics of Paint Technology Part II*. (Antar Prakash Center for Yoga, 2008).

73 Wynstra, J. Hydroxyl terminated polyester oligomers. US3449467 (1969).

74 Schoen Lowhardt, A. A. Preparation of hydroxyl-terminated polyesters. US3894075 (1975).

75 Havard, J. Powder coating of epoxy resin, carboxylic acid-terminated polyester, styrene-maleic. WO2001094463 (2001).

76 Sreeves, J. E. Powdered coating composition of carboxyl terminated polyester, epoxy resin and zinc oxide. US4145370 (1979).

77 Strong, A. B. *Fundamentals of Composites Manufacturing, Second Edition: Materials, Methods and Applications*. (Society of Manufacturing Engineers, 2008).

78 Victorius, C. Thermosetting powder coating composition of an acrylic polymer, dodecanedioic acid, cellulose acetate butyrate and a cross-linking agent. US4027066 (1977).

79 Craven, J. M. Powder coating composition for automotive topcoat. US4402983 (1983).

80 Tracton, A. A. *Coatings Technology Handbook, Third Edition*. (CRC Press, 2005).

81 Harper, C. A. *Handbook of Plastic Processes*. (Wiley, 2006).

82 Jin, F.-L., Li, X. & Park, S.-J. Synthesis and application of epoxy resins: A review. *Journal of Industrial and Engineering Chemistry* 29, 1-11, doi:http://dx.doi.org/10.1016/j.jiec.2015.03.026 (2015).

83 Xu, H. J., Jin, F. L. & Park, S. J. Synthesis of a novel phosphorus-containing flame retardant for epoxy resins. *Bulletin of the Korean Chemical Society* 30, 2643-2646, doi:10.5012/bkcs.2009.30.11.2643 (2009).

84 Plunkett, RJ The History of Polytetrafluoroethylene: Discovery and Development, pages 261-266 in "High Performance Polymers: Their Origin and Development. Proceedings of the Symposium on the History of High Performance Polymers at the American Chemical Society Meeting held in New York, April 15–18, 1986." Seymour RB and Kirshenbaum GS, Editors, Elsevier, New York, 1986. ISBN 0-444-01139-0.

85 Teng, H. Overview of the Development of the Fluoropolymer Industry *Appl. Sci.* 2, 496-512 (2012).

86 Center, P. T. E. & Landrock, A. H. *Fluidized-bed coating with plastics: technology and potential for military applications*. (Defense Technical Information Center, 1964).

87 Kellams, R. W. & Dyer, C. H. Electrostatic fluid bed powder coating system. US3865079 (1975).

88 Tipler, P. A. *College Physics*. 467 (Worth, 1987).

89 Gomez, A., De La Mora, J. F. & Tang, K. Electrospray employing corona-assisted cone-jet mode. US5873523 (1999).

90 Rosato, D. V., Rosato, M. G. & Rosato, D. V. *Concise Encyclopedia of Plastics*. (Springer US, 2000).

91 Koleske, J. V. *Paint and Coating Testing Manual*. Vol. 14th (ASTM International, 1995).

92 Ryntz, R. A. & Yaneff, P. V. *Coatings Of Polymers And Plastics*. (Taylor & Francis, 2003).

93 Liberto, N., Liberto, N. P. & Division, A. f. F. P. o. S. P. C. *User's Guide to Powder Coating, 4th Edition*. (Society of Manufacturing Engineers, 2003).

94 Utech, B. *A Guide to High-performance Powder Coating*. (Society of Manufacturing Engineers, Association for Finishing Processes, 2002).

95 Giguere, R. J., Bray, T. L., Duncan, S. M. & Majetich, G. APPLICATION OF COMMERCIAL MICROWAVE-OVENS TO ORGANIC-SYNTHESIS. *Tetrahedron Lett.* 27, 4945-4948, doi:10.1016/s0040-4039(00)85103-5 (1986).

96 Gedye, R. *et al.* THE USE OF MICROWAVE-OVENS FOR RAPID ORGANIC-SYNTHESIS. *Tetrahedron Lett.* 27, 279-282, doi:10.1016/s0040-4039(00)83996-9 (1986).

97 Caddick, S. MICROWAVE-ASSISTED ORGANIC-REACTIONS. *Tetrahedron* 51, 10403-10432, doi:10.1016/0040-4020(95)00662-r (1995).
98 Dallinger, D. & Kappe, C. O. Microwave-assisted synthesis in water as solvent. *Chem. Rev.* 107, 2563-2591, doi:10.1021/cr0509410 (2007).
99 de la Hoz, A., Diaz-Ortiz, A. & Moreno, A. Microwaves in organic synthesis. Thermal and non-thermal microwave effects. *Chemical Society Reviews* 34, 164-178, doi:10.1039/b411438h (2005).
100 Kappe, C. O. Controlled microwave heating in modern organic synthesis. *Angewandte Chemie-International Edition* 43, 6250-6284, doi:10.1002/anie.200400655 (2004).
101 Kappe, C. O. & Dallinger, D. Controlled microwave heating in modern organic synthesis: highlights from the 2004-2008 literature. *Mol. Divers.* 13, 71-193, doi:10.1007/s11030-009-9138-8 (2009).
102 Lidstrom, P., Tierney, J., Wathey, B. & Westman, J. Microwave assisted organic synthesis - a review. *Tetrahedron* 57, 9225-9283, doi:10.1016/s0040-4020(01)00906-1 (2001).
103 Varma, R. S. Microwave-assisted synthesis of organics and nanomaterials. *Abstracts of Papers of the American Chemical Society* 237 (2009).
104 Sinnwell, S. & Ritter, H. Recent advances in microwave-assisted polymer synthesis. *Australian Journal of Chemistry* 60, 729-743, doi:10.1071/ch07219 (2007).
105 Pozar, D. M. *Microwave Engineering*. (Addison-Wesley, 1993).
106 "ARTICLE 1 - Terms and Definitions". life.itu.ch. International Telecommunication Union. 19 October 2009. 1.15. industrial, scientific and medical (ISM) applications (of radio frequency energy): Operation of equipment or appliances designed to generate and use locally radio frequency energy for industrial, scientific, medical, domestic or similar purposes, excluding applications in the field of telecommunications.
107 Cottrell, T. L. *The Strengths of Chemical Bonds*. 2 edn, (Butterworth, 1958).
108 Bilecka, I. & Niederberger, M. Microwave chemistry for inorganic nanomaterials synthesis. *Nanoscale* 2, 1358-1374, doi:10.1039/b9nr00377k (2010).
109 Kappe, C. O., Dallinger, D. & Murphree, S. S. *"Practical Microwave Synthesis for Organic Chemists"*. (Wiley-VCH, 2009).
110 Gabriel, C. *et al.* Dielectric parameters relevant to microwave dielectric heating. *Chemical Society Reviews* 27, 213-224, doi:10.1039/A827213Z (1998).
111 Smith, A. D. *et al.* Dielectric Properties of Free-Radical Polymerizations: Molecularly Symmetrical Initiators during Thermal Decomposition. *Industrial & Engineering Chemistry Research* 49, 1703-1710, doi:10.1021/ie901201h (2010).
112 Mingos, D. M. P. & Baghurst, D. R. Applications of microwave dielectric heating effects to synthetic problems in chemistry. *Chemical Society Reviews* 20, 1-47, doi:10.1039/cs9912000001 (1991).
113 Nelson, S. O. & Trabelsi, S. Factors Influencing the Dielectric Properties of Agricultural and Food Products. *J. Microw. Power Electromagn. Energy* 46, 93-107 (2012).
114 Debye, P. Polar Molecules. *New York: The Chemical Catalog Co*, doi:10.1002/jctb.5000484320 (1929).
115 Tierney, J. & Lidström, P. *Microwave Assisted Organic Synthesis*. (Wiley, 2009).
116 Magee, M. D. Dielectric relaxation time, a non-linear function of solvent viscosity. *Journal of the Chemical Society, Faraday Transactions 2: Molecular and Chemical Physics* 70, 929-938, doi:10.1039/F29747000929 (1974).

117 Nuchter, M., Ondruschka, B., Bonrath, W. & Gum, A. Microwave assisted synthesis - a critical technology overview. *Green Chemistry* 6, 128-141, doi:10.1039/b310502d (2004).

118 Langa, F., DelaCruz, P., DelaHoz, A., DiazOrtiz, A. & DiezBarra, E. Microwave irradiation: more than just a method for accelerating reactions. *Contemporary Organic Synthesis* 4, 373-386, doi:10.1039/co9970400373 (1997).

119 Loupy, A., Perreux, L., Liagre, M., Burle, K. & Moneuse, M. Reactivity and selectivity under microwaves in organic chemistry. Relation with medium effects and reaction mechanisms. *Pure Appl. Chem.* 73, 161-166, doi:10.1351/pac200173010161 (2001).

120 Perreux, L. & Loupy, A. A tentative rationalization of microwave effects in organic synthesis according to the reaction medium, and mechanistic considerations. *Tetrahedron* 57, 9199-9223, doi:10.1016/s0040-4020(01)00905-x (2001).

121 Chia, H. L., Jacob, J. & Boey, F. Y. C. The microwave radiation effect on the polymerization of styrene. *Journal of Polymer Science Part a-Polymer Chemistry* 34, 2087-2094, doi:10.1002/(sici)1099-0518(199608)34:11<2087::aid-pola1>3.0.co;2-x (1996).

122 Kappe, C. O. & Dallinger, D. The impact of microwave synthesis on drug discovery. *Nat Rev Drug Discov* 5, 51-63 (2006).

123 Moseley, J. D. & Kappe, C. O. A critical assessment of the greenness and energy efficiency of microwave-assisted organic synthesis. *Green Chemistry* 13, 794-806, doi:10.1039/C0GC00823K (2011).

124 Mallakpour, S. & Rafiee, Z. Application of Microwave-assisted Reactions in Step-Growth Polymerization (A Review). *Iranian Polym. J.* 17, 907-935 (2008).

125 Chemat, F. & Esveld, E. Microwave super-heated boiling of organic liquids: Origin, effect and application. *Chemical Engineering & Technology* 24, 735-744, doi:10.1002/1521-4125(200107)24:7<735::aid-ceat735>3.0.co;2-h (2001).

126 Stuerga, D. A. C. & Gaillard, P. Microwave Athermal Effects in Chemistry: A Myth's Autopsy: Part I: Historical background and fundamentals of wave-matter interaction. *J. Microw. Power Electromagn. Energy* 31, 87-100, doi:10.1080/08327823.1996.11688299 (1996).

127 Stuerga, D. A. C. & Gaillard, P. Microwave Athermal Effects in Chemistry: A Myth's Autopsy: Part II: Orienting effects and thermodynamic consequences of electric field. *J. Microw. Power Electromagn. Energy* 31, 101-113, doi:10.1080/08327823.1996.11688300 (1996).

128 Kappe, C. O., Pieber, B. & Dallinger, D. Microwave Effects in Organic Synthesis: Myth or Reality? *Angewandte Chemie-International Edition* 52, 1088-1094, doi:10.1002/anie.201204103 (2013).

129 Bu, J. U. & Jung, K. G. Microwave oven with multi-infrared sensors disposed at different distance intervals from the rotating table plane. US5693247 (1997).

130 Nakata, T., Horinouchi, A. & Taino, K. Temperature control for microwave oven. US4553011 (1985).

131 Durka, T., Stefanidi, G. D., Van Gerven, T. & Stankiewicz, A. On the accuracy and reproducibility of fiber optic (FO) and infrared (IR) temperature measurements of solid materials in microwave applications. *Measurement science and technology* 21 (2010).

132 Herrero, M. A., Kremsner, J. M. & Kappe, C. O. Nonthermal Microwave Effects Revisited: On the Importance of Internal Temperature Monitoring and Agitation in Microwave Chemistry. *The Journal of Organic Chemistry* 73, 36-47, doi:10.1021/jo7022697 (2008).

133 Hoogenboom, R. & Schubert, U. S. Microwave-Assisted Polymer Synthesis: Recent Developments in a Rapidly Expanding Field of Research. *Macromolecular Rapid Communications* 28, 368-386, doi:10.1002/marc.200600749 (2007).

134 Ebner, C., Bodner, T., Stelzer, F. & Wiesbrock, F. One decade of microwave-assisted polymerizations: quo vadis? *Macromol Rapid Commun* 32, 254-288, doi:10.1002/marc.201000539 (2011).

135 Kempe, K., Becer, C. R. & Schubert, U. S. Microwave-Assisted Polymerizations: Recent Status and Future Perspectives. *Macromolecules* 44, 5825-5842, doi:10.1021/ma2004794 (2011).

136 Wiesbrock, F., Hoogenboom, R. & Schubert, U. S. Microwave-Assisted Polymer Synthesis: State-of-the-Art and Future Perspectives. *Macromolecular Rapid Communications* 25, 1739-1764, doi:10.1002/marc.200400313 (2004).

137 Komorowska-Durka, M., Dimitrakis, G., Bogdał, D., Stankiewicz, A. I. & Stefanidis, G. D. A concise review on microwave-assisted polycondensation reactions and curing of polycondensation polymers with focus on the effect of process conditions. *Chemical Engineering Journal* 264, 633-644, doi:http://dx.doi.org/10.1016/j.cej.2014.11.087 (2015).

138 Pourjavadi, A., Zamanlu, M. R. & Zohuriaan-Mehr, M. J. Microwave-induced synthesis of partially aromatic polyamides via the Yamazaki phosphorylation reaction. *Angewandte Makromolekulare Chemie* 269, 54-60 (1999).

139 Imai, Y. in *Step-Growth Polymers for High-Performance Materials* Vol. 624 *ACS Symposium Series* Ch. 27, 421-430 (American Chemical Society, 1996).

140 Tang, X. *et al.* Polycondensation of sodium tetrazodiphenyl naphthionate and pyromellitic dianhydride under microwave irradiation and the performance of the third-order nonlinear optics. *Journal of Applied Polymer Science* 88, 1121-1128, doi:10.1002/app.12126 (2003).

141 Lin, L. *et al.* Rapid microwave-assisted green production of a crystalline polyimide for enhanced visible-light-induced photocatalytic hydrogen production. *Journal of Materials Chemistry A* 3, 10205-10208, doi:10.1039/C5TA01078K (2015).

142 Hurduc, N., Abdelylah, D., Buisine, J.-M., Decock, P. & Surpateanu, G. Microwave effects in the synthesis of polyethers by phase transfer catalysis. *European Polymer Journal* 33, 187-190, doi:http://dx.doi.org/10.1016/S0014-3057(96)00069-9 (1997).

143 Valério, A., Fortuny, M., Santos, A. F., Araújo, P. H. H. & Sayer, C. Poly(Urea–Urethane) Synthesis by Miniemulsion Polymerization Using Microwaves and Conventional Polymerization. *Macromolecular Reaction Engineering* 9, 48-59, doi:10.1002/mren.201400029 (2015).

144 Mallakpour, S. & Dinari, M. A Green Route for Synthesis of Different Polyureas Based on Phenylurazole: Rapid Solid-state, Microwave-assisted Technique. *High Performance Polymers* 22, 314-327, doi:10.1177/0954008308101788 (2010).

145 Komorowska, M., Stefanidis, G. D., Van Gerven, T. & Stankiewicz, A. I. Influence of microwave irradiation on a polyesterification reaction. *Chemical Engineering Journal* 155, 859-866, doi:http://dx.doi.org/10.1016/j.cej.2009.09.036 (2009).

146 Yamada, S., Takasu, A., Takayama, S. & Kawamura, K. Microwave-assisted solution polycondensation of l-lactic acid using a Dean-Stark apparatus for a non-thermal microwave polymerization effect induced by the electric field. *Polymer Chemistry* 5, 5283-5288, doi:10.1039/C4PY00639A (2014).

147 Leenslag, J. W. & Pennings, A. J. Synthesis of high-molecular-weight poly(L-lactide) initiated with tin 2-ethylhexanoate. *Die Makromolekulare Chemie* 188, 1809-1814, doi:10.1002/macp.1987.021880804 (1987).
148 Singla, P., Mehta, R., Berek, D. & Upadhyay, S. N. Ring Opening Polymerization of Lactide in a Monomode Microwave using Stannous Octoate and Dibutyltin Dimethoxide Catalysts. *Journal of Macromolecular Science, Part A* 51, 350-361, doi:10.1080/10601325.2014.882701 (2014).
149 Jakubowycz, S. Esterification process using a catalyst consisting of sand, stannous tin and aluminate. US5571938 (1996).
150 Ridland, J., Lindall, C. M. & Slack, N. Esterification catalysts. WO2000071252 (2000).
151 Jones, L. O., Lo, P. Y. & Woods, D. G. Optimized catalyst addition to enhance esterification catalyst performance. EP1301459 (2003).
152 Kricheldorf, H. R., Yashiro, T. & Weidner, S. Isomerization-Free Polycondensations of Maleic Anhydride with α,ω-Alkanediols. *Macromolecules* 42, 6433-6439, doi:10.1021/ma9009356 (2009).
153 Takasu, A., Oishi, Y., Iio, Y., Inai, Y. & Hirabayashi, T. Synthesis of aliphatic polyesters by direct polyesterification of dicarboxylic acids with diols under mild conditions catalyzed by reusable rare-earth triflate. *Macromolecules* 36, 1772-1774, doi:10.1021/ma021462v (2003).
154 Buzin, P., Lahcini, M., Schwarz, G. & Kricheldorf, H. R. Aliphatic Polyesters by Bismuth Triflate-Catalyzed Polycondensations of Dicarboxylic Acids and Aliphatic Diols. *Macromolecules* 41, 8491-8495, doi:10.1021/ma8017662 (2008).
155 Garaleh, M., Lahcini, M., Kricheldorf, H. R. & Weidner, S. M. Syntheses of aliphatic polyesters catalyzed by lanthanide triflates. *Journal of Polymer Science Part A: Polymer Chemistry* 47, 170-177, doi:10.1002/pola.23136 (2009).
156 Göbölös, S., Tálas, E., Hegedüs, M., Bertóti, I. & Margitfalvi, J. L. Condensation of allyl alcohol with ammonia over phosphoric acid catalyst supported on controlled pore glass. *Applied Catalysis A: General* 152, 63-68, doi:http://dx.doi.org/10.1016/S0926-860X(96)00340-7 (1997).
157 Nakato, T., Kusuno, A. & Kakuchi, T. Synthesis of poly(succinimide) by bulk polycondensation of L-aspartic acid with an acid catalyst. *Journal of Polymer Science Part A Polymer Chemistry* 38, 117-122 (2000).
158 Adlington, K. *et al.* Mechanistic Investigation into the Accelerated Synthesis of Methacrylate Oligomers via the Application of Catalytic Chain Transfer Polymerization and Selective Microwave Heating. *Macromolecules* 46, 3922-3930, doi:10.1021/ma400022y (2013).
159 Dallinger, D., Lehmann, H., Moseley, J. D., Stadler, A. & Kappe, C. O. Scale-Up of Microwave-Assisted Reactions in a Multimode Bench-Top Reactor. *Organic Process Research & Development* 15, 841-854, doi:10.1021/op200090k (2011).
160 Schmink, J. R., Kormos, C. M., Devine, W. G. & Leadbeater, N. E. Exploring the Scope for Scale-Up of Organic Chemistry Using a Large Batch Microwave Reactor. *Organic Process Research & Development* 14, 205-214, doi:10.1021/op900287j (2010).
161 Amore, K. M. & Leadbeater, N. E. Microwave-Promoted Esterification Reactions: Optimization and Scale-Up. *Macromolecular Rapid Communications* 28, 473-477, doi:10.1002/marc.200600751 (2007).
162 Nakamura, T. *et al.* Large-Scale Polycondensation of Lactic Acid Using Microwave Batch Reactors. *Organic Process Research & Development* 14, 781-786, doi:10.1021/op900325e (2010).

2 Experimental and Equipment

2.1 Overview

This chapter describes the equipment, techniques and methods used to synthesise, characterise and test the polyesters discussed throughout this thesis. The specific equipment used for both conventional heating (CH) and microwave heating (MWH) is outlined in detail. Some techniques and equipment described are different to standard procedures as they are implemented specifically for an industrial process with bespoke equipment and are therefore outlined in detail.

2.2 Processing Methods and Equipment Overview

2.2.1 Conventional Heating Equipment and Set-up

2.2.1.1 Adipic Acid, 1,6-Hexanediol Polyesterification at 185 and 150 °C

All CH adipic acid, 1,6-hexanediol experiments were conducted using a standard distillation set-up and 50 mL Drysyn® heating mantle (Asynt, UK), shown below in Figure 2-1. A K-type thermocouple was inserted through the stillhead into the reaction bulk to measure the internal temperature. Internal bulk temperature measurement was necessary as MWH reactions used an internally inserted fibre optic for temperature feedback and control. Therefore, an internal

reference is needed for CH to confirm processing temperatures were identical to MWH.

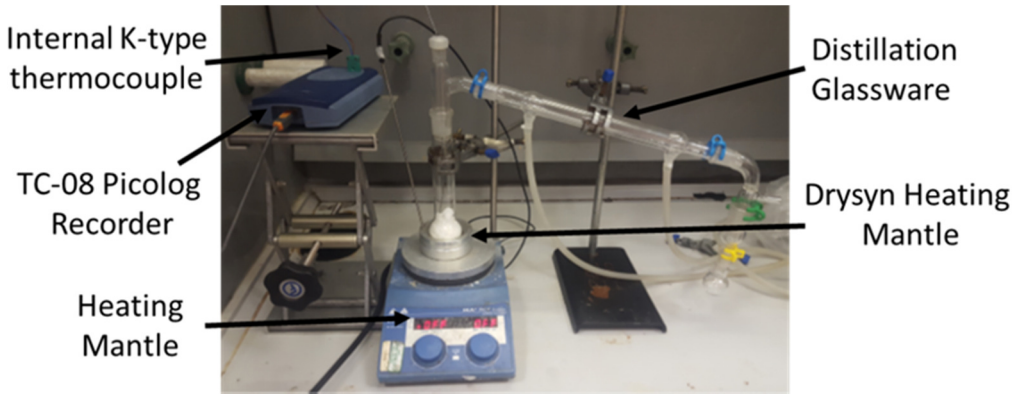


Figure 2-1. Picture of a standard adipic acid, hexanediol reaction set-up using the Drysyn® heating mantle and a long necked round bottomed flask.

The internal temperature monitoring hardware was a thermocouple data logger TC-08 (Picolog, UK) and was logged using Picolog™ software on a computer.

A long necked round bottom flask was used to remain consistent with microwave reactions, see section 2.2.2.

2.2.1.2 Polyester Synthesis Using Highly Stable Resin Monomers (Neopentyl glycol, Terephthalic acid, Trimethylolpropane system) Used in Industry

For all CH reactions involving industrially used monomers an electrothermal heating mantle (Bibby scientific, UK) was used. As such, apart from the heating mantle differences, the set-up was identical to the one described in Figure 2.1.

2.2.2 Small scale microwave heating equipment and set-up

2.2.2.1 Sairem Miniflow 200SS

The Sairem Miniflow 200SS (Sairem, France) is a lab specific, single mode microwave cavity with a maximum power input of 200 W and is shown below in Figure 2-2. Unlike conventional and domestic microwaves, the microwaves are generated using a solid state generator. The advantages to using a solid state microwave generator include:

1. Compact size and lightweight.
2. Can operate at low power levels (as low at 1 W) and adjust power by 1 W increments.
3. Longer operation lifetimes.
4. Adjustable microwave frequency.

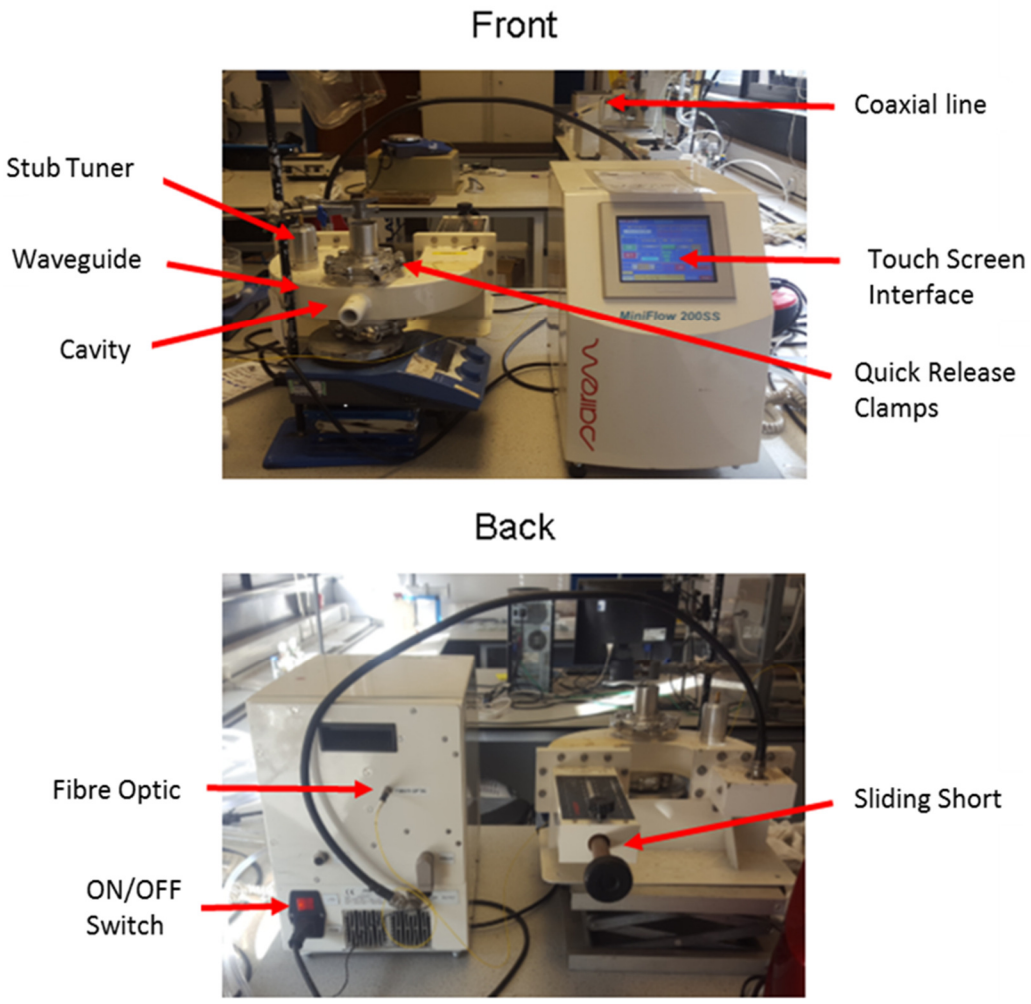


Figure 2-2. Picture of the Sairem Miniflow ss200 system with annotations.

The Miniflow 200SS displayed continuous monitoring of both the forward and reflective power. This allowed matching of the waveform with the reaction mixture to maximise the amount of absorbed power. This matching process was completed by moving the sliding short and stub tuner, shown in Figure 2-2, until the lowest reflective power was displayed on the touchscreen interface.

Figure 2-2 shows the T1 Fibre Optic Temperature probe (Neoptix, Canada), which is used instead of a normal K-type thermocouple due to the safety risks associated with a metal thermocouple *e.g.* arcing.

For all MWH experiments presented in this thesis the Miniflow 200SS was used at a frequency of 2.45 GHz.

2.2.2.2 2 kW Batch Reactor with Pulsed Microwaves

A 2 kW batch reactor was assembled with the capability of using a pulsed microwave setting (discussed in Chapter 5), a schematic of this is shown in Figure 2-3.

The magnetron and magnetron control box were a 2 kW microwave generator (Sairem, France), connected in series to an E-stop for emergency shutdown. The waveguide used was WR340 with a High Power Automatic Impedance/Power Analyzer and Matching System (S-team, Slovak Republic) for automatic tuning of the waveform. The cavity was developed and milled at the University of Nottingham (UoN), UK. Connected to the cavity was a sliding short for coupling the microwaves (UoN, UK). The fibre optic used was a T1 Fibre Optic Temperature Probe (Neoptix, Canada) attached to a reflex signal conditioner (Neoptix, Canada). The magnetic stirring mantle used was an IKA Basic (IKA, Germany).

The microwave forward and reflected power were logged on a computer/workstation using HOMSOFT software (S-team, Slovak Republic) and the temperature was logged using Neoptix software.

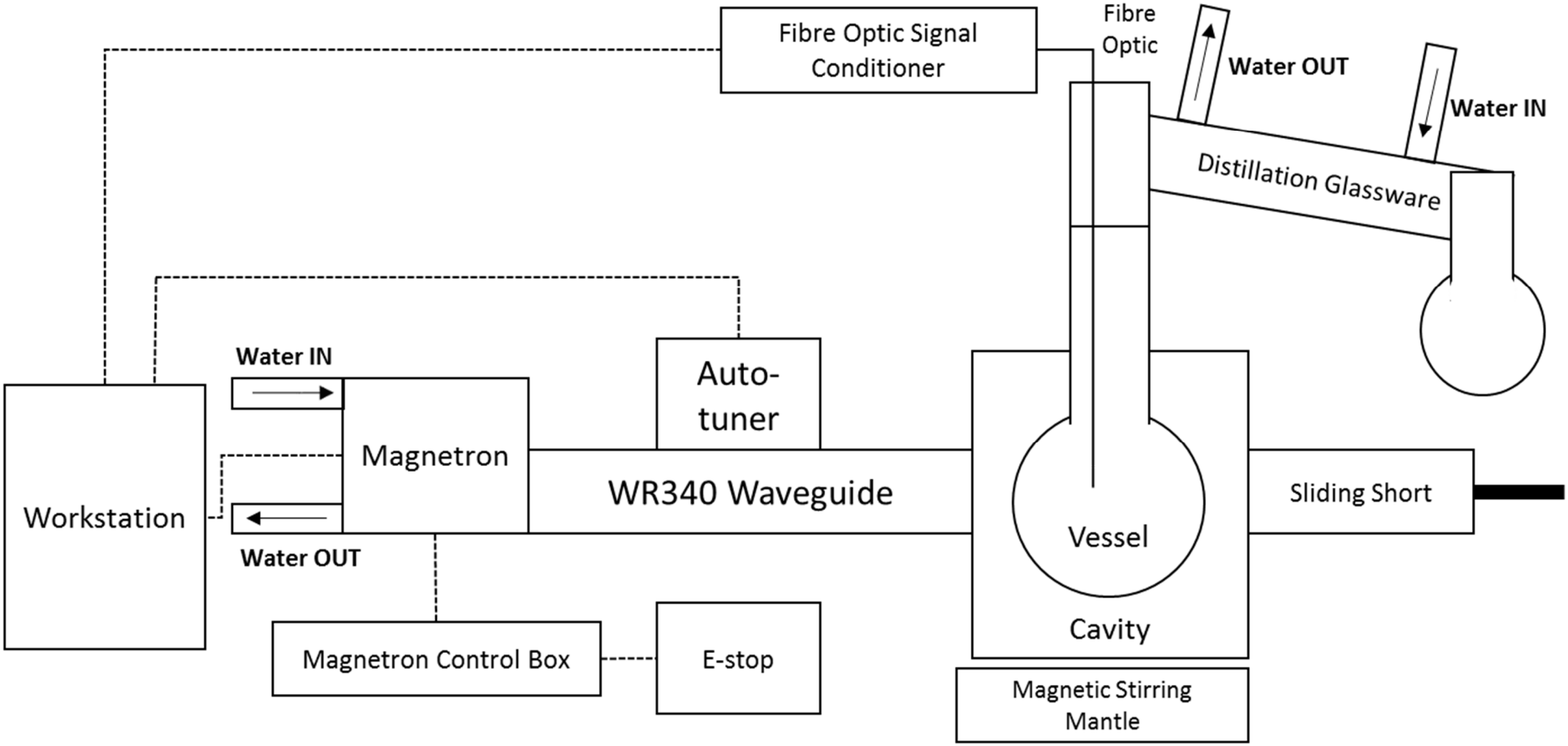


Figure 2-3. 2 kW pulse rig schematic.

2.2.3 5 L 2 kW Hybrid Batch Reactor

For the scaled-up reactions, a hybrid rig was developed at the UoN with input from the sponsoring company and Asynt. The vessel was developed to allow both CH and MWH to be implemented in the same reactor at a 5 L scale, this allowed direct comparisons to be made between both heating techniques. The vessel was designed to mimic the equipment that is currently employed at the sponsoring company's research site where 5 L CH reactions are conducted on a regular basis.

To confirm this was a viable design proposition, electromagnetic (EM) simulations, an example of which is shown in Figure 2-4, were conducted by Dr. Angeliki Sklavounou and an optimised reactor geometry was deduced. This geometry allowed all the necessary ports/holes (stirrer, charging, and distillation) to be included in the design as well as accommodating the microwave waveguide.

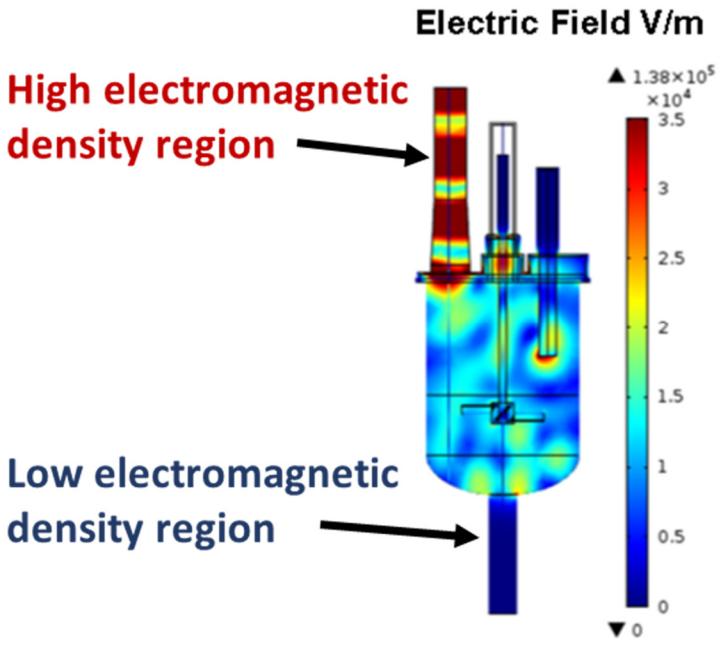


Figure 2-4. Example of an EM simulation of the 5 L hybrid rig. The scale shows the intensity of the magnetic field in V/m with the red areas signalling high intensities and the blue low.

A technical diagram for the rig is shown below in Figure 2-5 , with a table of the system components (required for the HAZOP and to use as a key for schematic annotations) with their tags in Table 2-1.

Table 2-1. Table of 5 L hybrid reactor system components and ID tags.

Node No.1	Node ID	Node Description	Elements
1	OL	Aluminium Over lid	n/a
2	CP	Charge Port	n/a
3	I&M	Impeller and Motor	Impeller & IKA Overhead Stirring Motor
4	SV	Swagelok valves	V1, V2, V3
5	P	Process Pipes (inc. drop out & side arm in & out)	P1, P2, P3
6	HS	Heating System: Julabo Oil Heater, Oil Pipe, Heating Blocks	J, OP1-5, HB1-3
7	TM	Temperature Monitoring : Fibre Optic, Signal Conditioner, 0 – 10V Analogue Output 1	FO, SG, AO1
8	D	Distillation System: Condenser, Dean Stark, Vacuubrand Vacuum Pump,	C, DS, VcP
9	G	Generator, Water Cooling	n/a
10	GC	Generator Control Sairem Box	n/a
11	CB	Circuit Breaker	AO2
12	SS	EMF detector, E-Stop	EMF, ES

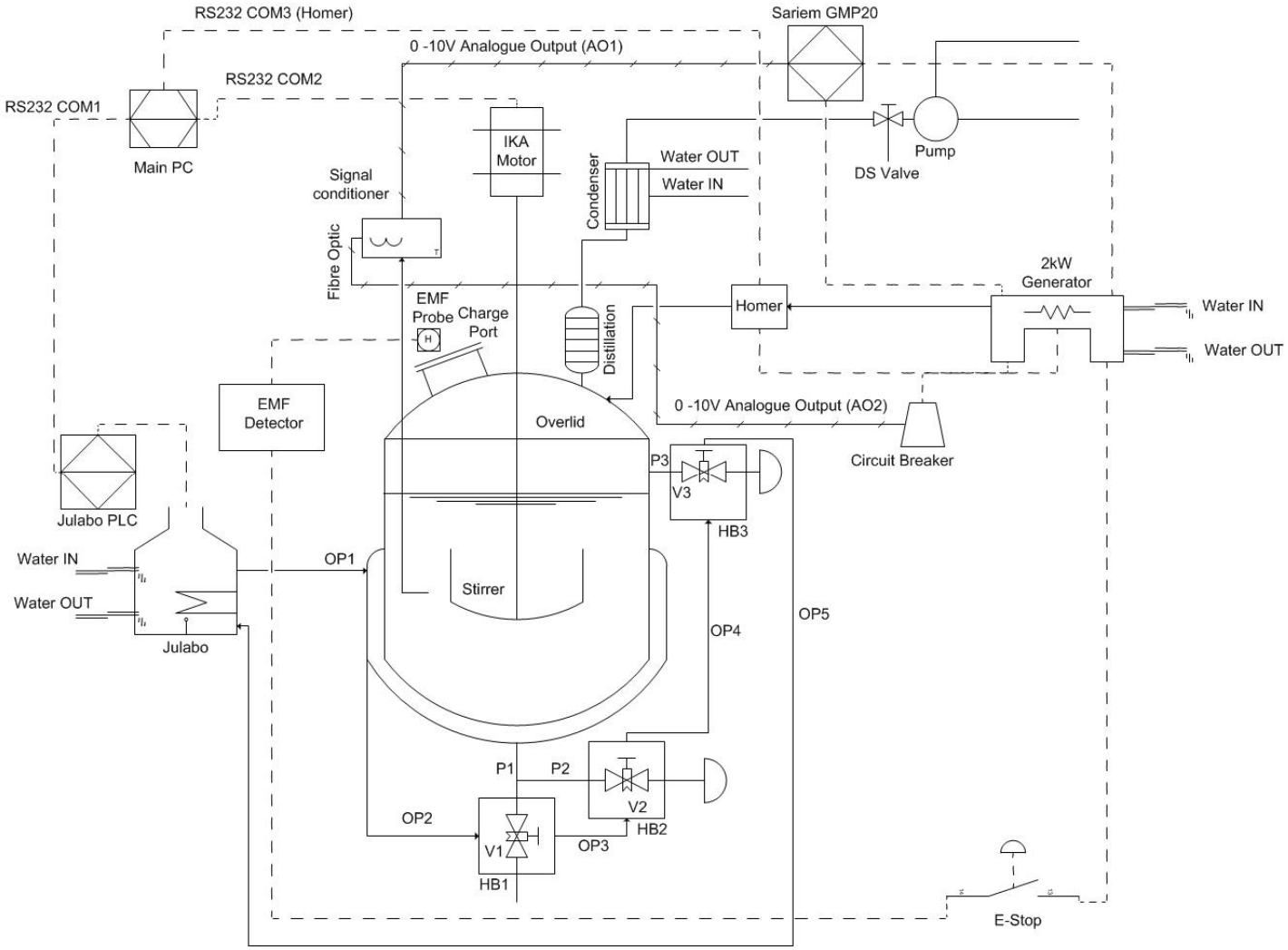


Figure 2-5. Technical drawing of 5 L hybrid rig.

The final design included the vessel which was made from 316 stainless steel (Asynt, UK) with a milled PTFE lid (UoN, UK) and a 316 stainless steel over lid (UoN, UK). The over lid was designed to clamp to the vessel using nuts and bolts to minimise microwave leakage. It was also designed to include an option to add a sidearm (Shown as valves V2 and V3, heating blocks HB2 and HB3 and the pipe OP4 in Figure 2-5) to pump reaction mixtures using a high powered pump, but this feature is not discussed in this thesis.

The supporting apparatus included a Julabo HT60-M3 heater (Julabo, Germany) with Thermal H350 heating fluid (Julabo, Germany) and triple insulated metal tubing (Julabo, Germany) to transport the heating fluid to and from the stainless steel vessel. This heater included a control box to set the temperature and ramps which was also connected to a computer to allow remote control. This computer was connected to a IKA Eurostar 100 mechanical overhead stirrer (IKA, Germany) with a 4 paddled impeller made from sintered silicon nitride ceramic (Syalons, Newcastle). Also attached to the computer was a High Power Automatic Impedance/Power Analyzer and Matching System (S-team, Slovak Republic). This is an auto-tuner and is used to control the matching of the EM wave with the sample. The microwaves were controlled by a custom made GMP20 microwave controller (Sairem, France) which controlled the microwave output from a 2 kW microwave generator (Sairem, France). Attached to the microwave control box was a Reflex Signal Conditioner (Neoptix, Canada) with a T1 Fibre Optic Temperature Probe (Neoptix, Canada) to read the internal bulk temperature of the reaction. The signal conditioner was attached to a circuit breaker with a 0 to 10 V Analogue output (UoN, UK). The voltage of the signal applied to the circuit breaker was calibrated with respect to temperature, shown in Figure 2-6. As the circuit breaker was attached to the microwave generator it allowed lower and upper voltage limits to be set to shut

off the power to the generator if overheating of the reaction mixture was detected. Above the charging port was an EM field (EMF) detector (UoN, UK) to detect any dangerous microwave leakages which was attached to an E-Stop (UoN, UK) in series. Attached to the inner PTFE lid was a 300 mm Vigurex distillation column with a water condenser attached in a Dean-Stark fashion, shown in Figure 2-7, to allow the condensate to be collected whilst enabling cleaning *via* boiling glycol and water. Attached at the bottom of the distillation apparatus was a DS valve to allow the condensate to escape, whilst allowing a sealed system to be created for vacuum application. Attached to the top of the condensing column was a Vacuubrand MD1C Vario plus pump (Asynt, UK).

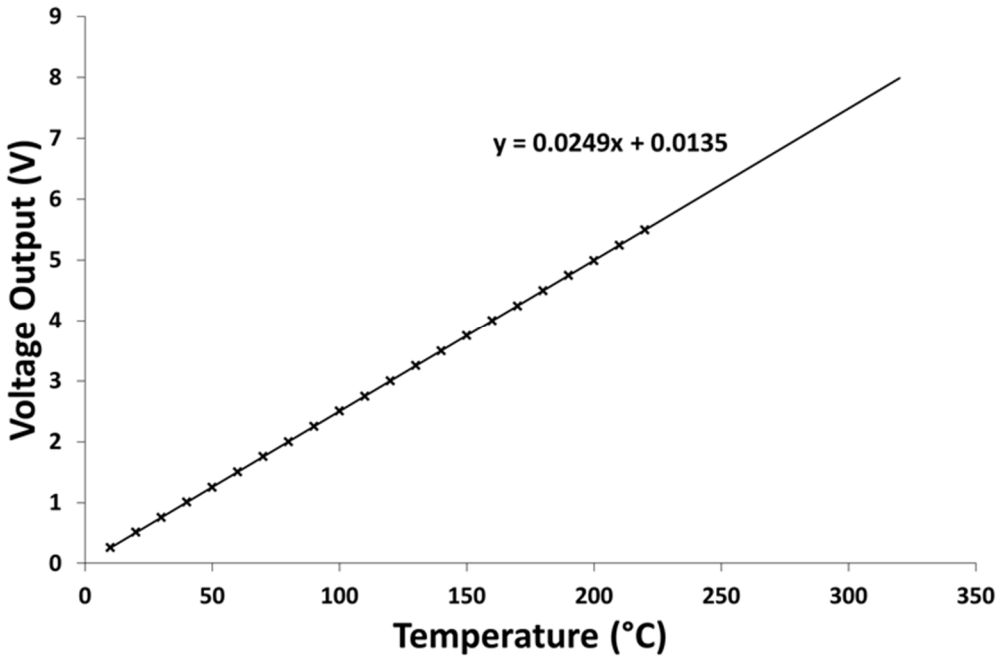


Figure 2-6. Calibration plot for the voltage output of circuit breaker.

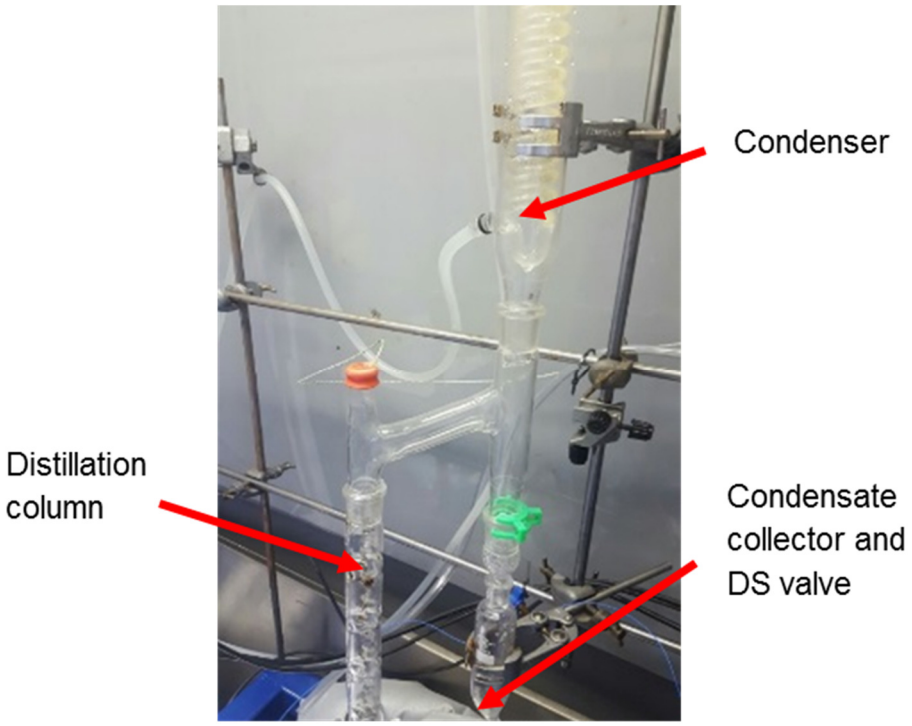


Figure 2-7. Picture of Dean-Stark like set-up.

2.3 Reaction Methods

2.3.1 Materials

1,6-Hexanediol (99 %), adipic acid (Reagentplus ≥99 %), tin(II) 2-ethylhexanoate (92.5 – 100 %), zinc(II) trifluoromethanesulfonate (98 %), bismuth(III) trifluoromethanesulfonate (purity not specified), bis(cyclopentadienyl)zirconium dichloride (≥98 %), crystalline phosphoric acid (≥99.999 %) and pyrophosphoric acid (≥90 %) were all purchased from Sigma Aldrich. Dihydroxybutyl tinchloride (96 %) was supplied by BNT chemicals GmBH. Purified isophthalic acid was purchased from Eastman chemicals (99.8 %). Neopentyl glycol flakes (≥99.0 %) and trimethylolpropane flakes (>98 %)

were purchased from Perstorp. All chemicals were used as received without purification.

2.3.2 Reaction Methods

2.3.2.1 Microwave Leakage Testing

Prior to any MWH experiment the equipment was tested for any microwave leaks using an ETS-Lingren HI-1600 Microwave Oven Survey Meter (ETS-Lingren, UK), shown in Figure 2-8 . Before use the meter was tested for battery and probe response followed by the needle being set to the zero position. Following this, the meter was set to 10 MW – 2450 MHz and a low microwave power (~10 W) was input from the microwave source. The microwave detector (A, Figure 2-8) was then passed around the microwave cavity and surrounding waveguide. If the dial exceeded a value of 1/5 MW/cm^2 the microwaves were deemed as unsafe and switched off. It was then necessary to tighten the bolts and retest the equipment. Once the acceptability level was achieved the experiment could begin.

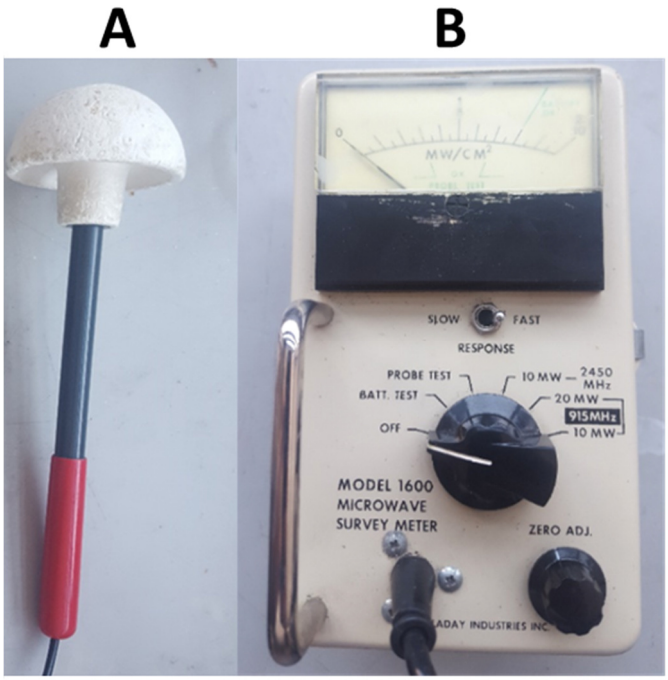


Figure 2-8. ETS-Lingren HI-1600 Microwave Oven Survey Meter consisting of microwave detector, A, and the readout, B.

2.3.2.2 Kinetic Sampling of Microwave Heated Reactions

During all the reactions conducted throughout this thesis regular samples were extracted during the polymerisations to allow kinetic analysis to be conducted. The general procedure for doing this safely is described below:

Samples were taken via a long needle or a spatula, depending on product viscosity. To ensure safe sampling when using microwave heating the microwaves were terminated before sampling commenced, with reapplication of microwaves after sampling. For 5 L reactions stirring was terminated before sampling and re-applied after. Once the sample was withdrawn from the bulk, it was immediately quenched and stored in a -20 °C freezer to inhibit any further polymerisation.

2.3.2.3 Adipic Acid, 1,6-Hexanediol Polycondensation at 50 mL Using Conventional and Microwave Heating at 185 and 150 °C (Chapter 3)

1,6-Hexanediol (15 g, 126 mmol), adipic acid (18.55 g, 126 mmol) and 1 % mol equivalent catalyst (1.26 mmol) (catalysts include; tin(II) 2-ethylhexanoate, dihydroxybutyl tinchloride, zinc(II) trifluoromethanesulfonate, bismuth(III) trifluoromethanesulfonate, bis(cyclopentadienyl)zirconium dichloride, phosphoric acid and pyrophosphoric acid) were placed into a 50 mL long neck flask. The flask was placed into a Drysyn® heating mantle for CH or a Sairem SS200 microwave cavity for MWH and distillation equipment was attached. A K-type thermocouple for CH or fibre optic for MWH was inserted into the sample to monitor the internal bulk temperature. Heating was commenced to an internal temperature set-point of 150 or 185 °C (dependant on experiment), and stirring started at 300 rpm. The start of the reaction (time = 0 secs) was defined to be when the heating commenced. For microwave reactions, the microwave power introduced was at a maximum power of 200 W (P_{max} = 200 W). Kinetic samples (~0.2 mL) of the reaction mixture were taken at 15 minute intervals following the procedure described in 2.3.2.2. After the cycle time elapsed, the product was discharged into a vial, quenched and placed into the -20 °C freezer. Once cooled the product observed was a waxy solid with colours ranging from colourless to brown, depending on catalyst used.

The ^{1}H NMR (300 MHz or 400 MHz, $CDCl_3$ or MeOD, 25 °C) for an AA and HD derived polyester are as follows: AA. δH 1.60 (4H, C**H**$_2$), δH 2.32 (4H, C**H**$_2$), HD δH 1.42 (4H, C**H**$_2$), δH 1.56 (4H, C**H**$_2$), (monomer/end group) δH 3.56 (2H, -O-C**H**$_2$), (backbone) δH 4.09 (2H, HO-C**H**$_2$).

2.3.2.4 Isophthalic Acid, Neopentyl Glycol Polycondensation Using Conventional and Microwave Heating at 200 and 225 °C (Chapter 4)

Typically, neopentyl glycol (15 g, 144 mmol), isophthalic acid (23.9 g, 144 mmol) and catalyst (1.44 mmol) were added to the long necked reaction vessel with a magnetic stirrer and an internal K-type thermocouple for CH or a fibre optic for MWH for internal temperature monitoring. Heating was commenced to distil at reaction temperature (200 or 225 °C) for 3 to 6 hours. The start of the reaction (time = 0 secs) was defined to be when the heating commenced. For microwave reactions the maximum input power was set to 150 W (P_{max} = 150 W). In some cases vacuum was added after a pre-determined period of time (discussed in chapter 4). Kinetic samples (~0.2 mL) were extracted throughout the reaction at either 15 or 30 minute intervals using the procedure described in 2.3.2.2. After the cycle time had elapsed, the product was discharged, quenched and placed into a -20 °C freezer. Once cooled the product formed a glassy solid with colours ranging from colourless to milky white, depending on the catalyst used and conversion level.

Note: For some reactions, the molar ratio of neopentyl glycol:isophthalic acid was changed to 1.1:1 or 1.2:1 (chapter 4 section 4.2.1.2.2). This was done by reducing the mass of isophthalic acid, not increasing neopentyl glycol.

Note 2: For the pre-heating experiments (chapter 4 section 4.2.1.2), NPG and water (1 mL) were initially added and heated to 85 – 90 °C to dissolve the diol, then addition of the catalyst and isophthalic acid followed.

The ^{1}H NMR (300 MHz or 400 MHz, $CDCl_3$ or DMSO-d_6, 25 °C) for an NPG and IPA derived polyester are as follows: IPA δH 7.65 (1H, CH), δH 8.13 (2H, C**H**), δH 8.60 (1H, C**H**), NPG δH 0.90 (6H, C$\mathbf{H_3}$), (monomer/end group) δH 3.40 (4H, HO-C$\mathbf{H_2}$), (backbone) δH 4.25 (3H, -O-C$\mathbf{H_2}$).

2.3.2.5 Industrial resin Polycondensation Using Conventional and Microwave Heating at 225 °C (Chapter 4)

Neopentyl glycol (18.1 g, 174 mmol), trimethylopropane (3.75 g, 28 mmol) and water (1 mL) were added to the long necked reaction vessel with a mechanical stirrer and K-type thermocouple for CH or fibre optic for MWH for internal temperature monitoring. The reaction was placed into an electrothermal heating mantle for CH or Sairem 200SS microwave cavity for MWH and heated to 90 °C for the diol to fully dissolve with a slow ramp of stirring from 30 to 100 rpm as dissolving occurred. Once dissolved, isophthalic acid (26.67 g, 161 mmol) and dihydroxybutyl tinchloride (0.42 g, 0.171 mmol) were added and the reaction was left to distil at 225 °C for 4 to 6 hours. For microwave reactions a maximum input power of 150 W (P_{max} = 150 W) was implemented. In some cases vacuum was added after 3 hours of reaction time (discussed in chapter 4). The start of the reaction (time = 0 secs) was defined as when the heating commenced. Kinetic samples (~0.2 mL) were extracted throughout the reaction at either 15 or 30 minute intervals following the procedure described in section 2.3.2.2. After the cycle elapsed, the product was discharged, quenched and placed into the -20 °C freezer. Once cooled the product formed was a colourless, glassy solid.

2.3.2.6 Pulsed Microwave Polycondensations (Chapter 5)

2.3.2.6.1 Adipic Acid, 1,6-Hexanediol Polycondensation at 185 °C

1,6-hexanediol (15 g, 126 mmol) was placed into a the 50 mL long neck flask with a fibre optic and magnetic stirrer. This was placed into the microwave cavity and distillation equipment was attached. Stirring was started at 300 rpm and the microwaves were applied with an average input power of 150 W until the 1,6-

hexanediol had dissolved (~60 °C). Adipic acid (18.55 g, 126 mmol) and 1 % mole equivalent catalyst (1.26 mmol) were added and the microwaves were re-applied at an average input power of 150 W. The start of the reaction (time = 0 secs) was defined when the microwave power was first applied. Due to the lack of temperature feedback control on the magnetron, once an internal temperature of 185 °C was achieved, the microwaves were terminated and re-applied once the temperature had dropped by ~3 °C. This was done throughout the experiment to achieve a constant average internal temperature of 185 °C. Kinetic samples (~0.2 mL) were taken every 15 minutes following the procedure described in section 2.3.2.2. After the cycle time had been completed, the product was discharged, quenched and stored in a -20 °C freezer. Once cooled the product formed was a waxy, colourless solid.

2.3.2.6.2 Neopentyl Glycol, Isophthalic Acid Polycondensation at 200 °C

Neopentyl glycol (15 g, 144 mmol) and water (1.5 mL) were added to the 50 mL long necked reaction vessel with an internal fibre optic and a magnetic stirrer. Stirring was started at 300 rpm and the microwaves were applied with an average input power of 150 W until the neopentyl glycol had dissolved (~90 °C). At this point isophthalic acid (23.93 g, 144 mmol) and dihydroxybutyl tinchloride (0.35 g, 1.44 mmol) were added. The start of the reaction (time = 0 secs) was defined as when the microwave power was first applied. Due to the lack of temperature feedback control on the magnetron, once the internal temperature was achieved, the microwaves were terminated and switched back on once the temperature had dropped ~3 °C. This was done throughout the experiment to achieve a constant average internal temperature of 200 °C. For power matching reactions, the average power input was lowered to sustain a constant

temperature of 200 °C (explained in chapter 5). Kinetic samples (~0.2 mL) were taken every 15 minutes following the procedure described in section 2.3.2.2. After a cycle time of 3 hours had been completed, the product was discharged, quenched and stored in a -20 °C freezer. Once cooled the product formed a colourless, glassy solid.

2.3.2.7 5 L Conventional and Microwave Polymerisations (Chapter 5)

2.3.2.7.1 Adipic Acid, 1,6-Hexanediol 5 L Polycondensations General Procedure at 185 °C

Hexanediol (2,000 g, 16.92 mol) was charged and the vessel was sealed. Heating was commenced (t = 0 mins) to an internal set point of 60 °C to melt the diol. Once the hexanediol had melted, adipic acid (2,470 g, 16.92 mol) and dihydroxybutyl tinchloride (4.17 g, 17 mmol) were charged. Heating was then ramped to an internal set point of 185 °C. After 30 mins, stirring was started at 50 rpm and increased at 10 rpm per minute till 150 rpm. After 1 hour cycle time, kinetic samples (~1 g) were taken every 30 minutes following the procedure described in section 2.3.2.2. After 4 hours reaction time, vacuum was added at 900 mbar, increasing to 300 mbar over 2 hours. After the cycle time had elapsed the product was discharged into a 5L tin and left to cool to room temperature overnight. The product created was a colourless, waxy solid.

2.3.2.7.1.1 Conventional Heating Temperature Information

For the CH experiments, the temperature was controlled using an external oil jacket around the reaction vessel. As such, for the internal set point to be

achieved, the external oil temperature was set to 10 °C higher than the required internal temperature. Therefore, initially an oil set point of 70 °C was used and the ramp was set from 70 to 195 °C. The temperature ramp from an oil set point of 70 to 195 °C took ~50 minutes to achieve an internal temperature of 185 °C.

2.3.2.7.1.2 Microwave Heating Temperature Information

For the MWH experiments, the magnetron was controlled *via* temperature feedback from a fibre optic which measured the internal bulk temperature. Therefore, the MWH set point was input as the target reaction temperature. As such, initially an internal temperature of 60 °C was selected for the hexane diol melt and the ramp was set from 60 to 187 °C (a few degrees higher than reaction temperature to allow oscillation as microwaves turn on and off). For the temperature ramp the P_{max} was increased over time from 200 W to 1.5 kW depending on the speed of heating. This led to the temperature ramp lasting ~1 hour 30 minutes instead of the targeted 50 minutes.

2.3.2.7.2 Industrial Resin Polycondensation using Conventional and Microwave Heating at 235 °C

Neopentyl glycol (1,810.3 g, 17.38 mol) and trimethylolpropane (37.5 g, 0.28 mol) were added to the vessel with water (200 mL). Heating was applied (t = 0 mins) to achieve an internal set point ~85 °C to melt/dissolve the diols. Once the diols had melt/dissolved stirring was slowly increased to 350 rpm to allow sufficient agitation of the mixture. Isophthalic acid (2,665.5 g, 16.03 mol) and dihydroxy butyltin chloride (1 g, 4 mmol) were combined and added to the vessel and stirring was reduced to 150 rpm. The internal temperature set point was

then raised to 130 °C. Once the internal temperature reached ~125 °C, a slow heating ramp was applied (6 - 8 °C/hour) to achieve an internal set point of 235 °C and the mixture was left to process at this temperature for 2 - 6 hours. Once clarity was achieved (explained in chapter 5), a sample was extracted (~50 g) following the procedure described in section 2.3.2.2. The sample was assessed for acid and hydroxyl value and a correction, if needed, was calculated (explained in chapter 5). The internal set point was reduced to 190 °C, stirring was increased to 350 rpm and isophthalic acid (371.8 g, 2.24 mol), adipic acid (55 g, 0.38 mol) and the required correction were charged into the reaction bulk. The internal set point was then raised to 235 °C and the sample was left to process for 14 – 18 hours. Once the cycle time had elapsed, a sample was taken (~50 g) and tested for hydroxyl and acid value. If the sample was not in the correct hydroxyl value range (discussed in chapter 5), corrections were made, if it was a high vacuum was added and the sample was left to react for 2 – 3 hours. A sample (~30 g) was taken and tested for acid value, if this was too high, vacuum was re-added and a sample was taken after a further 2 – 3 hours, if it was within specification the product was discharged from the vessel into a 5 L tin. This was left to cool to create a colourless/light yellow glassy solid.

2.3.2.7.2.1 Conventional Heating Temperature Information

As in section 2.3.2.7.1.1 the temperature was controlled via external oil temperature. Therefore, for the initial diol melt the oil set point was at 90 °C, the post acid addition oil set point was 140 °C and the ramp was from 140 to the 245 °C processing temperature. For the second stage addition the oil set point was dropped to 200 °C.

2.3.2.7.2.2 Microwave Heating Temperature Information

As in section 2.3.2.7.1.2 the temperature was controlled via an internal fibre optic. Therefore, for the initial diol melt the internal set point was at 80 °C at a P_{max} of 200 to 800 W, the condensing internal set point was 130 °C (P_{max} = 400 W to 1.5 kW) and the ramp was from 130 to the 237 °C processing temperature. The ramp was conducted by setting different temperature steps on the GMP20 magnetron controller. The set points, powers and durations used are described below in Table 2-2.

Table 2-2. Internal temperature set points, maximum power inputs and power application duration for the ramp to temperature in the industrial polyester synthesis.

Set Point (°C)	P_{max} (W)	Power Application Duration (Minutes)
150	500	180
170	500	180
190	500	180
220	500	180
237	450	600

Once at 237 °C processing temperature a P_{max} of 450 W was used to sustain this temperature.

2.4 Analytical Techniques

2.4.1 Proton (^{1}H) Nuclear Magnetic Resonance (NMR)

NMR spectroscopy is a robust, common technique used for characterising all chemical species which contain NMR active nuclei. NMR active nuclei are defined by their nuclear spin, I, which is a non-zero value *e.g.* $^1/_2$, 1, $^3/_2$, 2 *etc.* [1]

The nuclear spin can be calculated from the mass number and the atomic number of the nucleus, shown in Table 2-3.

Table 2-3. Values of atoms nuclear spin in relation to mass number and atomic number.

Mass number	Atomic number	Nuclear spin (I)
Odd	Even or Odd	$^1/_2$, $^3/_2$, $^5/_2$ etc.
Even	Even	0
Even	Odd	1, 2 ,3 etc.

For this report, only ^{1}H NMR will be discussed. This is the most common type of NMR spectroscopy alongside ^{13}C and ^{31}P, which all have spins of I = $^1/_2$.

All spectra were recorded using a Bruka DPX-300 (300 MHz) and Bruka AV-400 (400 MHz). The chemical shifts were recorded in ppm and referenced relative to a deuterated solvent of $CDCl_3$, MeOD or DMSO-d_6 depending on the sample being analysed and the level of conversion. Sample concentrations were ~10 mg/mL with respect to the deuterated solvent. To analyse the spectra ACD/Labs or MestReNova software was used.

^{1}H NMR analysis was primarily used to calculate conversions of the monomer to polymer from the integration of the diol and ester peaks, A and B respectively, shown in Figure 2-9 and Equation 2-1.

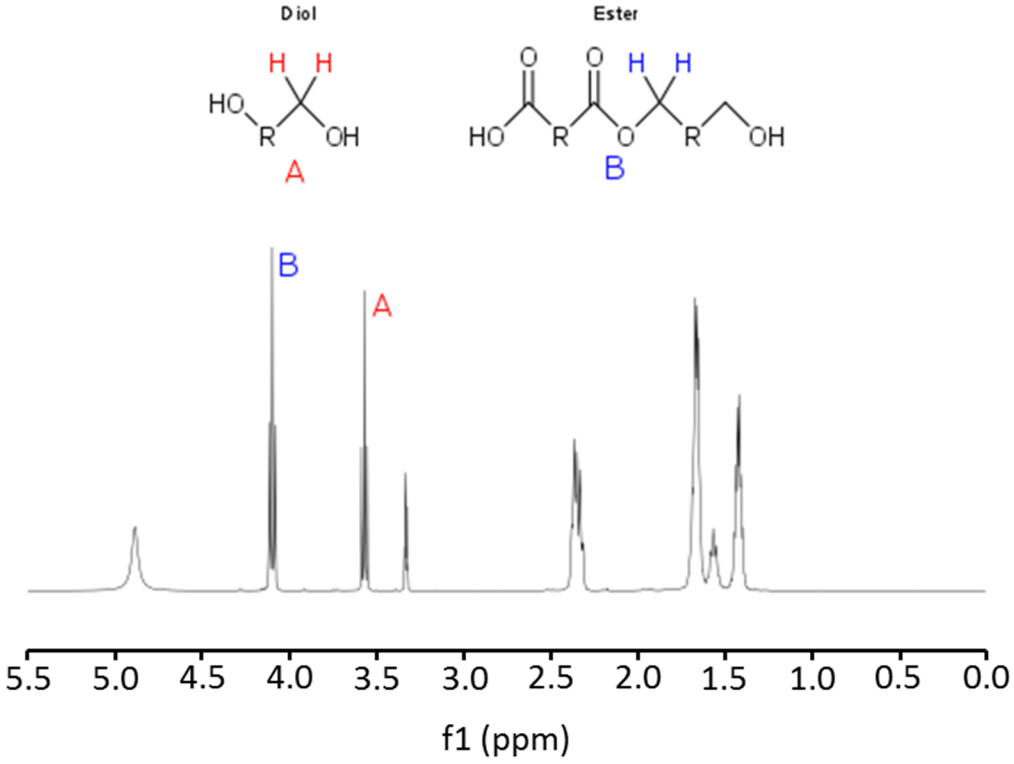


Figure 2-9. NMR spectra for a standard adipic acid, hexanediol polycondensation reaction indicating the relevant peaks needing to be intergrated for the conversion calculation. A = diol peaks and B = ester peaks.

$$\textbf{Monomer to polymer conversion} = \frac{B}{A+B} \times 100\% \qquad \text{Equation 2-1}$$

Equation 2-1 shows that to calculate the overall conversion of the kinetic samples and the final product, the integral of the ester peak was divided by the sum of the integrals for the ester and diol peaks. This was then multiplied by 100 % to give a percentage which is the value reported.

2.4.2 Differential Scanning Calorimetry (DSC)

For thermal property analysis of the polyester species, differential scanning calorimetry (DSC) was conducted. This technique monitors the heat flow to and from a sample with respect to a reference as it is subject to a temperature profile *i*.e. cooled or heated. [2-4] This allows the equipment to detect changes in the polymer's morphology and the determination of values such as melting points (T_m) and glass transition temperatures (T_g).

DSC analysis was completed using a TA-Q2000 DSC (TA Instruments, USA), calibrated using sapphire and indium standards. Two different experimental methods were used depending on the product and are outlined below:

a) Adipic acid, 1-6,hexanediol polyester

The sample (1 - 4 mg) was first cooled to -90 °C followed by heating to 80 °C at a ramp rate of 20 °C/min, this was taken the first "temperature cycle". A second temperature cycle from -90 °C to 80 °C at 20 °C/min followed. The second temperature cycle was used as the curve to attain the T_m value as the first cycle was used to remove any thermal history from the sample. The T_m was described as the peak in the heat capacity during the temperature ramp from -90 to 80 °C, expected between 45 and 60 °C for the molecular weights (MWt's) targeted.

b) Isophthalic acid, Neopentyl Glycol resin and Industrial resin:

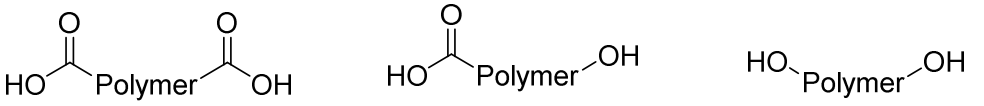
The sample (1 - 4 mg) was first cooled to 0 °C followed by a heating ramp of 20 °C/min to 140 °C as the first temperature cycle. This was followed by a second temperature cycle from 0 °C to 140 °C at 20 °C/min. The second temperature cycle was used as the curve to attain the T_g value as the first cycle was used to remove any thermal history from the sample. The T_g was taken as the mid-point

in the change in heat capacity, this was expected to be between 45 and 60 °C for the MWt's targeted.

For all experiments Tzero platinum pans (TA instruments, USA) were used. Prior to analysis the pans were closed using a pan press. A flow of N_2 (50 mL/min) was present around the samples during experiments, this was to create an inert atmosphere and stop any oxidising effects occurring. The data was analysed using the Universal Analysis software (TA instruments, USA).

2.4.3 Titration

When synthesising a polyester it can be terminated in 3 different ways, shown in Figure 2-10. These terminating groups can be evaluated using titration techniques to give information on end group identity and molecular weight. [5]



Carboxyl terminated | "racemic" hydroxyl and carboxyl terminated | Hydroxyl terminated

Figure 2-10. Representation of terminating groups in a linear polyester.

When polyesters are synthesised in industry, acid value (AV) and hydroxyl value (OHV) titrations are commonly implemented. [6,7] Both of these methods will be employed in this thesis and the methods are detailed in section 2.4.3.1 and 2.4.3.2.

2.4.3.1 Acid Value (AV) Titration Method

A 0.1 M methanolic KOH solution was used as the basic titrant and was prepared by dissolving KOH pellets (12 g, 0.214 mol) in water (100 mL). Once the KOH pellets were dissolved, methanol (1,900 mL, 46.97 mol) was added.

The basic solution was then standardised to calculate its exact molarity. This was achieved by dissolving hydrogen potassium phthalate (KHP) (0.6 – 0.8 g) in water (25 mL), the dissolution was assisted by heating to 50 °C and stirring for ~10 minutes. The mixture was cooled to room temperature and 3 drops of 1 mol. % thymolphthalein indicator solution was added. The mixture was titrated against the basic solution and the molarity was calculated using Equation 2-2. This standardisation was repeated in triplicate for accuracy.

$$\boldsymbol{Molarity} = \frac{\mathbf{1000} \times \boldsymbol{sample\ mass\ (g)}}{\mathbf{204.22} \times \boldsymbol{titre\ (mL)}} \qquad \textit{Equation 2-2}$$

Sample mass refers to the mass of KHP in grams to 4 decimal places and 204.22 refers to the molar mass of KHP.

The result of the molarity from Equation 2-2 was then inserted into Equation 2-3 to work out the “F factor”.

$$\boldsymbol{F\ factor} = \boldsymbol{Molarity} \times \mathbf{56.1} \qquad \textit{Equation 2-3}$$

The molarity is multiplied by 56.1 as this is the molar mass of KOH in g.mol^{-1}.

For sample AV determination a known quantity (2.5 – 3.0 g) of polyester was dissolved in 50 mL of 3:1 (v/v) xylene:methoxy propanol containing 1 mL/L of 1 mol. % thymolphthalein indicator solution. Dissolution was aided by heating and stirring the sample at 70 °C for ~15 minutes. Once dissolved, the sample was

cooled to room temperature and titrated against the standardised 0.1 M KOH solution. The acid value was then calculated using Equation 2-4.

$$\boldsymbol{Acid\ Value} = \frac{\boldsymbol{F\ factor} \times \boldsymbol{sample\ titre}}{\boldsymbol{sample\ mass}} \qquad \textit{Equation 2-4}$$

With sample titre a volume expressed in mL and sample mass in grams to 4 decimal places.

This analysis was conducted in triplicate for accuracy and a mean value was calculated.

2.4.3.2 Hydroxyl Value (OHV) Titration Method

Hydroxyl values were conducted using an 808 Titrando autotitration unit (Metrohm, UK) containing 0.6 M KOH solution and an 805 Dosimat dispenser (Metrohm, UK) to dispense accurate amounts of acetylating reagent. Dynamic titrant addition was conducted using an accurate 20 mL dispenser. A pH probe monitoring the conductance of the solution identified the equivalence point and relayed the data back to the Tiamo 2.0 software (Metrohm, UK) on a computer.

The 0.6 M KOH was prepared by dissolving KOH pellets (95.7 g, 1.74 mol) in water (125 mL). Once all the KOH pellets had dissolved methanol (1.875 L,) was added. The solution was standardised for exact molarity by dissolving a known mass of KHP (2.5 – 3.0 g) in water (100 mL). The solution was heated to 50 °C and stirred for ~10 minutes to aid the dissolution of the KHP. Once the KHP solution had cooled to room temperature it was titrated using the 808 Titrando. This was done in triplicate to achieve a reproducible, average result.

For polyester titrations a known mass of polyester (2.5 g – 3.0 g) was dissolved in xylene (20 mL), with heating at 80 °C and stirring to aid dissolution. After, the

solution was left to cool to room temperature and acetylating reagent (10 mL) (see section 2.4.3.2.1.1) was accurately dispensed into the samples. The samples were refluxed for 20 minutes after which a 3:1 (v/v) pyridine:water mixture (20 mL) was added and refluxed for a further 10 minutes. The acetylation steps which occurred are described schematically in Figure 2-11.

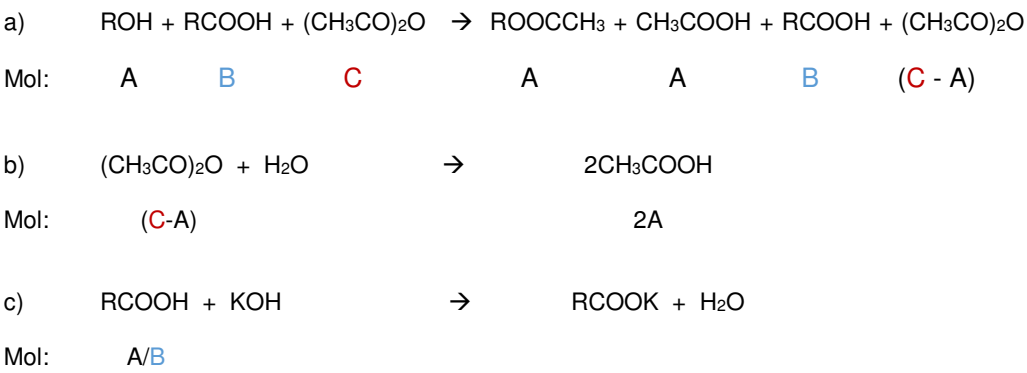


Figure 2-11. Reaction scheme for the hydroxyl value process of a polyester. a) Acylation of hydroxyl groups. "A" moles of hydroxyl group are acetylated with "C" moles of acetic anhydride producing "A" moles of acetic acid and "(C – A)" moles of acetic anhydride. b) Conversion of remaining acetic anhydride to acetic acid via hydrolysis. "(C - A)" moles of acetic anhydride hydrolysed to form "2A" moles acetic acid. c) Titration of all acidic groups. "A" moles of remaining acetic acid groups and "B" moles of acid groups from the original sample.

Post reflux the mixture was left to cool to room temperature and acetone (100 mL) was washed down the condenser neck. The solution was then autotitrated against the 0.6 M KOH solution.

The OHV sample analysis was conducted in triplicate for accuracy with a set of blanks. The blanks were prepared following the same procedure as above but omitting the initial sample and therefore dissolution of the sample in xylene. As such, when washing the final reaction mix, 120 mL of acetone was used instead of 100 mL to create a mixture with identical volumes to the samples.

The OHV was then calculated using Equation 2-5 below:

$$OHV = \frac{(B - S) \times M \times 56.1}{W}$$ Equation 2-5

Where B is the volume (mL) of titre used in the blanks, S is the volume (mL) of titre used in the samples, M is the molarity of the KOH solution, 56.1 is the M_n of KOH and W is the mass of sample (g).

2.4.3.2.1.1 Preparation of Acetylating Reagent

p-Toluenesulfonic acid (6 g, 0.035 mol) was dissolved in n-butyl acetate (450 mL, 3.42 mol) at 60 ºC and cooled to room temperature. Once cooled acetic anhydride (10 mL/100 mL of solution) was added. This solution was prepared weekly as the acetic anhydride reacted at room temperature over long periods of time to form acetic acid.

2.4.4 Gel Permeation Chromatography (GPC)

GPC is an essential technique widely employed throughout all aspects of polymer chemistry. It allows determination of MWt and MWt distributions (polydispersity, Đ) of polymers based on their hydrodynamic volume when swelling in a particular solvent. [8] These changes in hydrodynamic volume are detected by the changes in refractive index (RI) when compared to a sample of pure eluent.

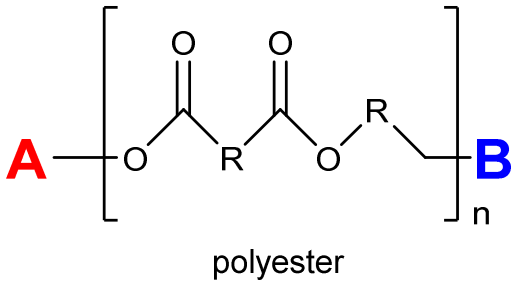
GPC analysis was performed using an Agilent 1260 Infinity series HPLC (Agilent Technologies, USA) with an online degasser, isocratic pump, automated liquid sampler, thermostatted column oven and refractive index detector. The columns used consisted of 2 × 7.5 mm I.D. by 300 mm Agilent PLgel MIXED-E (Agilent Technologies, USA) , 3 µm particle size Columns (Linear Separation range – up to 25 k g.mol^{-1} relative to polystyrene). A 7.5 mm

ID by 50 mm Agilent PLgel 3 µm guard column was also present to reduce the chance of blockages. The eluent used was tetrahydrofuran (THF) (HPLC grade, ≥99.99 %, inhibitor free) (Sigma-Aldrich, USA). Sample preparation involved dissolving the polymer in THF (1 – 2 mg/mL) and then passing the sample through syringe filters (Whatman, 25 mm, 0.2 µm). Analysis was run by flowing the sample through the columns at 1 mL/min at 40 °C and data were analysed using Astra 6.1 software (Wyatt technology, USA).

2.4.5 Matrix-Assisted Laser Desorption/Ionisation Time-of-Flight Mass Spectrometry (MALDI-ToF MS)

A Bruker Ultraflex III spectrometer was implemented for the confirmation of the polyester repeating unit and the determination of end group composition for the polyesters synthesised during this thesis. Sample preparation was achieved by dissolving polyester sample in THF (10 mg/mL). This solution was then mixed with the matrix solution (2,5-dihydroxybenzoic acid (DHB) dissolved in acetonitrile (~10 mg/mL)) at a 1:4 sample:matrix (v/v) ratio. 1µL of this mixture was then spotted onto a stainless steel MALDI plate and left to air dry. The sample was then inserted into the equipment and the software was set to reflectron mode. The MALDI laser was used to vaporise the sample with the matrix. The samples were then fired down the MALDI chamber to the detector and separated using ToF MS. The collected sample data was analysed with respect to mass-to-charge ratio (m/z) using the FlexAnalysis software (Bruker, UK). The experimentally derived values were then compared to the expected (M_{obv}) values of the fragmented molecules, which were calculated using a spreadsheet and known molecule masses.

As previously discussed, polyesters can have a variety of terminating groups, Figure 2-10. Therefore, these different structures were calculated based on the polyester backbone with the different terminating groups, shown in Figure 2-12.



polyester

A = H or ROH B = OH or OOCRCOOH

Figure 2-12. Representation of polyester backbone for MALDI analysis. A can consist of a hydrogen or diol unit, B can be a hydroxyl group or a diacid.

Note: after calculation of the backbone and terminating group masses an ion with positive charge is added to the mass, typically H^+, Na^+ or K^+.

MALDI ToF MS allows for both high and low molecular weight polyesters to be analysed due to its high sensitivity, non-averaging and soft ionization technique.[9,10] However, MALDI results are not quantitative, therefore MWt's cannot be accurately calculated due to the different compositions and lengths of fragments having different affinities for being ionised and fired down the MALDI chamber.

2.4.6 Determination of Product Discolouration – Gardner Scale Colorimetry

Colour of the final polyester product was an important factor when synthesising products for coating applications. It is widely accepted that the high

temperatures and long cycle times employed in polycondensation reactions lead to side reactions or oxidation which can produce “yellow/browning” of final products.[11-13]

Therefore, the amount of “yellow/browning” was quantitatively assessed using the Gardner scale (GS). The GS is a method widely used and adapted in industry for the production of coatings, surfactants and fatty acids. [14-17] The scale consists of a set of standardised colours, ranging from a colourless solution, to a dark red. These colours are assigned a number from 1 – 18, shown in Figure 2-13.

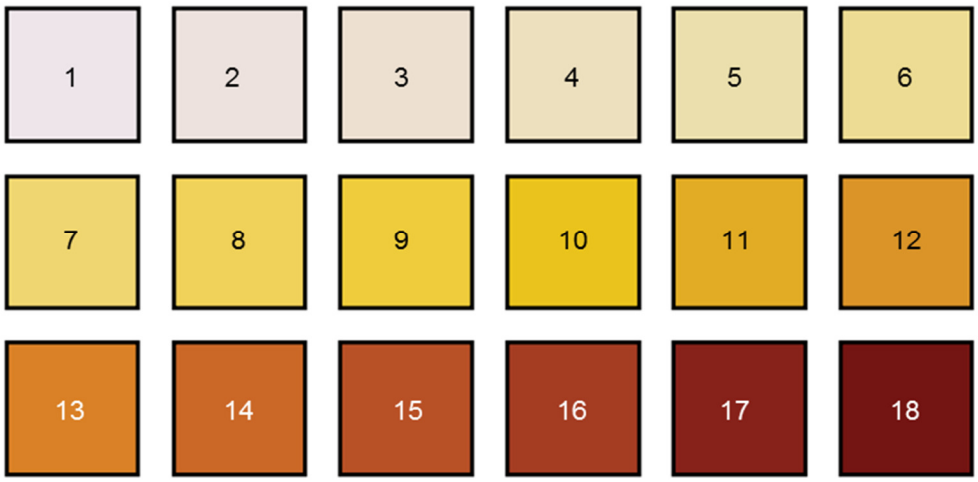


Figure 2-13. Gardner scale colour calibration examples for the Lovibond colorometer. [18]

Samples were measured at Croda (Runcorn, UK) using a Lovibond PFXi-950 colorimeter. Samples were produced by dissolving polyester in THF at 33 % w/v and dispensing ~3 mL into glass cuvettes (10 mm path length). Gardner colour is calculated by triangulating the chromaticity coordinates (±0.1 Gardner) compared to the reference colour standards.

2.4.7 Dielectric Property Analysis - Cavity Perturbation Technique

Dielectric property assessment is a vital part of evaluating the viability of a chemical reaction when wanting to implement MWH. The dielectric properties assess which substances interact with the EM field more favourably than others and how efficiently the materials convert microwave energy into heat. This ability is denoted by the term tanδ and is calculated using other dielectric factors, as described in Equation 2-6.

$$\tan \delta = \frac{\varepsilon''}{\varepsilon'} \qquad \textit{Equation 2-6}$$

Where ε' is the dielectric constant and represents the ability of the material to store EM energy and ε'' represents the dielectric loss which is the ability of the material to convert the stored EM energy into heat. [19-21]

It is generally accepted that a material is considered to heat efficiently using microwave energy if their tanδ value is 0.1 or above. [22] However, when considering materials in a chemical reaction, it is important to take into account the relative dielectric properties between the materials in order to determine which material will heat the most efficiently.

The dielectric cavity used to determine dielectric properties of the materials in this thesis is based on the design and theory by Hutcheon *et al.* [23,24] and a schematic is described in Figure 2-14.

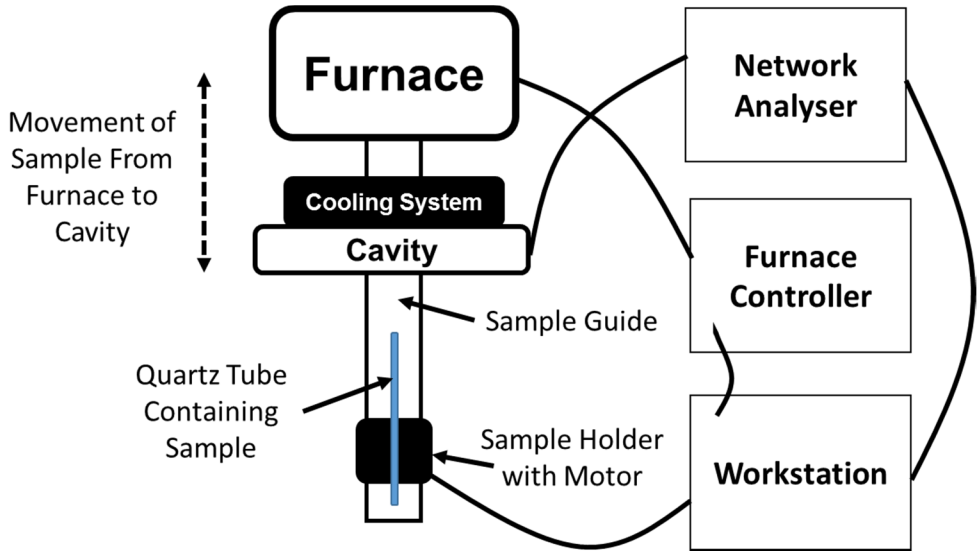


Figure 2-14. Schematic representation of the dielectric cavity used in cavity perturbation.

Initially, the dielectric properties of an empty quartz tube of known mass and inner diameter were recorded at room temperature in quintuplicate. This tube was then packed with a known mass of sample to a height of 15 - 25 mm, ensuring that with powder samples there were no air pockets. The dielectric properties of the sample were then recorded at room temperature in quintuplicate. The sample tube was then inserted into the furnace and dielectric measurements taken in the cavity whilst heating at 10 °C increments from 40 °C to a specified temperature. The specified temperature was either 30 °C above the targeted reaction temperature for the sample/chemical being analysed or just before the sample/chemicals evaporation temperature, depending on which occurred first.

2.5 References

1 Abraham, R. J., Fisher, J. & Loftus, P. *Introduction to NMR Spectroscopy*. 3rd edn, (Wiley, 1993).

2 Menczel, J. D. & Prime, R. B. *Thermal Analysis of Polymers: Fundamentals and Applications*. (Wiley, 2009).

3 Hatakeyama, T. & Quinn, F. X. *THEREMAL ANALYSIS - Fundamental Applications to Polymer Science*. 2nd edn, (John Wiley & Sons Ltd, 1999).

4 Seidel, A. *Characterization and Analysis of Polymers*. (Wiley, 2008).

5 Harris, D. C. *Quantitative Chemical Analysis*. (W. H. Freeman and Company, 2007).

6 Gardner, H. A. & Sward, G. G. *Paint Testing Manual*. (American Society for Testing & Materials, 1972).

7 Flory, P. J. FUNDAMENTAL PRINCIPLES OF CONDENSATION POLYMERIZATION. *Chem. Rev.* 39, 137-197, doi:10.1021/cr60122a003 (1946).

8 Carraher, C. E. *Carraher's Polymer Chemistry*. 8th edn, (CRC Press, 2011).

9 Rizzarelli, P., Puglisi, C. & Montaudo, G. Matrix-assisted laser desorption/ionization time-of-flight/time-of-flight tandem mass spectra of poly(butylene adipate). *Rapid Commun. Mass Spectrom.* 20, 1683-1694 (2006).

10 Williams, J. B., Gusev, A. I. & Hercules, D. M. Characterization of Polyesters by Matrix-Assisted Laser Desorption Ionization Mass Spectrometry. *Macromolecules* 30, 3781-3787, doi:10.1021/ma970123c (1997).

11 Robert, B. & Hans, T. After-condensation of polycondensation polymers in an electrical high frequency field. US 3535285 (1970).

12 Israilov, D. & Rodivilova, L. A. Polycondensation of some diacid chlorides of phosphorus-containing acids with 2,2-DI-(4-hydroxyphenyl)propane. *Polymer Science U.S.S.R.* 8, 1557-1561, doi:http://dx.doi.org/10.1016/0032-3950(66)90172-9 (1966).

13 Acton, Q. A. *Hydroxy Acids—Advances in Research and Application: 2013 Edition*. 34-38 (ScholarlyEditions, 2013).

14 Engineers, N. B. C. *The Complete Book on Adhesives, Glues & Resins Technology*. (NIIR Project Consultancy Services, 2007).

15 Schmitt, T. M. *Analysis of Surfactants, Second Edition*. (Taylor & Francis, 2001).

16 Brice Robert, M. & Robert, P. C. Method of making refined fatty acids from soap stocks. US 2812343 (1957).

17 O'Brien, R. D. *Fats and Oils: Formulating and Processing for Applications, Second Edition*. 201-202 (CRC Press, 2004).

18 ASTM International, Standard Test Method for Color of Transparent Liquids (Gardner Color Scale). (2013).

19 Dallinger, D. & Kappe, C. O. Microwave-assisted synthesis in water as solvent. *Chem. Rev.* 107, 2563-2591, doi:10.1021/cr0509410 (2007).

20 Smith, A. D. *et al.* Dielectric Properties of Free-Radical Polymerizations: Molecularly Symmetrical Initiators during Thermal Decomposition. *Industrial & Engineering Chemistry Research* 49, 1703-1710, doi:10.1021/ie901201h (2010).

21 Mingos, D. M. P. & Baghurst, D. R. Applications of microwave dielectric heating effects to synthetic problems in chemistry. *Chemical Society Reviews* 20, 1-47, doi:10.1039/cs9912000001 (1991).

22 Kappe, C. O., Dallinger, D. & Murphree, S. S. *"Practical Microwave Synthesis for Organic Chemists"*. (Wiley-VCH, 2009).

23 Hutcheon, R. *et al.* A system for rapid measurements of rf and microwave properties up to 1400-degrees-c .2. Description of apparatus, data-collection techniques and measurements on selected materials. *J. Microw. Power Electromagn. Energy* 27, 93-102 (1992).

24 Hutcheon, R. M. *et al.* in *3rd Symp on Microwave Processing of Materials, at the 1992 Spring Meeting of the Materials Research Soc.* (ed Off Ind Technol A. Dv Ind Concepts Mat Program Continental Electr Amer Ceram Soc Renewable Energy) 541-551 (Materials Research Soc, 1992).

3 Adipic Acid, 1,6-Hexanediol Polycondensation Reaction

3.1 Overview

Chapter 3 is dedicated to detailing the work conducted on the melt polycondensation between adipic acid (AA) and 1,6-hexanediol (HD) with both conventional (CH) and microwave heating (MWH). This polycondensation was selected as the pilot system for developing an understanding of this type of polymerisation which would then be applied to the industrial process of the project sponsors, discussed in later chapters. This was because the AA and HD monomers react at lower temperatures and the resin produced is more manageable in terms of viscosity, solidification temperature and reaction times.

The aim of this chapter was to assess the reaction profile, optimise the reaction cycle time for the MWH reaction and then compare it to that of the CH alternative. This led to determining any advantages that could be gained from adopting MWH as a heating method. An investigation was conducted to assess if mass transfer strategies would have the any effect on the polycondensation reaction profile and if so, define which strategy was the most effective for each heating method.

It is well known that polyesters require high temperatures and long reaction times,[1-3] so MWH was applied to these systems to define if it was a more efficient heat transfer method than CH. If this were the case, MWH could lead to increased reaction rates, reducing process cycle times. This proposal drew direct analogies with what has been previously reported in the literature, which described MWH polycondensations conducted with lower temperatures at similar rates to CH. These different efficiencies were hypothesised to be related

to a different heating mechanism being dominant in the MWH process. Consequently, different organometallic and non-organometallic catalysts, which have difference proposed reaction mechanisms, were adopted to define if they had an effect on the polycondensation mechanism/kinetics and whether this was dependent or independent of heating method applied.

3.2 Initial Evaluation of Process Cycle Time

Initially, it was decided to evaluate the overall processes cycle time. As the reactions reported in this section of the study were being conducted to assess the differences in conversion between the two heating techniques, a typical reaction time needed to be identified. This involved finding a cycle time where +90 % conversion was achieved. Therefore a CH reaction was conducted whilst taking samples throughout the cycle at regular intervals. The sample was then subjected to NMR analysis to define when the polyesterification reached a “maximum conversion asymptote” and the reactions can be terminated. A typical CH reaction was prepared as described above, using tin(II) 2-ethylhexanoate ($Sn(Oct)_2$) as the catalyst and sampled at 30 minute intervals, and the data detailing the conversion recorded as the reaction proceeded is shown in Figure 3-1.

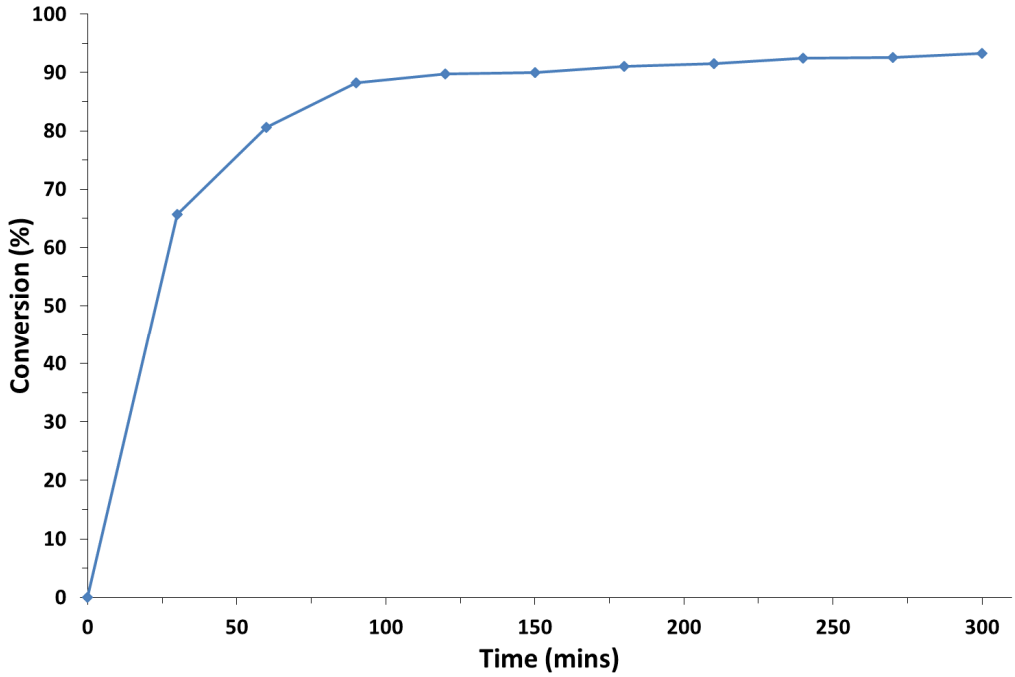


Figure 3-1. Plot of kinetic analysis of reaction conversion with time for a 5 hour adipic acid, hexanediol polyesterification conducted at 185 °C using CH and an $Sn(Oct)_2$ catalyst and no mass transfer methods applied.

Figure 3-1 demonstrates a typical polyester, step-growth reaction profile that was observed from these experiments. The level of conversion is initially rapid but then dramatically slows once a high conversion (typically ≥85 %) is reached. The data presented show that once a reaction time of ~100 minutes is reached there is only a small increase in final conversion (~ 5%) until the reaction is terminated at 300 minutes (typically at 93 to 97 % conversion). In practice, the final 100 – 200 minute time frame is important for the final materials mechanical properties as the polymers molecular weight (MWt) is built up significantly during this section of the cycle time which, in turn, increases the mechanical and thermal properties exhibited by the polyester.

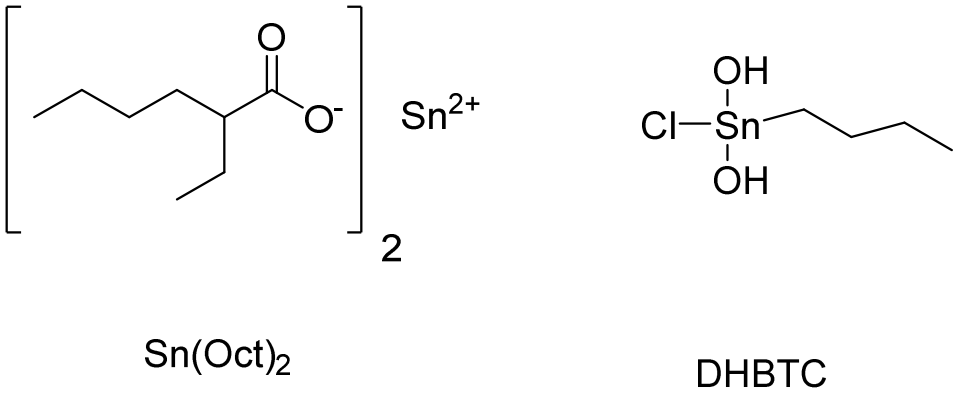
Therefore, a polycondensation can be split up into two sections; the first being the initial reaction with rapid conversion to form small chains (oligomers) and the second being the combination of these chains to build high MWt.

In this chapter the focus will be on the first stage of the reaction. Critically investigating how the choice of heating mode affected the initial section of the reaction profile (i.e. 0 – 95% conversion). Therefore, it was decided that the reactions would generally be terminated after 180 minutes.

3.3 Investigation into Comparing Tin Catalyst Reactivity Between Conventional and Microwave Heated Reactions

Tin compounds catalysts are an integral part of several types of reactions including; the Stille cross coupling,[4,5] carbamate synthesis,[6] glucose isomerisation[7,8] and esterification/transesterification.[9-11] They are not only used widely in academic research, but are also extensively used in industrial esterification processes.[12,13]

Due to this large interest in ton related catalysts, an initial investigation was conducted into the catalyst efficiency of two tin catalysts, one which was liquid at room temperature, tin(II) 2-ethylhexanoate (tin octanoate/$Sn(Oct)_2$), and one which was solid, dihydroxybutyl tinchloride (DHBTC). $Sn(Oct)_2$ has been extensively used and studied as an inorganic tin catalyst in esterifications, [9,10] ring opening polymerisations (ROP) [14-16] and has been widely applied in various microwave reactions. [17-20] DHBTC has primarily been used in polyesterifications. [21,22] The structure of the catalysts are shown in Figure 3-2.



Sn(Oct)$_2$ DHBTC

Figure 3-2. Chemical structures of the different tin catalysts used.

3.3.1 Mass Transfer Studies to Assess the Dominant Factor Within the Polycondensation

As discussed in chapter 1 section 1.2.3, an important principle in ester/polyester synthesis is Le Chatelier's principle, due to their reversible nature.[23] Therefore, it is important to apply a mass transfer (condensate removal) strategy to drive the equilibrium toward ester/polyester formation.

There are a number of ways to aid condensate removal that are adopted in industry, these include; the application of vacuum to the reaction headspace,[24,25] gas sparging of the reaction bulk *i.e.* bubbling inert gas through the reaction,[26,27] stirring rate *etc.* To investigate the effect the influence of mass transfer upon the overall system, experiments were conducted to understand whether it is reaction kinetics or diffusion that is the dominant factor in determining reaction cycle rate/time with the chemistry and apparatus used in this study. To do this the reaction was split up into two separate studies, shown pictorially in Figure 3-3.

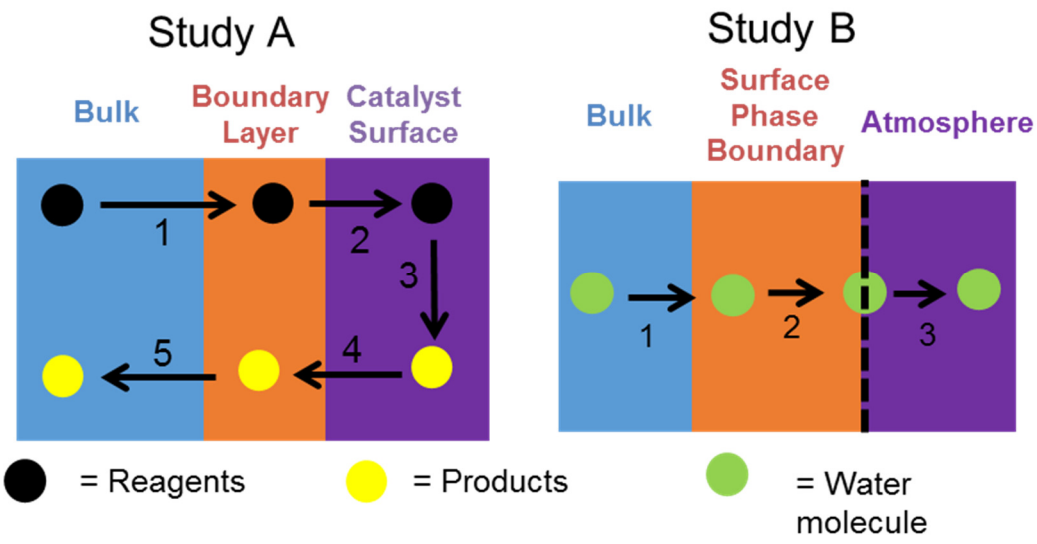


Figure 3-3. Pictorial representation of reagent and product movement through the different phases within a polycondensation reaction.

Study A, Figure 3-3, will focus on the diffusion of the reagents and products to and from the catalyst surface and through the bulk to catalyst boundary layer. The numbering represents the following:

1. Movement of reagents towards catalyst surface through bulk material.
2. Diffusion of reagents towards catalysts through boundary layer.
3. Reaction between reagents on catalyst surface.
4. Diffusion of product and condensate from catalyst surface through boundary layer.
5. Movement of product and condensate from boundary layer to bulk.

Study B, Figure 3-3, will focus on the movement of the water by-product formed when conducting a polycondensation. The numbering represents the following movements:

1. Movement of water between bulk liquid phase and phase boundary.
2. Diffusion of water from phase boundary to boundary layer.
3. Diffusion of water from boundary layer to bulk gas/atmosphere.

3.3.1.1 Stirring Rate Evaluation

Prior work by Yokoyama et al.[28] upon the degradation reactions in the synthesis of poly(ethylene terephthalate) suggested that increasing the stirring rates increased the conversion of monomer to polymer. Therefore, experimental work was conducted to evaluate if it was true for the specific polycondensation investigated in this study. Also, evaluating the stirring rates allowed the deduction of whether movements of monomers/products and the diffusion of water from the reaction through different layers is key to reaction rate. (Figure 3-3, Study A - steps 1, 2, 4 & 5 Study B - Steps 1 & 2).

The experiments conducted involved undertaking a CH experiment at 150 °C with differing stirring rates. The stirring rates chosen were; no stirring, 200 rpm, 400 rpm and 600 rpm, and the data from these experiments are shown in Figure 3-4.

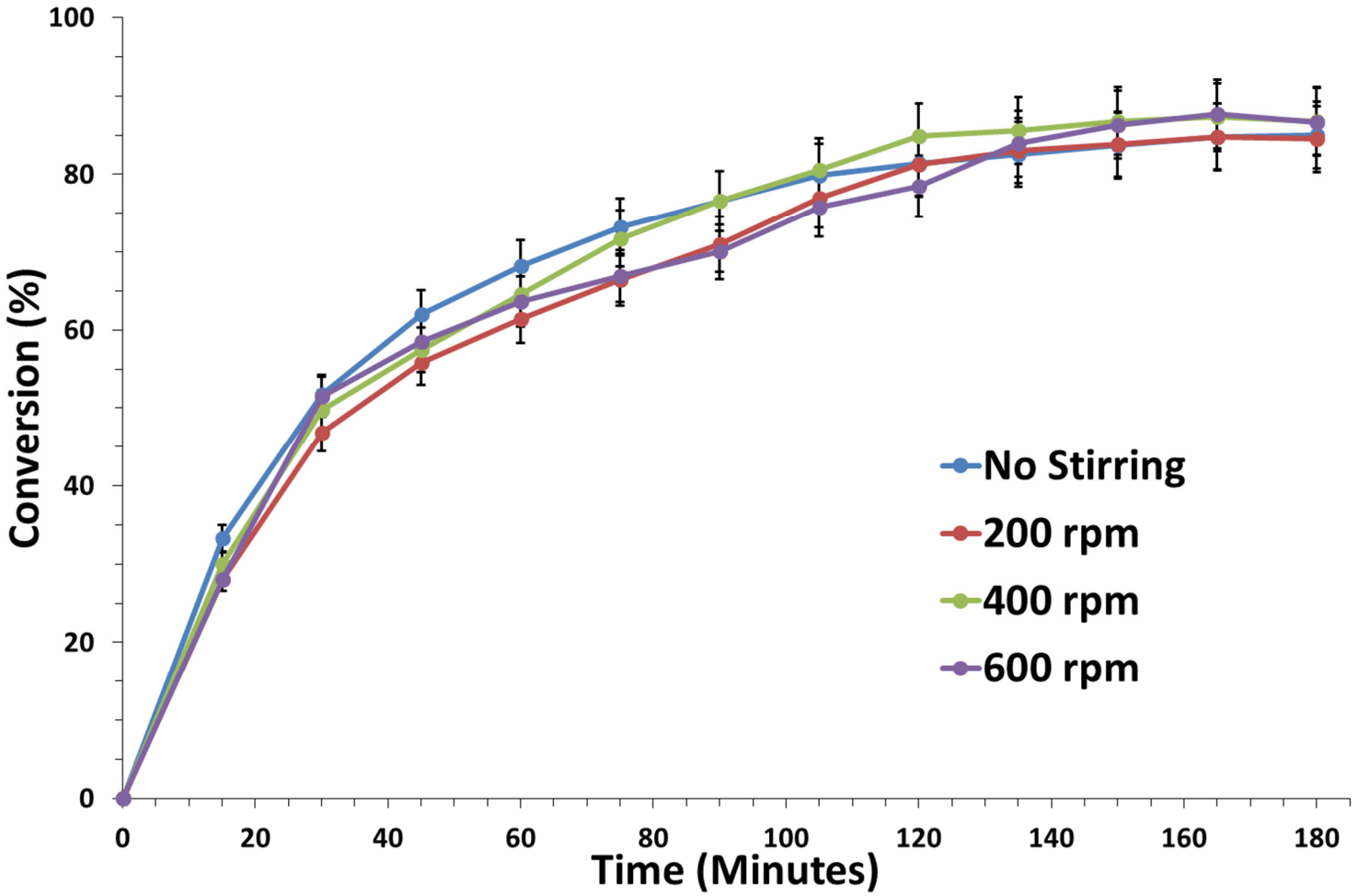


Figure 3-4. Comparison of the effect of stirring rates upon the conversion versus time for adipic acid, hexanediol polycondensation using a dihydroxybutyl tinchloride catalyst conducted at 150 °C using CH and with no mass transfer applied.

The data in Figure 3-4 demonstrated that the slight differences in the conversions achieved related to altering the stirring rates were within the observed experimental error. Additionally, a final conversion range of 84 – 87 % (200 and 600 rpm) was deduced. Both these observations showed that there was negligible difference between the different stirring rates. This slight difference were most likely due to the appearance of a vortex on the surface of the reaction medium achieved at higher stirring rates. This vortex increased the surface area of the mixture and so aided faster evaporation of the condensate. Nevertheless, overall it was concluded that stirring rate did not affect the apparent rate of the reaction for this polymerisation. Therefore, stirring rate was assumed to not be influencing the rate/efficiency of the mass transfer in the system.

This result was attributed to the fact that the catalyst used was homogeneous in nature. A homogeneous catalyst is solvated within the reaction mixture; allowing it to interact with the reagents, independent of the rate of stirring rate, because they are in the same phase. Stirring rate is typically more important when using a heterogeneous catalyst *i.e.* when the reaction mixture and catalyst are in different phases. This makes stirring an essential part of increasing the ability for diffusion to and from the catalyst surface to take place and therefore chances of reagents reacting with the catalyst. [29,30]

3.3.1.2 Assessment of Vacuum Level to Determine Optimum Level

On reviewing the characteristics of the apparatus used in these experiments, it was concluded that vacuum would be a more appropriate method of mass transfer than sparging. This was due to the geometry required for the microwave reaction vessel to ensure its safe operation, see chapter 2 section 2.2.1 for a

description. The long neck is required to prevent microwave energy leakage, hence fitting a sparge made of a non-microwave absorbing material *i.e.* non-metallic, down the vessel's neck along with the sheath required for the fibre optic (FO) was not practical due to space restrictions. By comparison it was relatively easy to attach a vacuum system to the condensation glassware to achieve a head space vacuum.

Therefore, the level of vacuum needed to aid removal of the condensate *via* increased diffusion of the condensate water from boundary layer to gas phase and so reduce the cycle time was investigated (Study B - Step 3). To achieve this a series of CH experiments were conducted at 150 °C with the following vacuum levels; no vacuum, 800, 600 and 200 mbar, Figure 3-5.

A note for these experiments was that an insufficient amount of repeats were conducted, due to time constraints, to confirm the difference between initial conversions between the vacuum levels. This is described in Figure 3-5 by the vast difference in conversion percentage between the 15 minute samples. This variance likely arose due to the differences in dissolution times depending on aggregation levels of the HD monomer (due to its hydroscopic nature). Therefore, this shows that outside factors can affect the reproducibility of these reactions substantially and that future work will be needed to assess any differences between vacuum rates and initial conversion rates. However, the final conversion will still be assessed as the difference in initial reaction speed shouldn't affect the final conversion substantially once the vacuum is added.

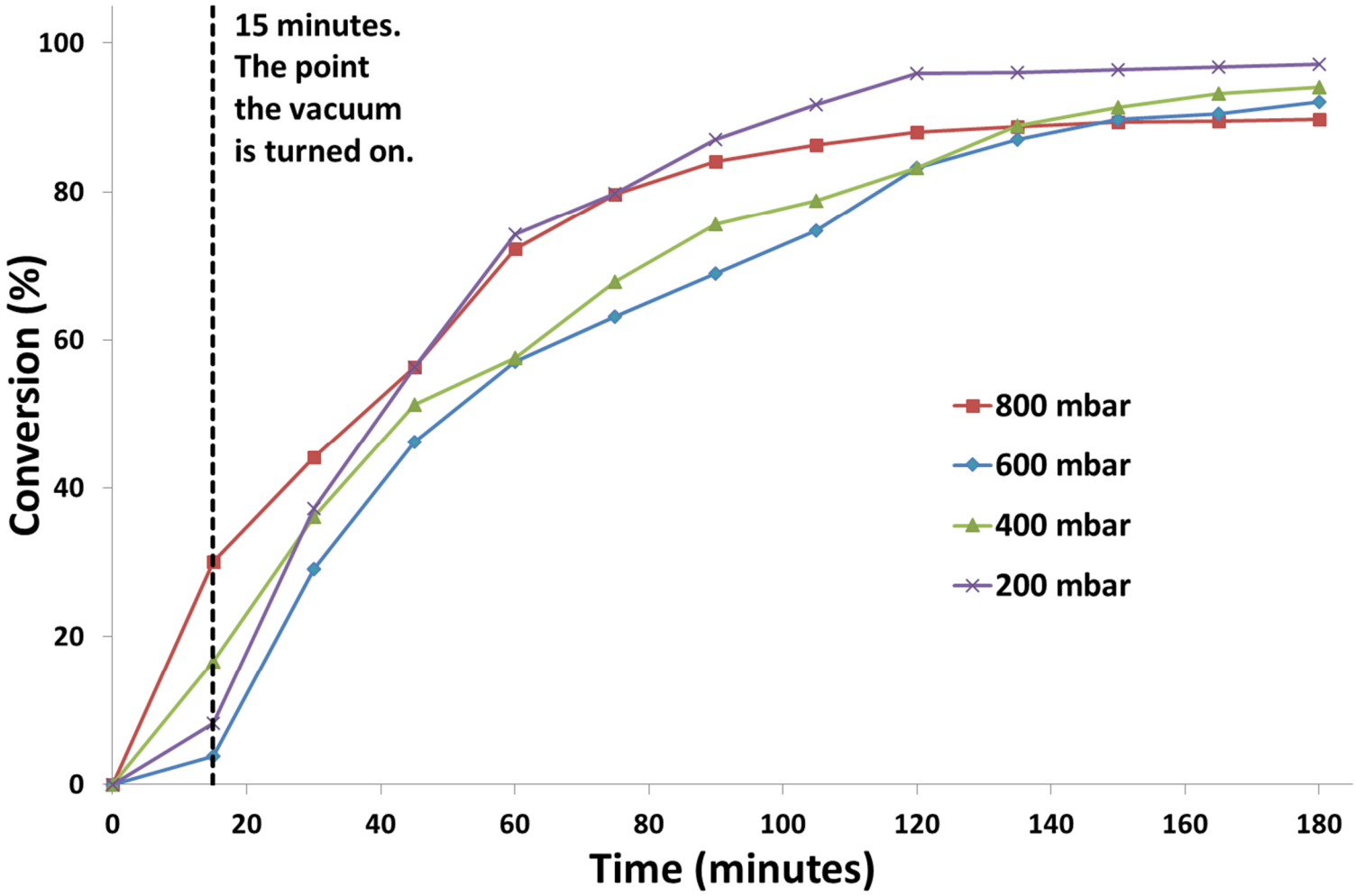


Figure 3-5. Plot of conversion versus time for adipic acid, hexanediol polycondensations using a dihydroxybutyl tinchloride catalyst using CH conducted at 150 °C with varying levels of vacuum applied.

In practice, the vacuum was not applied until 15 minutes of cycle time had elapsed, indicated by the dotted line in Figure 3-5. This gave the reagents time to melt and form a semi-homogenous melt/dispersion of diacid and diol and consequently prevented the fine powder from being removed from the reactor by the vacuum.

Figure 3-5 showed that the higher the vacuum also resulted in a larger the final conversion. This is demonstrated by the final conversion percentages, shown in Table 3-1. This therefore proves that adding a higher vacuum level is imperative to achieving a highly converted polyester.

Table 3-1. Final conversion percentages for AA, HD polycondensations conducted at 150 °C using the dihydroxybutyl tinchloride catalyst with varying levels of vacuum.

[a] Pressure (mbar)	[b] Final Conv. (%)
200	97
400	94
600	92
800	90

[a] Vacuum started after 15 minutes of reaction. [b] Calculated using polymer to monomer peak ratio in ^{1}H NMR.

The data in Table 3-1 define that between 800 and 200 mbar there is an increase in final conversion of 7 %. This is a significant difference, especially when considering that polycondensation reactions have been shown to significantly reduce in rate towards the higher conversion levels (see Figure 3-1). As expected, there was also a significant difference observed in the MWt of the final polyesters related to this increase in conversion, described in Table 3-2. This is because the low Mwt species in the reaction medium had mostly reacted and so it was larger oligomers that started reacting together and building a higher molecular weight in the final material.

Table 3-2. Final conversion percentages and their MWt values for the polyesters synthesised in the vacuum level study.

[a] Pressure (mabr)	[b] Final Conv. (%)	[c] M_n^{GPC} ($g.mol^{-1}$)	[c] M_w^{GPC} ($g.mol^{-1}$)	[c] Đ
200	97	4,890	13,460	2.75
400	94	3,360	10,890	3.24
600	92	2,430	5,430	2.23
800	90	1,950	4,040	2.08

[a] Vacuum started after 15 minutes of reaction [b] Conversion calculated via ^{1}H NMR. [c] Calculated using THF GPC and ASTRA processing software relative to a polystyrene standard.

3.3.2 Conventional versus Microwave Heating of Polycondensations using Tin Catalysts Conducted at 185 °C

As discussed previously, tin is an important catalyst in many chemical processes/applications and so it has been chosen as the initial catalyst for this thesis.

Firstly, experiments were performed to test the dielectric response of the catalysts, mentioned previously in Figure 3-2. This was performed before microwave heating experiments were conducted to assess how the reagents were likely to respond to an applied electromagnetic (EM) field. This enabled an estimated relative ranking to be developed of how these molecular structures would absorb the EM energy and translate this absorbed energy into heat. It also allowed the experimental procedures and reaction mixtures to be tailored such that the applied energy was being directly input to the desired molecules, a process that is referred to as selective heating (chapter 1 section 1.3.5).

To test the dielectric response a method developed by Hutcheon et al. was followed.[31,32] This method was done using a cavity perturbation technique, as described in, chapter 2 section 2.4.7. The most relevant dielectric property to

this study is tanδ due to it being a barometer of how efficiently a material will contribute to the heating of a chemical system. This is because it takes into account both the level of energy absorbed and the efficiency of conversion of that energy into molecular motion (chapter 1 section 1.3.3). Thus, the higher the tanδ, the better a substance will contribute to heating the bulk or promoting a chemical transformation, and this data is presented below in Figure 3-6.

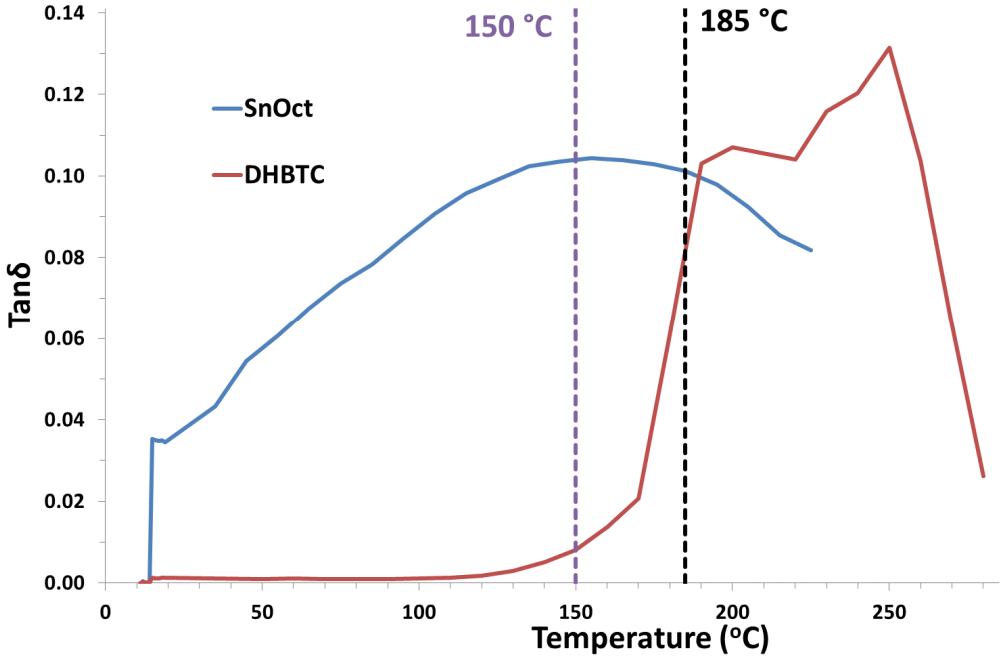


Figure 3-6. A plot of the variation in tanδ with temperature for $Sn(Oct)_2$ and DHBTC, performed using cavity perturbation technique at 2.45 GHz.

Figure 3-6 shows that at both 185 °C (black dotted line) and 150 °C (purple dotted line) $Sn(Oct)_2$ is shown to exhibit a higher tanδ than DHBTC. This suggests $Sn(Oct)_2$ has a better relative heating potential than DHBTC when EM energy is applied. Also as the value in in the region of 0.1 it can be regarded as a material which will interact well with applied EM energy. [33] Therefore, if the reaction rate is determined by the catalyst when implementing MWH, it would be hypothesised that the $Sn(Oct)_2$ catalysed reactions would proceed at a slightly faster rate once at processing than if DHBTC is the catalyst utilised.

The reason attributed for the large difference in tanδ from room temperature to processing temperature was due to the physical form of the catalysts. $Sn(Oct)_2$ is a liquid at room temperature, therefore it is readily heated under MWH as soon as it is added. Whereas, DHBTC is a solid at room temperature and does not melt until 150 °C. Therefore it is expected to have lower dielectric properties at lower temperatures than $Sn(Oct)_2$. Also, at 185 °C it will not be fully molten and this is why it still has lower dielectric properties than $Sn(Oct)_2$ at this temperature. However, once the catalyst dissolved into the solution the dielectrics will change due to interactions with other moieties in the mixture. Unfortunately, these mixtures cannot be evaluated for dielectric data due to the fact that they are likely to commence a reaction during the measurements. Therefore, the dielectric data of the raw catalysts will be used as the barometers of their efficiency under microwave heating. The actual response of DHBTC will therefore depend of the level and quality of dissolution achieved in the reaction mixture under study. [34]

Therefore, this hypothesis was tested by conducting esterifications using identical conditions, but differing the heating method and both catalysts at 185 °C. This data is presented in Figure 3-7.

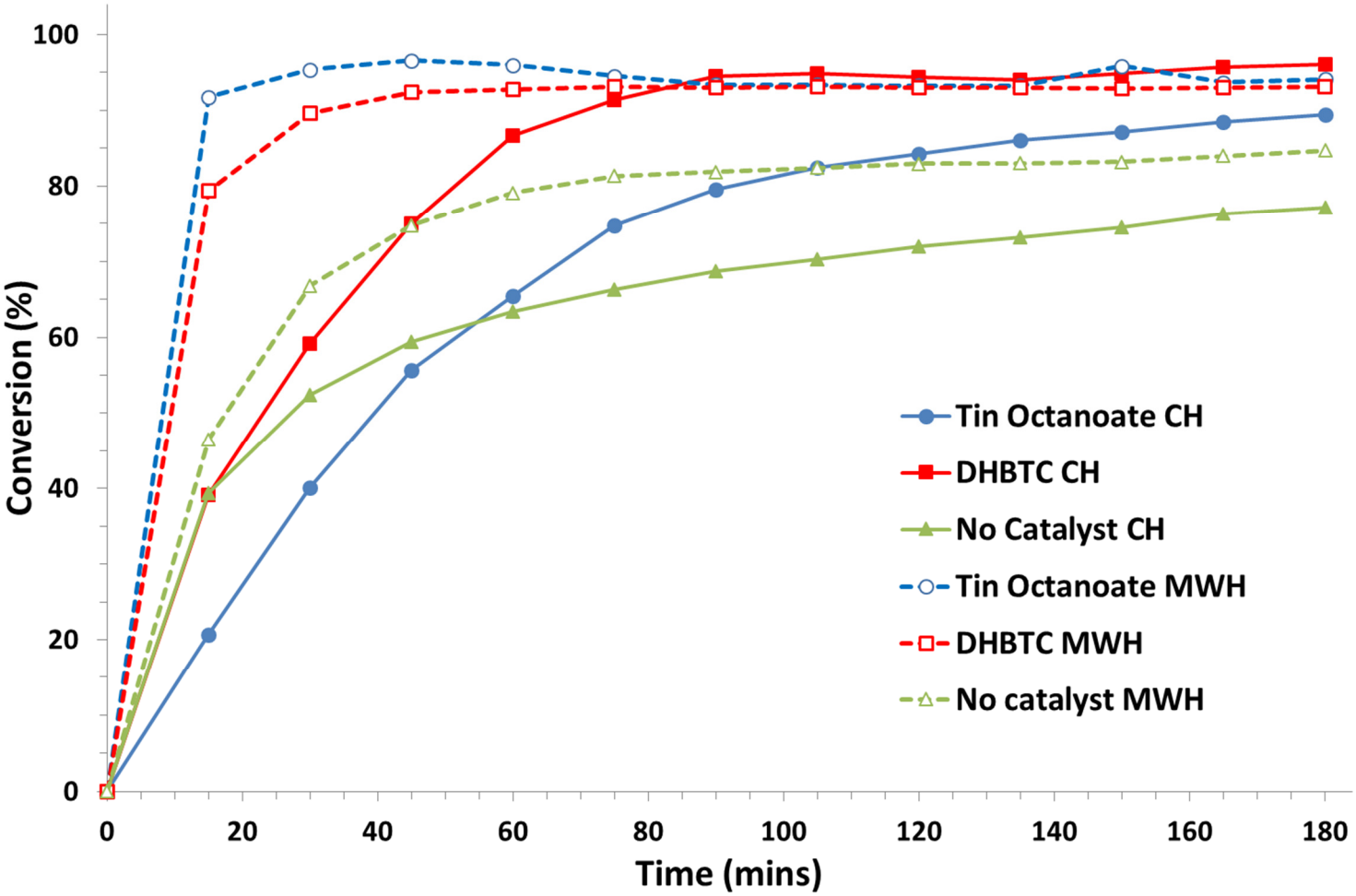


Figure 3-7. Plot of conversion versus time for adipic acid, hexanediol polyesterifications using different tin catalysts and varying the heating method used at 185 °C with no mass transfer applied.

From study of the data in Figure 3-7, it was observed that when comparing MWH to CH for each individual catalyst, there is an increased reaction rate by implementing MWH. Both MWH reactions reached a conversion of 80 % in significantly shorter times when compared to their respective CH reactions. This suggested that the heat/energy and/or mass transfer in MWH was much more efficient than in CH equivalents. This improved heat transfer efficiency was evident from analysis of the temperature profiles, an example of which is shown below as Figure 3-8.

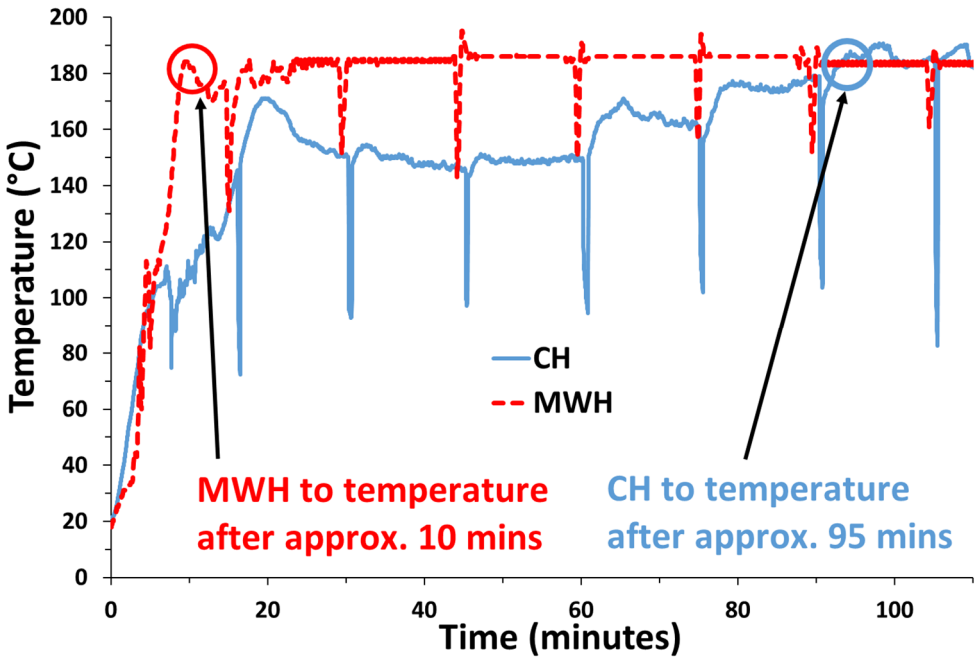


Figure 3-8. Comparison of CH and MWH heating profiles for an adipic acid, hexanediol polycondensation conducted at 185 °C using $Sn(Oct)_2$ with circles depicting when the internal temperature achieved reaction temperature.

Figure 3-8 details that by implementing MWH, processing temperature is reached in almost 10 % of the time as CH. This helps explain why in Figure 3-7 there is an obvious initial rate increase for the MWH compared to the CH reactions.

In Figure 3-8 there are clear temperature fluctuations at 15 minute intervals for both heating methods which are attributed to the sampling of the reaction mixture. These temperature fluctuations occur because the thermocouple/FO is removed from the reaction mixture during sampling, reducing the temperature recorded. Once the thermocouple/FO is re-inserted, the reading returns to the bulk temperature value.

A second observation from Figure 3-7, is that the catalyst efficiency is altered based on the heating methods. For CH, the DHBTC catalysts produced the fastest reaction rate and achieved the highest level of final conversion. Whereas, with MWH, the $Sn(Oct)_2$ catalyst produced the fastest initial reaction rates and achieved a marginally higher final conversion. This finding agreed with the earlier dielectric analysis, Figure 3-6, which suggested that $Sn(Oct)_2$ was a more dielectrically active species than DHBTC and therefore predicted that, of the two catalysts, it would promote polyester formation *via* selective heating more readily. However, the change in catalyst efficiency between the heating methods could potentially be explained by the mechanisms involved in the polyester formation. The proposed mechanisms for both of these catalysts are detailed in Figure 3-9.

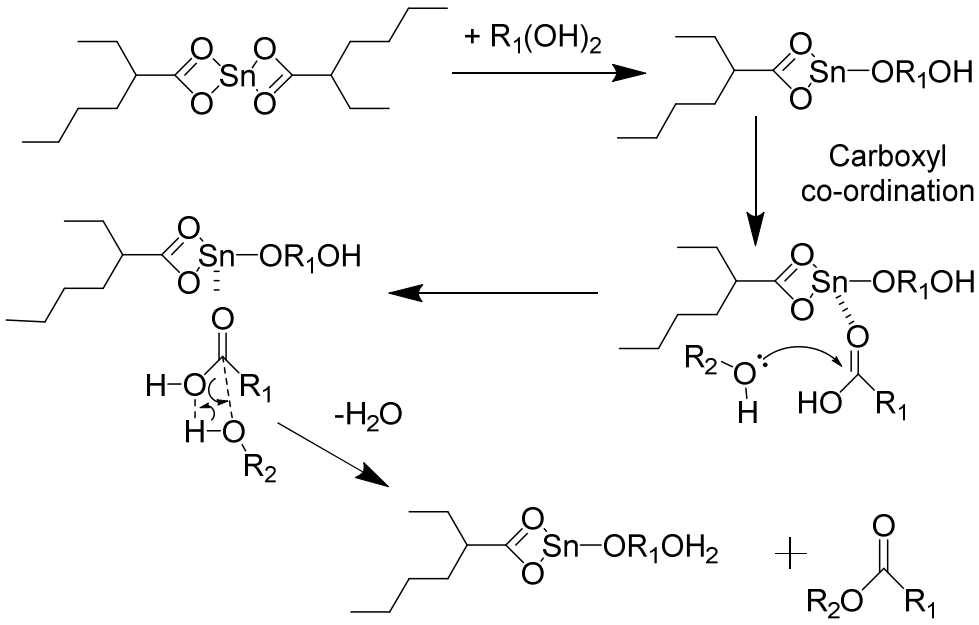
$\underline{Sn(Oct)_2}$

a) Carboxyl co-ordination to pre-catalyst

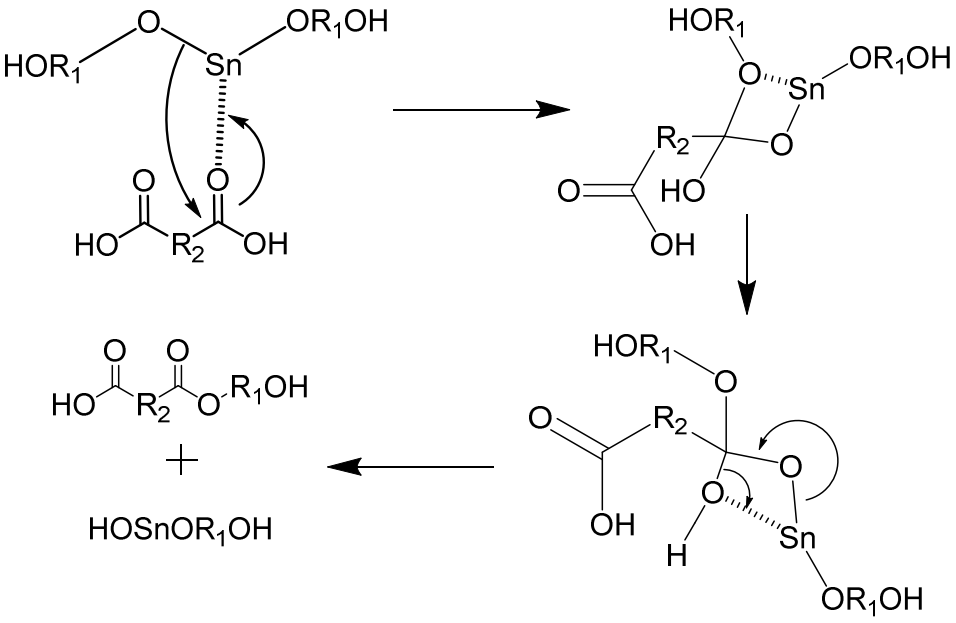
$Sn(Oct)_2 + R_1(OH)_2 \rightleftharpoons OctSnOR_1OH + OctH$

$OctSnOR_1OH + R_1(OH)_2 \rightleftharpoons Sn(OR_1OH)_2 + OctH$

Pre-catalyst



b) Insertion of pre-catalyst into ester chain



DHBTC

c) Lewis Acid mechanism

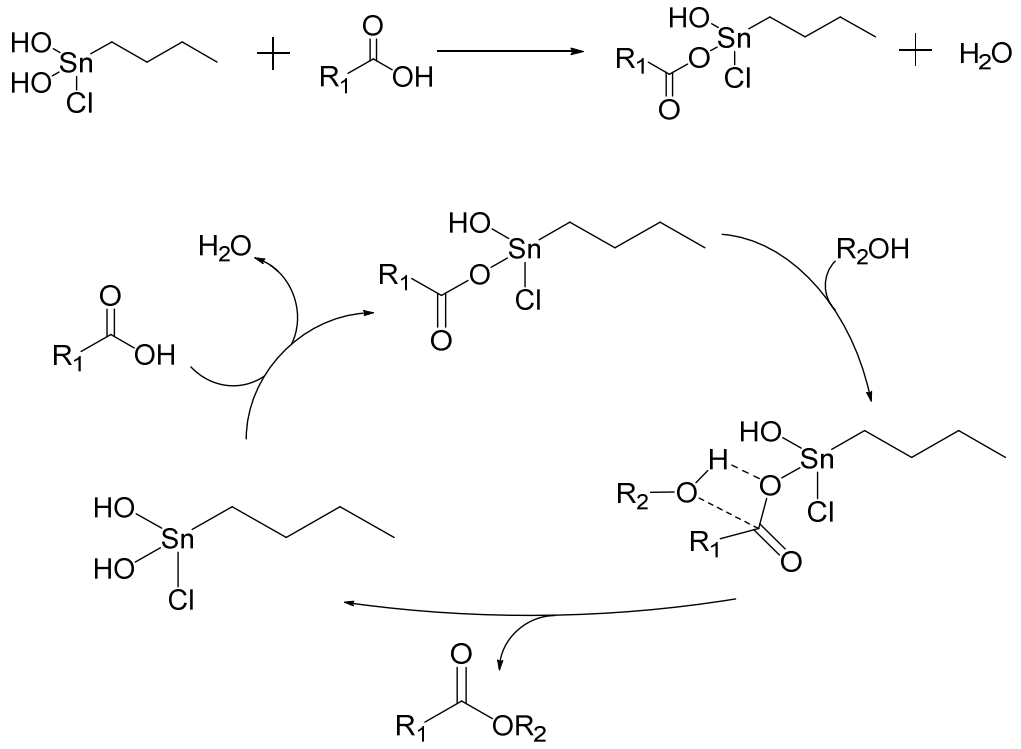


Figure 3-9. Proposed mechanisms for the tin catalysed reactions. a = $Sn(Oct)_2$ via carboxyl coordination, b = $Sn(Oct)_2$ insertion mechanism and c = DHBTC Lewis acid.

Figure 3-9 details the proposed reaction catalytic mechanisms involved in the polyesterifications. In the case of $Sn(Oct)_2$, there are 2 possible routes. Scheme (a) involves coordination of the ester to the pre-catalyst Sn centre to create a strong dipole, and therefore electrophile, at the carboxyl group. This allows insertion of the alcohol group at the carbon and the displacement of a molecule of water. This scheme suggests that the Sn centre is only coordinated to the carboxyl/ester and does not become involved in the growing chain by creating a formal bond, rather the bond between the Sn centre and the polyester is only associative. Scheme (b) is an insertion mechanism with pre-catalyst formation. It is based on the coordination insertion mechanism which has been suggested

for the ROP of lactide. [35,36] Unlike scheme (a) there is a covalent bond formed with the Sn centre and the growing ester chain. This is proceeded by intramolecular H-bonding to help catalyse the reaction. This is also similar to the proposed mechanism for DHBTC, scheme (c) in Figure 3-9, which is based on a Lewis acid mechanism. [9,37] In this reaction scheme, the Sn catalyst species is inserted into the carboxyl/ester chain and forms a covalent tin-alkoxide bond. This can then form intermolecular H-bonds with the alcohol and catalyse ester formation.

Therefore, it was proposed that in the case of $Sn(Oct)_2$, if the mechanism was based on scheme (b), which involves the covalent insertion of the catalyst onto the growing ester chain, then the effect of utilising MWH would be similar to the DHBTC species. But, there is in fact a significantly increased efficiency in the $Sn(Oct)_2$ catalysed sample compared to the DHBTC sample. Therefore, it was hypothesised that scheme (a) is the most likely mechanism for a melt step growth polycondensation which involved linear diacids and diols when using $Sn(Oct)_2$. These findings also suggest that when the catalyst is inserted into the polyester chain, the MWH effect is reduced. This explanation is also supported by the fact that microwave energy is a non-ionising energy, *i.e.* it is not sufficiently intense to break chemical bonds. Rather, it will just increase their energetic state. Therefore, when the catalyst contains an associatively bonded "ester adduct" within the reactions catalytic transition state, the MWH promotes the catalysis cycle at the heart of the reaction to a higher degree than in CH. This is because it can include a larger degree of separation between the charged species that form this associative bond, which is a heating mechanism known as ionic conduction (chapter 1 section 1.3.2).

These findings suggest that in a MWH polyesterification, the catalyst choice is very important when trying to achieve high reaction rates. Therefore, different catalysts have been investigated and will be discussed further in section 3.4.

3.3.3 Temperature Effects on the Reaction Rates of the Adipic Acid, Hexanediol System – a Comparison of Conventional and Microwave Heating at Lower Temperatures

Due to the observation of the catalysts efficiency swap in section 3.3.2, there was an investigation into conducting the reactions at a lower processing temperature. This was assessed for the following reasons:

i. Lower temperatures are less energy intensive on the large scale as it takes significantly less time and energy to achieve and maintain the target temperature at the tonne scale.
ii. At lower temperatures, non-organometallic catalysts can be investigated, which is beneficial for environmental and product discolouration reasons.
iii. At a lower temperature the reaction rate would be reduced, hence it was easier to monitor its progress *via* kinetic experiments. At 185 °C using MWH a conversion of 90 % is attained within 15 minutes.
iv. If MWH helps accelerate the reaction rate, hopefully the observed differences between the MWH and CH equivalent experiments will be amplified when conducting at a lower temperature, due to the decrease in overall rate.

Therefore, a temperature of 150 °C was chosen to perform the polycondensations and the data attained is presented in Figure 3-10.

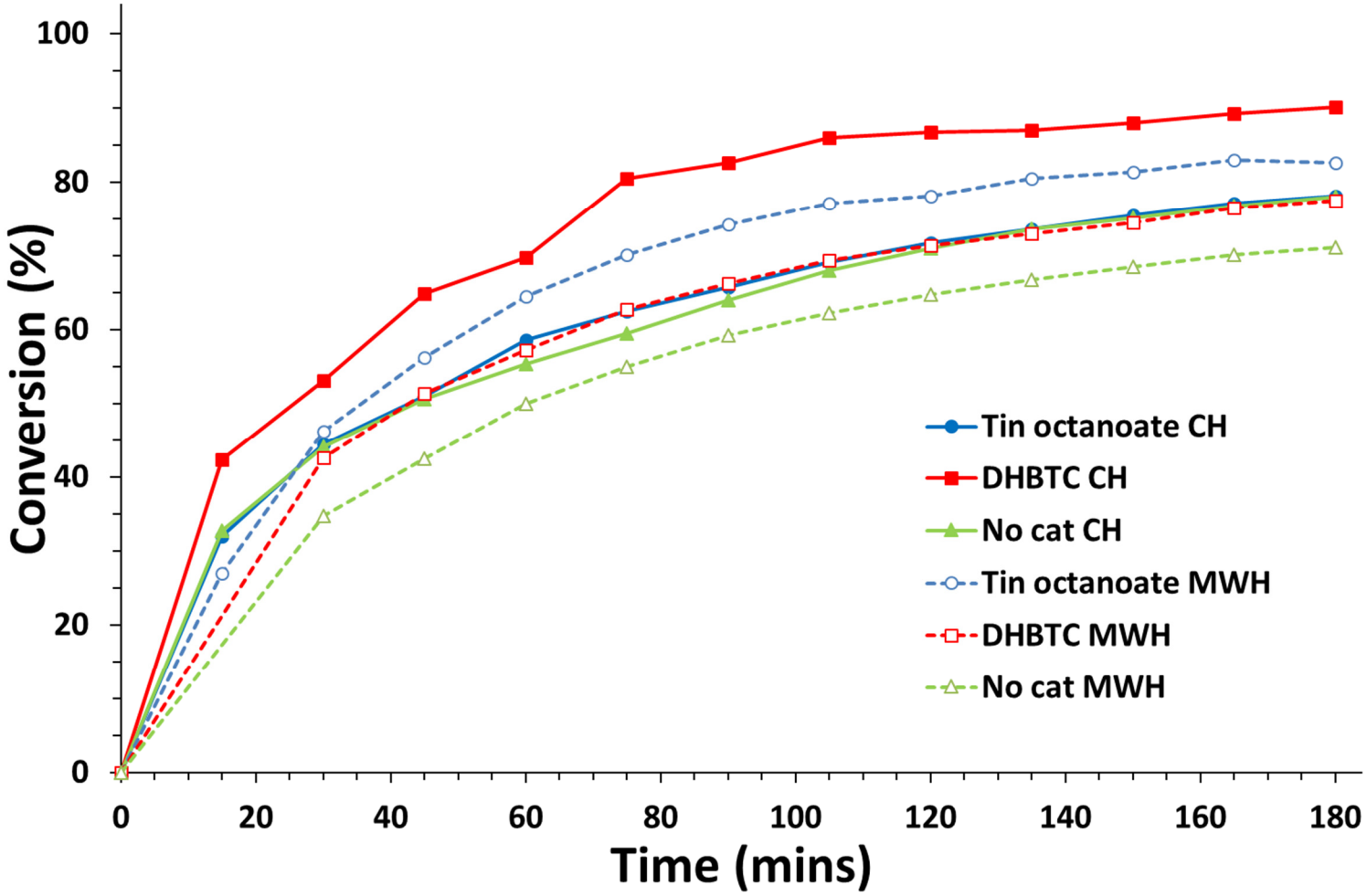


Figure 3-10. Comparison of conversion rate versus time for adipic acid, hexanediol polycondensations at 150 °C using different tin catalysts with no mass transfer applied.

Figure 3-10 contains interesting data which demonstrates a significant contrast to the observations made at 185 °C in Figure 3-7. At 150 °C when either DHBTC or no catalyst was applied, the CH experiments are shown to react at a faster rate than the MWH reactions. When using DHBTC the difference is significant, with a 43 % conversion for CH compared to 23 % for MWH after 15 minutes and final conversions of 90 and 77 % for CH and MWH respectively. However, when using $Sn(Oct)_2$, there is again an increased reaction rate in MWH, but this difference is not as prominent as when processing at 185 ºC (within 5 % for each data point).

Interestingly, the fastest reaction rates and highest conversion occur when using the DHBTC catalyst with CH. This suggests that at lower temperatures, when using CH techniques, this catalyst is more active than the $Sn(Oct)_2$. There is also an argument to say that this is the case at lower temperatures when using MWH as well. This is due to the fact that the $Sn(Oct)_2$ has a significantly higher tan (δ) value than DHBTC, 0.103 compared to 0.008 (Figure 3-6, purple line), so it is expected that the $Sn(Oct)_2$ MWH reaction would be significantly faster than the DHBTC. This is because the potential to selectively transfer energy into the catalyst to drive the catalytic cycle will be less than in the $Sn(Oct)_2$ case. This confirms that catalyst choice is imperative when conducting polyesterifications. However, in actual fact, the initial reaction rates and conversions for the reactions processed using MWH are very similar (27 % conversion for $Sn(Oct)_2$ and 23 % for DHBTC after 15 minutes). This data may suggest that at lower temperature mass transfer of the condensate is also exerting more of an influence over the reactions than at 185 ˚C

However, Figure 3-10 still confirms that there is a switch in catalyst efficiencies which strengthens the hypothesis that the catalytic mechanisms present can be effected by the heating method used. This led to the conclusion that the lower

temperature is effecting the mechanisms that were proposed which involve the formation and scission of covalent bonds in the microwave system more significantly than those that are thought to contain associative bonds. This would support the mechanistic conclusions above due to the fact that microwave energy is non-ionising and thus is not going to promote the scission of these bonds. Therefore, different catalysts will be investigated later in this thesis.

3.4 Differing Catalyst Studies

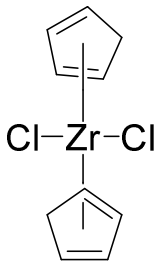
Due to the interesting results found when using 2 different tin catalysts, as detailed in section 3.3, it was decided to investigate the application of different non-tin esterification catalysts. The catalysts chosen included both organometallic and non-organometallic species. The former group contained organometallic catalysts with different metal centres and the latter non-metal based catalysts were added to define if MWH could allow the process to include a “greener” catalyst, introducing the potential that they could be sourced from renewable sources.

3.4.1 Organometallic Catalysts Investigation

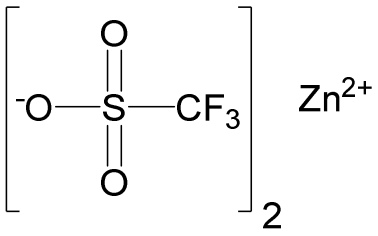
This section reports the evaluation of various reaction catalysts with both CH and MWH at differing reaction temperatures. Firstly, a range of organometallic catalysts were investigated at 185 °C, with in depth analysis of and comparison between the products resulting from the application of the different catalysts.

After this, the temperature was lowered to 150 °C and these products were again compared.

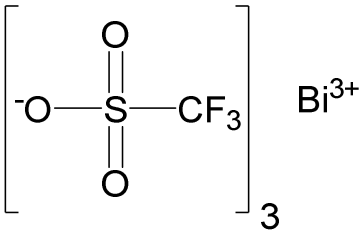
Figure 3-11 details the molecular structures of the organometallic catalysts investigated in this section of the study.



Bis(cyclopentadienyl)zirconium(IV) dichloride



Zinc(II) trifluoromethanesulfonate



Bismuth(III) trifluoromethanesulfonate

Figure 3-11. Chemical structures of the new organometallic catalysts investigated further.

Bis(cyclopentadienyl)zirconium(IV) dichloride (ZrDC) was investigated as it posed significant interest with the industrial sponsors due to a previously filed patent by Knifton et al. [38] and the use of zirconium has been previously been reported in esterifications. [39,40]

Similarly, trifluoromethanesulfonate (triflate) catalysts have also previously been investigated for use as polyesterification catalysts. [41-43] The bismuth derivative was chosen as Buzin et al. had demonstrated that it achieved the highest M_n of all the triflates tested. [41] Zinc triflate was selected based upon

research conducted by Shekarriz et al. who showed that using a zinc triflate catalyst in esterifications can accelerate the reactions under MWH conditions.[44]

3.4.1.1 Organometallic Catalyst Reaction Mechanism Discussion and Comparison of System Differences

ZrDC has been extensively used as a Ziegler-Natta catalyst for the polymerisation of alkenes to polyolefins and the proposed coordination insertion mechanism by which these polymerisations achieve chain growth is described in Figure 3-12. [45,46]

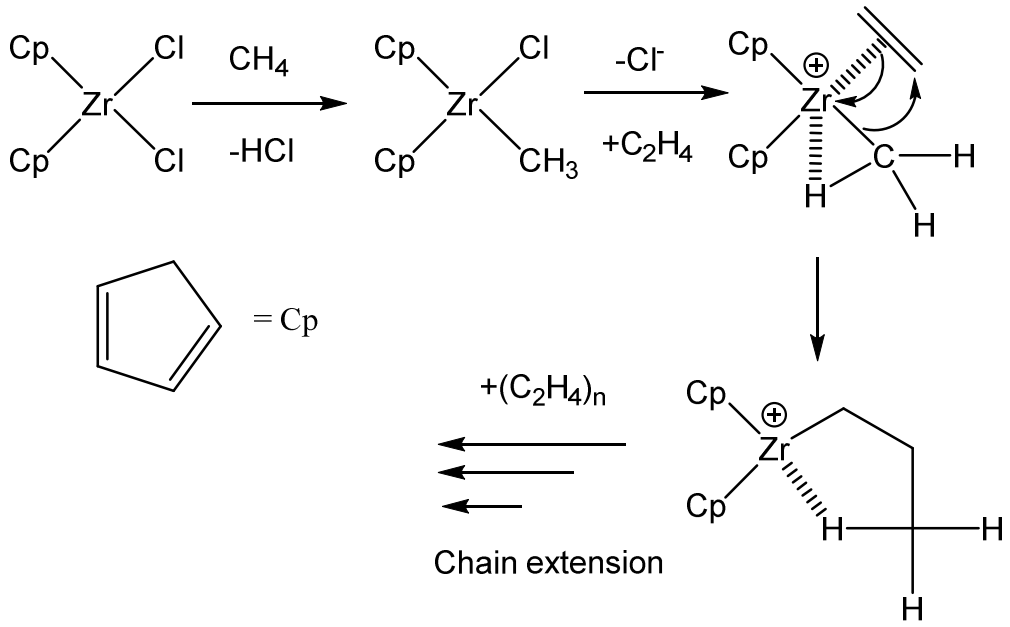


Figure 3-12. Ziegler-Natta polyolefin synthesis mechanism using bis(cyclopentadienyl)zirconium(IV) dichloride.

To date, there has been no literature report of an investigation into the esterification mechanism, only the patent filing mentioned above. [38] Therefore, it was proposed that that the mechanism would be based on the Ziegler-Natta coordination insertion mechanism, but centred upon the coordination of the carbonyl group rather than the alkene. This proposed mechanism is shown in Figure 3-13.

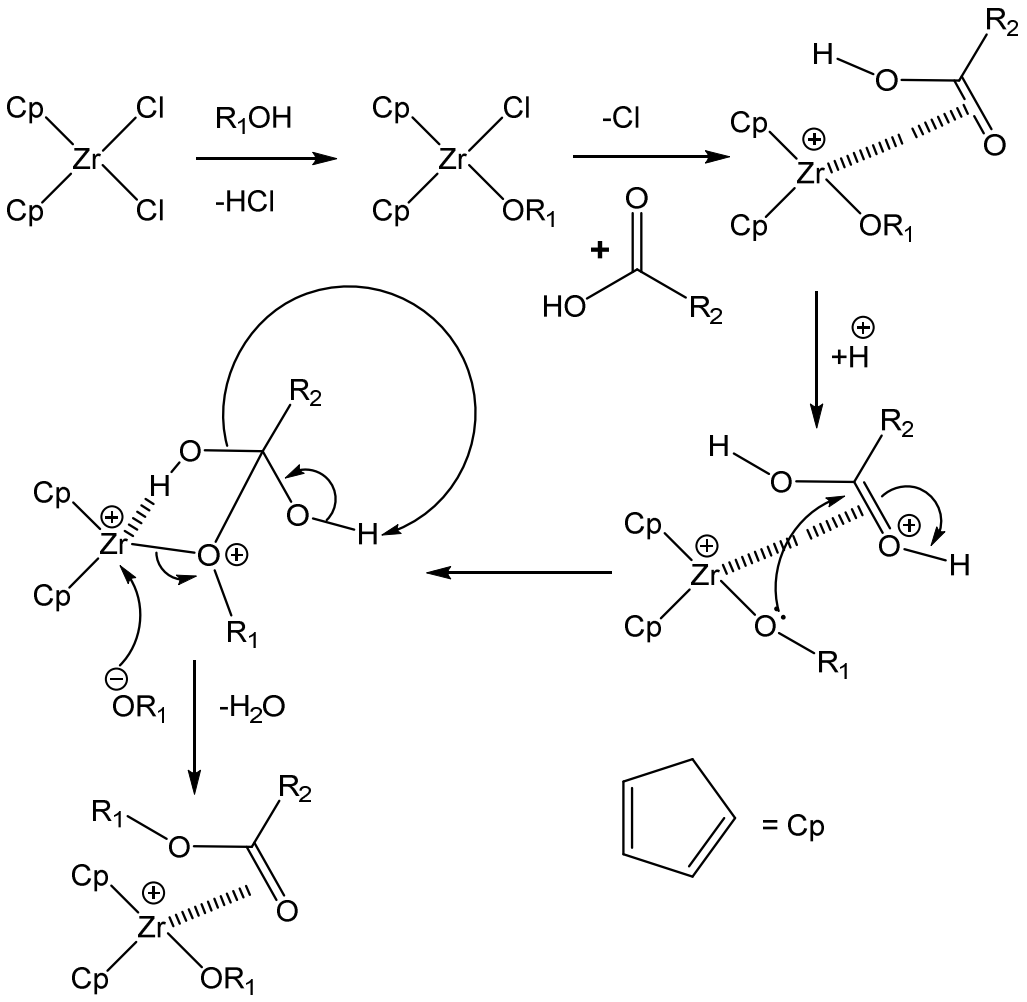


Figure 3-13. Proposed mechanism for the polyesterification based upon a Ziegler-Natta like bis(cyclopentadienyl)zirconium(IV) dichloride.

In the case of the triflate complexes, it was originally hypothesised by Buzin *et al.* [41] that the reaction proceeds *via* a protic mechanism, as shown in Figure 3-14. This was proposed due to the consistently higher yields achieved when using a more acidic triflate. But, later work by Garaleh *et al.*[47] reported contradictory results to this, which suggested a mechanism involving the complexation of carboxyl groups, see Figure 3-15. This was proposed because some less acidic triflates were found to polymerise to higher yield and at a faster rate than more acidic ones. Furthermore, metal carboxylates are, in general,

more stable than metal alkoxides. The work in this thesis will put forward an argument which agrees with Buzin's original protic mechanism.

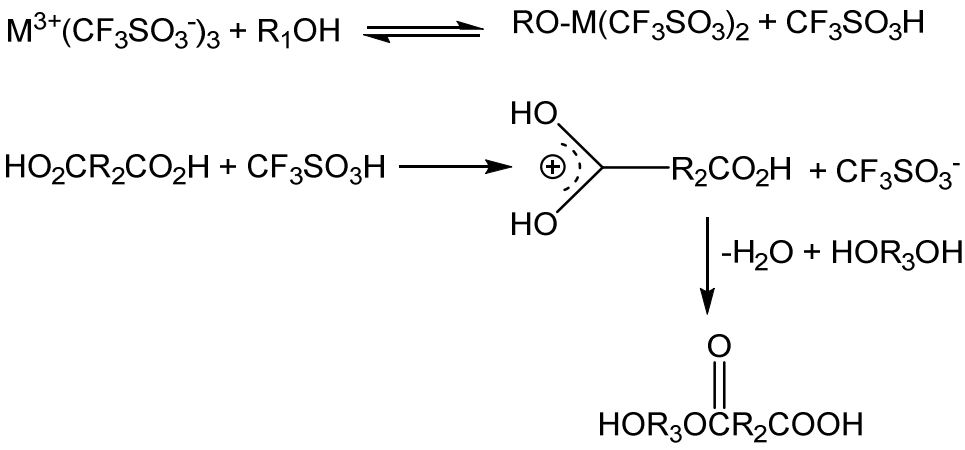


Figure 3-14. Protic esterification mechanism suggested by Buzin et al for triflate catalysts. [41]

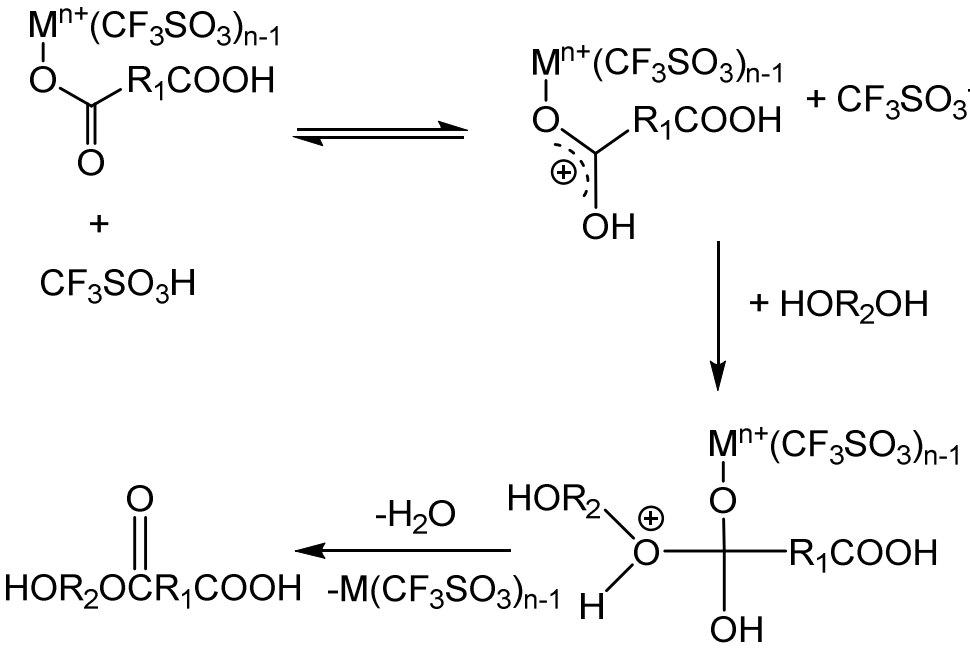


Figure 3-15. Complexation of carboxyl group esterification mechanism for triflate proposed by Garaleh et al. [47]

3.4.1.2 Comparison of Conventionally versus Microwave Heated Organometallic Catalysed Reactions at 185 °C

As reported for the tin catalysts, reactions were conducted at a processing temperature of 185 °C to initially analyse the reaction kinetics using both CH, Figure 3-16, and MWH, Figure 3-17. To aid comparison, the tin results have been included within these figures.

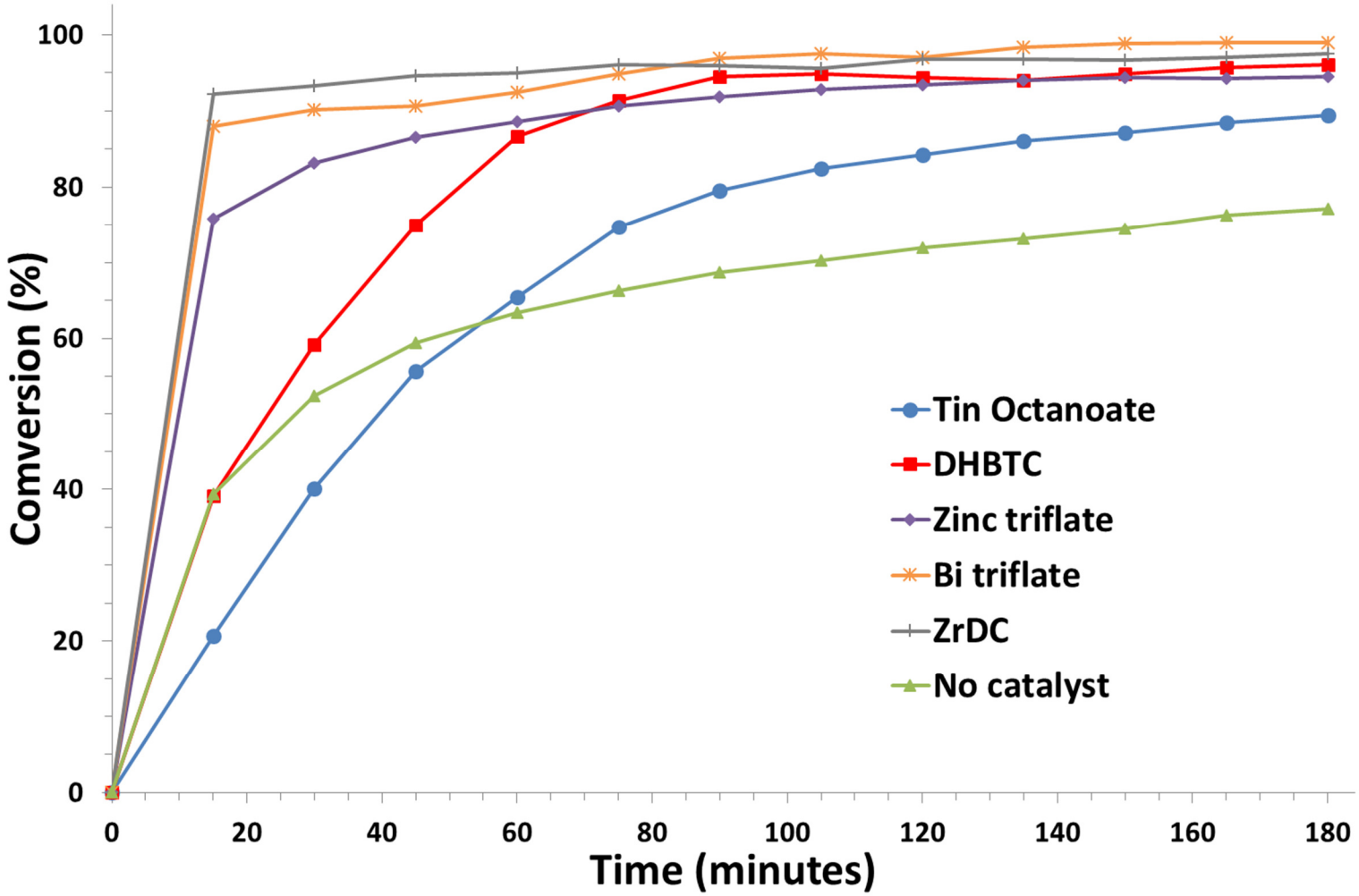


Figure 3-16. Plots of conversion versus time for adipic acid, hexanediol CH polyesterifications at 185 °C using differing metal catalysts with no mass transfer applied.

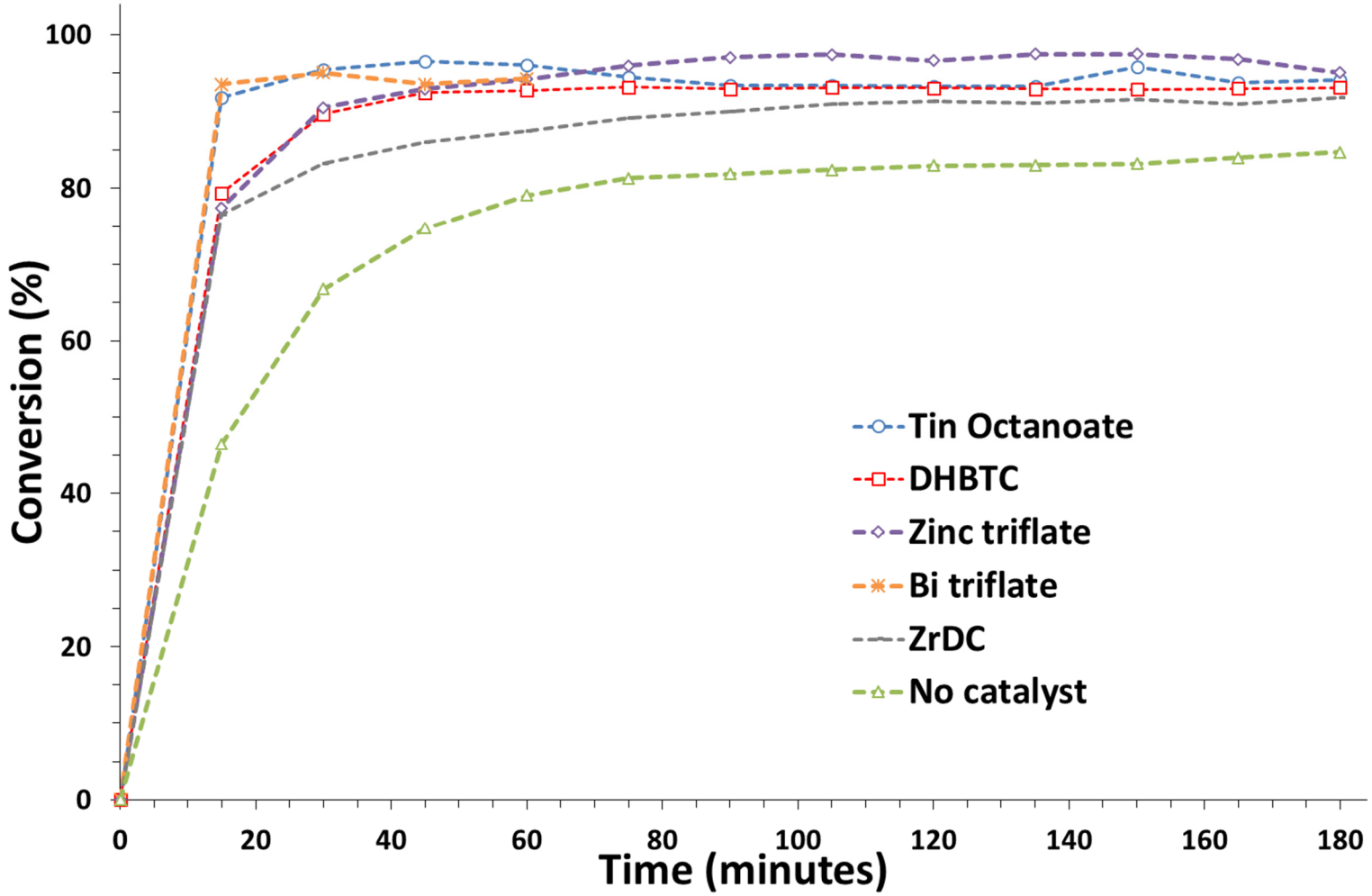


Figure 3-17. Plots of conversion versus time for adipic acid, hexanediol MWH polyesterifications at 185 °C using differing metal catalysts with no mass transfer applied

Figure 3-16 displays that when CH is employed, all of the second generation organometallic catalysts achieve a high conversion in a significantly shorter times than either of the tin catalysts. Even the industrially used DHBTC exhibited a slower initial reaction rate when compared to these alternatives. The conversion after 15 minutes for the CH reactions shown in Table 3-3.

Table 3-3. Polyester conversions after 15 minutes of reaction time for each catalyst system using CH.

Catalyst	[a] Conv. after 15 minutes (%)
Tin Octanoate	21
DHBTC	39
Zinc triflate	76
Bi triflate	88
ZrDC	92
No catalyst	39

[a] Calculated using polymer to monomer peak ratio in ^{1}H NMR.

The data in Table 3-3 indicated a clear dependence on catalyst type for reaction rates of monomer to polyester formation. The results in Table 3-3 and Figure 3-16 also suggested that by using a different catalyst system, CH reactions may be able to be performed at lower temperatures and still achieve relatively fast conversions. This will be discussed further in section 3.4.1.3.

Figure 3-17, which detailed the rate of the experiments with MWH applied, shows that again there is a difference in reaction efficiencies between the heating methods for the catalysts evaluated. This is exemplified in Table 3-5 compares the order exhibited by the different catalysts to achieve a reaction conversion of 90 % when implementing the different heating methods.

Table 3-4. Order at which catalysts enabled the polyesterification to reach 90 % conversion for both CH and MWH.

[a] Rank to 90 % Conv.	CH	MWH
1st	ZrDC	Bi triflate
2nd	Bi triflate	Tin octanoate
3rd	Zinc triflate	Zinc triflate
4th	DHBTC	DHBTC
5th	Tin octanoate	ZrDC

[a] Calculated using polymer to monomer peak ratio in ^{1}H NMR. Note. "No catalyst" did not reach 90 % conversion for either CH or MWH over the cycle time analysed.

Table 3-4 confirms that, no matter what heating method is used, it is crucial that a catalyst is used if a polyesterification is to be commercially viable. If a catalyst is not employed, the activation energy (E_a) is not lowered sufficiently for there to be efficient reaction between the diol and diacids. This was proved by neither CH or MWH achieving a conversion of 90 % after the 180 minute cycle time.

Figure 3-17 and Table 3-4 also demonstrate a change in catalyst efficiencies for the newly adopted organometallic catalysts, as had been observed with the tin complexes. Whilst, ZrDC is the most efficient catalyst in the CH reactions (less than 15 minutes to 90 % conversion), it becomes the least efficient with MWH (90 minutes to 90 % conversion).

From Table 3-4, $Sn(Oct)_2$ is shown to have its reaction efficiency increased by the greatest margin when compared to the other catalysts with MWH application. In CH it is the least efficient catalyst by a considerable margin (90 % conversion in 180 mins), but in MWH it is the second most efficient (90 % conversion in ~15 mins). This finding supports the mechanistic evaluation described in section 3.3.2. This is due to the mechanism of the $Sn(Oct)_2$ catalysed reactions being the only catalyst which promoted ester synthesis *via*

exclusively associative bonds. Using all other catalysts, there are covalent bonds made between the growing polyester chain and the metal. Alternatively, it could be that the other catalyst are not significantly affected by the application of MWH because they are already exhibiting a fast rate of conversion up to 90%. Thus, any difference in the system may be masked by and inability to improve the mass transfer in the system. This will have to be investigated by lower temperature experimentation in section 3.4.1.3.

Considering the triflate catalysts from the CH and MWH reactions displays that in both circumstances the Bi metal centre catalyses the reaction at a faster rate than Zn. This helped determine which mechanism from Figure 3-13 and Figure 3-14 was most likely when correlating with the catalysts pH, shown in Table 3-5.

Table 3-5. pH of triflate catalysts.

Catalyst	[a] pH
Bi triflate	1.37
Zinc triflate	4.96

[a] Calculated using a Mettler Toledo Seveneasy pH meter and dissolving the catalyst at 0.05 mol/L in deoinised H_2O, as in Garaleh et al. [47]

Table 3-5 describes the increased acidity of the Bi triflate sample. Hence, this agreed with the previous report by Buzin *et al.*[41] which suggested the protic mechanism. This protic mechanism also agreed strongly with the reaction rate differences between CH and MWH, as these were similar to the Lewis acid based mechanism in DHBTC. Therefore, the minimal differences between CH and MWH would further suggest this protic mechanism.

Another factor to consider is the dielectric properties of the catalysts at 185 °C which are shown in Figure 3-18.

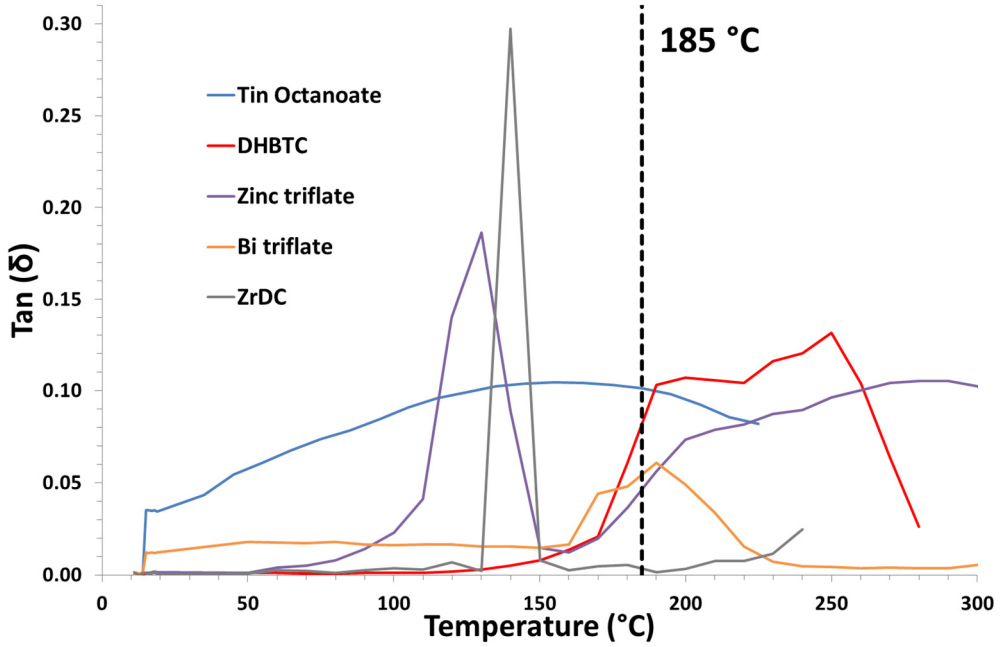


Figure 3-18. Dielectric properties of all catalysts in respect to temperature, calculated using cavity perturbation technique performed at 2.45 GHz after drying of samples in a 120 °C oven.

Figure 3-18 details that at 185 °C, $Sn(Oct)_2$ marginally has the highest tanδ value ahead of DHBTC. Then there is drop to the two triflates and ZrDC is approaching zero. This data trend loosely fits with the order of conversion to 90 % in the MWH reactions, shown in Table 3-4, but, the triflate species are higher than expected. This could suggest that a triflate species is generally a more efficient species when using MWH for polycondensations than the tin and zirconium complexes considered. This could be due to them solvating more readily into the reaction mixture than the other catalysts which would lead to more collisions with the reacting species or the formal charges found on the metal and ligand species in solution (this would lead to significant interaction with the EM field via an ionic conduction mechanism).

The most interesting result from Table 3-4 is from the ZrDC catalyst. When using CH, it is by far the most efficient catalyst, but when using MWH it is the least. This can be explained when examining the dielectric properties of this

material at the chosen reaction temperature. It was shown that the tanδ value is almost zero (approx. 0.002). This, paired with the proposed formal bond formation with the metal centre mechanism described in Figure 3-13 quantitatively shows that the catalyst selection is a very important aspect when considering MWH as a viable option for a linear melt polyesterification. The difference in the reaction profile of the triflates and tanδ values also suggest that the metal centre plays an important role in MWH reactions.

The polyesters synthesised using the organometallic catalysts were subject to standard polymer analysis techniques which are detailed in the following discussions.

3.4.1.2.1 Size Exclusion Chromatography (SEC) of Adipic Acid, Hexanediol Reaction at 185 °C Using Organometallic Catalysts

To analyse the polyesters MWt values, Gel Permeation Chromatography (GPC) was conducted to evaluate their M_n^{GPC}, M_w^{GPC},M_p^{GPC} and polydispersities (Đ). A typical GPC trace for these polyesters is shown below in Figure 3-19.

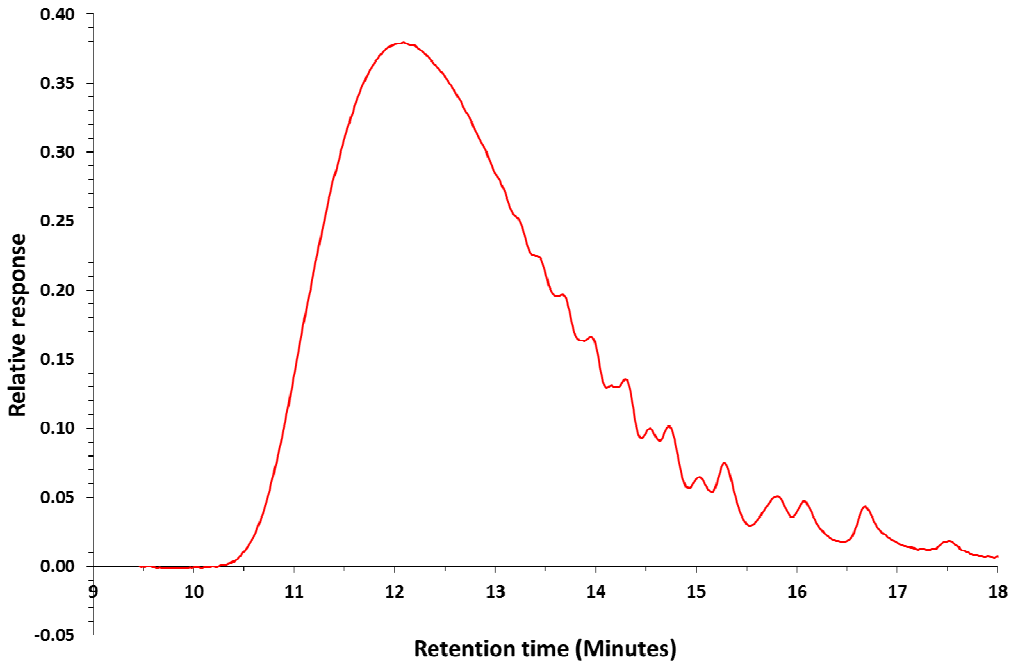


Figure 3-19. Typical GPC trace for a polyester. Sample shown is a polyester synthesised using $Sn(Oct)_2$ catalyst and MWH.

A polyester GPC trace has a typical characteristic in the form of the "long tail" towards the longer retention times. This is shown in the trace above by the response signal after the maximum (~12.5 minutes). This "long tail" is typical due to the high amount of shorter, oligomeric chains synthesised in polycondensations. It is typical to have a large amount of oligomeric species in a polyester sample due to the slow nature of building high MWt chains (chapter 1 section 1.3.2).

The GPC MWt data for the polyesters synthesised using the differing catalysts is detailed below in Table 3-6.

Table 3-6. GPC data for AA HD reactions at 185 °C using different metal catalysts.

Catalyst	Heating method	[a] Final Conv. (%)	[b] M_n^{GPC} (g.mol^{-1})	[b] M_w^{GPC} (g.mol^{-1})	[b] M_p^{GPC} (g.mol^{-1})	[b] $Đ^{GPC}$
None	CH	77	1,000	1,820	1,480	1.83
	MWH	85	1,660	2,300	2,200	2.33
DHBTC	CH	96	4,580	10,700	12,500	2.36
	MWH	93	2,460	6,380	6,980	2.59
Tin Octanoate	CH	89	1,580	3,630	1,940	2.07
	MWH	94	3,900	8,940	10,300	2.33
Zinc triflate	CH	98	1,760	3,700	3,210	2.08
	MWH	95	1,760	3,840	3,750	2.18
Bismuth triflate	CH	99	400	580	370	1.43
	MWH	89	940	570	320	2.44
ZrDC	CH	95	2,980	7,160	7,150	2.43
	MWH	92	2,510	5,150	5,600	2.08

a Calculated using polymer to monomer peak ratio in 1H NMR. b Calculated using THF GPC and ASTRA processing software relative to a polystyrene standard.

Generally, larger M_n, M_w and M_p's are observed in the samples with higher conversions. This was expected as a higher conversion is directly related to a larger percentage of the monomers/oligomers reacting to form higher molecular weight polymer. Also, the Đ's are approximately 2.0, which is an expected value for a polyester due to the high amount of oligomeric species, as described in Figure 3-19 and in accordance with the Flory-Schlutz distribution. [2,48]

From Table 3-6, the Bi triflate samples produced unexpected GPC results. When using this catalyst, the highest conversion rate had been observed in both heating method reactions when compared to the other catalysts. Thus, it was expected to exhibit the highest M_n^{GPC} value. But, the GPC data suggested that it contained species that were primarily dimeric to tetrameric (M_n^{GPC} = 400 g.mol^{-1} for CH and 940 g.mol^{-1} for MWH). Additionally, a Đ value of 1.43 was recorded

for the CH reaction which suggested that either polymer decomposition (i.e. depolymerisation) had occurred or that this catalyst was only efficiently catalysing monomer to low oligomer formation and not that of oligomer to polymer.

This decomposition/lack of polymer formation was also observed visually when inspecting and comparing the final product characteristics of the polyesters. All of the catalysed products formed a waxy solid with colours from colourless to dark yellow with the exception of the Bi triflate catalysed polyesters which produced a brown, oil substance with a layer of yellow oil on top.

One hypothesis was that the oxidation of the Bi with atmospheric air occurred and caused this discolouration/decomposition of the catalysts such that the polymerisation is halted and/or promotes depolymerisation. This hypothesis was tested by conducting a polycondensation at 185 °C under an inert atmosphere. But, the final product from this inert reaction was identical to the non-inert product, thus this was concluded not to be the root cause of this observation and the following hypotheses were proposed.

Bi triflate was not stable at higher temperatures (in the previous work by Buzin *et al.* the reactions were conducted at 80 °C) [41] and so degrades over time and thus is deactivated during the oligomer formation. This degradation therefore contaminated the reagents and no polymerisation occurred. However, the literature recorded melting point of Bi triflate is above 300 °C, so it was thought that it should not have degraded below this temperature.

Hence, the most probable explanation was that the Bi triflate catalyst reacts with the water condensate to degrade the catalytic species *via* hydrolysis.

3.4.1.2.2 Colorimetry - Gardner Scale (GS) Colour Analysis of Adipic Acid, Hexanediol Reaction at 185 °C Using Organometallic Catalysts

Due to the fact that the polyesters being synthesised are being considered for coatings, a quantitative method of colour analysis was desired. This is because a colourless polyester is easier to use as a base to add pigment. Therefore, Gardner Scale (GS) colour analysis was performed on all the products. The GS is a colour analysis technique used by industry to test to what extent a resin, surfactant, fatty acid *etc.* has "yellowed/browned" during a reaction/processing. [49] It has been used in this thesis to analyse what effect the catalyst and heating method had on discolouring the polyester materials synthesised. The technique methodology is explained in detail in chapter 2 section 2.4.6 using a Lovibond PFXi-950 and the results are shown below in Table 3-7.

Table 3-7. Gardner scale analysis of AA HD polyester synthesised at 185 °C using different catalysts and heating methods.

Catalyst	Heating method	[a] GS Number	[a] GS Hue
Tin Octanoate	CH	6.5	7.0
	MWH	7.9	11.0
DHBTC	CH	0.5	0.0
	MWH	0.2	0.0
Zinc triflate	CH	3.6	1.0
	MWH	7.2	7.0
Bi triflate	CH	[b] too dark for analysis	
	MWH	8.6	6.0
	inert atmosphere	16.0	6.0
ZrDC	CH	5.9	5.0
	MWH	4.2	3.0
No catalyst	CH	0.2	0
	MWH	2.2	0

[a]Calculated using a Lovibond PFX1-950 and GS colour standards 1-18.
[b]sample double diluted to achieve a number of 16.7 and hue of 9.0.

Relating the data described in Table 3-7 to the previous section on MWt's, the CH Bi triflate catalyst produced a product that had a GS number which was unmeasurable, *i.e.* it was too dark to measure a value at the specified concentration. This further suggests there was depolymerisation or degradation of the catalyst. To obtain a value, the sample was doubly diluted but even at this level the value measured was still exceptionally high (16.7). When comparing the MWH to the CH sample of Bi triflate catalysed polyesters, it was shown that the MWH sample had a reduced GS value, indicating less discolouration. This suggested that the heating mechanism that was active in MWH could help minimise the effect of hydrolysis of the catalyst. However, this trend of MWH producing lower GS numbered products was not observed for all the catalysts. Overall, considering the catalysts, the GS analysis shows that there is no obvious trend between the discolouration of the product and the heating method/conversion. Thus, this suggested that the catalyst selection is the dominant factor in product discolouration.

This conclusion is exemplified by the polymerisation using DHBTC, Bi triflate and ZrDC, exhibiting a lower GS number when implementing MWH. Whilst in those using tin octanoate, zinc triflate and no catalyst it is the CH method which produces the lower GS number.

The catalyst dielectric heating efficiency in the microwave at reaction temperature was then compared to the GS number of the product. This was achieved by plotting the tanδ value at 185 °C against the GS number, and the following association was observed (Figure 3-20).

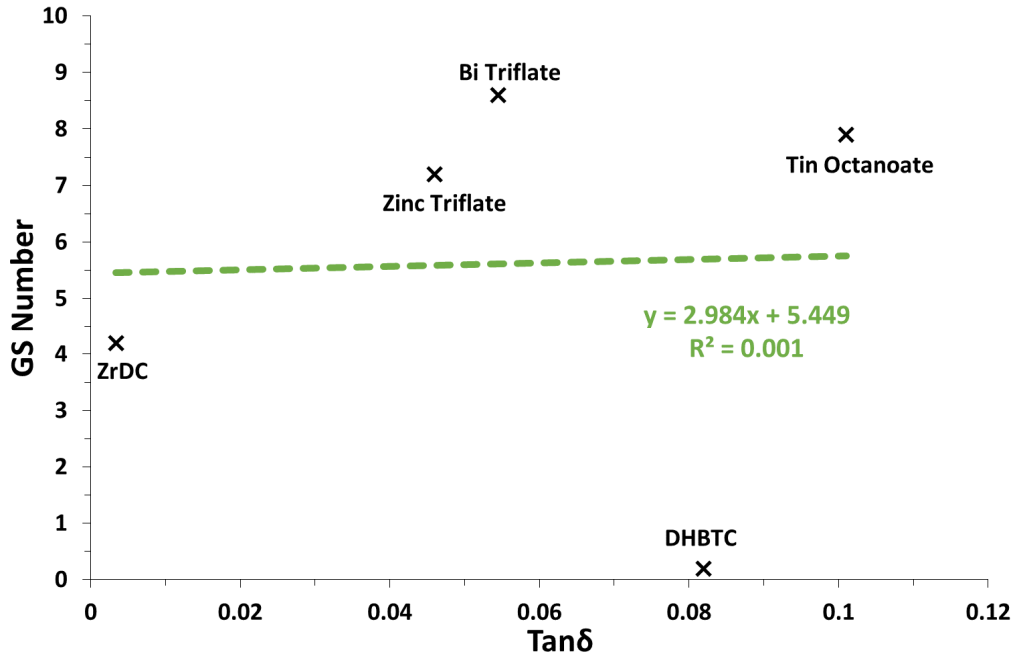


Figure 3-20. Plot of the relationship between tanδ value at reaction temperature and GS number for an adipic acid, hexanediol polycondensation at 185 °C using MWH. Green line indicates the line of best fit.

From the plot in Figure 3-20 there is no suggestion of a trend between tanδ and GS number of the MWH product. This, therefore, suggested that the discolouration observed when particular catalysts were employed in the MWH polymerisations was independent of the heating method. This conclusion was proposed because, if discolouration was promoted in MWH at this reaction temperature, then the catalysts with higher tanδ values would create a more discoloured product. This is because a catalyst with a higher tanδ would lead to a larger proportion of EM energy heating the catalyst and this would therefore have led to the catalyst hydrolysis reactions being promoted.

However, if the value derived for the DHBTC is discounted from the comparison, there is a much stronger positive exponential trend between catalyst EM interaction and GS number (R^2 = 0.8918 (Figure 3-21) compared to 0.0010 (Figure 3-20)). The differentiated behaviour of the DHBTC catalyst could

potentially be due to the difference in the catalysts structure. In all the other catalysts investigated the metal is an ion being balanced by counter ions. Whereas, the DHBTC catalyst contains ligands formally bonded to the metal centre. Therefore, it would be expected that the mechanism in which it is effected by the EM field would be differentiated from that of the other catalyst but also this structure may mean that the catalyst is less likely to undergo hydrolysis.

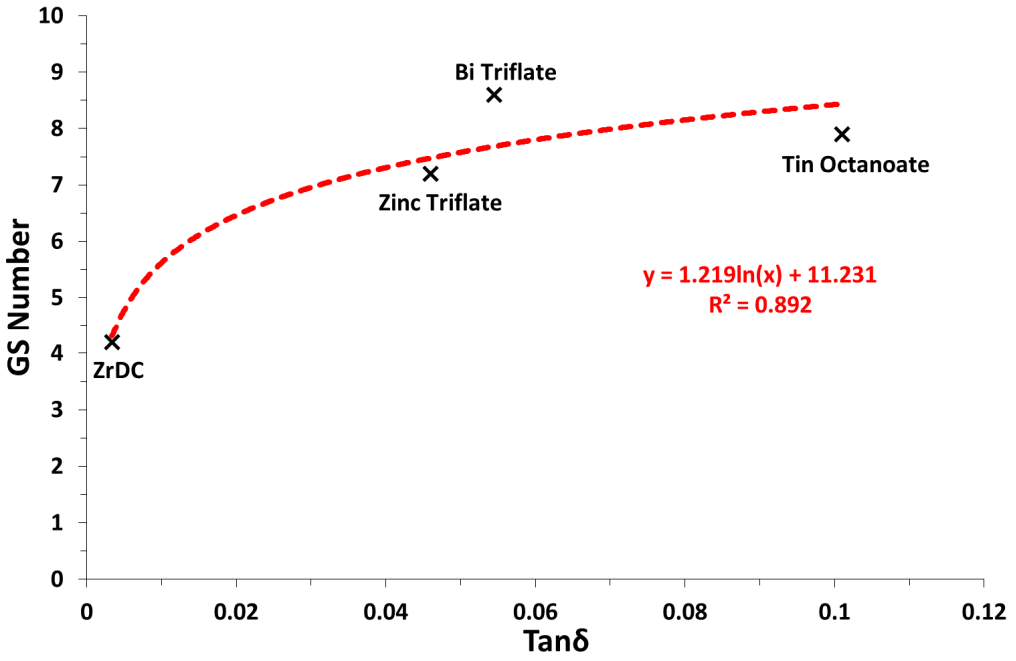


Figure 3-21. Plot of the relationship between tanδ value at reaction temperature and GS number for an adipic acid, hexanediol polycondensation at 185 °C using MWH with DHBTC omitted.

In the case of $Sn(Oct)_2$ it was interesting that the product produced such a high GS number as the product was visually colourless compared to some other products with lower GS numbers, Figure 3-22.

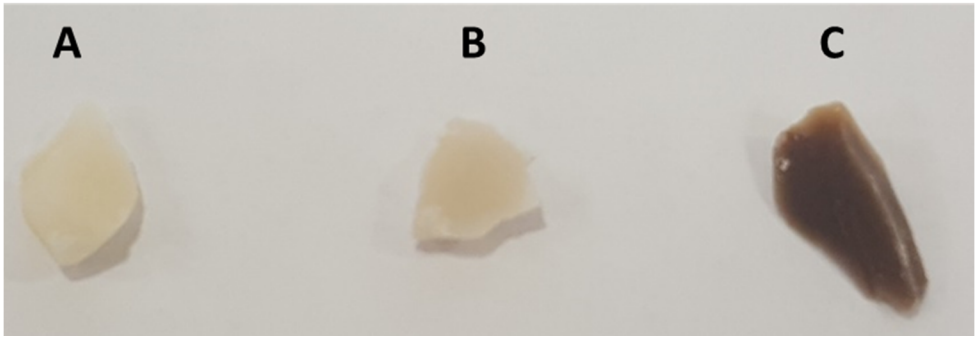


Figure 3-22. Picture of three polyester samples produced under CH using different catalysts. A = $Sn(Oct)_2$, B = Zinc triflate, C = ZrDC.

The sample containing $Sn(Oct)_2$ (sample A, Figure 3-22) is visually a similar level of “whiteness” to the sample containing Zinc triflate (sample B) and both much whiter than the sample containing ZrDC. Therefore, sample A would not be expected to exhibit a GS number as high as was recorded. However, the GS evaluation also takes into account the Hue of the dissolved sample which is related to the sample clarity when it is being analysed. In the case of $Sn(Oct)_2$ this helps explain why its GS number was measured to be so high, because it is only sparingly soluble in the THF, as shown in Figure 3-23.

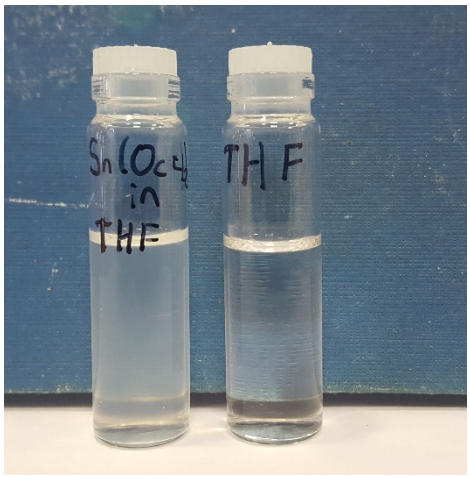


Figure 3-23. Solubility of $Sn(Oct)_2$ in THF, left, compared to pure THF, right.

Consequently, it should be noted that the solubility of the catalyst and polymer may have an influence on this colour defining technique. In this study, this

potential skewing of the results was reduced as much as possible by the application of long stirring times and identical concentrations in the analytical process.

Comparing conversion versus GS number showed that, again, there was no strong trend observed in either the MWH, CH or by analysing both sets of data as a whole, Figure 3-24.

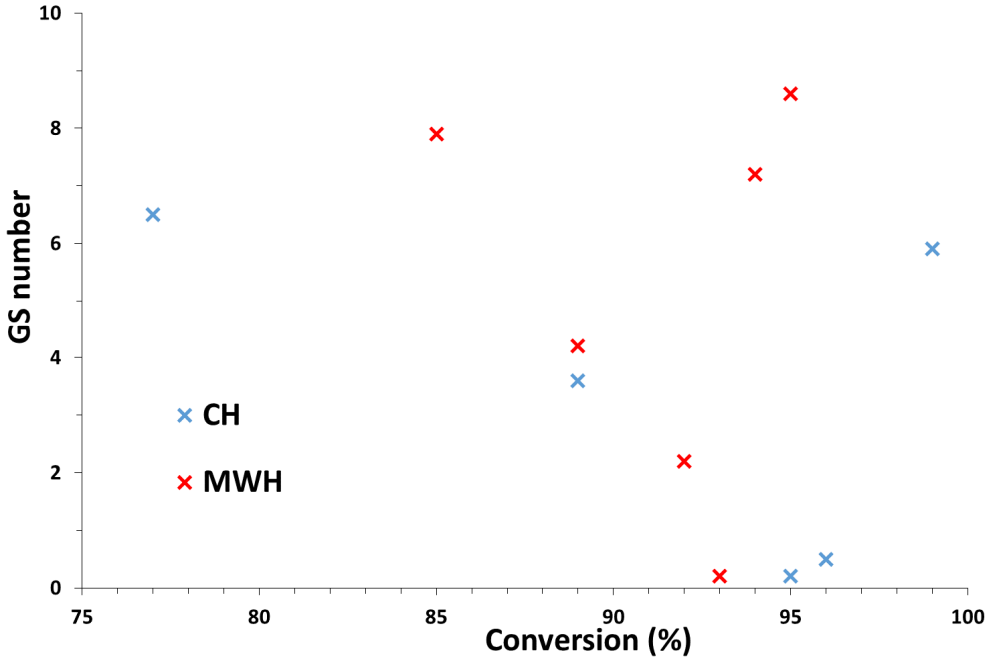


Figure 3-24. GS number versus conversion trend for AA, HD polycondensations using different catalysts and heating methods. X-axis plot starts from 75 % conversion. Note. The CH Bi triflate catalysed reaction has been omitted due to having a too high GS number to analyse.

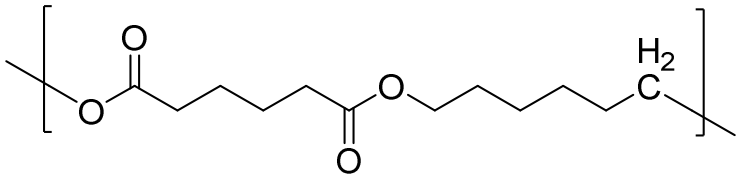
With no general trend shown in Figure 3-24, it was concluded that the level of conversion achieved does not play a crucial role in discolouration of the product. Therefore, it was proposed that metal type is much more important.

Temperature effects on colour will be discussed later in this thesis in section 3.4.1.3.2.

3.4.1.2.3 Matrix Assisted Laser Desorption/Ionisation-Time of Flight Mass Spectrometry (MALDI-ToF MS) for Repeating Unit Analysis of Adipic Acid, Hexanediol Reaction at 185 °C Using Organometallic Catalysts

Following the method described in chapter 2 section 2.4.5, MALDI was performed on the polyester samples. This was conducted to determine whether there was a clear repeating unit observed *via* this type of analysis and assessment of the end group functionality. For the products produced in this section a mixture of end groups was expected i.e. one OH and one COOH. This was because the stoichiometry of the reaction was 1:1, therefore there was an identical amount of acid to hydroxyl groups. This therefore should statistically create a mixture of end functionalisation.

For the AA, HD polyester, the repeating unit is shown below in Figure 3-25.



Exact Mass: 228.14

Figure 3-25. Repeating unit of AA, HD polymer in MALDI analysis with exact mass.

For all samples discussed in this section, there was the consistent, repeating unit (*e.g.* in Figure 3-26) of 228.14 observed and therefore this confirmed the identity of polyester that had been synthesised. The only exception to this were the Bi triflate samples which did not produce a MALDI spectrum, further suggesting that no polyester had been formed. It confirmed that only oligomers had been produced which were all present tin the matrix zone of the MALDI data and so must be discounted.

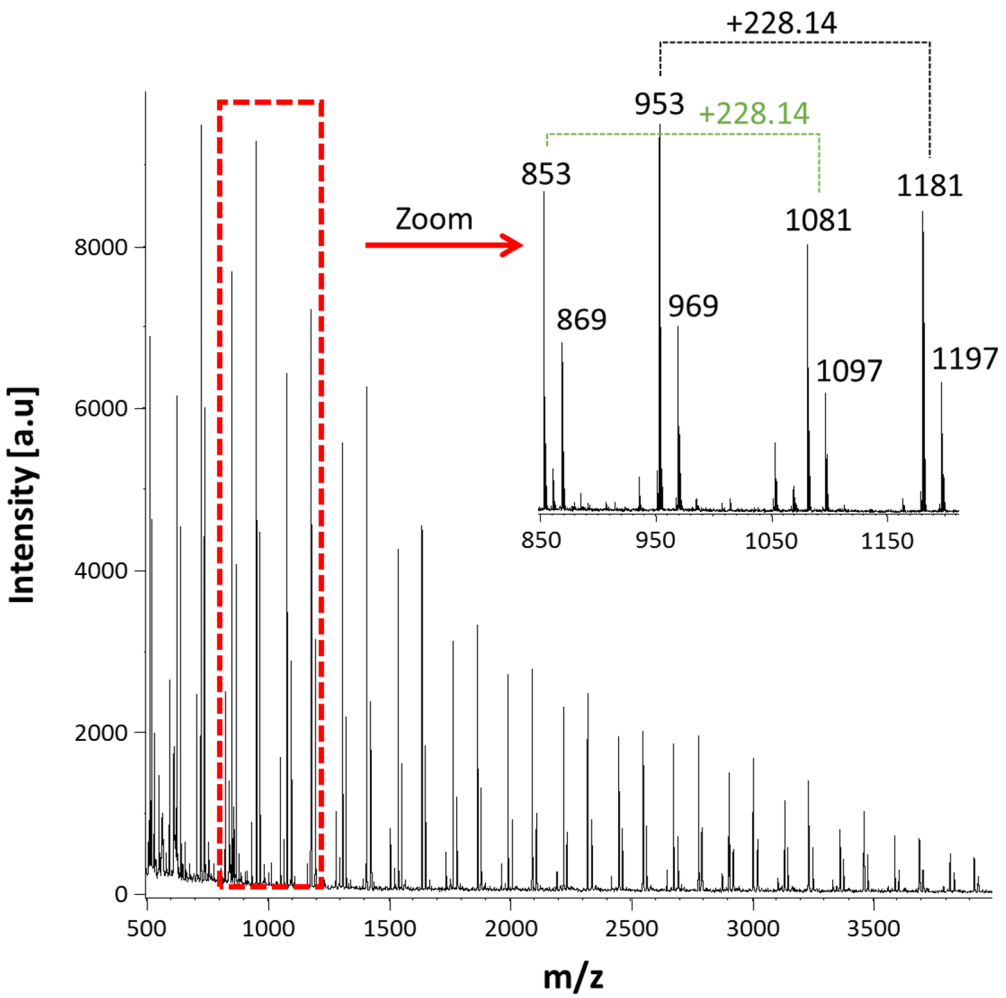


Figure 3-26. Standard MALDI spectra for a synthesised adipic acid, hexanediol polyester, showing the 228.14 repeating unit gap. The spectra shown is from polymer produced using the zirconium catalyst and CH.

The most prominent series shown in Figure 3-26 centres around m/z = 953.36, with a 228.14 gap (shown in black). This peak represents a charged polyester fragment which is balanced by a sodium counter ion and is terminated by a mixture of end groups, *i.e.* one end is carboxyl (COOH) and one end is hydroxyl (OH). This suggests that all polyesters synthesised contain material which possess a mixture of OH and COOH terminal groups. The exception to this was the material synthesised with the zinc catalyst the results from which are discussed below.

A secondary fragmentation series was observed in Figure 3-26, which is shown in green. This was related to material that was a doubly COOH terminated series. Again, this secondary series was observed in all the samples with the exception of that synthesised using the zinc catalysts, the data from which is discussed below.

The polyester which presented an alternative primary and secondary series in the MALDI data was that produced using the zinc triflate catalyst. Using this catalyst and both heating methods created a polyester with the green COOH terminated series as the primary product, as shown in Figure 3-27.

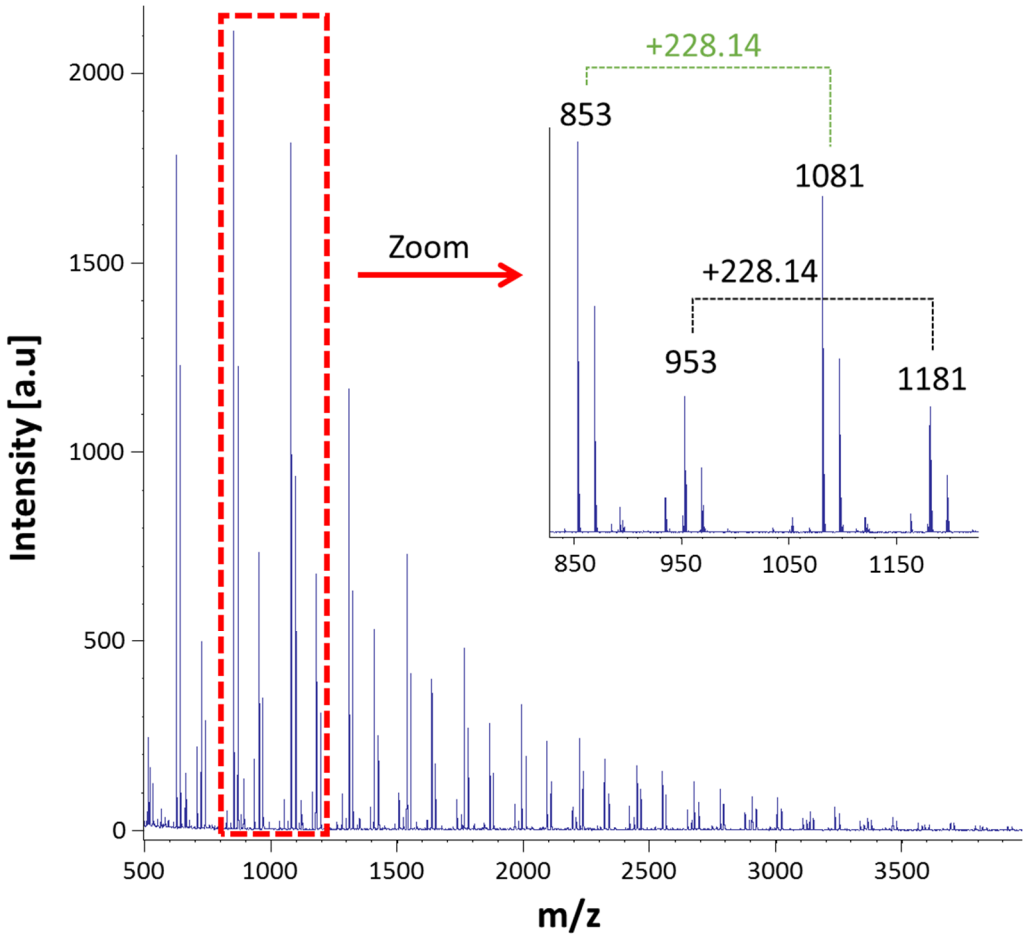


Figure 3-27. Zinc triflate catalysed AA, HD polyester, showing a different primary series to the other catalysts.

Although MALDI is not a quantitative technique *i.e.* the highest peak does not necessarily correlate to the most abundant chain length, due to different fragments having different affinities to being fired down the MALDI chamber. This difference in primary peak showed that there was a different terminal series by changing the catalyst because the polymers synthesised in this section were of identical monomer composition and therefore the fragments of each separate sample had the same affinity to be ionised and fly down the spectrometer.

Therefore, this was a positive result for a coatings application because it is commonplace to create a pre-polymer, either OH or a mixture of end groups, which is then reacted further with an excess of acid to create a COOH terminated polyester. [50,51] This COOH terminated polyester can then be cured using a cross-linking agent to form a hard, durable coating. [52,53] Hence, creating a COOH terminated polyester at a 1:1 molar ratio of diol to diacid could be a substantially beneficial synthesis route for a powder coating as it reduces the number of stages within the process and removes the need for a stoichiometric excess of diacid or diol, potentially improving batch to batch consistency.

3.4.1.2.4 Acid Value Titration Analysis of Adipic Acid, Hexanediol Reaction at 185 °C Using Organometallic Catalysts

To support the findings from the MALDI data, acid value (AV) analysis was conducted on the polyesters. The technique and brief background is described in chapter 2 section2.4.3. This analysis allowed determination of how acidic the samples were and therefore gave an indication of end group composition as well as conversion of monomer. The data for the polycondensations is shown below in Figure 3-28.

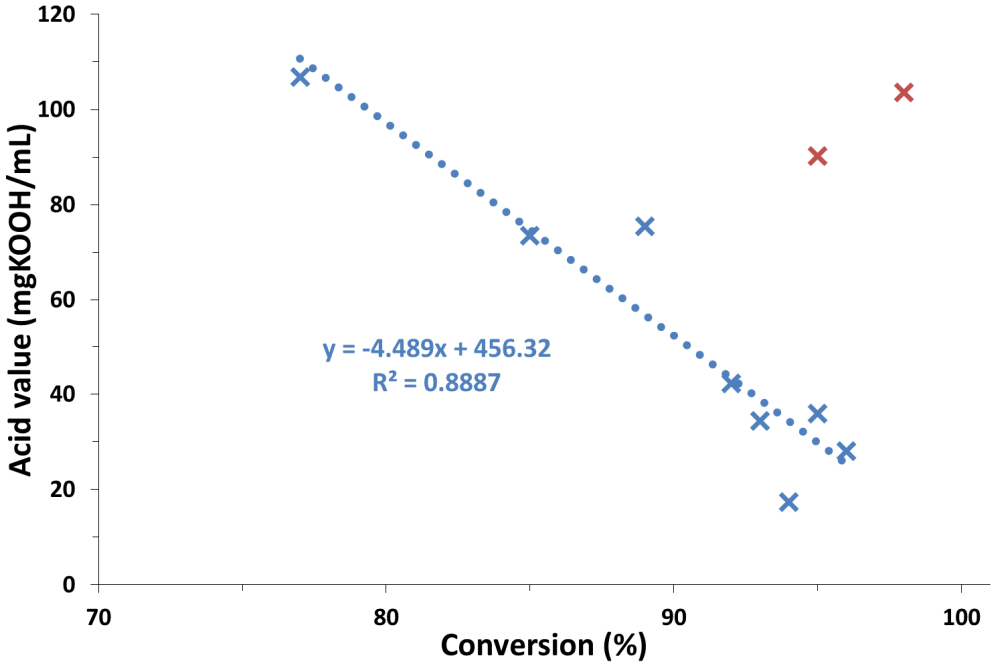


Figure 3-28. Plot of conversion versus acid value of adipic acid, hexanediol polycondensations using the studied organometallic catalysts at 185 °C. Red crosses = zinc triflate catalysed samples. Blue crosses = $Sn(Oct)_2$, DHBTC, ZrDC and no catalysed samples.

The data presented in Figure 3-28 is divided into 2 data sets. The blue data set described the AV of the polyesters synthesised using the catalysts; $Sn(Oct)_2$, DHBTC, ZrDC and no catalyst, and the red data set the zinc triflate. There are no data points included for the Bi triflate catalyst as the solution was too dark to enable any colour change in the titration solution to be defined and consequently AV analysis was impossible to perform.

When considering the blue data set, it is clear that a polyester which was processed to a high conversion had a low AV and vice versa. This was expected as the more converted a polymerisation reaction mixture is, then the less monomer and so chain ends there will be present. This leads to less acidic groups in the sample and so it requires less KOH to neutralise the sample. This strong trend is demonstrated by a high R^2 value of 0.8887 between the data points.

The red series was generated from polymerisations using zinc triflate as the esterification catalyst. The data was discounted from the overall data set when calculating the linear fit above. This was because the product indicated the differential terminal group characteristics as discussed with the MALDI results. Therefore, the product's data (a) lie significantly away from the trend line defined by the other organometallic catalysts and (b) does not follow the expected "higher conversion = lower AV" trend like all the other data points (however there are really too few points to define that this trend definitively). These observations suggests the following hypotheses:

i. Zinc triflate is a poor polycondensation catalyst's and creates many oligomeric species, leading to high conversion but low M_n.
ii. A high percentage of the chains are COOH terminated.

Consequently, by cross-referencing this data with the GPC and MALDI data the following conclusions were drawn.

The M_n^{GPC} proposes that for both MWH and CH a DP of between 7 and 8 was observed, which is in the oligomeric region. This is lower than similar conversions exhibited by the other catalysts (e.g. DHBTC CH DP = ~20 @ 96 %, MWH DP = ~11 @ 93 %), suggesting an increased amount of shorter chains were created than with the other catalysts which contributed to the explanation of the higher AV. Thus, to further define which of the hypotheses above were responsible for the apparent anomalous data, the MWH polymerisation with no catalyst and CH $Sn(Oct)_2$ reactions, which have very similar M_n^{GPC} values as the exhibited by the product from the zinc triflate reactions were cross-referenced, this comparison is shown in Table 3-8.

Table 3-8. Comparison of zinc triflate AV's compared to polyesters using different catalysts with similar M_n^{GPC} values.

Catalyst	Heating Method	[a] Final Conv. (%)	[b] M_n^{GPC} ($g.mol^{-1}$)	[c] AV (mgKOOH/g)	[d] M_n^{AV} ($g.mol^{-1}$)
Tin Octanoate	CH	89	1,580	75.44	740
No catalyst	MWH	85	1,660	73.45	760
Zinc triflate	CH	98	1,760	103.64	540
Zinc triflate	MWH	95	1,760	90.27	620

[a] Calculated using polymer to monomer peak ratio in ^1H NMR. [b] M_n^{GPC} calculated using THF GPC with polystyrene standards. [c] Calculated using titration against 0.1M KOH. [d] Calculated using the modified Stockmayer equation (M_n^{AV} = 56,000/AV)

Table 3-8 indicates a M_n^{GPC} spread of approximately 200 $g.mol^{-1}$ and an M_n^{AV} spread of 220 $g.mol^{-1}$ between the samples, which equates to less than one repeating unit. Therefore, if the same terminal group combinations were present in all of these samples, the AV's should be similar. This is shown to be the case when comparing the $Sn(Oct)_2$ and no catalyst reaction products, were the AV differs by 2 units. However, the data from the zinc triflate products exhibited both (a) significantly higher AV's than $Sn(Oct)_2$ and no catalyst (30 and 15 units for CH and MWH respectively) and (b) difference between the samples produced by MWH and CH which have exhibited the same GPC predicted MWt.

Therefore, there was significant evidence which suggested an excess of COOH terminated polyesters. This was due to COOH termination being the primary series for the zinc triflate catalyst in MALDI analysis and the AV's of the zinc triflate samples being significantly higher than comparable MWt samples from products catalysed using other catalysts. This result has been shown to be true for both heating methods with CH and MWH achieving notably higher AV's than other catalysts. This difference between the catalysts can be explained by the mechanisms and polymerisation environments being different between the

catalysts. The protic mechanism employed in the triflate catalysis cycle promoted acidic terminal groups as these are the species which are formed for the diols to react with. But, in Bi triflate, the acidity of the catalytic solution is so high (pH = 1.37) that there is quick addition of diol to the end groups to counter balance this. Whereas, the zinc catalysts was acidic enough to catalyse the reaction, but not promote diol capping due to the milder acidic conditions (pH = 4.96).

Comparing the heating methods showed that there was an increase in AV and therefore in COOH termination with the application of MWH. This suggested that by implementing MWH there is a specific heating mechanism which promoted the formation of COOH terminal groups. It can also be of interest to industry for the previously discussed single step reaction potential and cross-linking benefits. However, this increase in AV may be because of the reduced conversion percentage, meaning there was more monomeric species in the product which would increase AV through an increase number of end groups.

3.4.1.2.5 Differential Scanning Calorimetry (DSC) Adipic Acid, Hexanediol Reaction at 185 °C Using Organometallic Catalysts

To assess the thermal properties of the polyesters synthesised, the samples were subjected to DSC analysis following the methods described in chapter 2 section 2.4.2. This was conducted to assess whether the polyesters synthesised agreed with the known literature values. For the AA, HD polyester, a T_m of 55 – 65 °C was expected for a M_n = 3,800 g/mol^{-1}. [54] A typical DSC trace is shown below in Figure 3-29. In Figure 3-30 T_m is plotted against final conversion and M_n^{GPC} to enable any trend in the data to be defined.

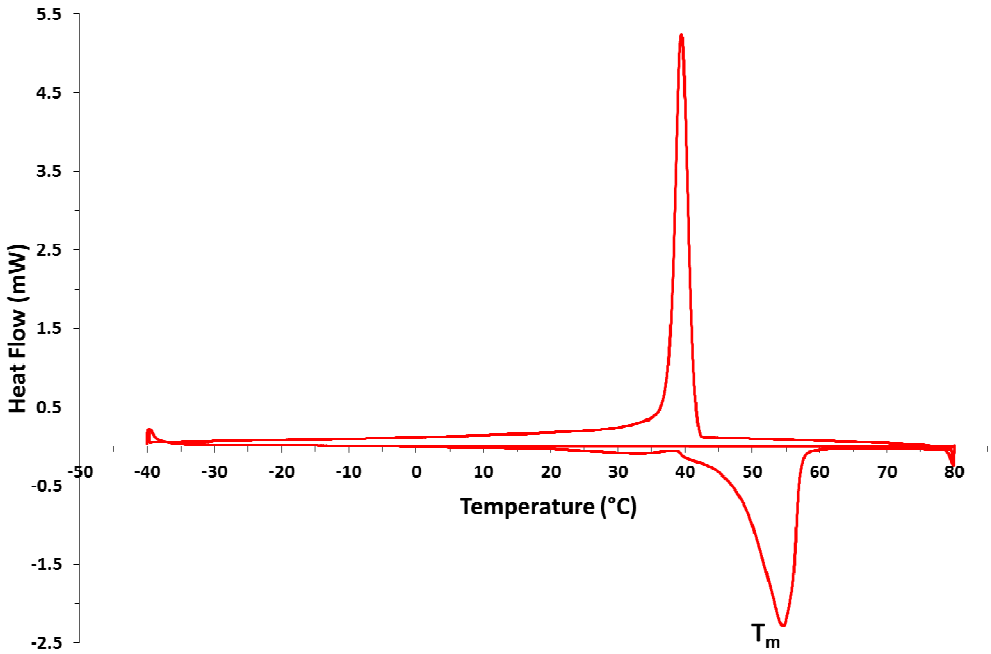


Figure 3-29. A typical DSC trace. Example shown is for DHBTC using CH.

For both plots in Figure 3-30, the Bi catalysed samples are omitted because there was no T_m peak in the DSC traces, this was regarded as further evidence that there was no polyester synthesised. Also, the zinc triflate catalysed samples have been omitted in the best fit calculations as it had been shown that this catalyst created a highly converted polyester with low M_n^{GPC} values and a potentially different combination of end-groups. But, for comparison the points have been included in the plots.

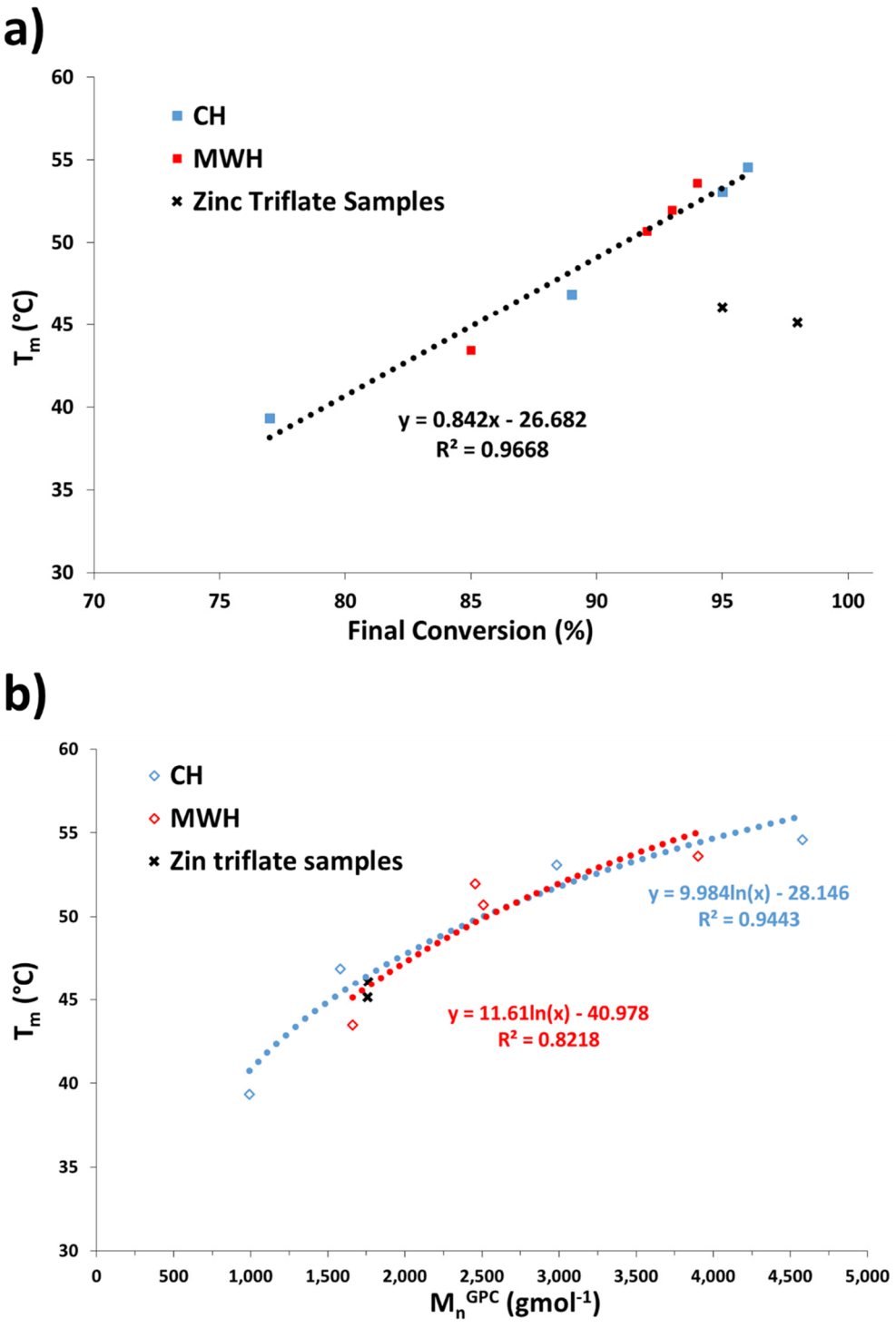


Figure 3-30. Graphical comparison of adipic acid, hexanediol polyesters synthesised at 185 °C of a) final conversion versus Tm compared to b) M_n^{GPC} versus T_m with CH and MWH in different colours for each graph. Blue = CH, red = MWH, ■ = Final conversion versus T_m and ◊ = M_n^{GPC} versus T_m. Note: for both plots the x-axis starts from 30 °C and for plot "a)" the y-axis from 60 % for clarity.

Assessing the values in graph (a), Figure 3-30, there was a strong trend between final conversion and T_m which suggested a higher final conversion is equal to a higher T_m value. This is a common result as a higher conversion from monomer to polymer equals a longer chain. Considering both CH and MWH data sets the data trends are closely aligned and therefore one best fit line is assigned to them. This suggested that heating method does not affect the relationship between final conversion and T_m. Considering graph (b), Figure 3-30, there was a general trend of a higher M_n^{GPC} value leading to a higher T_m, however, the data followed a logarithmic fit and began to plateau. This suggested that once a certain/critical T_m was achieved, an increase in MWt would not increase the product's thermal properties. This is expected as once a high MWt is achieved the difference in length between the polymer chains is proportionately decreased. Therefore, a maximum T_m is achieved for each polymer sample.

This suggested that high temperature processing led to better MWt control when using CH. This occurs because of the different heating efficiencies in the reaction mix due to the difference in catalyst tanδ values and the difference in reaction mechanisms. To probe the underpinning reasons behind this difference, tanδ at reaction temperature was correlated to T_m, and this data is shown in Table 3-9.

Table 3-9. Correlation between tan of organometallic catalysts and T_m of the polyesters synthesised at 185 °C.

Catalyst	[a] tanδ	[b] T_m (°C)	[c] M_n^{GPC} (g.mol^{-1})
Tin Octanoate	0.101	53.6	3,900
DHBTC	0.082	52.0	2,460
ZrDC	0.003	50.7	2,510

[a] Calculated using cavity perturbation technique. [b] Calculated using a TA-Q2000 DSC.[c] Calculated using THF GPC and ASTRA processing software relative to a polystyrene standard.

The data in Table 3-9 proposed there was a positive relationship between the tanδ of the catalyst and the observed $T_{m,}$ with a higher tanδ value correlating to a higher T_m, but these also generally followed M_n^{GPC}. This suggested that by implementing a highly dielectrically active catalyst when implementing MWH, the reaction was processing at a faster rate, increasing polyester MWt and inherent thermal properties. It also proposed that the associative mechanism suggested for the $Sn(Oct)_2$ mechanism does aid quick promotion of polyester formation over a Lewis acid based system, likely due to the non-ionising nature of MWH promoting the associative forces in the $Sn(Oct)_2$ mechanism more so than the formal bond making/breaking in the Lewis acid catalysis.

3.4.1.3 Conventionally versus Microwave Heated Reactions at 150 °C

As previously investigated with the tin catalysed system, the effect of implementing a lower temperature was considered. This was of specific interest because such efficient conversions were being achieved at 185 °C that it made probing the differences in behaviour of the different systems more difficult. Therefore, it was proposed that lowering the temperature would allow the reaction to be analysed in greater detail. Again, reactions were conducted for both CH and MWH and this data is presented below in Figure 3-31 and Figure 3-32.

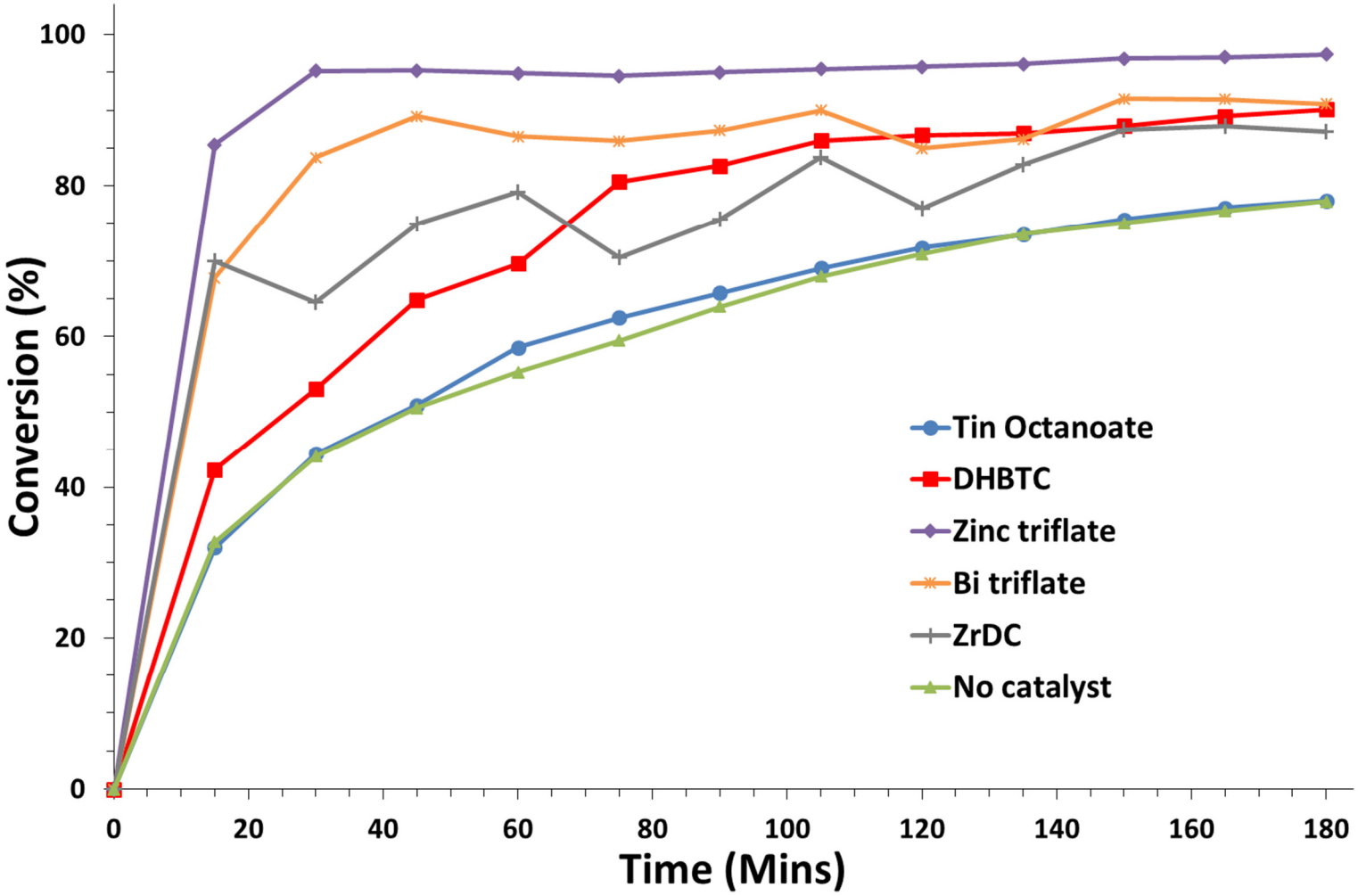


Figure 3-31. Plot of conversion versus time for adipic acid, hexanediol polyesterifications at 150 °C with CH using differing metal catalysts and with no mass transfer applied.

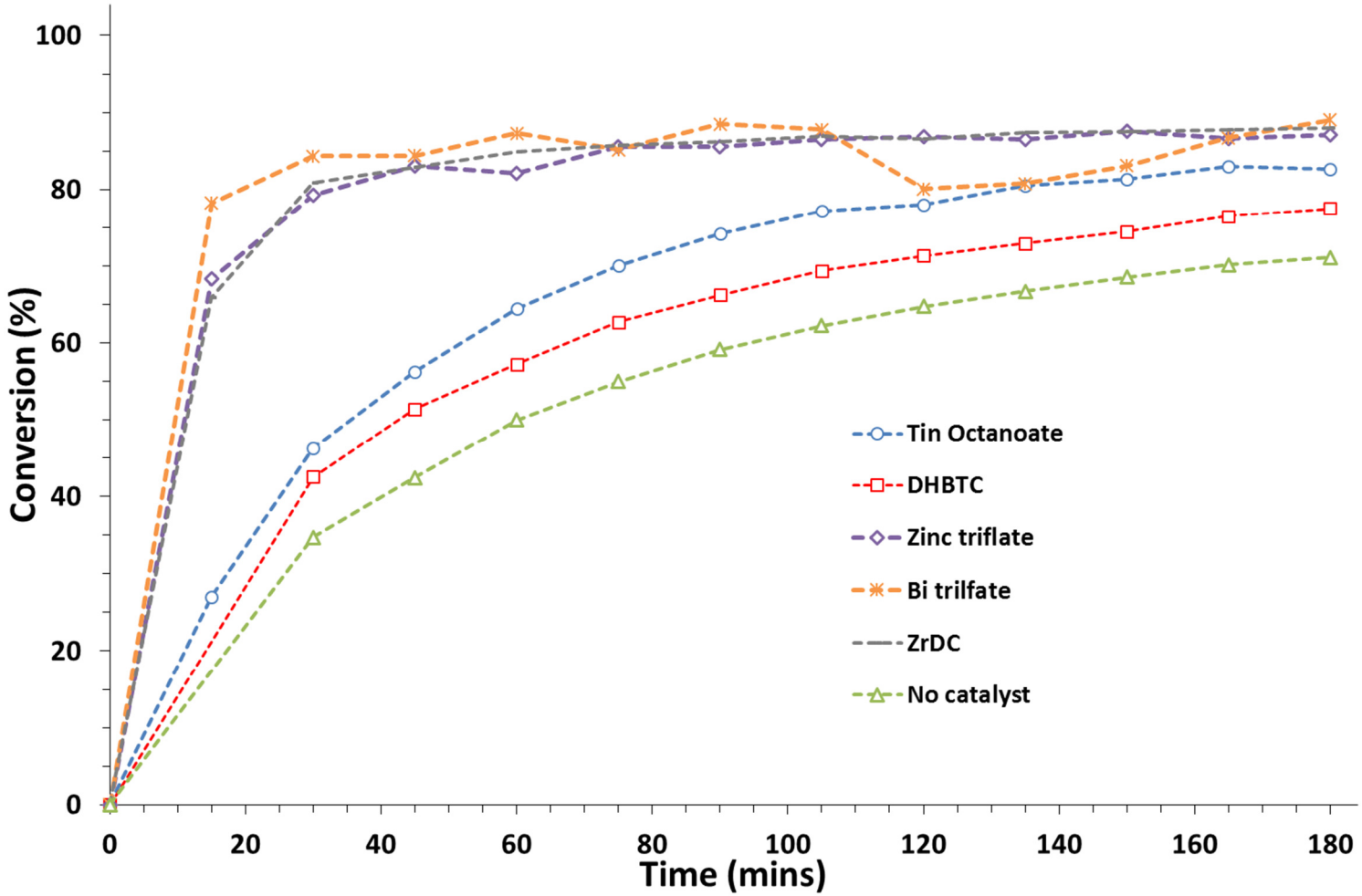


Figure 3-32. Plot of conversion versus time for adipic acid, hexanediol polyesterifications at 150 °C MWH using differing metal catalysts with no mass transfer applied.

Figure 3-31 suggested that at 150 °C and using CH there was a change in catalyst and reaction efficiencies when compared to 185 °C. The zinc and ZrDC catalysts had "swapped" their position in the relative efficiency rates, with the zinc triflate now exhibiting the fastest reaction rate. Meanwhile, at this temperature, the $Sn(Oct)_2$ reaction rate was observed to be very similar to when no catalyst is present. This suggested that at 150 °C with CH, this catalyst was essentially ineffective and was not contributing toward lowering the reaction's activation energy (E_a) *i.e.* energy needed to overcome the bond breaking and making of the polycondensation. This lack of activity in polycondensations is reinforced by a review by Hu et al. [55] which describes many example polycondensations of lactide to PLA using a $Sn(Oct)_2$ catalyst which implement temperatures exceeding 150 °C.

Additionally, in general it was observed that the reactions involving the second series of organometallic catalysts (especially triflates) at 150 °C proceeded at higher reaction rates than the tin catalysts at 185 °C when implementing CH, this was exemplified by the comparison of time taken to reach 90 % conversion in Table 3-10.

Table 3-10. Comparison of time to 90 % conversion between tin at 185 °C and triflate catalysts at 150 °C when using CH.

Catalyst	Temperature (°C)	[a] Time to 90 % Conv. using CH (minutes)
DHBTC	185	75
Tin Octanoate	185	180
Zinc triflate	150	20
Bi triflate	150	45

[a] Calculated using polymer to monomer peak ratio in ^{1}H NMR.

Table 3-10 shows that by implementing a triflate catalysts within the system, it was possible to achieve 90 % conversion at 150 °C in times significantly quicker

than the tin catalysed reactions at 185 °C. For an industrial system, this difference of 35 °C creates significant economic and environmental benefits including; reduced heat up and cool down times, reduced energy costs for heating, lower hazards, *etc.*

At 185 °C, Figure 3-32 showed that the Bi triflate catalyst reaction rate was observed to be the most efficient when MWH was adopted. This further suggested that the Bi triflate catalyst was a very efficient catalyst for these polyesterifications. The properties of the polyester products synthesised at 150 °C are discussed later in this chapter to show that Bi triflate becomes a promising catalyst at this temperature.

Again, Figure 3-32 demonstrated that the $Sn(Oct)_2$ catalyst obtains an increased reaction rate when implementing a MWH method compared to CH. Whereas, DHBC performed worse in the MWH experiments than in the CH. Interestingly for $Sn(Oct)_2$, although it was discussed earlier that it does not react well at 150 °C using CH, shown by its similar reaction rate to no catalyst in Figure 3-31, there is a clear increase in reaction rate with MWH applied. This further suggests that there is a specific microwave effect, promoting the catalysis of the system *via* the associative mechanism. This observation is strengthened by the fact that the DHBTC's reaction rate decreases when using MWH, showing that a formally bonded mechanism is not promoted.

ZrDC is shown to have a similar activity to the triflate catalysts in MWH, whereas in CH it performed at a reduced rate. This suggested that at this temperature there is promotion of reaction rate *via* MWH at this temperature. When assessing the previously suggested mechanisms it was shown that there is a significant amount of associative bonds in the ZrDC reaction, further suggesting that in MWH there was an affinity to increase reaction rates when associative bonds are present in the catalytic mechanism. Again, this was

further shown by the increase in reaction rate for the $Sn(Oct)_2$ catalyst. Comparing this to the reactions at 185 °C, where there was a decrease in reaction rate when MWH applied compared to CH, suggests that these newly applied organometallic catalysts actually performed better at lower temperatures due to the higher temperatures leading to side reactions with the catalyst.

Continuing with the comparisons between the MWH reactions at 150 °C, the $Sn(Oct)_2$ catalysed reaction rate was slower than both the zinc and ZrDC catalysed reactions. As such, if the dielectric properties of the catalysts were the main factor in deducing reaction rate this would not have been the case. This is shown when considering the dielectric properties of the catalysts at 150 °C, shown in Figure 3-33.

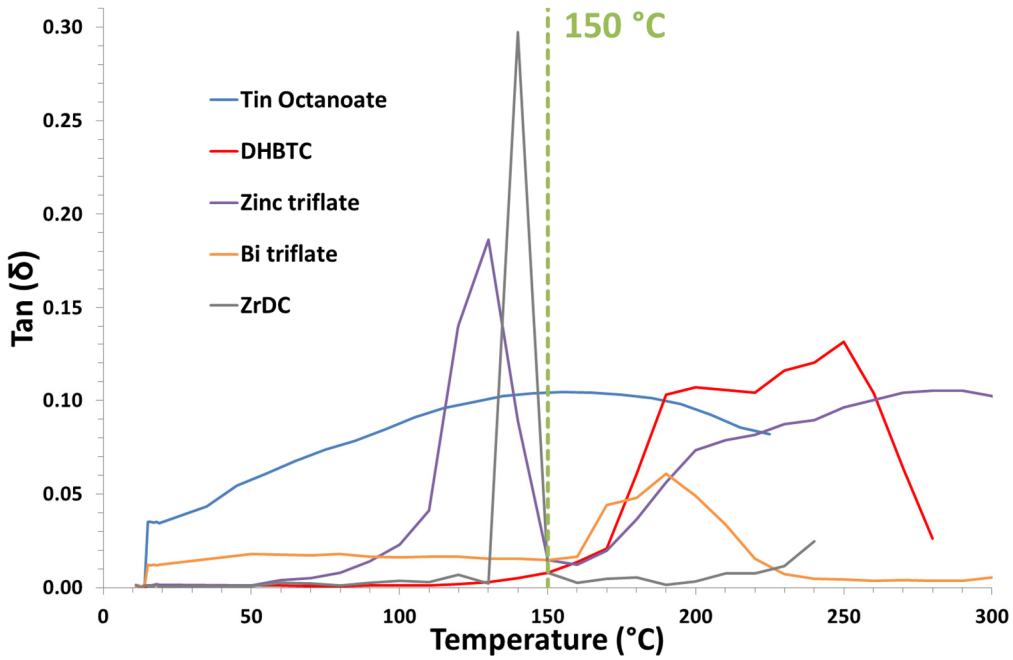


Figure 3-33. Dielectric properties of the organometallic catalysts used at 150 °C.

Assuming that the same trend was followed as was observed in the comparison of the tin catalysed reactions, there should be a direct correlation with tanδ value

and reaction rate. With the higher tanδ value catalysts leading to a faster reaction rate. But, in Figure 3-32, it was shown that $Sn(Oct)_2$ had a significantly slower reaction rate than ZrDC, Bi and zinc catalyst, even though the tanδ value at 150 °C is significantly higher, shown in Figure 3-33.

This is explained by 4 possible scenarios:

i. The $Sn(Oct)_2$ catalyst was not as active at lower temperatures and therefore did not catalyse the reaction, unlike the other catalysts used.
ii. The high dielectric properties of the zinc and ZrDC catalyst before 150 °C helped to catalyse the reaction as it is heating up to reaction temperature.
iii. The dielectrics of the catalyst in solution are different than those of the neat catalyst based on the physical form that they are in. Typically, materials that are in solid physical form will exhibit low dielectric responses due to the dipoles movement being restricted. Catalyst that are well solvated by/in the reaction medium may show significantly different dielectric properties.
iv. A combination of elements from points (ii) and (iii) above combine to improve the overall catalysts dielectric response in the reaction medium. The higher dielectric response of the catalyst at lower temperature increase the level of solvation of the catalyst by promoting the interaction with the other materials in the mixture to give a better dielectric profile for the catalyst at the chosen reaction temperature.

With specific regard to explaining the reduced reaction rate of the $Sn(Oct)_2$ catalyst. Scenario (i) is supported by the lack of rate increase in the CH reactions. The CH reaction profile in Figure 3-32 shows that at this temperature, the $Sn(Oct)_2$ did not catalyse the reaction due to the heating profile being identical to the non-catalysed reaction profile. Therefore, even though using

$Sn(Oct)_2$ and MWH did speed up conversion rate when compared to CH, it was not excited enough by the applied field to overcome this higher E_a barrier in the kinetics of the reaction.

However, as previously mentioned in this section, this difference in the CH and MWH profiles with $Sn(Oct)_2$ suggested that the microwaves were selectively heating the catalyst to a higher temperature than when CH heating was applied. However, this will require more investigation to be understood as a selective heating phenomenon.

A combination of effects introduced by Scenario (ii), (iii) and (iv) may have significant influence because reaction temperature is not achieved instantaneously. Rather, as the medium reaches a transition point during the heat-up process where the reagents start to react. This point was achieved once the mixture had homogenised and passed the boiling point of the condensate (100 °C). Therefore, polyesterification could occur at temperatures lower than the 150 °C reaction temperature. Consequently, because the heating of the catalyst is a dominant step in achieving a fast reaction rate, a sustained period at ~130 °C in zinc triflate and ~140 °C in ZrDC could have led to an increased rate for these catalysts. Similarly these effects may have resulted from better interaction with the reaction mixture resulting in the mixture reaching a homogeneous state more quickly with the MWH as a result of the catalysts electromagnetic interaction between 100 and 130 °C.

In an attempt to investigate these theories, an assessment of a typical heat-up profile of the reaction was conducted. A typical result for the polyesterification using an organometallic catalysts, *e.g.* zinc triflate, is shown in Figure 3-34.

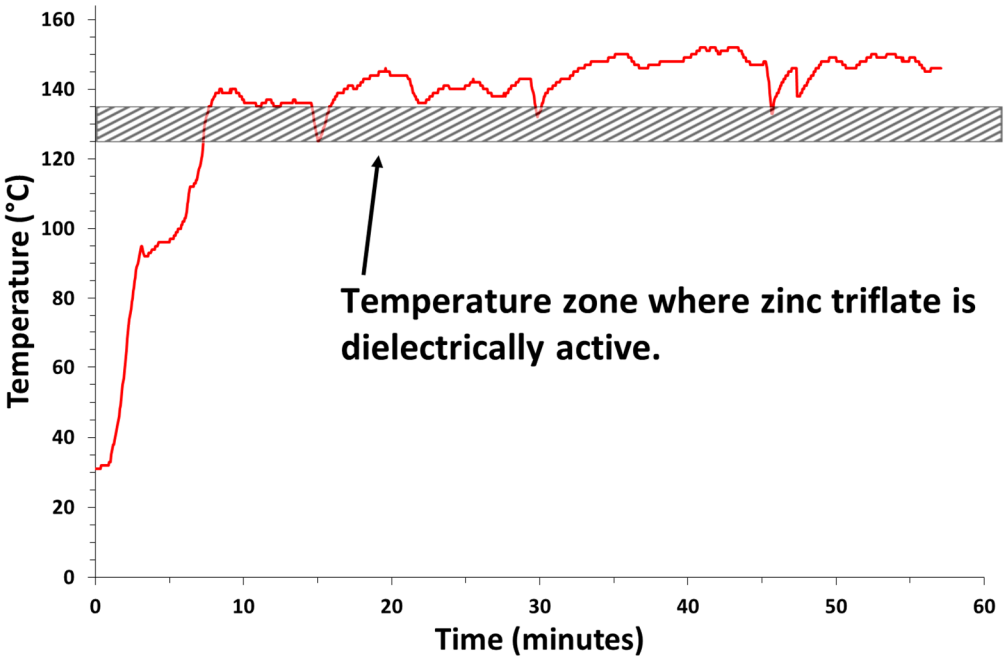


Figure 3-34. A typical heating profile for an adipic acid, hexanediol reaction to 150 °C using MWH. The catalyst used was zinc triflate and only the first hour is plotted.

The highlighted zone in Figure 3-34 refers to the region of temperatures where zinc triflate was predicted to be dielectrically active (125 to 135 °C). It was observed that the reaction passed through this temperature zone rapidly (less than 1 minute) at the beginning of the reaction and only re-enters it because of the temperature dips due to sampling. Therefore, assuming tanδ was the dominant factor in indicating polyesterification reaction efficiency under MWH, scenario (ii), which is essentially a direct reduction in heat up time is highly unlikely. Thus, the influence of the higher catalyst dielectric properties below the reaction temperature are likely to only improve the compatibilisation or solvation of the catalyst and monomers which then directly affect the MWH rate via a better availability of catalyst and/or improved EM response for the solvated catalyst. Therefore, solution dielectric analysis would be a beneficial technique to employ into this system to assess the changing dielectric properties of the solution with time and this would help expand on scenario (ii) and (iii).

3.4.1.3.1 Size Exclusion Chromatography (SEC) of Adipic Acid, Hexanediol Reaction at 150 °C Using Organometallic Catalysts

GPC was used to analyse the M_n^{GPC} and Đ of the polyester products synthesised at 150 °C and the data is shown below in Table 3-11.

Table 3-11. GPC data for AA HD reactions at 150 °C using different metal catalysts.

Catalyst	Heating Method	[a] Final Conv. (%)	[b] M_n^{GPC} (g.mol^{-1})	[b] M_w^{GPC} (g.mol^{-1})	[b] M_p^{GPC} (g.mol^{-1})	[b] Đ
No Catalyst	CH	72	380	1,180	120	3.08
	MWH	73	430	1,310	110	3.04
DHBTC	CH	90	1,690	3,640	2,770	2.16
	MWH	77	1,040	1,960	1,810	1.88
Tin Octanoate	CH	75	380	1,280	120	3.37
	MWH	83	1,250	2,410	1,810	1.93
Zinc triflate	CH	97	2,520	5,810	6,170	2.30
	MWH	87	1,710	3,630	2,320	2.12
Bi triflate	CH	91	1,910	4,450	2,710	2.33
	MWH	86	1,880	4,470	2,710	2.47
ZrDC	CH	87	1,530	4,200	2,740	2.62
	MWH	88	1,810	3,860	2,710	2.13

[a] Calculated using polymer to monomer peak ratio in ^{1}H NMR. [b] Calculated using THF GPC and ASTRA processing software relative to a polystyrene standard.

Table 3-11 demonstrated that for the reactions using no catalyst and $Sn(Oct)_2$ with CH there was a low level of reaction achieved at 150 °C, with M_n^{GPC} values in the dimeric region. This again suggested that the $Sn(Oct)_2$ catalyst was not effective, if at all, at these lower temperatures with CH. But, there is colourless polyester formation in the MWH sample, with a M_n^{GPC} in the oligomeric region. Hence, as there was an improvement in molecular weight, rate and final conversion when MWH was applied, this presents more evidence for the catalytic species being selectively heated or for an increase in mechanistic

efficiency through MWH due to the associative nature of the catalyst. This suggested that either the catalyst was at a local, higher temperature than the bulk increasing its efficiency and promoting polyesterification or the weak associative bonds in the mechanism are rapidly made and broken by implementing MWH.

At 185 °C there was shown to be depolymerisation/degradation when implementing the Bi triflate catalyst, with a highly discoloured and oily product formed, dimeric M_n^{GPC} values reported in section 3.4.1.2.1 and MALDI data within the matrix zones in section 3.4.1.2.3. But, at 150 °C there was suggestion of polyester formation with M_n^{GPC} values of 1,910 and 1,890 presented in Table 3-11 and Đ values typical of polyester formation, as explained previously by the Flory-Schultz distribution. [2,48] In fact, the polymers synthesised using these catalysts are now some of the largest recorded, showing a far better performance at this lower temperature for this catalyst. This tends to suggest that, of the proposed explanations in section 3.4.1.2 for the different performance of the Bi catalyst at 185 °C, temperature may be the main influencing factor. This is because at the high temperature of 185 °C there is clear depolymerisation/degradation, but, once the temperature is lowered there is polyester formation. This may also be because the hydrolysis of the catalysts is reduced at these lower temperatures due to the reduced amount of water condensate rapidly produced (lower temp led to a lower reaction rate) and therefore both temperature and hydrolysis were key factors in the performance of the catalyst.

Assessing the new organometallic catalysts potentially suggested that by using these at lowered temperatures a product can be achieved which is comparable to products produced at 185 °C in terms of MWt e.g. zinc triflate CH @ 150 °C = 2,520 $g.mol^{-1}$, $Sn(Oct)_2$ CH @ 185 C = 1,580 $g.mol^{-1}$).

3.4.1.3.1.1 Comparison of Molecular Weights from the polyesterification reactions between 185 and 150 °C

One interesting difference when analysing all the polyester products synthesised at the same processing temperatures, independent of catalysts choice, was the change in correlation between M_n^{GPC} value and final conversion between the reactions at 185 and 150 °C, shown in Figure 3-35.

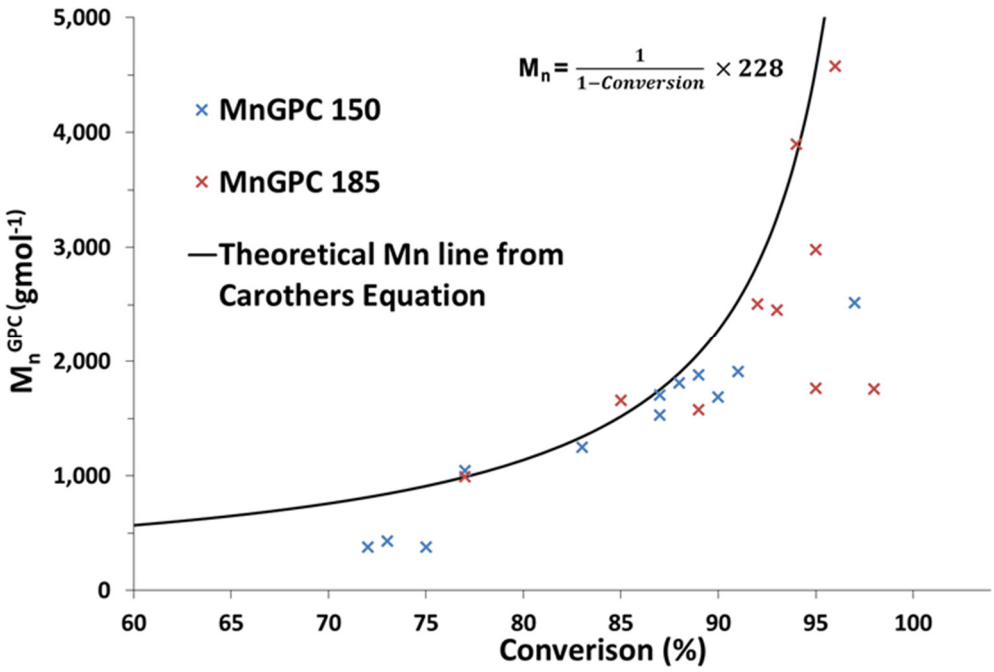


Figure 3-35.Plots of MnGPC against level of conversion for the adipic acid, hexanediol polycondensations at 150 °C (blue) and 185 °C (red) using organometallic catalysts. For 185 °C Bi triflate has been omitted due to the depolymerisation/degradation. Line of best fit added as the theoretical M_n values based on Carothers equation. [56]

The data presented in Figure 3-35 demonstrated that the theoretical relationship, proposed by Carothers, fit well. However, there was some discrepancy between the two temperatures, with the polymers processed at 185 °C fitting the theory at high conversions more closely than the polymers processed at 150 °C. Whereas, at lower conversions and molecular weights it is the polymers processed at 150 °C which fit with the theoretical line more

closely, especially around 90 % conversion. This suggested an increased in polyester synthesis control for the polycondensations at lower processing temperatures. This was explained by the lower temperatures not allowing quick elongation of the polyester chain, whereas, at the higher temperatures, some significantly longer chains were created due to the increased number of species with enough energy to react. Therefore, by processing at a lower temperature, specific MWt's could be targeted more easily as the reaction is more consistent in terms of MWt growth with increased conversion and this was true with all catalysts and either heating method. However, to fully deduce this, reactions need to be conducted to higher MWt's to assess if the fit is still consistent.

3.4.1.3.2 Colorimetry - Gardner Scale Colour Analysis of Adipic Acid, Hexanediol Reaction at 150 °C Using Organometallic Catalysts

As discussed in section 3.4.1.2.2 for the 185 °C polyesterifications, GS colour analysis was conducted on all the polymers synthesised at 150 °C, and the data from this analysis is shown in Table 3-12.

Table 3-12. Gardner scale analysis of AA HD polyester synthesised at 150 °C using different catalysts and heating methods.

Catalyst	Heating Method	[a] GS # at 150 °C	[a] GS Hue at 150 °C	[a] GS # at 185 °C	[a] GS Hue at 185 °C
Tin Octanoate	CH	7.6	9.0	6.5	7.0
	MWH	11.7	11.0	7.9	11.0
DHBTC	CH	0.1	0.0	0.5	0.0
	MWH	0.1	0.0	0.2	0.0
Zinc triflate	CH	4.9	3.0	3.6	1.0
	MWH	0.4	0.0	7.2	7.0
Bi triflate	CH	2.0	0.0	[b] too dark for analysis	
	MWH	2.0	0.0	8.6	6.0
	CH inert	1.2	0.0	16.0	6.0
ZrDC	CH	5.0	2.0	5.9	5.0
	MWH	1.0	0.0	4.2	3.0
No catalyst	CH	1.3	1.0	0.2	0
	MWH	0.1	0.0	2.2	0

[a] Calculated using a Lovibond PFX1-950 and GS colour standards 1-18. The results from the 185 °C product have been included for ease of comparison. [b] sample double diluted to achieve a number of 16.7 and hue of 9.0.

Table 3-12 displays that, as at 185 °C in section 3.4.1.2.2, the $Sn(Oct)_2$ reactions were shown to have surprisingly high GS values for a substance which was, by visual inspection, essentially colourless in its solid form. However, at 150 °C the GS values were even higher than at 185 °C. Again, like in 3.4.1.2.2, this is attributed to the insolubility of the $Sn(Oct)_2$ catalyst in the THF used to dissolve the products within the analytical method. The increase in values from 185 to 150 °C was attributed to the lower conversions achieved in the 150 °C samples. This lower conversion left over more unreacted diacid monomer, which is insoluble in THF and therefore interfered with the sample, indicated by the extremely high hues.

Whilst it was generally observed that all the products from the 150 °C polymerisation produced lower GS values (except $Sn(Oct)_2$, zin triflate CH and

no catalyst CH), one result that was surprising when compared to those for the products at 185 °C was that of the Bi triflate. At 185 °C, the GS values of the Bi products were the highest out of all the catalysts used, which included a need to doubly dilute the CH sample in order to get a reading. In Table 3-12, the Bi triflate values were noted to be very low by comparison, with both CH and MWH being 2.0, which compared very favourably to conducting the reaction under an inert atmosphere which generated a GS value of 1.2. This suggested that at lowered temperatures, the Bi triflate catalyst was not hydrolysing with the condensate or degrading due to temperature and was therefore capable of catalysing the reaction. This, correlated with the MWt data discussed above in section 3.4.1.3.1, which indicated that polymer rather than oligomers had been synthesised at 150 °C. This was a significant result as it allowed the reactions to take place at a lower temperature, whilst not effecting the final product with serious discolouration or depolymerisation. These findings therefore further suggested that the Bi catalyst was degrading/depolymerising due to both the temperature of the reaction and the water content. This, coupled with the fact the triflate reactions are shown to progress faster at 150 °C than the tin at 185 °C, presented a strong case for a reduction in processing temperature to be considered when applying the non-tin based organometallic catalysts used in this study.

Overall, there was a positive indication that when using MWH at 150 °C the level of decolourisation observed was reduced. In half of the products (zinc triflate, no catalyst and ZrDC) when MWH was implemented there was a reduction in GS number. With the largest reduction found in the zinc triflate catalysed sample which dropped from 4.9 using CH to 0.4 using MWH. This is a significant difference and could be the difference between an industrially viable process/product and not. For the other products only $Sn(Oct)_2$ didn't

reduce in GS when implementing MWH, but this is most likely due to the catalysts interaction with the solvent, as previously discussed. This correlation is different to what was found at 185 °C as there was no trend found between MWH and CH in terms of discolouration. This suggested that by implementing MWH at 150 °C the energy was being selectively input into the reaction sites and not into the vessel/bulk. This selective heating would therefore minimise the temperature of the evaporating water, hypothesised as the cause for discolouration, and therefore limit the discolouration.

Interestingly, when plotting the tanδ values against the GS number for the 150 °C data, a trend was observed, unlike at 185 °C were no trend was found, as shown in Figure 3-36.

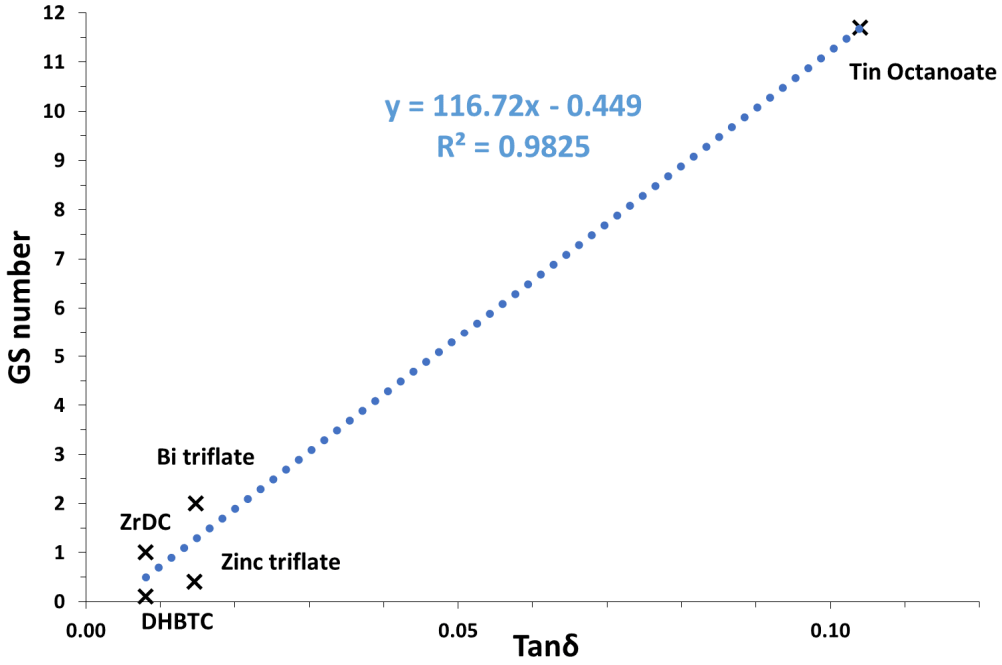


Figure 3-36. Representation of relationship between highest tanδ catalyst and highest GS number catalyst for a AA, HD polycondensation at 150 °C.

The data presented in Figure 3-36 suggested that, at 150 °C, there was a correlation between catalyst tanδ at reaction temperature and the final products discolouration. This therefore suggested that for the AA, HD system at 150 °C

the ability of the catalyst to absorb EM energy is key in final colour of the product. But, as previously discussed, the $Sn(Oct)_2$ samples are visually white and the GS values may be down to poor miscibility in the solvent. However, the low levels of discolouration in the products with low tanδ values could theoretically be due to the fact that water is an extremely good microwave absorber. This property would lead to the water efficiently coupling to the microwaves and superheating after being produced during the condensation reaction, increasing the evaporation rate. In contrast, the high tanδ value of $Sn(Oct)_2$ would lead to the EM irradiation being used to heat the catalyst more and water proportionally less. This would therefore lead to the water being cooler and there being a higher probability of it hydrolysing the catalyst and creating discolouration. This theory is tested by omitting $Sn(Oct)_2$ a new correlation is created which shows that in fact, there is no correlation between the catalyst tanδ at reaction temperature and GS number, shown in Figure 3-37.

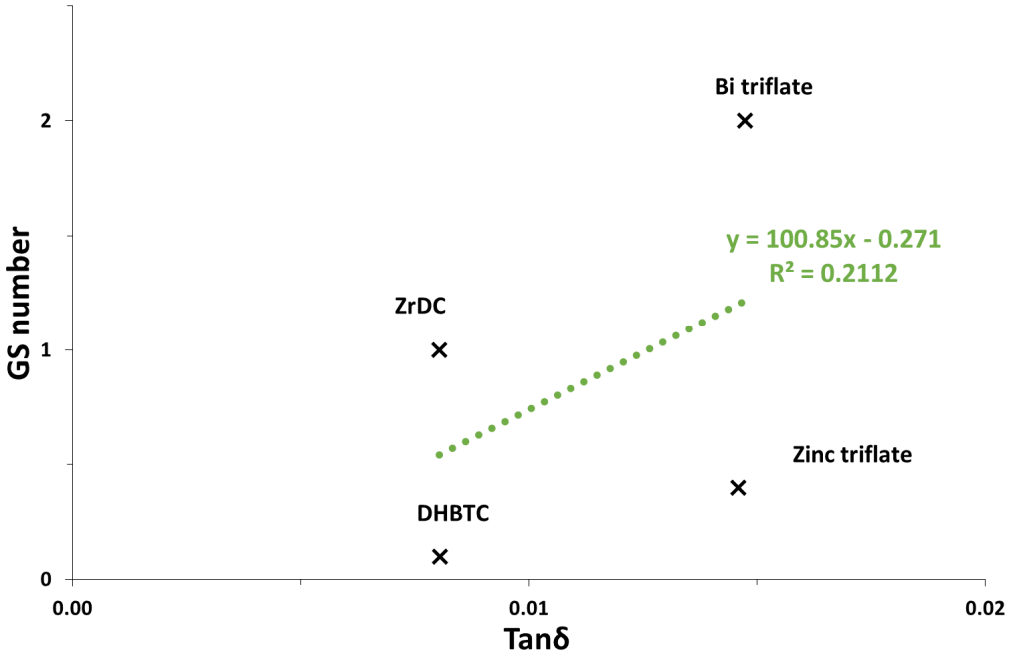


Figure 3-37. Representation of relationship between highest tanδ catalyst and highest GS number catalyst for a AA, HD polycondensation at 150 °C with the $Sn(Oct)_2$ catalysed product data omitted.

Figure 3-37 demonstrates that in fact the dielectric properties of the catalyst do not greatly affect the final discolouration of the product at either temperature investigated. This is likely due to the fact that the catalyst is only a small percentage of the reaction mix and therefore does not affect the bulk conditions significantly. Therefore, the reason behind the large discolouration in the $Sn(Oct)_2$ samples was deduced as the insolubility of the $Sn(Oct)_2$ catalyst in THF.

The samples with no change between CH and MWH are DHBTC and Bi triflate, Table 3-12. This allows either heating method to be used in terms of discolouration when using either of these catalysts, accordingly other product qualities must be considered such as MWt, reaction rate and AV.

3.4.1.3.3 Matrix Assisted Laser Desorption/Ionisation-Time of Flight Mass Spectrometry (MALDI-ToF MS) of Adipic Acid, Hexanediol Reaction at 150 °C Using Organometallic Catalysts

MALDI analysis was undertaken on all the samples synthesised. It was discovered that some of the polyesters did not undergo MALDI spectra effectively, as both the CH and MWH polyesters synthesised using no catalyst and the CH polyester using $Sn(Oct)_2$ produced no spectra. This was explained by the data for these samples from the previous analysis were the M_n^{GPC} and final conversion values were found to be so low that it suggested that polymeric species hadn't been formed. Therefore, it was proposed that product peaks could not be found in the MALDI analysis because they were located within the matrix peaks. This can happen with any molecular fragment that is below ~500 M_n as the matrix (2,5-dihydroxybenzoic acid) has MALDI cluster peaks up to this value.

For the all the other polyesters, using either heating methods, the results showed that the most prominent peaks exhibited dual COOH terminated polymers. This is in contrast to the reactions at 185 °C where all but zinc triflate had a primary series of a mixture of terminal groups, irrespective of conversion percentage and MWt. A hypothesis to suggest why this happened was that processing at 150 °C led to evaporation of the diol, creating a stoichiometric excess of diol. This would occur more prominently at 150 °C than 185 °C because 150 °C is slightly lower than the melting point of the diacid (152 °C), therefore, only a small amount of diacid monomers will be reacting. As such, although the boiling point of HD was still 100 °C more than the reaction, these conditions led to an increased number of diols evaporating instead of reacting when compared to 185 °C.

This hypothesis was investigated further by conducting AV analysis, as detailed below.

3.4.1.3.4 Acid Value titration analysis of Adipic Acid, Hexanediol Reaction at 150 °C Using Organometallic Catalysts

AV analysis was implemented on the crude polyester products to investigate if conducting the polycondensations at a lower temperature would affect which end groups dominated the termination of the chains. Again, as in the products analysed at 185 °C in section 3.4.1.2.4, a mixture of end groups was expected due to the 1:1 stoichiometry of acid to hydroxyl groups. This data was then correlated to conversion and compared to the previous analysis on the polyesters synthesised at 185 °C. Below in Figure 3-38 is a graphical comparison of the results.

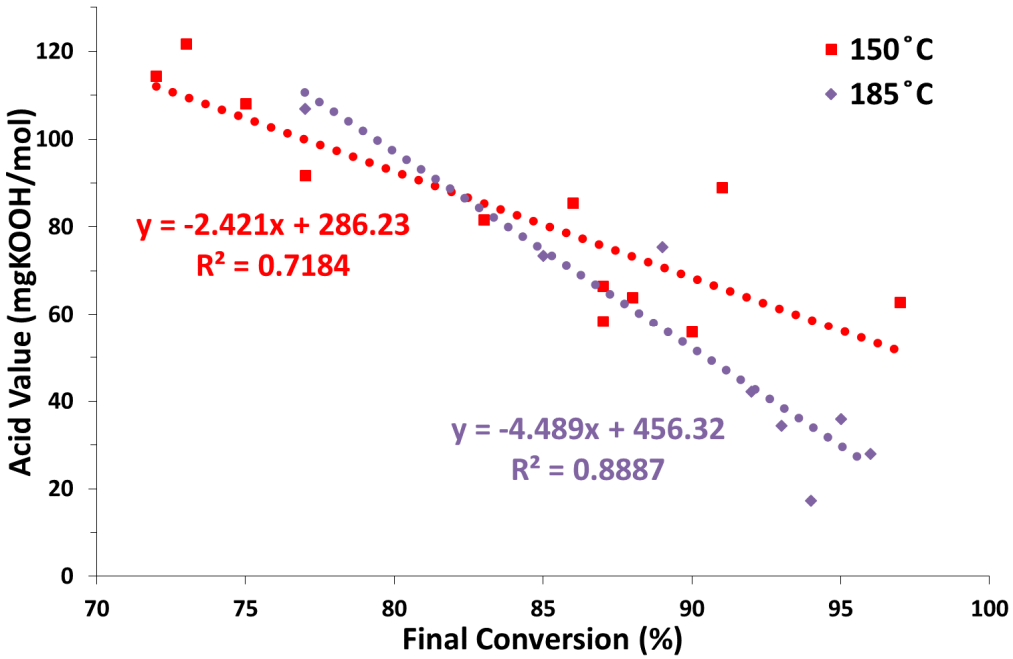


Figure 3-38. Comparison of final conversion percentage versus AV for AA, HD polyesterifications at 150 and 185 °C using organometallic catalysts, independent of heating method. ■ = 150 °C, ♦ = 185 °C NOTE: for the 185 °C data set, the zinc triflate data has been omitted as it was shown to skew the data.

The data in Figure 3-38 showed that, as would be expected, a low conversion leads to a higher AV due to the increased number of chain ends and oligomers/monomers present in the samples at both temperatures and heating methods. However, comparing the data from the two processing temperatures shows that there was a thermally related difference between the correlation between AV and conversion. The polyesters processed at 150 °C create a series which suggested that as the reaction progressed to higher conversion levels, a higher AV was achieved than at 185 ºC. It was proposed that this potentially occurred for because:

i. The previously discussed evaporation of diol at 150 °C, leading to a stoichiometric excess of acid and promoting the formation of COOH terminated chains.

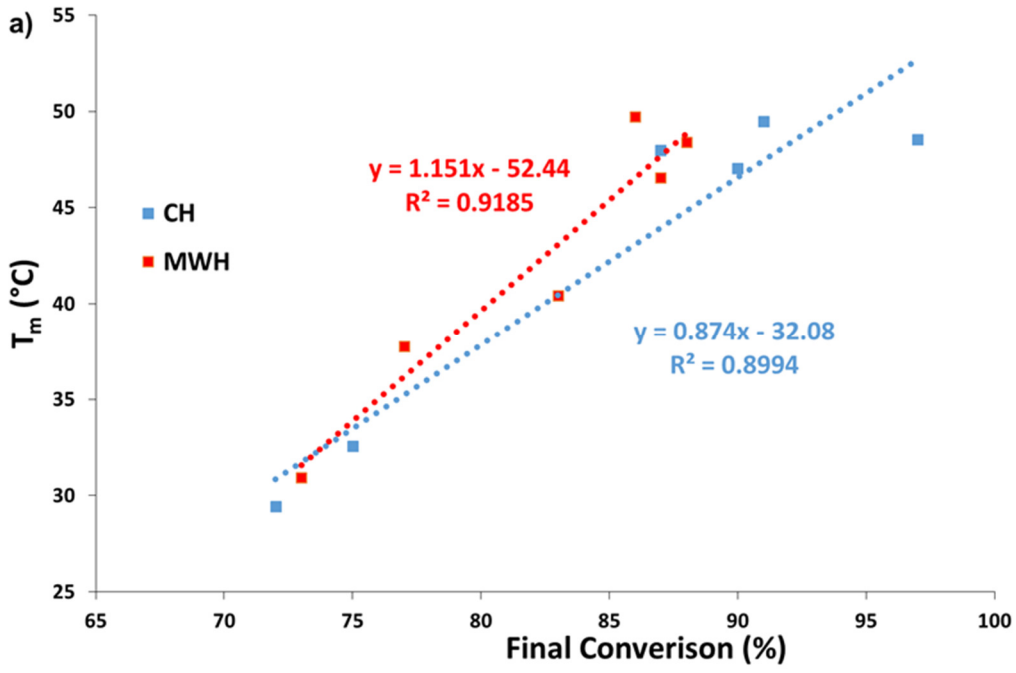
ii. Processing at 185 °C promoted the combination of higher MWt chains towards the higher conversion levels. This is because the high

temperature will overcome the mass transfer and viscosity problems encountered once polyester reach higher MWt's. This is shown by the products at 185 °C having significantly increased MWt's than the products processed at 150 °C.

3.4.1.3.5 Differential Scanning Calorimetry of Adipic Acid, Hexanediol Reaction at 150 °C Using Organometallic Catalysts

As for those samples that resulted from polymerisations performed at 185 °C, the 150 °C polyester samples were subject to DSC analysis. For these polyesters, T_m values of ~45 - 55 °C were expected as the final conversions and so MWt's synthesised were observed to be lower than at 185 °C, discussed in section 3.4.1.2.5.

The data from the DSC analysis is shown below in and compared with final conversion % and M_n^{GPC}.



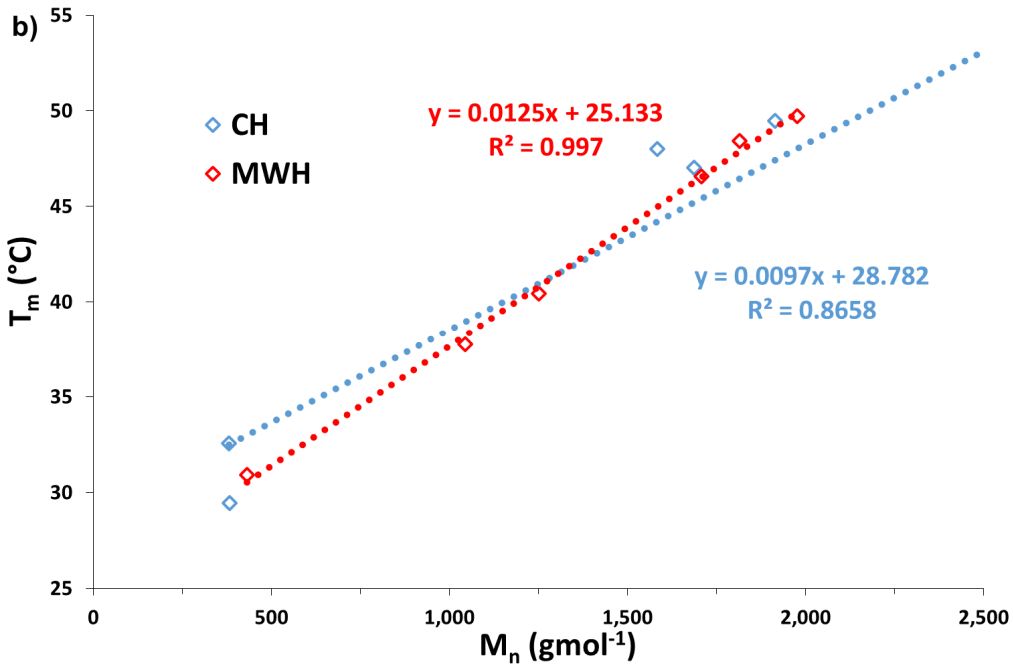


Figure 3-39. Graphical comparison of adipic acid, hexanediol polyesters synthesised at 150 °C of a) final conversion versus Tm compared to b) Mn versus Tm with CH and MWH in different colours for each graph. Blue = CH, red = MWH, ■ = Final conversion versus T_m and ◊ = M_n versus T_m. Note: the x-axis starts at 25 °C and for graph "a" the y-axis begins at 60 %.

Again, Figure 3-39 suggested a strong correlation between both final conversion versus T_m and M_n^{GPC} versus T_m. Interestingly, at 150 °C there was a stronger correlation between the MWH reactions when compared to the CH. This is especially evident in graph (b), Figure 3-39, with the MWH reactions having an almost perfect correlation (R^2 = 0.997). Therefore, at 150 °C, it was hypothesised that MWH is enabling better MWt control than CH. This observation was explained by relating it to the heating input when using MWH. In MWH the EM energy is transferred into the bulk of the reaction medium and thus the reagents/catalyst are heated directly. This promoted the energy being more efficiently used toward driving the chemical reactions instead of heating outside factors *i.e.* vessel. It ensured less of the thermal gradient across the vessel in the MWH case, ensuring that all the oligomers are experiencing the

same thermal conditions. It was proposed that both of these factors led to the effective promotion of reactions and more efficient/controlled polymer growth. This was not observed at 185 °C as the elevated temperature negated this differentiation in energy input efficiency and highly heated all aspects of the vessel and reaction mixture. Therefore, at 185 °C the polymerisations were deduced as mass transfer limited which led to CH achieving similar heating efficiencies as the MWH case at this temperature.

3.4.2 Investigation into Differences in Non-Organometallic Catalyst Activity for the Adipic acid, Hexanediol Polycondensation

After the positive results when implementing organometallic catalysts, non-organometallic catalysts were investigated. These types of catalysts were of particular interest due to their specific potential advantages over most organometallic catalysts which include;

i. Easy preparation and availability.
ii. Inert to discolouration by water and air (oxygen).
iii. No metal contamination.
iv. Ease of use in scale-up.[57]

Due to ever changing environmental and governmental legislation, organometallic catalysts are being viewed less favourable within the industrial community. As such, it is of specific interest for industry to transition away from organometallic catalysts to non-organometallic catalysts.

Therefore, a brief literature search was conducted into the use of non-organometallic catalysts in polymer synthesis, with a focus on polycondensations/esterifications. A highly researched area of polymer

synthesis when using non-organometallic catalysts is ROP e.g. poly(ε-capralactone) using phosphoric acid, [58] poly(lactic acid) (PLA) using p-toluenesulfonic acid (pTSA), [59,60] or bis(thiourea). [61] Additionally, a variety of enzymes have been successfully used to produce both polymers. [62-65] The application of ROP to synthesise these products has become of increasing interest due to the ability to source ROP monomers from renewable feedstocks. Also, these polymerisations can be processed at low temperatures and the generated products are low weight, strong and can be easily moulded.[66]

For melt polycondensations a strong acid catalyst is usually employed. Examples of these include; camphorsulfonic acid,[67] pTSA,[68] phosphoric acid and its dimer [69-71]

Therefore, for this section, crystalline phosphoric acid (PA) and its dimer, pyrophosphoric (PPA), were selected and investigated. This is because of:

i. Their previous use in the literature, as shown above.
ii. The relatively high boiling point (b.p.) compared to other acidic catalyst. But these are still lower than the previously used tin catalysts. (PA = 158 °C, pTSA = 116 °C and $Sn(Oct)_2$ = 296 °C)
iii. They have been reported in the literature as having been successfully used in polymerisations under MWH. [72-74]

The proposed mechanism exhibited by these non-organometallic catalysts is known as the Fischer esterification mechanism. This mechanism proceeds *via* the non-organometallic catalyst acting as a Lewis acid, as shown in Figure 3-40.

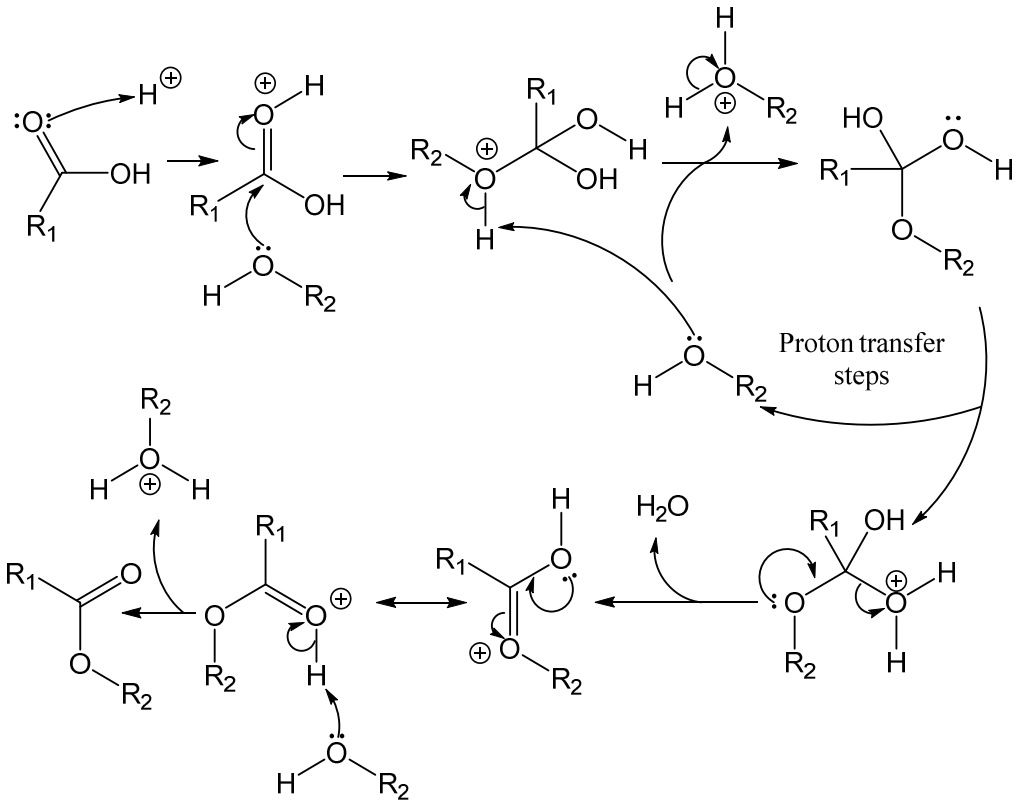


Figure 3-40. Fischer esterification mechanism.[75]

As was the case for all previous reactions reported, processing temperatures of 185 and 150 °C were implemented with a 3 hour cycle period. As before, these two temperatures will be discussed separately with comparisons made to the DHBTC industrial benchmark catalyst. As before, the final products were assessed using the standard polyester analysis techniques used in this thesis to-date.

3.4.2.1 Conventionally versus Microwave Heated Reactions Using Non-Organometallic Catalysts at 185 °C

Reactions were conducted which utilised PA and PPA as the catalyst of choice using both CH and MWH at 185 °C and the kinetic profiles were plotted for comparison against DHBTC, and this data is shown in Figure 3-41.

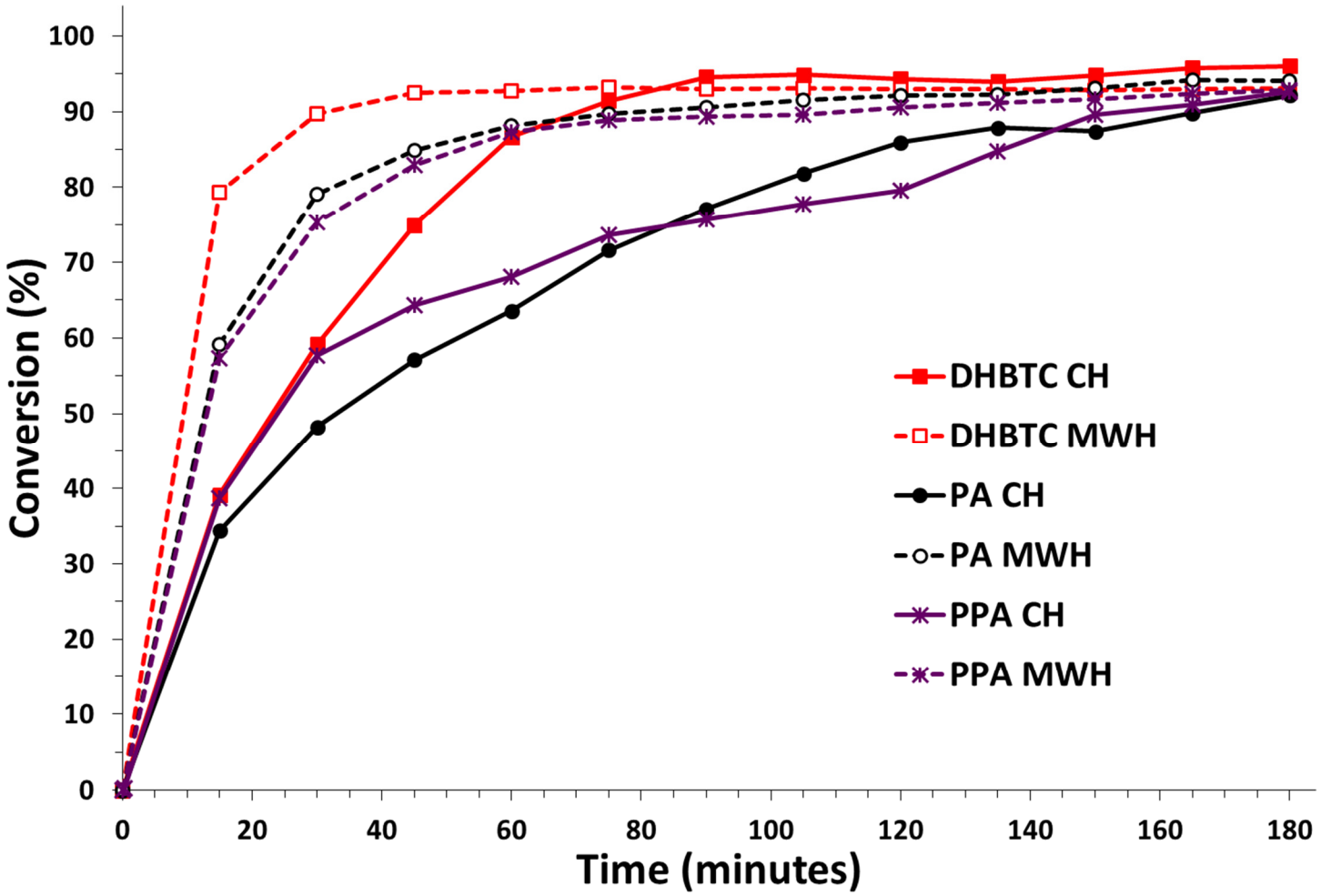


Figure 3-41. Plot of conversion % versus time for AA, HD polycondensation at 185 °C using different heating methods, non-organometallic catalysts and an industrially used DHBTC tin catalyst for comparison and with no mass transfer application.

Figure 3-41 demonstrates that the MWH reactions proceeded at a faster rate at 185 °C than the CH reactions. Additionally, it was observed that PA and PPA react at similar rates for both CH and MWH, with the MWH reaction profiles being almost identical. There is a larger disparity between the CH reactions during the first hour, but this differencel is negligible over the full reaction cycle. Again, a similar final conversion is achieved between CH and MWH over the full reaction cycle of 180 minutes. However, the highest achieved conversion plateau of ~90 % conversion was reached in 90 minutes for the MWH reactions and 150 and 165 minutes for the CH reactions (PPA and PA respectively). It was proposed that the similarity in reaction rate may be due to the conversion of PPA to form PA in the presence of the water condensate generated from the polycondensation.[76,77]

This data showed that these non-organometallic catalytic species could be used as a catalyst for this polycondensation and when implementing a MWH strategy, reaction rates accelerated when compared to the CH reactions. It has also been shown that using a non-organometallic catalyst and MWH can increase the reaction rate when compared to the industrially used tin catalyst when used in a CH method. Adopting these conditions would be beneficial when compared to the current methods because of the environmental/toxicology benefits of using the non-organometallic catalysts and the greater energy efficiency when using MWH.

Furthermore, when implementing a MWH system there is an increased safety aspect when compared to the CH methods. This is because microwave energy input can be instantaneously switched off, such that all heating of the system is terminated. In contrast, when using CH, ceasing the energy input to the hot oil does not immediately remove the heat input rather the hot thermal transfer fluid will continue to heat the reactor contents until it is drained/removed from the

system. Therefore, when using CH the product/vessel will stay at a higher temperature for longer, increasing the risk of causing thermal run away.

3.4.2.1.1 Size Exclusion Chromatography (SEC) of Adipic Acid, Hexanediol Reaction at 185 °C Using Non-Organometallic Catalysts

The polyesters produced were analysed for their MWt via GPC and the analysis is shown in Table 3-13.

Table 3-13. GPC data for adipic acid, hexanediol reactions at 185 °C using non-organometallic catalysts compared to an industrially used tin catalyst.

Catalyst	Heating Method	[a] Final Conv. (%)	[b] M_n^{GPC} (g.mol^{-1})	[b] M_w^{GPC} (g.mol^{-1})	[b] M_p^{GPC} (g.mol^{-1})	[b] Đ
DHBTC	CH	96	4,580	10,700	12,500	2.36
	MWH	93	2,460	6,380	6,980	2.59
PA	CH	94	2,750	6,700	6,800	2.47
	MWH	94	3,130	8,250	7,420	2.60
PPA	CH	93	3,370	7,280	6,720	2.13
	MWH	93	3,210	7,040	6,640	2.19

[a] Calculated using polymer to monomer peak ratio in ^{1}H NMR. [b] Calculated using THF GPC and ASTRA processing software relative to a polystyrene standard.

For the PPA catalyst, there are similar MWt and Đ values reported in Table 3-13 for both the CH and MWH polyester products. But, this was expected as the conversions are essentially identical. Interestingly, when comparing the Đ values with the other catalysts, they were noted to be significantly lower and therefore this suggested that the polymerisation had been more controlled. This suggests that the mechanism for the polycondensation when using the dimeric phosphoric species helps promote a more controlled chain growth than could be achieved by use of the organometallic catalysts. It was proposed that this

could be due to the increased availability of the H^+ ions due to the more labile nature of the bonds in the dimer.

For the PA catalyst, there was some disparity between the results of the CH and MWH experiments. Even though there was an identical conversion for both the polyesters, the MWH reaction produces a polymer with a M_n^{GPC} of approx. 400 $g.mol^{-1}$ higher which equates to approximately 1.5 repeating units, a value that is significant for these shorter chained polyesters. This suggested that MWH assisted the building of higher MWt polyester chains when compared to the CH system when using this catalyst. This can be explained by either the efficient heating of the catalyst system (most likely the proton) which forces polymerisation to overcome steric barriers, or the potential of MWH to heat the polyester chain ends to increase reactions with other chains.

This result would also suggest that the similarity in the rates between PA and PPA, which been attributed to the conversion of PPA to PA in the presence of condensate water, was in-fact due to some other root cause in the case of MWH. Otherwise the PPA would also have exhibited a higher MWH polymer molecular weight. Therefore, this similarity in reaction rate was likely due to the similar amount of free H^+ ions in the catalytic sample, a result of adding an identical mol % of catalyst.

Table 3-13 suggested that when implementing CH, the DHBTC catalysed products have a higher conversion and therefore M_n^{GPC} than the non-organometallic catalysed products, which may define why this species is currently used industrially. But, when considering the MWH results, the acidic catalyst produce polymers of higher M_n^{GPC} with similar conversion percentages. It was proposed that this observation was related to the mechanism of the polycondensations. With the acidic catalysts, the mechanism involves the Fischer esterification mechanism (see Figure 3-40), which progresses *via* the

presence of free H^+ ions. These H^+ ions were very active under the EM energy due to their high charge to weight ratio and will facilitate polymerisation. [78] This explanation is supported by the measured dielectric responses exhibited by the catalysts. When the dielectric experiments were conducted, the dielectric loss of PA and PPA was too high for the network analyser to record at 2.45 GHz, so the measurements had to be conducted at 910 MHz. This will mean that the results shown are not the exact values for the catalysts in the reaction medium due to the microwave frequency being 2.45 GHz, but the general trend of the values will be identical, Figure 3-42.

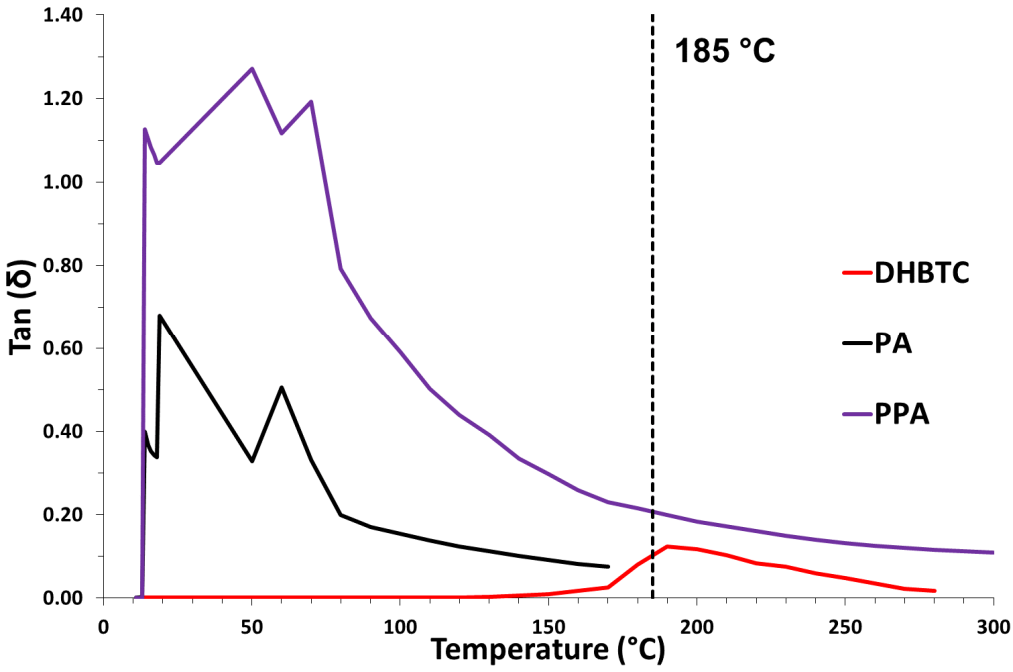


Figure 3-42. Dielectric properties of all non-organometallic catalysts with DHBTC for reference with respect to temperature, calculated using cavity perturbation technique at 910 MHz. Note: as the b.p. of PA is 153 °C the dielectric analysis was stopped at 150 °C due to safety concerns.

The dielectric data presented in Figure 3-42 suggested that the non-organometallic catalytic species were highly reactive to an EM field at low temperatures. This was explained by PA and PPA having low melting points, ~40 and 60 °C respectively, and typically a material which exhibits a

liquid/molten physical form will generally produce higher dielectric properties than when it is solid due to increased ease of molecular movement which allows the dipoles/ions greater freedom to align with the phase of the incident field. . As the temperature increased towards the reaction temperature, the tanδ value slowly decreases, but for PPA it was still approx. 2 times higher than DHBTC. Also, the maximum tanδ value of PPA is approximately twice that of PA. This is surprising as PPA is the dimer and which would suggest less rotation of the molecule due to its more bulky nature. But, previous research by Adlington et al. suggested that di/tri/oligomeric species have higher dielectric properties than their mono and polymeric counterparts. [79] Therefore, this result can be explained by their proposal that these oligomeric structures are still small enough to have free dipole movement while exhibiting a greater viscosity which means that there is greater molecular friction created from this movement.

3.4.2.1.2 Colorimetry – GS colour analysis of Adipic Acid, Hexanediol Reaction at 185 °C Using Non-Organometallic Catalysts

GS colour analysis of the polyesters is detailed below in Table 3-14.

Table 3-14. GS colour analysis of AA HD polyester synthesised at 185 °C using non-organometallic catalysts and industrially used DHBTC tin catalysts with different heating methods.

Catalyst	Heating Method	[a] GS Number	[a] GS Hue
DHBTC	CH	0.1	0.0
	MWH	0.1	0.0
PA	CH	0.4	0.0
	MWH	0.5	0.0
PPA	CH	0.3	0.0
	MWH	0.3	0.0

[a] Calculated using a Lovibond PFX1-950 and GS colour standards 1-18.

The data in Table 3-14 confirmed that the use of a non-organometallic catalyst had a positive result for the polycondensation when discolouration is considered. The GS numbers were observed to be small enough to be comparable with the industrially used catalyst and therefore their use had not discoloured the final product. The hue was also shown to be zero for all samples, indicating no cloudiness when dissolved in the solvent. There was also minimal difference in GS values between the heating methods which was positive for MWH due to the polyester product spending elongated periods at the high processing temperature as a consequence of the more efficient heat-up times witnessed for MWH, discussed in section 3.3.2. This is positive as high temperature has been discussed in section 3.4.1 as a main factor in discolouring the final products

3.4.2.1.3 Matrix Assisted Laser Desorption/Ionisation-Time of Flight Mass Spectrometry (MALDI-ToF MS) of Adipic Acid, Hexanediol Reaction at 185 °C Using Non-Organometallic Catalysts

The MALDI analysis on the non-organometallic catalysed polyesters produced spectra which were consistent with those previously discussed in section 3.4.1.2.3. The primary series involved a mixture of end groups with a secondary series based around the solely COOH terminated polyester. Therefore, for both types of heating method, these acidic catalysts did not appear to specifically favour a specific end group functionality and thus AV analysis was only performed for data completion.

3.4.2.1.4 Differential Scanning Calorimetry of Adipic Acid, Hexanediol Reaction Product Synthesised at 185 °C Using Non-Organometallic Catalysts

DSC was performed on the non-organometallic catalysed polyesters and the T_m's were compared to those of the DHBTC catalysed polyesters, this data is shown below in Table 3-15.

Table 3-15. DSC results for an AA HD polyester processed at 185 °C for the non-organometallic catalysed reactions compared to industrially used DHBTC. MWt data has been added for comparison

Catalyst	Heating Method	[a] Final Conv. (%)	[b] T_m (°C)	[c] M_n^{GPC} (g.mol^{-1})	[c] Đ
DHBTC	CH	96	54.6	4,580	2.36
	MWH	93	52.0	2,460	2.59
PA	CH	94	54.1	2,750	2.47
	MWH	94	54.9	3,130	2.60
PPA	CH	93	55.7	3,370	2.13
	MWH	93	54.9	3,210	2.19

[a] Calculated using polymer to monomer peak ratio in ^{1}H NMR. [b] Calculated using TA-Q2000 DSC. [c] Calculated using THF GPC and ASTRA processing software relative to a polystyrene standard.

The data shown in Table 3-15 is mostly consistent with the MWt data, which has been added for comparison. The value which was higher than expected is the PA catalysed reaction implementing CH. For example, this products M_n^{GPC} was almost 2k g.mol^{-1} lower than the product processed with DHBTC, but, the T_m values are within 0.5 °C. With this difference in MWt it was expected that the T_m would be reduced, as in the MWH DHBTC sample (T_m = 52 °C). But, this increased T_m value in the CH PA product may occur due to a plateau in the T_m value once a certain value of M_n^{GPC} is reached or between certain M_n^{GPC} values. Considering the MWH products, there was a 3 °C increase in the non-

organometallic catalysed samples at similar conversions. But this can be explained by the increased M_n^{GPC} of these samples compared to CH.

3.4.2.2 Conventionally versus Microwave Heated Reactions at 150 °C using Non-Organometallic Catalysts

To continue with the investigation into lower temperature melt polycondensations, reactions were conducted at 150 °C as had been done in the organometallic catalysed reactions.

Initially, the reaction was evaluated for kinetics and comparisons were drawn between CH and MWH. Again, the DHBTC catalyst profile is included for comparison. This data is shown in Figure 3-43.

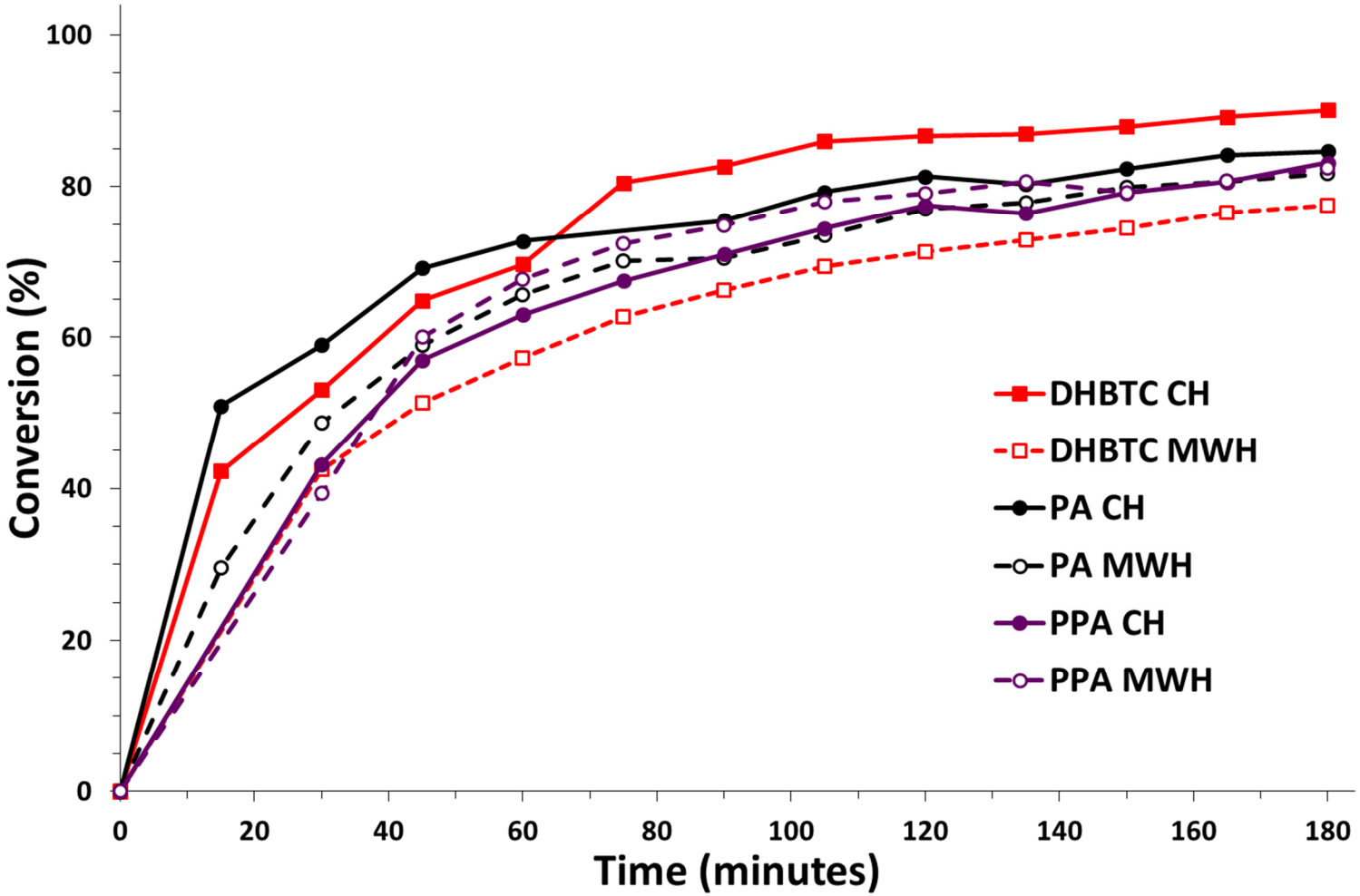


Figure 3-43. Plot of conversion % versus time for AA, HD polycondensation at 150 °C using different heating methods, non-organometallic catalysts and an industrially used DHBTC tin catalyst for comparison and with no mass transfer application.

Figure 3-43 shows the DHBTC catalysed reactions achieved the highest final conversion when CH was adopted at 150 °C, whilst by comparison when MWH was employed it exhibited the lowest final conversion. The data confirmed that catalyst selection is vitally important when implementing MWH in polycondensations.

PA was shown to have the fastest initial reaction rate when using CH, but once a conversion of ~70 % was reached, the conversion plateaued. This suggested that at 150 °C, PA is a more efficient catalyst when synthesising low MWt's, due to the high density of free H^+ ions, but once higher conversions and MWt's are reached, the effect reduces. This is because the final conversion achieved is similar to the other non-organometallic catalysed reactions.

Considering the MWH reactions in Figure 3-43, initially PA had a faster reaction rate than PPA and DHBTC. But, once a reaction time of 45 minutes was reached, the PPA and PA curves aligned, as in the 185 °C reactions shown in Figure 3-41. This suggested that at the two temperatures investigated, the non-organometallic catalyst reacted using a similar mechanism, even though the dielectric properties of PPA were significantly different. As at 185 °C, this is potentially due to the presence of similar levels of free H^+ ions when using both catalysts, leading to similar reaction rates or it could be because of conversion of PPA to form PA in the presence of the condensate. .[76,77] However, when considering the 185 °C reaction it is likely to be because of the similar levels of H^+ ions in the reaction mix as there was shown a differences between the PA MWH and CH MWt's, whereas there wasn't in MWH. This suggested a different mechanism in the MWH PA reaction which promoted chain elongation relative to the CH and both PPA reactions.

3.4.2.2.1 Size Exclusion Chromatography (SEC) of Adipic Acid, Hexanediol Reaction at 150 °C Using Non-Organometallic Catalysts

The polyesters synthesised were then analysed using standard polymer analysis techniques as in previous sections. The resultant GPC analysis of the non-organometallic catalysed products is shown in Table 3-16, where again the values obtained are compared to the DHBTC catalyst for a comparison with an industrially used catalyst.

Table 3-16. GPC analysis of non-organometallic catalysed adipic acid, hexanediol polycondensations compared to industrially used DHBTC polyester.

Catalyst	Heating Method	[a] Final Conv. (%)	[b] M_n^{GPC} (g.mol^{-1})	[b] M_w^{GPC} (g.mol^{-1})	[b] M_p^{GPC} (g.mol^{-1})	Đ
DHBTC	CH	90	1,690	3,640	2,770	2.16
	MWH	77	1,040	1,960	1,810	1.88
PA	CH	86	1,600	3,240	2,320	2.03
	MWH	82	1,560	3,140	2,340	2.01
PPA	CH	83	1,650	3,250	2,320	1.97
	MWH	82	1,700	3,330	2,340	1.96

[a] Calculated using polymer to monomer peak ratio in ^{1}H NMR. [b] Calculated using THF GPC and ASTRA processing software relative to a polystyrene standard.

The polyesters synthesised using PA and PPA were observed to have reached similar final MWt's from the application of the two heating methods. Both catalysts had similar M_n^{GPC} and Đ values. Comparing the products to the DHBTC catalyst showed that the M_n^{GPC}'s achieved in the non-organometallic catalysed products were similar to the CH DHBTC product, even though there is a reduction in final conversion. However, this lower value in the CH DHBTC product is likely due to the increased Đ, supported by the increased M_w^{GPC} and

M_p^{GPC} values and the slightly increased T_m, reported later in section 3.4.2.2.4. Unlike at 185 °C, there was close control for both catalysts due to the low Đ values. However, these Đ values were expected to be lower due to the lack of formation of higher MWt chains due to the lower conversions achieved.

As discussed in 3.4.2.1.1, when comparing the DHBTC to the non-organometallic catalysed polyesters, there was higher M_n^{GPC}'s for the non-organometallic catalysed polyesters at the final conversions achieved. This was shown by the lower conversions achieved in the PA and PPA catalysed reactions having similar MWt properties to the highly converted DHBTC. This further suggested that the non-organometallic catalysts have high efficiencies at the initial stages of the reaction.

3.4.2.2.2 Colorimetry – GS Analysis of Adipic Acid, Hexanediol Reaction at 150 °C Using Non-Organometallic Catalysts

GS colour analysis of the polyesters is detailed below in Table 3-17.

Table 3-17. GS colour analysis of AA HD polyester synthesised at 150 °C using non-organometallic catalysts and industrially used DHBTC tin catalysts with different heating methods.

Catalyst	Heating Method	[a] GS Number	[a] GS Hue
DHBTC	CH	0.1	0
	MWH	0.1	0
PA	CH	0.4	0
	MWH	0.2	0
PPA	CH	0.2	0
	MWH	0.2	0

[a] Calculated using a Lovibond PFX1-950 and GS colour standards 1-18.

Similar to section 3.4.2.1.2, Table 3-17 showed there was negligible discolouration effects when implementing the non-organometallic catalysts. It was also observed from the data in Table 3-17 that there was only a difference between the heating methods when using the PA catalyst. But, this difference of 0.2 GS units was an insignificant amount and it was clear that using any of the catalysts detailed above would result in a colourless polyester resin.

3.4.2.2.3 Matrix Assisted Laser Desorption/Ionisation-Time of Flight Mass Spectrometry (MALDI-ToF MS) of Adipic Acid, Hexanediol Reaction at 150 °C Using Non-Organometallic Catalysts

MALDI analysis on the non-organometallic catalysed polyesters produced spectra which were consistent with the previously discussed samples in section 3.4.1.2.3. The primary series involved a mixture of end groups with a secondary series based around the COOH terminated polyester. Therefore, again these acidic catalysts are not specifically favouring a specific terminal group functionality and AV analysis was only performed for data completion.

3.4.2.2.4 Differential Scanning Calorimetry of Adipic Acid, Hexanediol Reaction at 150 °C Using Non-Organometallic Catalysts

DSC was performed on the acid catalysed polyesters and the thermal properties compared to the DHBTC catalysed polyesters below in Table 3-18.

Table 3-18. DSC results for an AA HD polyester processed at 150 °C for the non-organometallic catalysed reactions compared DHBTC.

Catalyst	Heating Method	[a] Final Conv. (%)	[b] T_m (°C)	[b] M_n^{GPC} (g.mol^{-1})	Đ
DHBTC	CH	90	47.0	1,690	2.16
	MWH	77	37.8	1,040	1.88
PA	CH	86	44.6	1,600	2.03
	MWH	82	45.3	1,560	2.01
PPA	CH	83	45.8	1,650	1.97
	MWH	82	46.5	1,700	1.96

[a] Calculated using polymer to monomer peak ratio in ^{1}H NMR. [b] Calculated using TA-Q2000 DSC.

The T_m's in Table 3-18 were all within the expected range for AA, HD polyesters of this conversion and MWt. Cross referencing the T_m values with the M_n^{GPC} values, Figure 3-44, there was a clear correlation shown by the high R^2 value, 0.9791, which supports the conclusion that the small difference in T_m was related to the final conversion percentage achieved in the CH and MWH reactions.

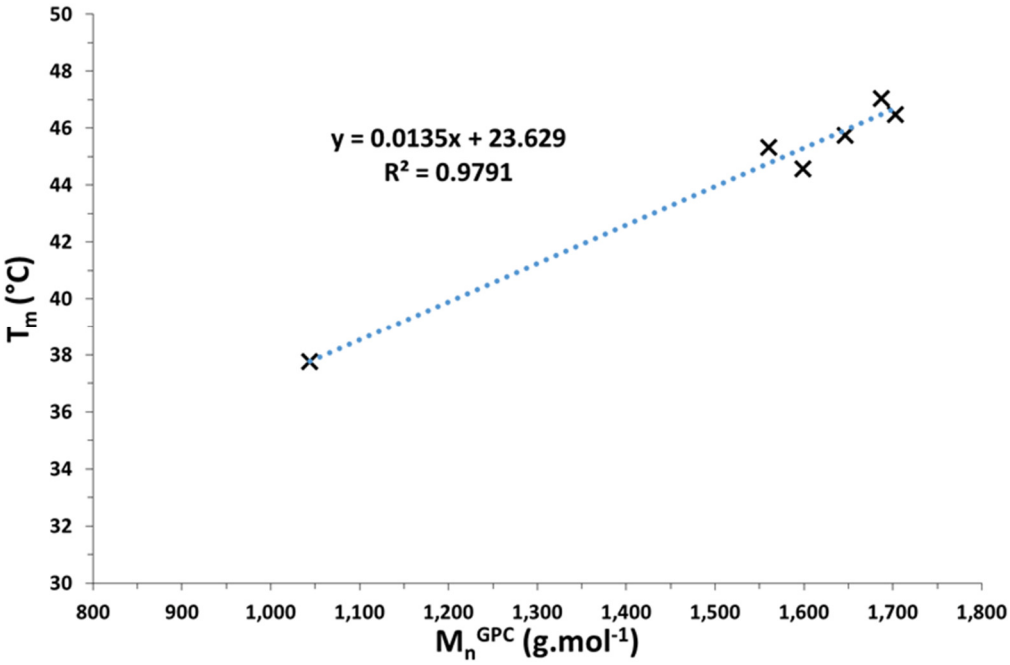


Figure 3-44. M_n^{GPC} versus Tm values for the AA, HD polyesters synthesised using DHBTC and non-organometallic catalysts independent of heating method.

3.5 Conclusions

3.5.1 Summary of Conclusions from Observations

Initially, the reaction cycle time was defined to allow maximum reaction comparisons in the initial heat-up stages of the reaction. It was concluded that for the AA, HD polycondensation, a cycle time of 3 hours was sufficient to allow kinetic reaction rate analysis to be conducted while producing a polyester product which had large enough MWt's to be subject to polymer analysis.

For the commonly used tin catalysts, mass transfer studies were conducted to assess if the process efficiency was determined by kinetics or diffusion. It was shown that the stirring rate had minimal effect on the reaction rate. It was concluded that this was because the system being investigated involved a homogeneous catalyst and low viscosities at the temperatures and MWt's investigated, allowing easy transport of the reagents and condensate throughout the system. The slight differences observed were attributed to the vortex created at higher stirring speeds, which increased the surface area at the mixtures boundary and therefore the available places for condensate to evaporate, however this effect was negligible to conversion rate. Vacuum was confirmed as an important factor when wanting to process the reactions towards completion. A higher vacuum was shown to promote longer chain formation towards the end of the reaction and increasing reaction rate in the initial stages. Therefore, it was deduced that the reaction rate is dictated by kinetics.

Implementing MWH produced a catalyst efficiency swap between $Sn(Oct)_2$ and DHBTC when compared to CH. This was shown by the DHBTC catalyst converting at a faster rate when using CH and $Sn(Oct)_2$ converting at a faster

rate when implementing MWH. This catalyst swap is observed at both 150 and 185 °C. This swap was attributed due to the two possible explanations;

i. Difference in dielectric properties.

ii. Mechanistic differences.

Difference in dielectric properties between the catalysts explained this difference because the dielectrics of $Sn(Oct)_2$ were high when compared to DHBTC at both temperatures investigated. This means that the microwaves will be more effective at selectively heating the $Sn(Oct)_2$ catalyst. Therefore, the reduction in E_a of the reaction that the catalyst provides will be emphasised.

The two mechanistic routes perform differently under MWH because the $Sn(Oct)_2$ catalyst forms a pre-catalytic species. This species forms associative bonds the growing polyester chain, catalysing polyester chain growth. In contrast, DHBTC inserts into the growing polyester chain to catalyse the reaction. It is hypothesised that the associative bond mechanism of $Sn(Oct)_2$ is favoured over the insertion mechanism for MWH reactions as microwaves are a non-ionising energy. This means they will not break covalent bonds. Therefore, breaking the bonds made in the DHBTC mechanism will require more energy than the associative bonds in $Sn(Oct)_2$.

For the tin catalysed reactions, both the MWH reactions at 185 °C are more efficient than the CH counterparts. But at 150 °C, the DHBTC catalysed CH reaction has the most efficient reaction rate. This is partially because the dielectric properties of the DHBTC are near zero at 150 °C and therefore the microwaves will not be effectively heating this component. The $Sn(Oct)_2$ catalysed reaction is consistently more efficient under MWH, but the increased reaction efficiency is minimised due to the reduced temperature which leads to

a reduction in water evaporation from the system. This reduction in water evaporation leads to increased backwards reaction of polyester to monomers.

An array of different organometallic catalysts were employed into the polycondensation with varying results between the CH and MWH experiments. At a reaction temperature of 185 °C, as found when using the tin catalysts, there was an efficiency swap between heating methods. This efficiency swap is ascribed to the differing dielectric properties of the catalysts, with higher tanδ values leading to more efficient heating in the EM field and therefore an increased reaction rate. Applying standard polymer analysis techniques showed that the properties of the end product were extremely varied. Bi triflate was found to not produce a polyester at this temperature. This was attributed to the Bi undergoing hydrolysis with the water at these high temperatures, concluded after a reaction under inert gas yielded an identical product. GS colour analysis was completed to assess if there was a difference in the heating techniques w.r.t. final product colour. It was shown that there was no correlation between heating method and final product colour, as well as no correlation between dielectric properties and level of discolouration in the MWH samples. MALDI analysis suggested that the zinc triflate catalysed reactions favoured an acid terminated polyester, unlike the other catalysts which suggested a primary mixture of terminal groups. These findings were cross-referenced with AV titrations to conclude that this suggestion was consistent. This was due to the high AV's at the MWt's and conversions produced by the zinc triflate catalysed samples. DSC analysis was conducted to confirm polymer formation and it was confirmed that there is a correlation between T_m and M_n^{GPC}. But, between heating methods there was no difference in correlation. This suggested that MWH doesn't alter the inherent thermal properties of the polymer.

Further catalyst studies were undertaken at 150 °C to assess the potential difference in MWH effects at reduced temperatures. As seen at 185 °C, there was a switch in the catalytic efficiencies between the heating methods. Interestingly, for the MWH reactions, the reaction rate does not follow with tanδ value as at 185 °C. An example was that $Sn(Oct)_2$ had high tanδ values compared to the other catalytic species, but the reaction rates were relatively slow. This was explained by the catalyst being less active at reduced temperatures. This was confirmed by the low M_n^{GPC}, and T_m values obtained form analysis. Although Bi triflate did not form polyester at 185 °C, there was polyester formation at 150 °C, with typical GPC and DSC traces. This suggested that hydrolysis of the Bi complex is less prominent at 150 °C, while fast reaction efficiencies were still retained. GS colour analysis was conducted and a positive effect on discolouration by using MWH was observed. All but one of the catalysts used with MWH produced less or identically discoloured product. This was attributed to the microwaves not promoting the hydrolysis side reactions that lead to discolouration due to the fact that water will be superheated by the microwaves. Therefore, the water is evaporated at a rate which is too fast to react with the catalyst. MALDI analysis of the polyesters showed that at 150 °C, the COOH terminating group is for all the polyesters. This is interesting as it was the mixture of end group series which was the most prominent at 185 °C. This was correlated with AV results but these were conflicting, with a higher converted polyester at 150 °C having higher AV's than at 185 °C, but a lower converted polyester having lower AV's than at 185 °C. This result is due to the higher temperatures promoting long chain formation over the lower temperatures, decreasing chain ends and therefore acid groups. DSC analysis of the polyesters suggested there was more controlled growth of the MWH species, with T_m following M_n^{GPC} and conversion % with a significantly closer

correlation than at 185 °C. This implies that the MWH mechanism at 150 °C is a more efficient way to target specific MWt's than when using CH.

Non-organometallic catalysts were evaluated for their use in melt polycondensations due to the increased environmental and processing benefits over the currently used organometallic alternatives.

At 185 °C, it was observed that the non-organometallic catalysts had a faster reaction rate when using MWH over CH. Again, this observation was due to the increased heating efficiencies when using MWH. GPC analysis suggested that when using both non-organometallic catalysed species and MWH, the polyesters synthesised were of a higher MWt than when using DHBTC at similar conversions. This was attributed to the free H^+ ions in the acids being active in an EM field due to their large charge to mass ratio. GS colour analysis displayed minimal discolouration from these catalysts, comparable to DHBTC. MALDI showed that the polyesters produced followed the mixture of terminal series. DSC was used to confirm polymeric species were present. Also, it was indicated that these catalyst could potentially increase the thermal properties of the polymers at similar MWt's, but this is only speculative with this amount of results.

At 150 °C, PA catalysed reactions were shown to have efficient initial reaction rates when using CH. But, once higher conversion levels were reached, the efficiency decreases. This suggests that the Fischer esterification mechanism favours shorter chained polymers. For the MWH reactions, there is minimal difference in the reaction profiles, attributed to the fact that PPA can be hydrolysed by the condensate to form PA. This negated any positive impact the dimeric species had on the reaction *via* high dielectric properties. Again, as at 185 °C, the MWt values of the non-organometallic catalysed samples were high when compared of the DHBTC catalysed samples. This further suggested that the Fischer esterification mechanism is an efficient mechanism pathway for low

MWt polyesters. Colorimetry confirmed that the non-organometallic catalysts don't discolour the final product and that lowering the processing temperature does not greatly reduce the GS numbers. MALDI confirmed that the primary series was based around a mixture of terminated chains, which is different to the organometallic catalysts at this temperature which were all COOH terminated. This was because of the acidic catalyst creating an acidic reaction environment, favouring a non-acidic polyester to balance the overall charge of the mixture. DSC analysis showed an increase in the T_m values for the polyesters synthesised using MWH. But, when the T_m's were compared to the M_n^{GPC} values, there was a clear correlation, explaining variance in thermal properties.

3.5.2 Mechanistic Conclusion

The mechanistic pathway in which the polyesterification reactions occurred was discussed in detail within this chapter. This highlighted a significant finding which is discussed below.

By evaluating the differences between the CH reactions and the MWH reactions at 185 °C it was shown that $Sn(Oct)_2$ catalysed the reaction at a reduced rate in the CH reactions, but once MWH was introduced, the reaction rate increased considerably. This was shown by considering the conversion after 15 minutes which went from 20 % in the CH system to 90 % in the MWH system. Whereas, the DHBTC catalyst increased from 40 % conversion after 15 minutes to 80 %. To ascertain why the efficiency of the polyesterification increased, dielectric analysis was conducted on the catalysts and it was shown that although the $Sn(Oct)_2$ had increased properties at 185 °C, these were

negligible and therefore this couldn't be the key to explain why there was such a large difference in reaction rate between the two heating methods and catalysts. Hence, it was hypothesised that there was a difference in the mechanisms involved in the catalytic cycle.

For $Sn(Oct)_2$ there was 2 proposed reaction mechanisms; one involving an associative coordination of the pre-catalyst with the carboxylic acid and one which included carboxyl insertion into the pre-catalyst metal centre. For the DHBTC catalyst a Lewis acid based mechanism was described, with coordination of the carboxyl onto the tin metal centre. Considering these mechanism it was deduced that the most probable mechanism for the $Sn(Oct)_2$ catalysed system was the associatively bonded system. This is because the increase in reaction rate between CH and MWH was so large compared to DHBTC that there must be a differentiating factor between the polyesterifications, which cannot be the dielectrics as they are too similar at reaction temperature. Therefore, the rapid increase in the $Sn(Oct)_2$ rate by implementing MWH was due to the labile nature of the associative bonds being easily manipulated by the EM energy. This is more probable than the formal bonded mechanism because of the non-ionising nature of EM energy *i.e.* it cannot make/break formal bonds. Therefore, by having only associative bonds with the metal catalyst, the reaction rate can be rapidly increased under MWH.

This increase in catalyst efficiency for $Sn(Oct)_2$ using MWH was also shown at a reduced temperature, were the CH reactions showed minimal to no catalysis. This increase in efficiency from CH to MWH was not observed in DHBTC, with the CH reaction processing at a faster rate and to a higher conversion. This further suggested that there was a mechanistic difference between catalysts.

Considering the other organometallic catalyst mechanisms showed that all of these proceeded *via* formal bonding mechanisms. This explained why there was

no obvious differences between the MWH and CH reaction efficiencies at 185 °C. Although, this may have been due to the extremely fast reaction rates observed in both MWH and CH at this temperature. However, at 150 °C there was a clear increase in reaction rate from CH to MWH for the ZrDC catalyst, but this was not as prominent as in $Sn(Oct)_2$. This can be explained by the large amount of associative interactions between the metal catalyst and the growing polymer chain. These interactions were readily excited by the EM energy and helped catalyse the reaction. Therefore, although there was formal bond making and breaking in the reaction mechanism, there was enough associative interactions to allow enhancement of the reaction rate *via* MWH.

Acidic non-organometallic catalysts were investigated in terms of their reaction mechanism and this was shown to proceed *via* the Fischer esterification mechanism. In this system there are a large amount of free H^+ ions involved in the catalytic cycle. In theory, this was positive for MWH applications due to the formal charges being readily manipulated by the EM energy. This led to an increased reaction rate for the 185 °C reactions, with the increases being similar to the DHBTC system. This was an expected result due to the fact that the mechanisms described for the Fischer esterification and Lewis acid esterification are similar, both with formal bond making and breaking. So although there were a large amount of readily excited H^+ ions in the non-organometallic synthesis, the mechanistic pathway was not as favourably accelerated as in a fully associatively bonded mechanism. However, it was shown that the MWH PA catalysed system did create a higher MWt product than the CH product. This therefore suggested that there was a difference in mechanism between the PA and PPA catalysts when MWH is implemented. Considering the 150 °C reactions showed that there was minimal difference between the CH and MWH reactions. This system therefore performed better

than the DHBTC system at these lowered temperatures, most likely due to the easily manipulated H^+ ions, but the formal making and breaking of bonds led to there being no increase in reaction rate.

3.6 References

1 Sokolsky-Papkov, M., Langer, R. & Domb, A. J. Synthesis of aliphatic polyesters by polycondensation using inorganic acid as catalyst. *Polymers for advanced technologies* 22, 502-511 (2011).

2 Scheirs, J. & Long, T. E. *Modern Polyesters: Chemistry and Technology of Polyesters and Copolyesters*. (Wiley, 2005).

3 Dowling, C. M. & Seshadri, R. Polyester polycondensation with titanyl oxalate catalyst and a catalyst enhancer. US6258925 (2001).

4 Stille, J. K. PALLADIUM CATALYZED COUPLING OF ORGANOTIN REAGENTS WITH ORGANIC ELECTROPHILES. *Pure Appl. Chem.* 57, 1771-1780, doi:10.1351/pac198557121771 (1985).

5 Stille, J. K. THE PALLADIUM-CATALYZED CROSS-COUPLING REACTIONS OF ORGANOTIN REAGENTS WITH ORGANIC ELECTROPHILES. *Angewandte Chemie-International Edition in English* 25, 508-523, doi:10.1002/anie.198605081 (1986).

6 Ichikawa, Y. *et al.* An Efficient Synthesis of Carbamates by Tin-Catalyzed Transcarbamoylation Reactions of Primary and Secondary Alcohols. *Synlett*, 1815-1818, doi:10.1055/s-0030-1258102 (2010).

7 Moliner, M., Roman-Leshkov, Y. & Davis, M. E. Tin-containing zeolites are highly active catalysts for the isomerization of glucose in water. *Proc. Natl. Acad. Sci. U. S. A.* 107, 6164-6168, doi:10.1073/pnas.1002358107 (2010).

8 Bermejo-Deval, R., Orazov, M., Gounder, R., Hwang, S.-J. & Davis, M. E. Active Sites in Sn-Beta for Glucose Isomerization to Fructose and Epimerization to Mannose. *ACS Catalysis* 4, 2288-2297, doi:10.1021/cs500466j (2014).

9 Casas, A., Ramos, M. J., Rodríguez, J. F. & Pérez, Á. Tin compounds as Lewis acid catalysts for esterification and transesterification of acid vegetable oils. *Fuel Processing Technology* 106, 321-325, doi:http://dx.doi.org/10.1016/j.fuproc.2012.08.015 (2013).

10 Ferreira, A. B. *et al.* Tin-Catalyzed Esterification and Transesterification Reactions: A Review. *ISRN Renewable Energy* 2012, 13, doi:10.5402/2012/142857 (2012).

11 Cho, C. S., Kim, D. T., Choi, H. J., Kim, T. J. & Shim, S. C. Catalytic activity of tin(II) chloride in esterification of carboxylic acids with alcohols. *Bulletin of the Korean Chemical Society* 23, 539-540 (2002).

12 Hutchins, J. E. & Wilson Earl, W. Tin salts catalysts for polyesterification process. US3194791 A (1965).

13 Vogt, H. C., Parekh, M. & Patton, J. T. Tin titanium complexes as esterification/transesterification catalysts. US 4020010 A (1977).

14 Sobczak, M. Ring-opening polymerization of cyclic esters in the presence of choline/SnOct2 catalytic system. *Polymer Bulletin* 68, 2219-2228, doi:10.1007/s00289-011-0676-8 (2012).

15 Kowalski, A. *et al.* Kinetics and Mechanism of Cyclic Esters Polymerization Initiated with Tin(II) Octoate. Polymerization of ε-Caprolactone and L,L-Lactide Co-initiated with Primary Amines. *Macromolecules 2*, 8170-8176 (2005).

16 Storey, R. F. & Sherman, J. W. Kinetics and Mechanism of the Stannous Octoate-Catalyzed Bulk Polymerization of ε-Caprolactone. *Macromolecules* 35, 1504-1512, doi:10.1021/ma010986c (2002).

17 Koroskenyi, B. & McCarthy, S. P. Microwave-assisted solvent-free or aqueous-based synthesis of biodegradable polymers. *Journal of Polymers and the Environment* 10, 93-104, doi:10.1023/a:1021120113910 (2002).

18 Pandey, A. & Aswath, P. B. Microwave synthesis of poly(L-lactic acid). *Journal of biomaterials science. Polymer edition* 20, 33-48, doi:10.1163/156856208x393482 (2009).

19 Bakibaev, A. A. *et al.* Polymerization of Lactic Acid Using Microwave and Conventional Heating. *Procedia Chemistry* 15, 97-102, doi:http://dx.doi.org/10.1016/j.proche.2015.10.015 (2015).

20 Deng, E. *et al.* Molecular Differentiated Initiator Reactivity in the Synthesis of Poly(caprolactone)-Based Hydrophobic Homopolymer and Amphiphilic Core Corona Star Polymers. *Molecules* 20, 20131–20145 (2015).

21 Sumner, C. E., Barnicki, S. D. & Dolfi, M. D. Process for the production of sterol and tocopherol concentrates. US 5424457 (1995).

22 Takekoshi, T., Bahr, S. R. & Winckler, S. J. Intimate physical mixtures containing macrocyclic polyester oligomer and filler. US 6960626 B2 (2005).

23 Gall, J. *The Systems Bible: The System always kicks back*. 3rd edn, (General Systemantics Press, 2002).

24 Bhatia, K. K. Polyesters production process. US5599900A (1997).

25 Bacaloglu, R., Fisch, M. & Biesiada, K. Kinetics of polyesterification of adipic acid with 1,3-butanediol. *Polymer Engineering and Science* 38, 1014-1022, doi:10.1002/pen.10268 (1998).

26 Goodman, E. S. H. *Handbook Of Thermoset Plastics*. (Jaico Publishing House, 2005).

27 Appleby, D. B. *et al.* Polyol polyester synthesis. CA 2089170 C (2007).

28 Yokoyama, H., Sano, T., Chijiwa, T. & Kajiya, R. Degradation Reactions in the Ethylene Glycol Terephthalate Polycondensation Process. *Journal of The Japan Petroleum Institute* 3, 194-198 (1978).

29 Naphadzokova, L. K., Kozlov, G. V. & Zaikov, G. E. Time-dependent transition from fractal to euclidean kinetics for model reaction of re-esterification. *Journal of the Balkan Tribological Association* 13, 329-333 (2007).

30 Fakirov, S. *Handbook of Condensation Thermoplastic Elastomers*. 256-257 (Wiley, 2006).

31 Hutcheon, R., Dejong, M. & Adams, F. A system for rapid measurements of rf and microwave properties up to 1400-degrees-c .1. Theoretical development of the cavity frequency-shift data-analysis equations. *J. Microw. Power Electromagn. Energy* 27, 87-92 (1992).

32 Hutcheon, R. *et al.* A system for rapid measurements of rf and microwave properties up to 1400-degrees-c .2. Description of apparatus, data-collection techniques and measurements on selected materials. *J. Microw. Power Electromagn. Energy* 27, 93-102 (1992).

33 Kappe, C. O., Dallinger, D. & Murphree, S. S. *"Practical Microwave Synthesis for Organic Chemists"*. (Wiley-VCH, 2009).

34 Hild, F. *et al.* Facile Determination of Molecular Structure Trends in Amphiphilic Core Corona Star Polymer Synthesis via Dielectric Property Measurement. *Macromolecular Rapid Communications* 27, 1295-1299, doi:10.1002/marc.201600149 (2016).

35 Kowalski, A., Duda, A. & Penczek, S. Kinetics and Mechanism of Cyclic Esters Polymerization Initiated with Tin(II) Octoate. 3. Polymerization of l,l-Dilactide. *Macromolecules* 33, 7359-7370, doi:10.1021/ma000125o (2000).

36 Kimura, Y. Molecular, Structural, and Material Design of Bio-Based Polymers. *Polym. J* 41, 797-807 (2009).

37 Niaounakis, M. *Biopolymers: Processing and Products*. (Elsevier Science, 2014).

38 Knifton, J. F. Process for preparing acetic and propionic acids and their esters. US4362822 (1982).

39 López, D. E., Goodwin Jr, J. G., Bruce, D. A. & Furuta, S. Esterification and transesterification using modified-zirconia catalysts. *Applied Catalysis A: General* 339, 76-83, doi:http://dx.doi.org/10.1016/j.apcata.2008.01.009 (2008).

40 Werber, F. X. Titanium and zirconium esterification catalysts. US305681 (1962).

41 Buzin, P., Lahcini, M., Schwarz, G. & Kricheldorf, H. R. Aliphatic Polyesters by Bismuth Triflate-Catalyzed Polycondensations of Dicarboxylic Acids and Aliphatic Diols. *Macromolecules* 41, 8491-8495, doi:10.1021/ma8017662 (2008).

42 Takasu, A., Oishi, Y., Iio, Y., Inai, Y. & Hirabayashi, T. Synthesis of aliphatic polyesters by direct polyesterification of dicarboxylic acids with diols under mild conditions catalyzed by reusable rare-earth triflate. *Macromolecules* 36, 1772-1774, doi:10.1021/ma021462v (2003).

43 Konishi, S., Yokoi, T., Ochiai, B. & Endo, T. Effect of metal triflates on direct polycondensation of lactic acid. *Polymer Bulletin* 64, 435-443, doi:10.1007/s00289-009-0148-6 (2009).

44 Shekarriz, M., Taghipoor, S., Khalili, A. A. & Jamarani, M. S. Esterification of carboxylic acids with alcohols under microwave irradiation in the presence of zinc triflate. *Journal of Chemical Research* 2003, 172-173, doi:10.3184/030823403103173381 (2003).

45 Shamiri, A. *et al.* The Influence of Ziegler-Natta and Metallocene Catalysts on Polyolefin Structure, Properties, and Processing Ability. *Materials* 7, 5069-5108, doi:10.3390/ma7075069 (2014).

46 Santos, L. S. What do we know about reaction mechanism? the electrospray ionization mass spectrometry approach. *Journal of the Brazilian Chemical Society* 22, 1827-1840 (2011).

47 Garaleh, M., Lahcini, M., Kricheldorf, H. R. & Weidner, S. M. Syntheses of aliphatic polyesters catalyzed by lanthanide triflates. *Journal of Polymer Science Part A: Polymer Chemistry* 47, 170-177, doi:10.1002/pola.23136 (2009).

48 Dunn, A. S. Polymer chemistry: An introduction (2nd edition) M. P. Stevens, Oxford University Press, New York, 1990. pp. xvii + 633, price £40 (hardback), £17.50 (paperback) ISBN 0-19-505759-7 (hardback) ISBN 0-19-506646-2 (paperback). *Polymer International* 25, 258-258, doi:10.1002/pi.4990250415 (1991).

49 Engineers, N. B. C. *The Complete Book on Adhesives, Glues & Resins Technology*. (NIIR Project Consultancy Services, 2007).

50 Weinert, R. J., Garcia, G. C., Robbins, J. E. & Fay, M. J. Coating derived from polyesters crosslinked with melamine formaldehyde. US 7727436 (2010).

51 Verborgt, J. Process for production acid polyester resins and powder coating products prepared from said resins. US 4065438 (1977).

52 Zhou, L., Thames, S. F., Smith, O. W., Boon, W. H. & Forschner, T. C. Carboxyl-functional polyester epoxy resin powder coatings based on 1,3-propanediol. US 6534178 (2003).

53 Bhattacharya, A., Rawlins, J. W. & Ray, P. *Polymer Grafting and Crosslinking*. 275 (Wiley, 2008).

54 Sigma-Aldrich. Material Safety Data Sheet - POLY(1,6-HEXAMETHYLENE ADIPATE), AVERAGE MN CA. 3,800. (2006).

55 Hu, Y., Daoud, W., Cheuk, K. & Lin, C. Newly Developed Techniques on Polycondensation, Ring-Opening Polymerization and Polymer Modification: Focus on Poly(Lactic Acid). *Materials* 9, 133 (2016).

56 Cowie, J. M. G. *Polymers: Chemistry & Physics of Modern Materials*. 2nd edn, 29 (Blackie, 1991).

57 Shaikh, I. R. Organocatalysis: Key Trends in Green Synthetic Chemistry, Challenges, Scope towards Heterogenization, and Importance from Research and Industrial Point of View. *Journal of Catalysts* 2014, 35, doi:10.1155/2014/402860 (2014).

58 Zhou, X. & Hong, L. Controlled ring-opening polymerization of cyclic esters with phosphoric acid as catalysts. *Colloid and Polymer Science* 291, 2155-2162, doi:10.1007/s00396-013-2950-9 (2013).

59 Pivsa-Art, S. *et al.* Preparation of Biodegradable Polymer Copolyesteramides from L-Lactic Acid Oligomers and Polyamide Monomers. *Energy Procedia* 56, 648-658, doi:http://dx.doi.org/10.1016/j.egypro.2014.07.204 (2014).

60 Ponmanee, L., Pechyen, C. & Sirisansaneeyakul, S. Synthesis of Polylactic Acid from Fermentative Lactic Acid by Direct Polycondensation for Materials Application. *Advanced Materials Research* 626, 495-499 (2013).

61 Spink, S. S., Kazakov, O. I., Kiesewetter, E. T. & Kiesewetter, M. K. Rate Accelerated Organocatalytic Ring-Opening Polymerization of l-Lactide via the Application of a Bis(thiourea) H-bond Donating Cocatalyst. *Macromolecules* 48, 6127-6131, doi:10.1021/acs.macromol.5b01320 (2015).

62 Sonti, V. R. & Mahesh, A. G. (Google Patents, 2010).

63 Ren, J. in *Biodegradable Poly(Lactic Acid): Synthesis, Modification, Processing and Applications* 15-37 (Springer Berlin Heidelberg, 2010).

64 Knani, D. & Kohn, D. H. Enzymatic polyesterification in organic media. II. Enzyme-catalyzed synthesis of lateral-substituted aliphatic polyesters and copolyesters. *Journal of Polymer Science Part A: Polymer Chemistry* 31, 2887-2897, doi:10.1002/pola.1993.080311202 (1993).

65 Kobayashi, S., Shoda, S.-i. & Uyama, H. in *Polymer Synthesis/Polymer Engineering* 1-30 (Springer Berlin Heidelberg, 1995).

66 Lim, L. T., Auras, R. & Rubino, M. Processing technologies for poly(lactic acid). *Progress in Polymer Science* 33, 820-852, doi:http://dx.doi.org/10.1016/j.progpolymsci.2008.05.004 (2008).

67 Ch. Behera, G. & Ramakrishnan, S. Transetherification polycondensation: The roles of the catalyst, monomer structure, and polymerization conditions. *Journal of Polymer Science Part A: Polymer Chemistry* 42, 102-111, doi:10.1002/pola.11009 (2004).

68 Mohammed, A. A. & Simonis, H. Process for the polycondensation of furfuryl alcohol. (1966).

69 Nakato, T., Kusuno, A. & Kakuchi, T. Synthesis of poly(succinimide) by bulk polycondensation of L-aspartic acid with an acid catalyst. *Journal of Polymer Science Part A Polymer Chemistry* 38, 117-122 (2000).

70 Chao, T. H., Wilcher, F. P., Ford, M. R. & Ringwelski, A. Z. Catalytic condensation process. (1991).

71 Sons, J. W. *Ullmann's Polymers and Plastics: Products and Processes*. 733-736 (Wiley, 2016).

72 Wang, H., Cheng, X., Shi, Y. & Le, G. Preparation and structural characterization of poly-mannose synthesized by phosphoric acid catalyzation under

microwave irradiation. *Carbohydrate polymers* 121, 355-361, doi:10.1016/j.carbpol.2014.12.046 (2015).

73 Hoogenboom, R., Schubert, U. S. & Wiesbrock, F. *Microwave-assisted Polymer Synthesis*. 211 (Springer International Publishing, 2016).

74 Velmathi, S., Nagahata, R., Sugiyama, J.-i. & Takeuchi, K. A Rapid Eco-Friendly Synthesis of Poly(butylene succinate) by a Direct Polyesterification under Microwave Irradiation. *Macromolecular Rapid Communications* 26, 1163-1167, doi:10.1002/marc.200500176 (2005).

75 Fischer, E. & Speier, A. Darstellung der Ester. *Berichte der deutschen chemischen Gesellschaft* 28, 3252-3258, doi:10.1002/cber.189502803176 (1895).

76 Corbridge, D. in *Studies in Inorganic Chemistry* Vol. Volume 20 169-305 (Elsevier, 1995).

77 "Phosphoric acid and phosphates". Encyclopedia of Chemical Technology. New York: The Interscience Encyclopedia, Inc. 1953. p. 421.

78 Gavish, N. & Promislow, K. Dependence of the dielectric constant of electrolyte solutions on ionic concentration: A microfield approach. *Physical Review E* 94, 012611 (2016).

79 Adlington, K. *et al.* Mechanistic Investigation into the Accelerated Synthesis of Methacrylate Oligomers via the Application of Catalytic Chain Transfer Polymerization and Selective Microwave Heating. *Macromolecules* 46, 3922-3930, doi:10.1021/ma400022y (2013).

4 Polymerisation of Isophthalic acid (IPA), Neopentyl glycol (NPG) and Trimethylolpropane (TMP) – Working Towards an Industrial Resin Process

4.1 Overview

Chapter 4 focuses on implementing a series of industrially used monomers in both the conventional (CH) and microwave heated (MWH) synthesis of polyester resin. The monomers examined were isophthalic acid (IPA), neopentyl glycol (NPG) and trimethylolpropane (TMP). These monomers are widely used in industry, with large volumes of polymers being produced and sold each year for coating applications.

Initially, only the linear reagents were investigated to gain insight into the reactivity of the system and gain an understanding of the product properties and morphology. This was conducted with CH, MWH and a subset of the catalysts used in chapter 3 including the tin catalysts and the non-organometallic catalysts. These were chosen as these produced the most promising results at the high temperatures with the previously investigated hexanediol, adipic acid system and, most importantly, did not discolour the product.

Additionally, pre-heating of a diol water mix was investigated using both CH and MWH because this was a commonly employed technique in the industrial processes. In this study, the system heat-up times were investigated to assess the differences between the heating methods and the advantages/disadvantages of pre-heating are discussed.

CH and MWH were then compared in terms of a comparison of the final polyester properties and it was identified that the MWH reactions can be processed to identical conversions in approximately half the time of the CH

reactions. Furthermore, the molecular weight (MWt) and thermal properties suggested that by implementing MWH there was an increase in polyester chain length for this fixed level of conversion.

Different reagent stoichiometries were investigated to assess how increasing the proportion of one monomer affects the polyesterification in both CH and MWH. It was shown that there was an optimal diol excess which helped increase the MWt of the polymers, but increasing this into a large excess was actually found to inhibit chain growth. It was also shown that an increase in diol excess helps to narrow the polydispersity (Đ) of the polyesters synthesised.

As in chapter 3, different temperatures were investigated to determine if a lower temperature could be utilised in polyester processing and in this chapter it was concluded that the polyesters can be synthesised at the lower temperatures using MWH. In fact MWH was also shown to achieve similar results at low temperatures than CH at high temperatures.

Finally, TMP monomer was added into the system to evaluate the full first stage of the industrial process at small scale for both CH and MWH. Again, a comparison of heat-up times was discussed and the reaction kinetics were evaluated. An increase in reaction rate was observed when implementing MWH. Also, large differences in MWt were observed between the products, with MWH producing a product with increased MWt. Furthermore, a high level of vacuum was applied to investigate prolonged exposure periods, resulting in a Weissenberg effect.

4.2 Results and Discussion

4.2.1 Isophthalic Acid, Neopentyl Glycol Polycondensation

For the initial investigation into using MWH as a viable option for an industrially processed polyester resin, no branching alcohol was introduced into the system. This was done to keep the product similar to the previous work on the linear adipic acid (AA), hexanediol (HD) system investigated in chapter 3. Therefore, the polyesters synthesised in this section were linear polyesters with NPG and IPA repeating units. The general scheme is shown below in Figure 4-1.

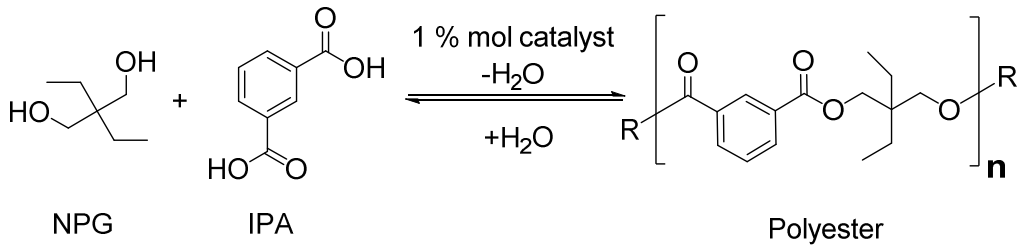


Figure 4-1. Scheme of an IPA, NPG polycondensation.

Neopentyl glycol is a diol which is extensively used in industry within many polyester resin applications,[1] for example, weather resistant coatings,[2] electrical resistant resins[3] and polyesters for use in aircraft and ship construction.[4] This is because it produces a final resin with:

a) Low initial colour.

b) Good colour stability.

c) Good powder flow and fluidisation properties.

d) Excellent balance between hardness and flexibility.

e) Good chemical and stain resistance.[5]

Isophthalic acid is a widely used diacid monomer for polyester resins used in powder coatings. It is a highly crystalline white powder with a high melting point (m.p.) of 343 °C. Because of this high melting point and therefore stability, the process temperatures employed are generally high to force both homogenisation of the reaction medium and to promote the condensation reactions with diols. [6] IPA is commonly used in powder coatings used for weather resistance, [2,7,8] the automotive industry [9] and general household items e.g. radiators and fridges. [10] IPA is a popular diacid monomer because:

a) It is stable and therefore easy to store for long periods.
b) It has excellent weathering characteristics when in a resin.
c) It has comparable impact resistance to acrylics.
d) It creates a more flexible resin than the terephthalic acid alternative which has the acids at the para positions.[5]

A subset of catalysts from Chapter 3 were investigated in this polymerisation. From the research conducted in Chapter 3, it was found that the discolouration of the final product was significant when using certain organometallic catalysts in the AA, HD reactions, especially at higher temperatures. Therefore, not all the catalysts from chapter 3 were investigated for this polycondensation system because the final product was used as a coating and therefore needed to be colourless. Furthermore, the processing temperatures employed in this chapter were higher than those in chapter 3 (+200 °C). As such, the catalysts being investigated were:

i) Dihydroxybutyl tin chloride (DHBTC).
ii) Phosphoric acid (PA).
iii) Pyrophosphoric acid (PPA).
iv) Tin(II) 2-ethylhexanoate (Tin octanoate/$Sn(Oct)_2$)

These had been shown to add the least amount of colour *via* visual inspection and Gardner Scale (GS) analysis at the higher processing temperatures. Although the $Sn(Oct)_2$ appeared visually colourless, the GS colour analysis showed it to have a high GS value. But, this was attributed to its lack of miscibility with the THF solvent the sample was dissolved in. Therefore, because of the visual inspection of colour assessment it was decided to progress with $Sn(Oct)_2$ in this chapter.

4.2.1.1 Evaluation of Tin versus Non-Organometallic Catalysts for Conventional and Microwave Heated Polycondensations of Isophthalic acid (IPA), Neopentyl glycol (NPG) at 200 °C

Initial catalyst studies were undertaken to assess the new monomer system with both CH and MWH for the tin and non-organometallic catalysts. An initial temperature of 200 °C was selected, which was lower than the industrial reaction temperature. This processing temperature was chosen to; (a) emphasise the differences in the catalysts efficiencies in MWH (due to large differences in dielectric values) and (b) to provide experience with these higher temperatures and product viscosities when compared to the AA, HD system. The results from the CH and MWH reactions are shown below in Figure 4-2.

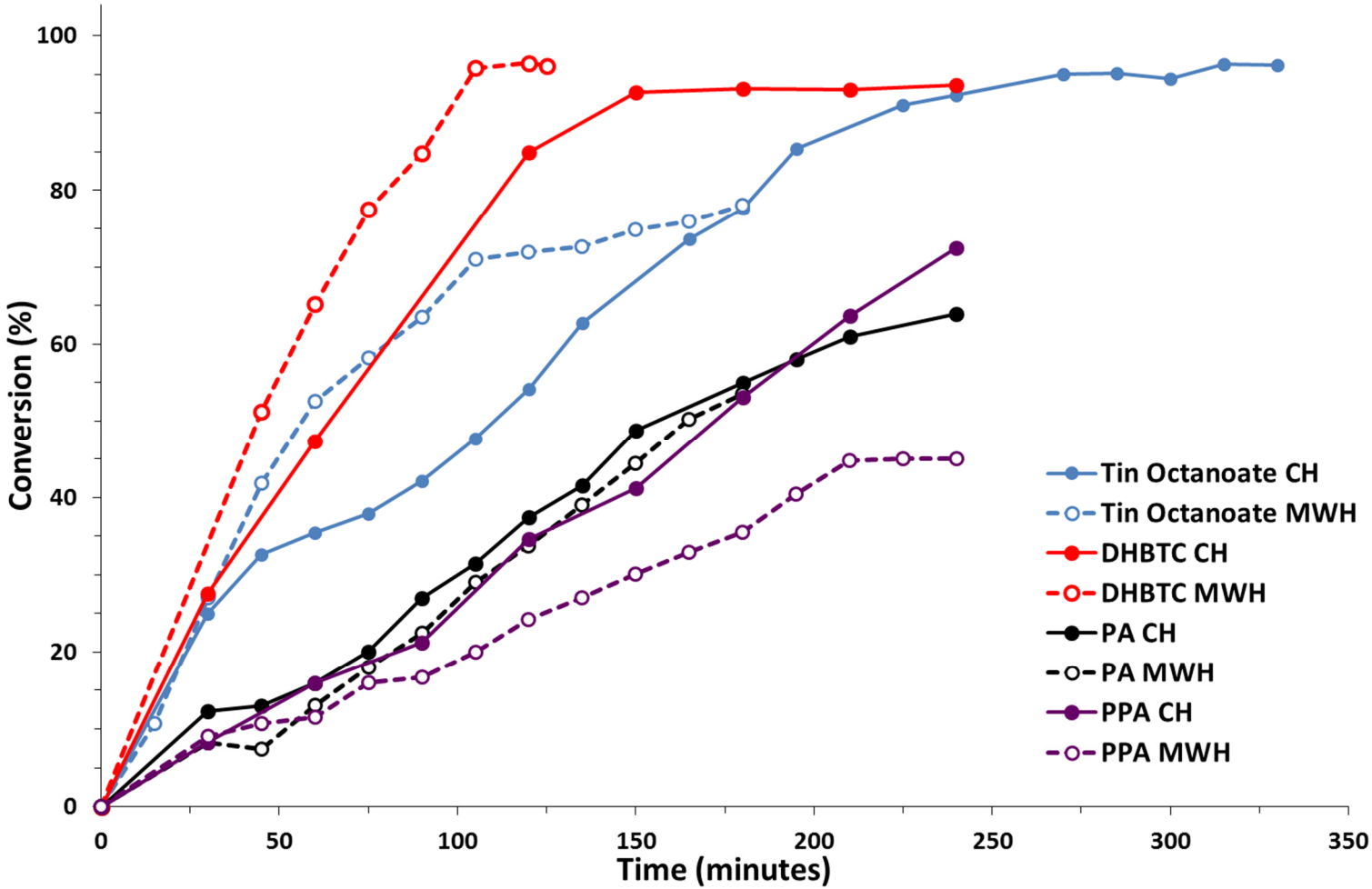


Figure 4-2. Conversion versus time for an IPA, NPG polycondensation at 200 °C showing the difference between catalysts and heating methods.

Observing the general profiles in Figure 4-2, only the two tin catalysts followed the expected polycondensation profile as previously described in Chapter 3. This suggested that the non-organometallic catalysts were not catalysing the reaction as efficiently as observed in the AA, HD study. This observation was attributed due to either the elevation in temperature affecting the catalysts in a negative way (decomposition of PA happens at ~213 °C), or the Fischer esterification mechanism not being efficient for these more crystalline monomers.

Interestingly, when comparing heating techniques from Figure 4-2 there was an increased reaction rate in the two tin compounds for MWH reactions, but a reduction in rate for the non-organometallic catalysts, especially PPA. This was surprising, because if the heating of the catalyst was an important factor in reaction rate, the PPA catalyst should have been efficient as the dielectric properties were higher than those of the two tin catalysts at 200 °C, shown in Figure 4-3. As in chapter 3, the dielectrics for the non-organometallic catalysts were processed at 910 MHz instead of 2.45 GHz as the dielectric losses of non-organometallic catalysts were too high for the network analyser to process at 2.45 GHz.

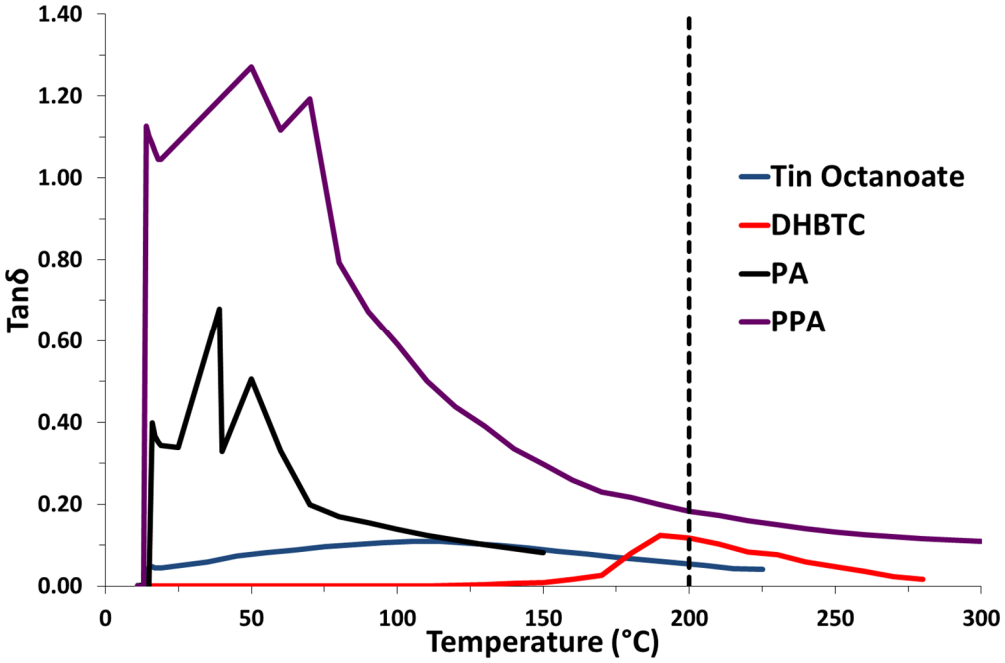
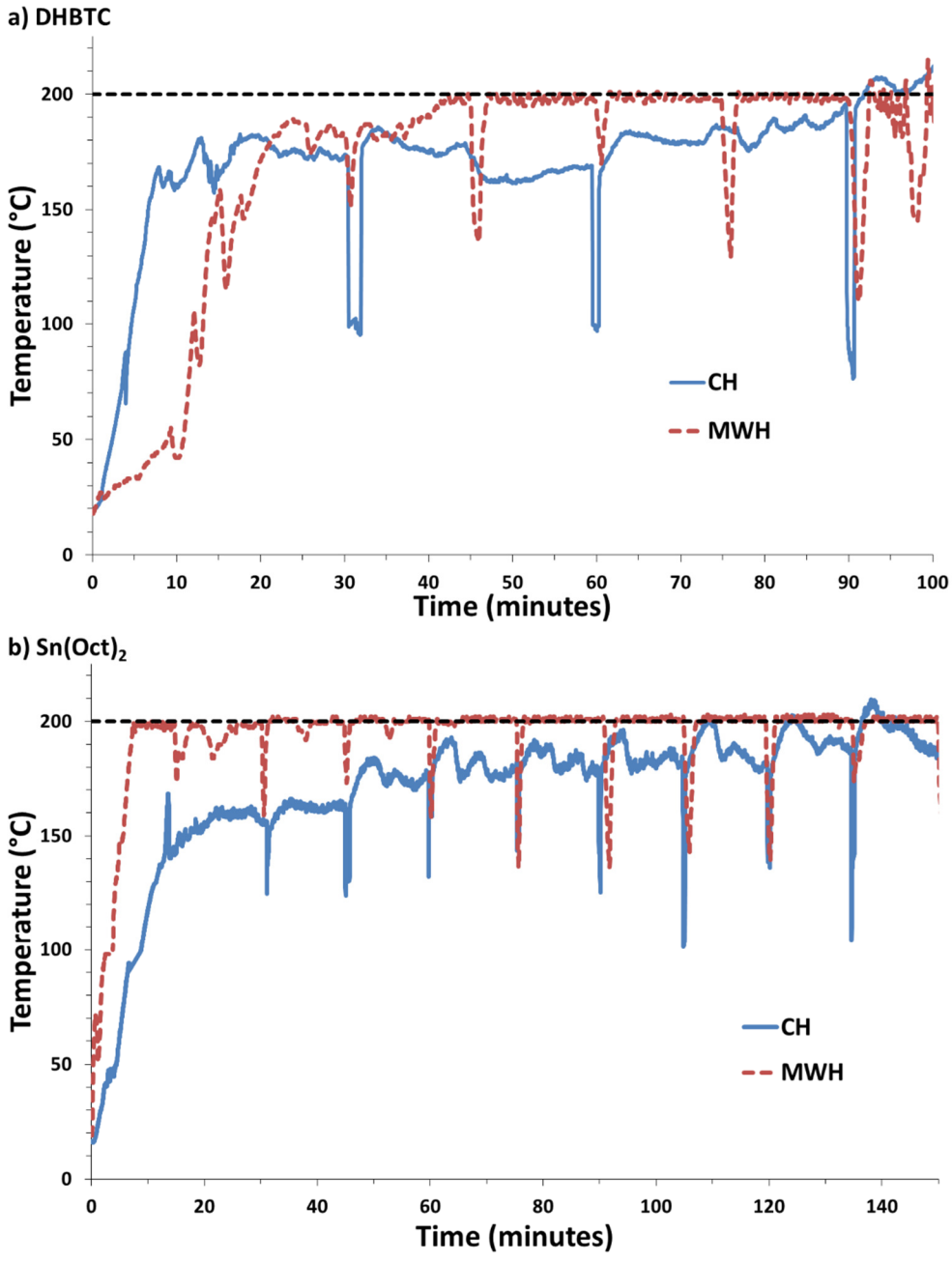


Figure 4-3. Dielectric properties of the catalysts used in the IPA, NPG polycondensation at 910 MHz.

The proportionally high tanδ value demonstrated in Figure 4-3 for PPA led to high amounts of energy being input into these non-organometallic catalysts (in MWH relative to CH) and therefore promoted to the conversion of PPA to PA. This subsequently led to the decomposition of PA due to the high reaction temperatures and the catalysts being over heated in the MWH, where the energy is proposed to be introduced directly to the catalysts as one of the materials that will selectively heat. Thus, this led to increased degradation of the catalyst at these high temperatures compared to the CH case and the reaction rate decreased when compared to CH.

One key observation during the reactions was the difference in system heat-up times that were observed. In the previous work on the AA, HD polyester in chapter 3, there was a vast difference in heat-up times between the MWH and CH reactions, with MWH reaching reaction temperature significantly quicker

than CH for all catalyst employed. This was attributed to the efficient heat transfer in MWH which led to rapid heating. But, in these crystalline monomer reactions, a catalyst specific dependency in heat-up times was observed, as described in Figure 4-4 and Table 4-1.



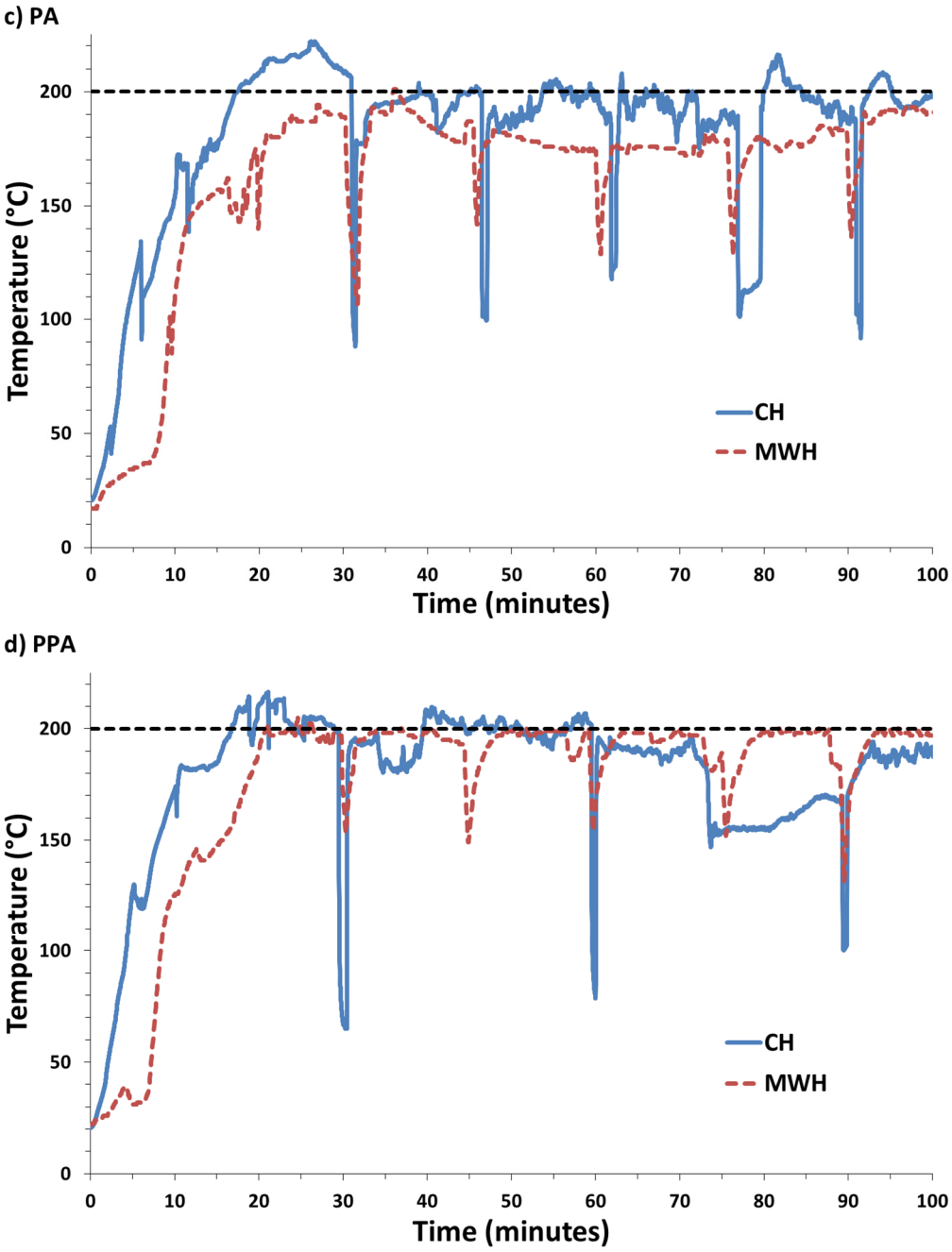


Figure 4-4. Initial heating profiles for IPA, NPG polycondensation at 200 °C using different catalysts. a) DHBTC, b) Sn(Oct)2, c) PA and d) PPA. With a black dotted line indicating 200 °C

Table 4-1. Heat-up times to 200 °C reaction temperature for an isophthalic acid, neopentyl glycol polycondensation.

Catalyst	Heating Method	Time to reach 200 °C (minutes)
DHBTC	CH	92
	MWH	43
$Sn(Oct)_2$	CH	109
	MWH	7
PA	CH	17
	MWH	36
PPA	CH	17
	MWH	21

From the heating profiles in Figure 4-4 and data in Table 4-1, it was noted that there was a large difference in heat-up times between the non-organometallic and tin catalysts. For the industrially used DHBTC, there was a slow heat-up time in CH, with 200 °C being achieved after 92 mins. Comparing this to MWH, which reaches 200 °C in 43 mins, and this partly explains why there was an increased reaction rate for the MWH reaction. This showed that when implementing CH, the heat transfer was not as efficient as MWH and therefore it elongated the heat-up time for the reaction bulk to reach a processing temperature of 200 °C and overcome this condensate cooling effect.

This slow heat-up time using CH was also observed for the $Sn(Oct)_2$ catalysed polymerisation, with MWH taking 7 mins and CH taking 109 mins to achieve processing temperature. This was attributed to the high dielectric properties of the catalyst and its physical state at room temperature (RT) i.e. it is in liquid physical for so can interact with the microwave energy for the start of the process. This allowed the species to absorb a large amount of energy and rapidly heat the reaction *via* conduction. By comparison DHBTC is solid at the outset thus does not interact so efficiently until later in the process.

Interestingly, in the cases of PA and PPA, there was a clear difference when compared to the tin catalysts. The CH reactions both heated-up to 200 °C in 17 mins, which was quicker than the corresponding MWH reactions of 36 and 21 mins for PA and PPA respectively. This was unexpected as the dielectric data from Figure 4-3 suggested that the non-organometallic catalysts were more efficient at turning electromagnetic (EM) energy into heat than the tin catalysts at lower temperatures. Therefore, these non-organometallic catalysts should have assisted the heat-up of the reaction bulk to a higher degree than DHBTC and $Sn(Oct)_2$.

This phenomenon was explained by comparing the dielectric properties of the monomer species with the catalysts, shown below in Figure 4-5.

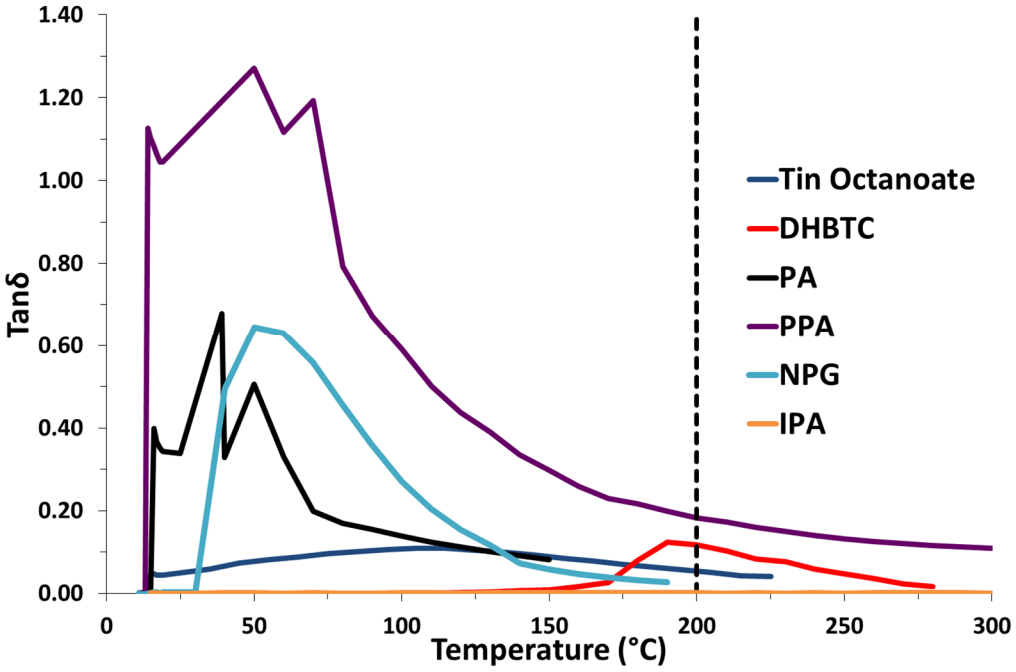


Figure 4-5. Dielectric properties of monomers and catalysts used in the IPA, NPG polycondensation at 910 MHz.

Figure 4-5 shows that when compared to the organometallic catalysts, NPG had a high tanδ value at lower temperatures. Therefore, between these values this was the species primarily being heated by implementing MWH, which was

a large percentage of the overall reaction bulk. But, it was observed that PA and PPA have similar and higher tanδ values than NPG at the lower temperatures. Therefore, a significant amount of EM energy was being input respectively to these species. This led to a small proportion of the reaction being selectively heated which led to poor dissipation of the energy throughout the system and slower heat-up times. Essentially there was penetration depth issues, i.e. where the system is too absorbent the energy does not fully penetrate into the centre of the reaction bulk thus heating is inefficient. The penetration depth (further details discussed in chapter 1) at reaction temperature and at a frequency of 910 MHz for each catalyst is shown in Table 4-2 and calculated using Equation 4-1. Although the reaction was processed at 2.45 GHz the data is reported at 910 MHz due to the acid catalysts having too high losses for analysis with the current equipment. Therefore the general trends will be similar but the exact values will vary.

$$\mathbf{d_p} = \frac{\boldsymbol{\lambda_o}\sqrt{\boldsymbol{\varepsilon'}}}{\mathbf{2\pi\varepsilon''}} \qquad \textit{Equation 4-1}$$

Table 4-2. Penetration depth of catalysts at 910 MHz and 200 °C used in the epolycondensation of isophthalic acid and neopentyl glycol.

Catalyst	[a] Dielectric Constant (ε')	[a] Dielectric Constant (ε'')	Penetration Depth (cm)
DHBTC	3.09	0.36	25.804
Tin Octanoate	4.65	0.22	52.232
[b] PA	43.03	3.23	10.817
PPA	185.83	33.89	2.143

[a] Calculated using cavity perturbation technique. [b] Results from 150 °C due to evaporation of catalyst after this temperature.

Table 4-2 described the high losses and constants for the acidic catalysts when compared to the tin alternatives. This led to the penetration depths of these acid catalysts being significantly reduced. Therefore when these acidic catalysts

were employed into the polycondensation there was a problem with energy penetration into the bulk and when the energy penetrated it was these species which were absorbing the bulk of the energy. This led to the energy being absorbed by the catalysts and used in the decomposition chemical transformation, not the polyesterification one intended.

By comparison in CH, the monomers were undergoing bulk heating, leading to the melting of the diol and therefore faster heat-up times for these non-organometallic catalysts. Furthermore, when considering the conversions in Figure 4-2, it was shown that the acidic catalyst proceeded at a significantly reduced rate than the tin species. Therefore, it was hypothesised that these non-organometallic species are not as active at these high temperatures (due to the decomposition temperature of PA previously discussed) and/or with these highly crystalline monomers. This lack of activity did not promote polymer formation and therefore the formation of water. This reduction in water formation led to a reduced cooling effect of the reflux when compared to the tin catalysts which therefore allowed the system to heat to reaction temperature in significantly reduced times.

When comparing the temperature control for each catalyst in Figure 4-4, there was considerably tighter control when using MWH over CH. This was especially true in the tin catalysed cases where the only deviation from the 200 °C reaction temperature was the dips that occurred when sampling. However, comparing the MWH temperature control between the tin and non-organometallic catalysts showed that the temperature control was much less accurate in the non-organometallic species and obvious oscillations were witnessed. This was because when using the tin catalysts the reaction was occurring at a faster rate, as shown in Figure 4-2. As such, the initial period of condensate reflux was reduced and therefore a more constant, lower amount of EM energy could be

input into the reaction for the remaining cycle time, lowering the chances of over/under heating. When considering the two heating methods for all catalysts there was significantly reduced control when implementing CH, with large temperature variations often occurring after sampling. This demonstrated how microwaves can be used for instant on/off energy input control, which is a large safety benefit over CH where the heating fluid will stay hot, even after the heating element has been terminated. It also demonstrated that for laboratory reactions it is easier to work with microwave energy than conventional systems because of the increased heating efficiency at higher temperatures can be more easily reached and maintained when MWH is applied.

When assessing the MWt properties of the final polyesters there were major differences in the final products resulting from the use of the different catalysts. This is shown below in Table 4-3 with the GPC traces in Figure 4-6.

Table 4-3. Comparison of GPC analysis for the different catalysts used in an IPA, NPG polycondensation at 200 °C.

Catalyst	Heating Method	[a] Final Conv. (%)	[b] M_n^{GPC} (g.mol^{-1})	[b] M_w^{GPC} (g.mol^{-1})	[b] M_p^{GPC} (g.mol^{-1})	[b] Đ
DHBTC	CH	94	2,070	4,340	4,490	2.09
	MWH	96	2,530	5,860	6,470	2.32
$Sn(Oct)_2$	CH	96	430	970	330	2.23
	MWH	70	500	1,290	900	2.57
PA	CH	64	350	820	580	2.33
	MWH	53	310	670	580	2.01
PPA	CH	72	560	1,210	920	2.14
	MWH	45	310	550	290	1.79

[a] Calculated using polymer to monomer peak ratio in ^{1}H NMR. [b] Calculated using THF GPC and ASTRA processing software relative to a polystyrene standard.

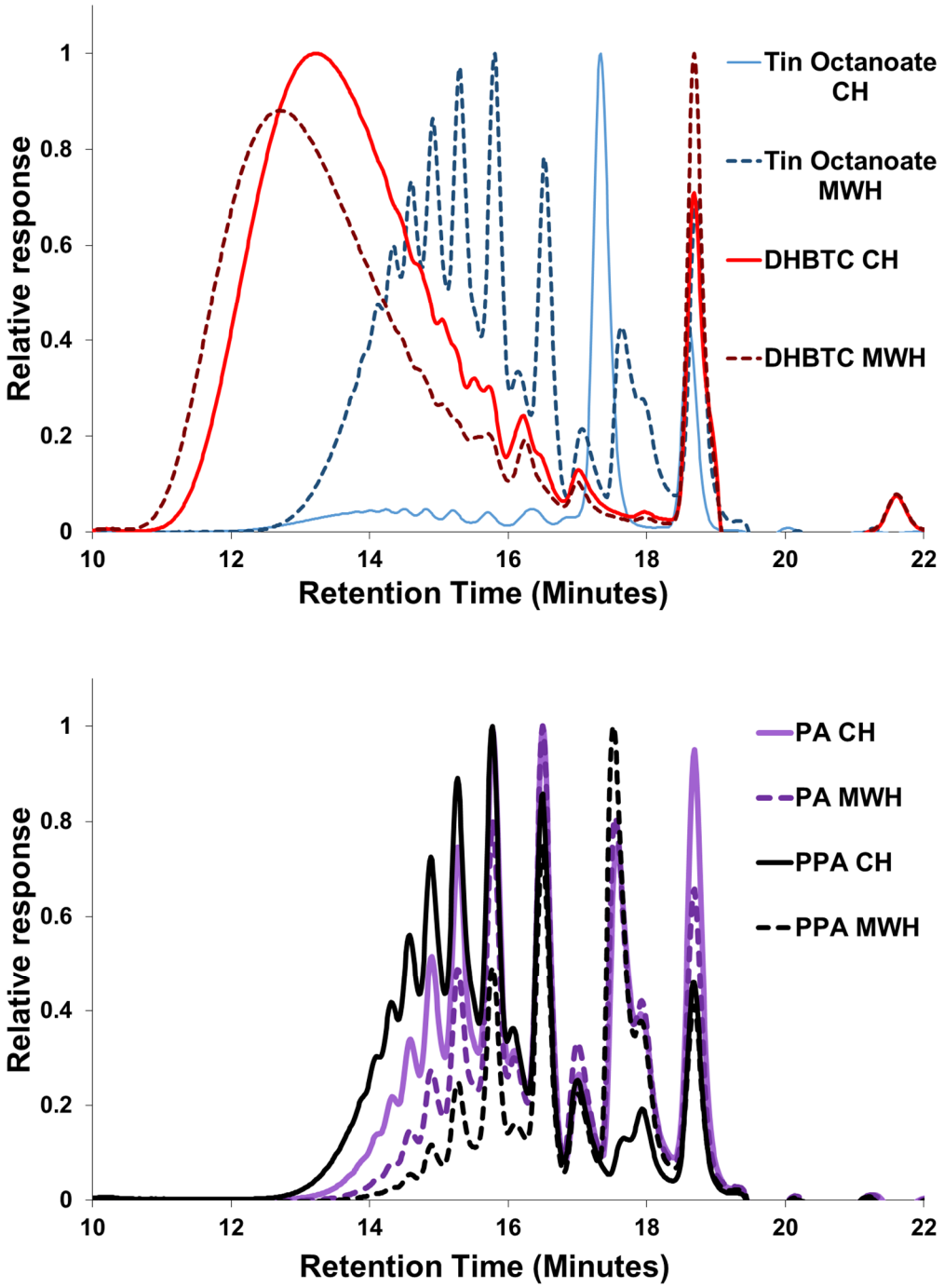


Figure 4-6. GPC traces of the polyester products from the reaction between isophthalic acid and neopentyl glycol at 200 C with differing catalysts. Blue line = tin octanoate catalyst, red = DHBTC catalyst, purple = PA catalyst, black = PPA catalyst.

Table 4-3 and Figure 4-6 confirmed that the non-organometallic catalysts produced low MWt polyesters which were in the dimer/trimeric region. This was expected as the reactions in Figure 4-2 were observed to proceed only to low

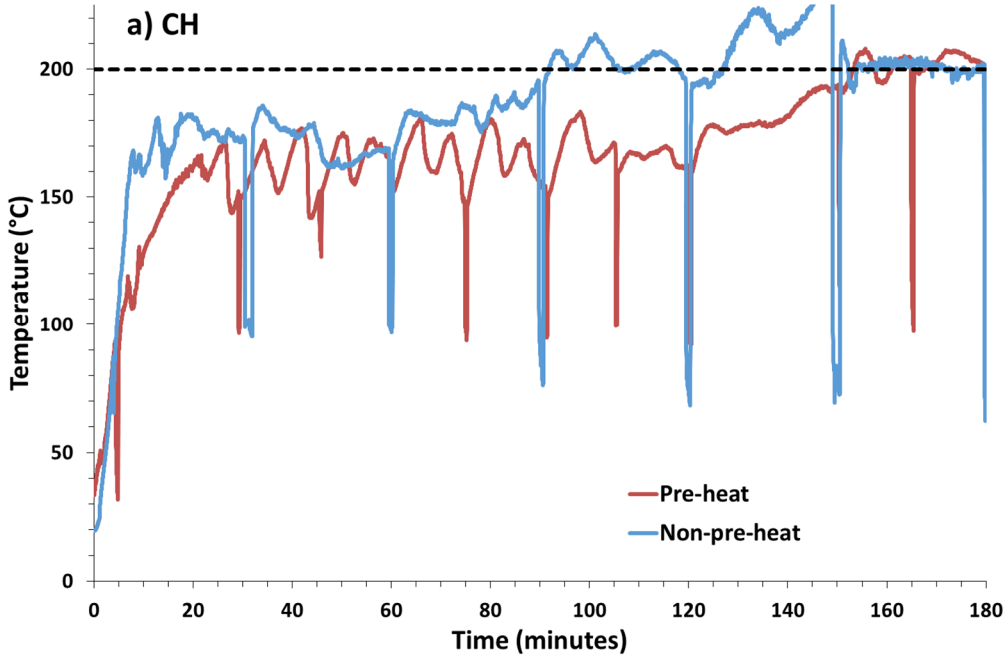
conversions. For both PA and PPA, the MWH reactions produced a lower MWt product than CH, which further suggested that processing at these high temperatures promoted catalyst decomposition for these highly dielectric active species as the selective heating may result in the catalyst being at a locally higher temperature in the MWH reactions than the CH reactions.

Considering the tin catalysts, $Sn(Oct)_2$ catalysed polyesters produced similar MWt's to the non-organometallic catalysts. The products were in the dimer/trimer region, even with high final conversions of 96 % in the case of the CH reaction. In contrast, the DHBTC catalysed reactions produced polyesters, with MWt's within the typically industrial targeted region as well as achieving an expected GPC trace. The MWH reaction was shown to achieve a M_n^{GPC} ~500 $g.mol^{-1}$ higher than the CH reaction. This was an interesting result as the CH reaction was processed for 4 hours, whereas the MWH reaction was 2 hours. These results equate to producing a better product in half the time when using MWH compared to CH, which was an encouraging result. This cycle time reduction was attributed partly due to the difference in heat-up times and partly due to the influence of selective MWH heating on the catalyst and/or the oligomers within the reaction mixture.

The MWt results presented in Table 4-3 suggests that for this monomer system, DHBTC was the most efficient catalyst. For both CH and MWH it was the only catalyst to produce a high MWt polyester product and the MWH results suggested that it was beneficial to use this alternative heating method. Therefore, any further work being reported in this chapter solely involved this catalyst.

4.2.1.2 Pre-heating of Diol Trials to Assess the Differences Compared to Not Pre-heating for Conventional and Microwave Heating

In industrial polyester synthesis it is commonplace to pre-heat the diol with water before addition of the diacid and catalyst as this aids homogenisation of the reagents. Therefore, trials were conducted using the DHBTC catalyst to assess the differences in heat-up times between CH and MWH using this pre-heating method. This involved adding the typical amount of NPG to the reactor and with 1.5 mL of deionised water. This mixture was then heated until the NPG had dissolved (80 - 90 °C) and charging of the diacid and catalyst then followed. The initial heating profiles are shown below in Figure 4-7 and compared to the non-pre-heated reactions.



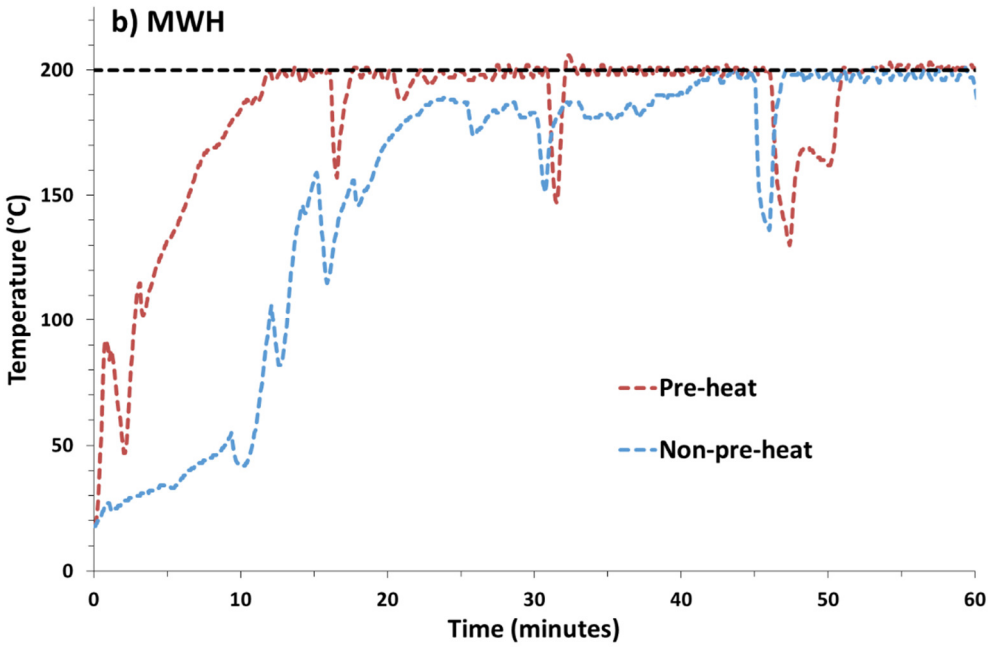


Figure 4-7. Pre-heating of diol trials for NPG, IPA polycondensation, a) CH, b) MWH

Figure 4-7 demonstrated that in the pre-heated reactions (red lines) there was a sharp decrease in temperature near the start of the reaction due to the addition the diacid and catalyst. This was due to the temperature monitoring apparatus being withdrawn to allow addition, this was coupled with the fact the diacid monomer and catalyst were being added as room temperature material and so cooled the reaction which was at ~90 °C.

Plot (a), Figure 4-7, refers to the reactions conducted when implementing CH. Using this heating method demonstrated that pre-heating the diol caused the heat-up time to increase ~60 mins compared to the non-pre-heated system. This was a substantial increase, especially considering that this is a common method employed in industrial processes. This was attributed to the fact that in the diol pre-melt reaction there was extra water which needed to be removed from the system to drive the dynamic equilibrium forward. This increased the amount of water removal that needed to be achieve to reach 100 % conversion by ~30 %. Additionally it increased the volume condensate refluxing in the

reactor, leading to some returning into the reaction mixture, cooling the bulk temperature and increasing heat-up time.

Considering the MWH reactions, plot (b), Figure 4-7, shows different results. The pre-heated reaction reached reaction temperature considerably faster than the non-pre-heated at ~13 and ~43 mins respectively. This was different to the CH reactions as water has very high dielectric values and so the extra water added to the reaction mix was rapidly heated under MWH. [11] This led to an increased rate of diol dissolution as well as evaporation of the extra water added, shown by the minimal dip in temperature at 110 – 120 °C. Therefore, this rapid dissolution of diol into the liquid phase with the excess water allowed the majority of the input power to be absorbed by the system. This outweighed the extra water needing to be evaporated and aided decreased heat-up times. This conclusion was supported by considering the reflected power from both reactions in Figure 4-8.

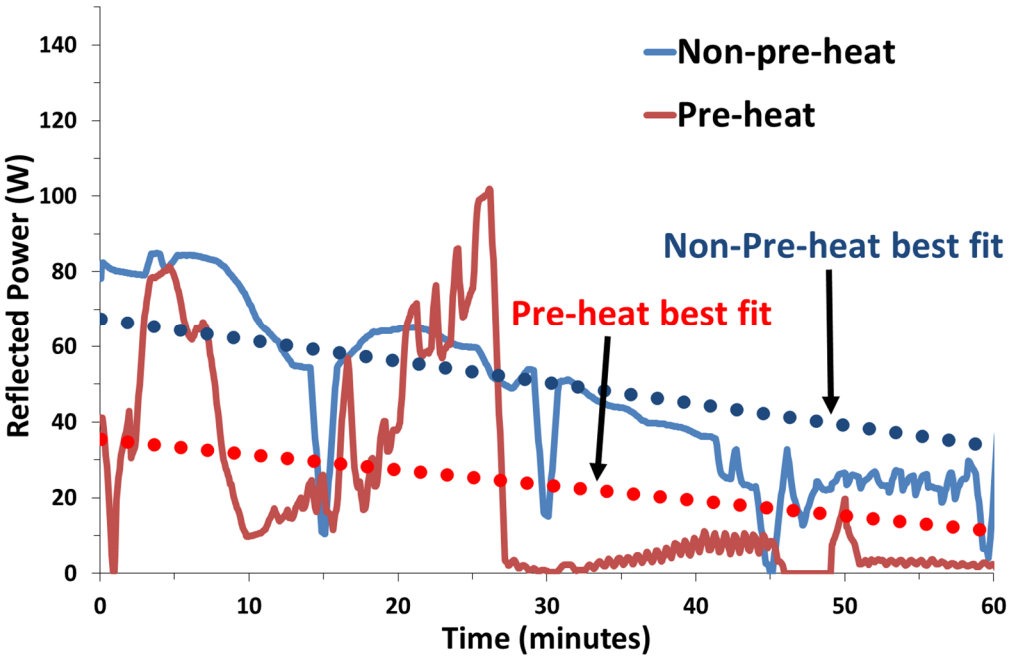


Figure 4-8. Reflected power comparison between pre-heated diol/water and non-pre-heated diol/water reactions.

Figure 4-8 details the variation in the reflected power as the reaction progressed. It was shown that the pre-heated reaction had a lower average reflected power, proven by the lower line of best fit. This suggested that, on average, between 20 and 30 more watts was being absorbed by the pre-heated system compared to the non-pre-heated system, due to the excess water addition. This explained why the heat-up times are vastly reduced in the pre-heated system when implementing MWH.

Additionally the large increase in reflected power at approximately 20 minutes was concluded to be the point at which the excess water had been completely removed and so the reaction dielectric had become dominated by the polymerisation reaction mixture alone.

Overall, this experimental work had shown that, on the 50 mL laboratory scale, it was dependent on the heating method as to whether employing a water/diol pre-heat was beneficial to the reaction profile. Implementing MWH into the pre-heated reactions created heat-up times which were ~25% of the times taken without pre-heating. Whereas, implementing water/diol pre-heating in CH elongated the heat-up time by ~65%. However, as pre-heating is the process method used in industry, it was the method implemented for all the following reactions to ensure that the results could be compared to known industrial production.

4.2.1.2.1 Differences in Polyester Properties Between Conventional and Microwave Heating

To assess the differences in the final polyesters synthesised between CH and MWH a series of repeats were conducted implementing both heating

techniques. These polyesters were then subject to standard polymer analysis and the results are discussed below.

All repeats demonstrated that by using MWH there was a clear reaction rate increase and higher conversions were achieved in shorter timeframes, as demonstrated by the data in Figure 4-9.

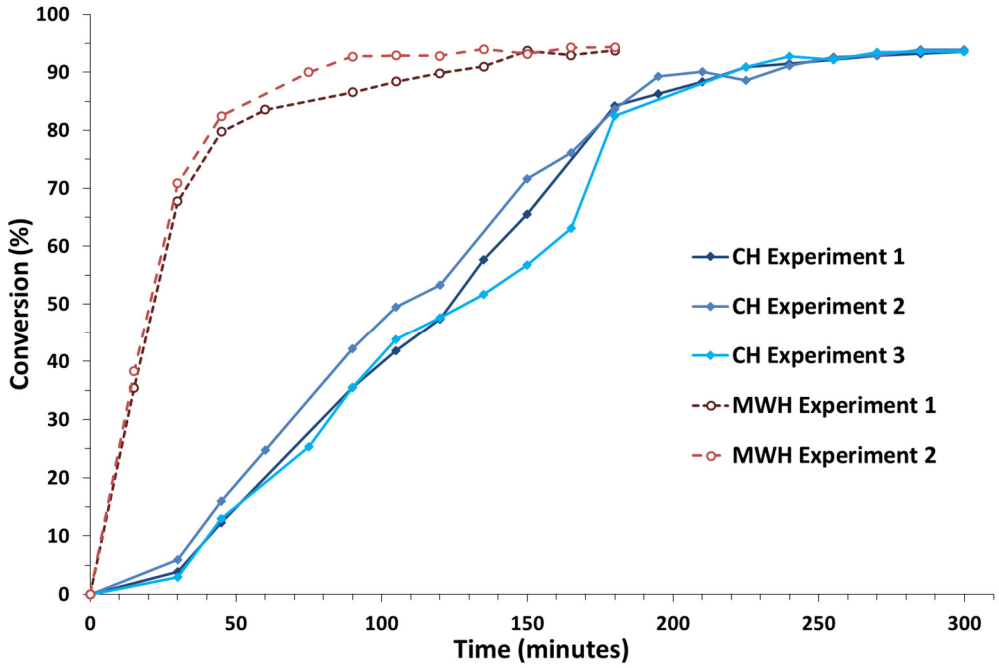


Figure 4-9. Comparison of heating methods in terms of conversion versus time for DHBTC catalysed polycondensation of NPG and IPA at 200 °C.

It was concluded that a significant contribution to the increase in reaction rate was due to a significant decrease in heat-up times required, as had previously been observed.

Furthermore, when assessing the final product properties a further interesting difference was observed, displayed in Table 4-4 and Figure 4-10 which present the GPC data for the polyesters synthesised above.

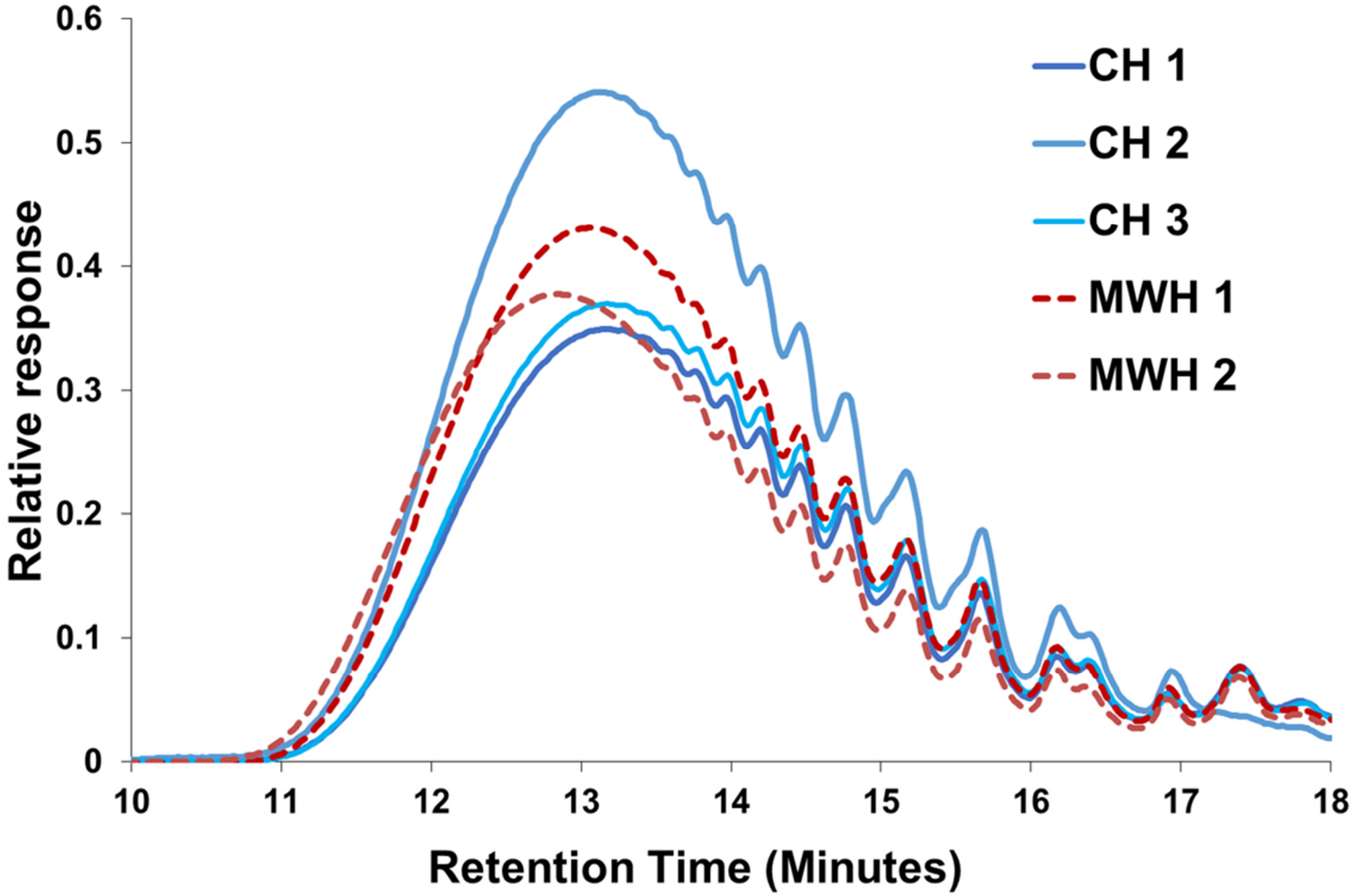


Figure 4-10. GPC traces for the polyester products synthesised at 200 °C using DHBTC catalyst with differing heating methods..

Table 4-4. Comparison of molecular weight data between CH and MWH for the repeated reactions of IPA and NPG polycondensation at 200 °C.

Heating Method	Cycle Time	[a] Final Conv. (%)	[b] M_n^{GPC} (g.mol^{-1})	[b] M_w^{GPC} (g.mol^{-1})	[b] M_p^{GPC} (g.mol^{-1})	[b] Đ
CH	300	94	1,800	4,370	7,450	2.41
			1,900	4,490	8,345	2.36
			1,850	4,445	8,350	2.42
MWH	180	94	2,030	4,730	7,780	2.34
			2,180	5,445	9,225	2.49

[a] Calculated using polymer to monomer peak ratio in ^{1}H NMR. [b] Calculated using THF GPC and ASTRA processing software relative to a polystyrene standard.

shows that the 5 polyesters produced from the reaction above had processed to identical conversion levels when assessing conversion *via* ^{1}H NMR. To reach this level, the MWH reactions had been processed for 3 hours and the CH for 5 hours. This had allowed the polyesters to be at reaction temperature (200 °C) for approximately the same period of time (~2 hours 30 mins) and therefore allowed a fair comparison between the analytical data from the different heating techniques. The MWt analysis showed that for the CH reactions the average M_n^{GPC} was calculated to be 1,850 g.mol^{-1}, compared to the average M_n^{GPC} for the MWH products which was 2,105 g.mol^{-1}. This suggested that implementing MWH led to a larger M_n^{GPC} by ~250 g.mol^{-1} when compared to the CH reactions, which was a significant amount for polyesters of this size (over 10 % increase).

These M_n^{GPC} increases were also confirmed by thermal property analysis, shown in Table 4-5.

Table 4-5 Comparison of average T_g data between CH and MWH for the repeated reactions of IPA and NPG polycondensation at 200 °C.

Heating Method	[a] Final Conv. (%)	[b] T_g (°C)	[b] Average T_g (°C)	T_g Standard deviation (°C)
CH	94	53.92 53.93 53.09	53.65	± 0.48
MWH	94	55.75 56.63	56.19	± 0.62

[a] Calculated using polymer to monomer peak ratio in ^{1}H NMR. [b] Calculated using TA-Q2000 DSC and Universal analysis software by TA.

The average T_g values and standard deviation of T_g values for the polyesters synthesised in Table 4-5 showed an increase of ~2 °C in the MWH products compared to CH. This correlates with the increase in MWt observed from the GPC traces in Figure 4-10.

Therefore, the data suggested that by implementing MWH led to an increase the polyester chain length. This could be attributed to:

i. MWH overcoming problems with mass transfer/removal of water which is a strong microwave absorber and therefore will be selectively heated, promoting evaporative removal from the reaction mixture to drive the equilibrium forward.
ii. Microwaves selectively heated the catalyst which to increase its catalytic activity within the system, helping polymerisation to occur and promoting the growth of longer chains.
iii. Microwaves selectively heated the chain ends of the monomers/oligomers, leading to higher temperatures at these sites and promoting MWt growth by overcoming steric barriers that prevent further reaction.

Point (i) was proposed to be the least likely scenario due to the high reaction temperatures. At a reaction temperature of ≥200 °C any condensate water was likely to be present in the form of superheated vapour. Being in this physical form led to poor interaction with the EM field due to the fact gases interact poorly with an EM field compared to material in a liquid/solution state. Therefore, it was proposed that the microwave energy would most probably have a negligible effect on the condensate at this temperature. Thus, it was thought that increased condensate removal would not be the root cause of the positive MWt effects to polymer growth observed.

Points (ii) and (iii) are similar on root cause but are difficult to both differentiate and definitively provide supporting data to prove their level of influence on the reaction. This is because it's impossible to gauge if the different substances in the system are at different local temperatures with the current technology available. But, the previous data/discussions in chapter 3 and the previous sections in this chapter have shown that the choice of catalyst is very important in polyester synthesis. Additionally, this and other work, [12] has demonstrated that oligomers are also more susceptible to being selectively heated than their corresponding monomers and both acid and diols have been shown to be functional groups that are susceptible to EM heating. Therefore, it was concluded that this increased MWt effect was as a result of a combination of points (ii) and (iii).

4.2.1.2.2 Investigation of how Changing the Stoichiometric Ratios of Monomers Affected the Isophthalic, Neopentyl Glycol Polycondensation with Conventional and Microwave Heating

When processing polyesters in industrial processes it is common to have an excess of either diacid or diol, depending on processing conditions and what

terminal functionality the end product is required to have. Therefore, to assess if changing the stoichiometric ratio of the monomers effected the polyester reaction profiles, a series of experiments were conducted which involved increasing the ratio of diol to diacid within the system. A relative increase in the diol component was investigated because it was the more likely of the monomers to be co-distilled off with the condensate during the reaction. This loss of reagent could therefore directly influence the ability of the reaction to reach high conversion and high MWt. As a result of this, in typical industrial processes, a 2 stage process in adopted, where the first stage involves an alcohol excess. Therefore, this scenario was mimicked in the laboratory based systems used within this. Furthermore, NPG has been found to exhibit significantly higher dielectric properties than IPA, as shown below in Figure 4-11. Therefore, having an excess of this monomer may aid the reaction rate by allowing a higher proportion of the bulk to efficiently couple with the EM energy. Conversely, this may also decrease the reaction rate as increasing the amount of more dielectrically active species may lead to penetration depth issues which, in turn, would therefore negate any specific microwave effects and the system would tend towards a bulk heating effect.

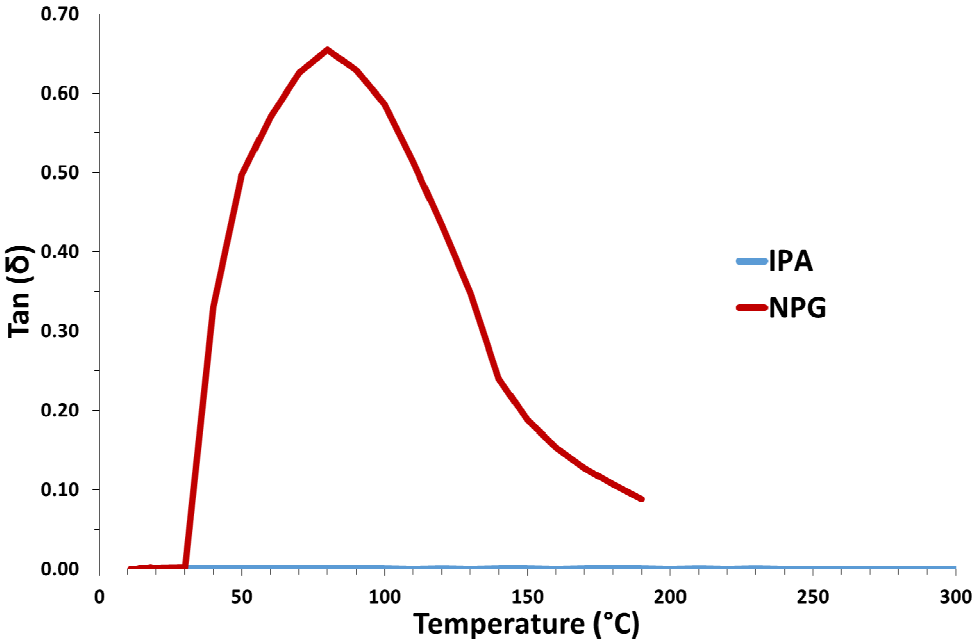


Figure 4-11. Dielectrics of IPA and NPG monomers with increasing temperatures.

Therefore, a series of experiments were conducted to assess the overall effect of increasing the NPG content of the reaction in CH and MWH polymerisations and is detailed in Figure 4-12. In these reactions, the stoichiometries were actually altered by decreasing the mass of IPA in the reaction mixture because adding more NPG would have led to the need for a larger reaction vessel, so reducing the ability to directly compare the results with those previously reported in this study.

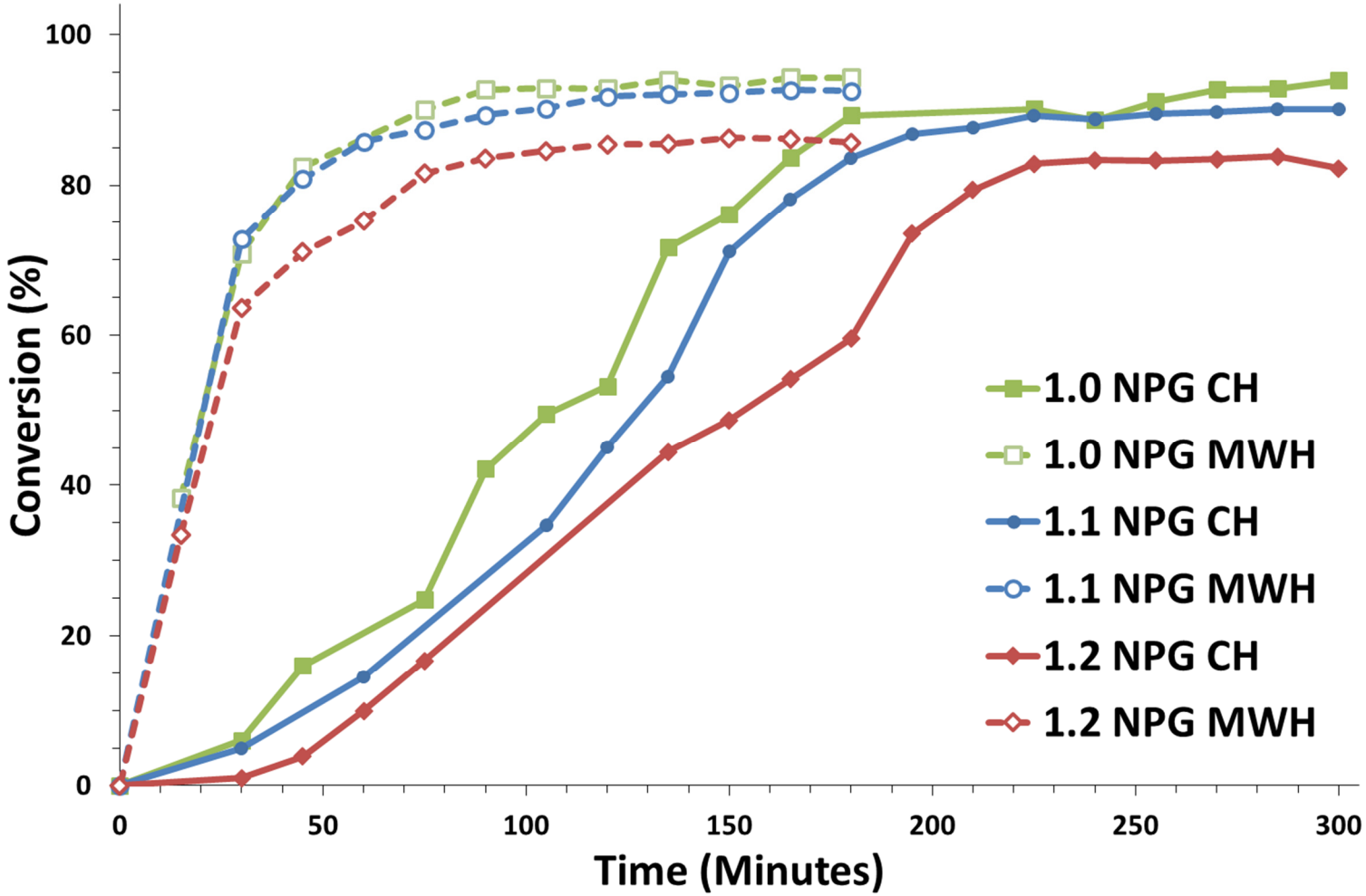


Figure 4-12. Conversion versus time for an IPA, NPG polycondensation using an increased stoichiometry of NPG for CH and MWH.

4-29

Figure 4-12 again demonstrated differences in reaction rates between the MWH and CH reactions. The MWH reactions were shown to be considerably more efficient than CH, with high conversion achieved in significantly short times. The times taken to achieve a conversion of 80 % are detailed below in Table 4-6.

Table 4-6. Reaction times to 80 % conversion in IPA, NPG polycondensation with increased NPG stoichiometry.

NPG:IPA Stoichiometry	Heating method	[a] Time to 80 % Conv. (minutes)
1:1	CH	110
	MWH	45
1.1:1	CH	170
	MWH	45
1.2:1	CH	210
	MWH	70

[a] Calculated using polymer to monomer peak ratio in ^{1}H NMR.

Table 4-6 details the large difference between the MWH and the CH systems. For all stoichiometry levels, implementing MWH over CH resulted in an increase in reaction rate and therefore reduction in cycle time to 80 % conversion.

Comparing the different stoichiometries, it was observed in Figure 4-12 and Table 4-6 that when implementing CH there was a faster conversion rate in the lower stoichiometric excess reactions. It was concluded that these results could be explained by the excess of NPG monomer which was not being co-stripped from the reaction mixture at level sufficient to give a "corrected" 1:1 stoichiometry during the procedure. As a result this led to an excess of unreacted diol monomer and as such using ^{1}H NMR analysis could never report 100 % conversion.

Therefore, these polyesters were then subjected to GPC and DSC analyses to obtain an indication of the final product polymer properties, shown in Table 4-7.

Table 4-7. GPC and DSC analysis on the neopentyl glycol, isophthalic acid polyesters using increasing stoichiometries of neopentyl glycol monomer.

NPG:IPA Stoichiometry	Heating Method	[a] Final Conv. (%)	[b] M_n^{GPC} ($g.mol^{-1}$)	[b] Đ	[c] T_g (°C)
1:1	CH	94	1,900	2.36	53.9
	MWH	94	2,020	2.34	55.8
1.1:1	CH	90	1,930	2.05	52.8
	MWH	93	2,510	2.15	51.3
1.2:1	CH	85	1,690	1.83	42.2
	MWH	86	1,930	1.85	45.0

[a] Calculated using polymer to monomer peak ratio in ^{1}H NMR. [b] Calculated using THF GPC and ASTRA processing software relative to a polystyrene standard.. [c] Calculated using TA-Q2000 DSC and Universal analysis software by TA.

Assessing the MWt values from Table 4-7 showed for each stoichiometry that processing with MWH created a product with a higher M_n^{GPC} value when compared to CH at the same stoichiometry. This again suggested implementing a MWH strategy was positively affecting the elongation of the polyester chains relative to CH *via* increasing conversion with time and/or a specific heating effect.

The Đ data from Table 4-7 suggested that increasing the molar percentage of NPG in the reaction led to narrower Đ's in both CH and MWH. For the 1.2:1 reactions this was because the majority of polyester chains were shorter (lower M_n^{GPC} and T_g than the other samples), therefore there weren't as many high MWt chains to offset the Đ. Although, this explanation did not persist for the 1.1:1 reaction. This was because the Đ was lower than with the 1:1 stoichiometry, even though the M_n^{GPC} values, especially in MWH, were higher.

Therefore, by increasing the stoichiometric excess to 1.1:1 it was suggested that this was approaching an optimised system, most specifically for the MWH system which showed no reduction in reactivity rate but resulted in a better quality product (higher MWt with lower PDI). This was attributed to a combination of effects; (a) having an excess of NPG created a more liquid reaction medium at the beginning of the reaction which both allowed better homogenisation/solvation of the diacid compared to reactions with lower levels of NPG and better/more immediate coupling with the EM energy and (b) it efficiently corrected for any co-stripping of the NPG caused by the evolution of the condensate. However, with both heating methods, having a larger NPG excess, as in the 1.2:1 reactions, created a reaction environment with too much diol (essentially an over correction) and therefore decreased the diol to diacid interactions which are needed to create ester bonds.

4.2.1.2.3 Increased Reaction Temperature to Assess Heating Differences between Conventional and Microwave Heating at an Industrially Used Temperature

For industrially processed polyester resins, temperatures of 200 – 250 °C are commonly implemented.[13-15] Therefore, elevated temperatures were investigated to assess whether the benefits of using MWH over CH persisted. For these reactions a temperature of 225 °C was selected. This was because the fibre optic (FO) used in MWH experiments for temperature logging had an upper safe operating limit of 240 °C. Therefore, 225 °C was low enough to keep the FO from being damaged in the event of a temperature overshoot.

Figure 4-13 shows a comparison of the conversion profiles for the CH and MWH reactions at 225 °C.

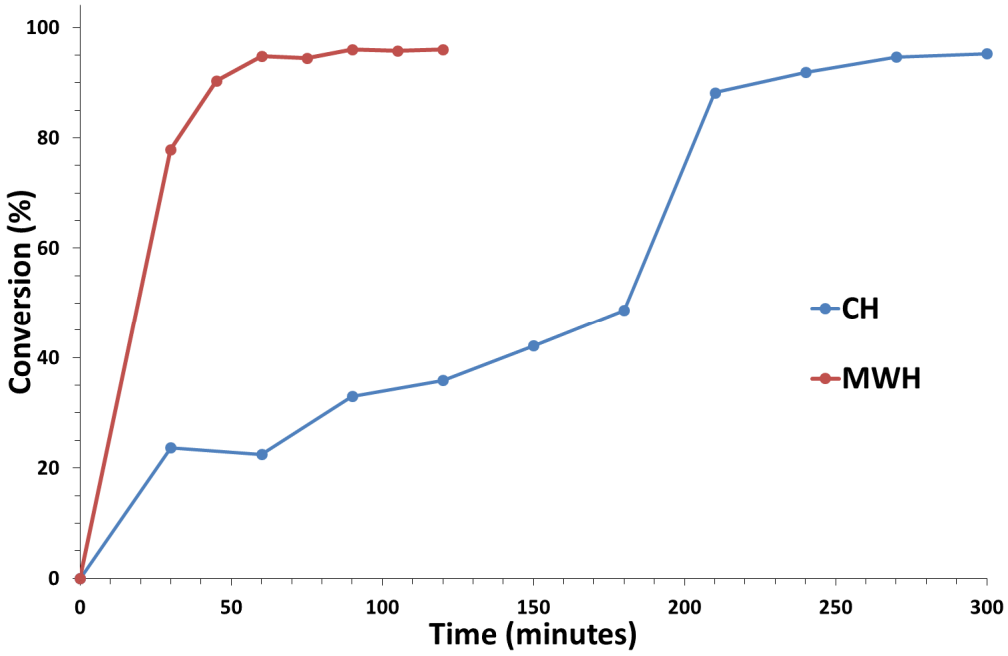


Figure 4-13. Comparison of CH and MWH for NPG, IPA polycondensation at 225 °C with diol/water pre-heat.

Figure 4-13 demonstrates that MWH led to vastly increased initial reaction rates when compared to CH. Comparing the time to 80 % conversion, MWH was shown to be over 10 times faster to this conversion (20 mins and 205 mins for MWH and CH respectively). Again, this demonstrated the transfer of energy into the reaction bulk was significantly more efficient when implementing MWH compared to CH. This was also be shown by comparing the heating profiles of the reactions, shown below in Figure 4-14.

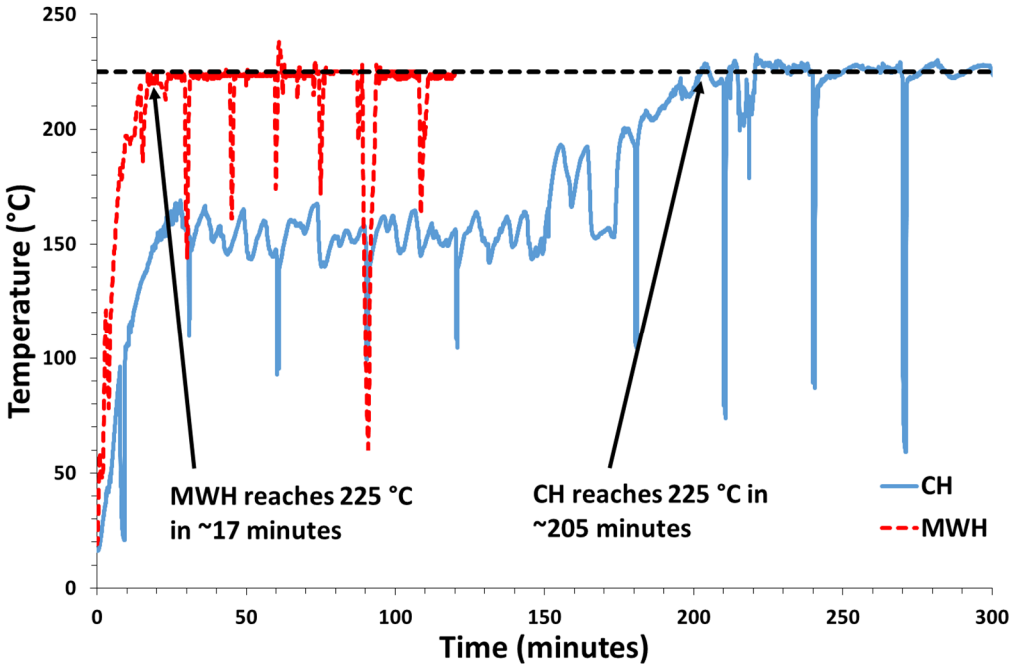


Figure 4-14. Heat-up times to 225 °C reaction temperature for isophthalic acid, neopentyl glycol polycondensation reaction.

Note: Dips in temperature relate to sampling intervals.

Figure 4-14 demonstrated that the heat-up time to 225 °C in MWH was ~12 times faster than in CH. When CH was implemented a temperature plateau between 160 - 170 °C was observed between ~30 and ~180 mins. This was due to the condensate refluxing back into reaction and cooling the bulk. Whereas, in the MWH reaction, this step was rapidly overcame due to the efficient heat transfer of MWH which heated the bulk straight to reaction temperature. To ensure the polyesters were similar conversions, the reaction was left at processing temperature for similar time periods (~100 mins). Therefore, this emphasised any intrinsic property differences produced between the products that occurred in the second "polymer MWt building" section of the process. Consequently, final conversions were found to be almost identical at 95 and 96 % for CH and MWH respectively. Therefore the samples were assessed for MWt and T_g values, and this data is presented in Table 4-8 and Figure 4-15.

Table 4-8. Comparison of molecular weight data between CH and MWH for the IPA and NPG polycondensation at 225 °C.

Heating Method	[a] Final Conv. (%)	[b] M_n^{GPC} (g.mol^{-1})	[b] M_w^{GPC} (g.mol^{-1})	[b] M_p^{GPC} (g.mol^{-1})	[b] Đ	[c] T_g (°C)
CH	95	2,020	5,000	5,470	2.48	59.4
MWH	96	2,070	4,760	5,040	2.30	60.0

[a] Calculated using polymer to monomer peak ratio in ^{1}H NMR. [b] Calculated using THF GPC and ASTRA processing software relative to a polystyrene standard.

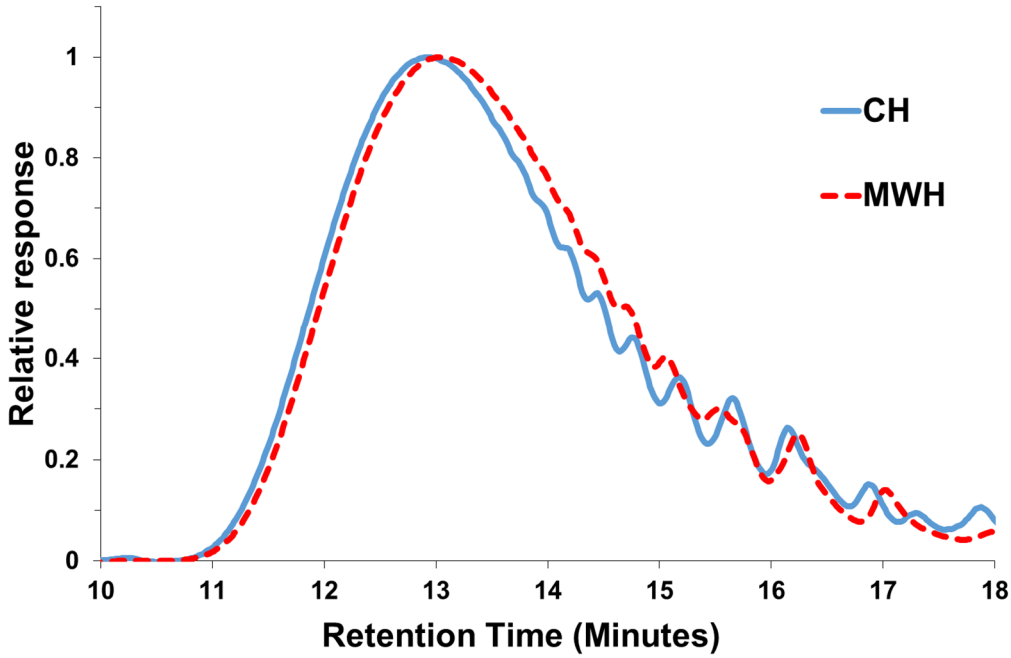


Figure 4-15. GPC trace comparison between heating methods used for the synthesis of an isophthalic acid, neopentyl glycol polyester at 225 °C after normalisation of traces.

Table 4-8 demonstrated that the polymers synthesised had similar properties. The slight differences produced were between the M_p^{GPC} values and Đ values. It was demonstrated that CH produced a higher M_p^{GPC} value than MWH by ~400 g.mol^{-1}, meaning that the mode peak was slightly larger in CH than MWH. Although, the Đ in MWH was shown to be lower than in CH, suggesting that there was more MWt control in the MWH reactions. This was due to the nature of the heating in MWH, with the energy penetrating straight into the reaction

system, heating the reactive sites or catalyst and not heating the surrounding materials. But, because the T_g, M_n^{GPC} and M_w^{GPC} values were so similar, it was deduced that the polyesters synthesised are comparable in properties. Therefore, at 225 °C, the reaction time when implementing MWH was 40 % of the CH reaction, creating large efficiency savings in terms of cycle times. This data is compared with the values from the reactions processed at 200 °C in Table 4-9.

Table 4-9. Comparison of polyester molecular weight after processing at different temperatures.

Heating Method	Processing Temp. (°C)	[a] Final Conv. (%)	[b] M_n^{GPC} (g.mol^{-1})	[b] M_w^{GPC} (g.mol^{-1})	[b] M_p^{GPC} (g.mol^{-1})	[b] Đ
CH	[c] 200	94	1,850	4,445	4,590	2.42
	[c] 225	95	2,020	5,000	5,470	2.48
MWH	[d] 200	94	2,030	4,730	4,980	2.34
	[e] 225	96	2,070	4,760	5,040	2.30

[a] Calculated using polymer to monomer peak ratio in ^{1}H NMR. [b] Calculated using THF GPC and ASTRA processing software relative to a polystyrene standard.[c] Reaction processed for 300 mins. [d] Reaction processed for 180 mins. [e] Reaction processed for 120 mins.

Table 4-9 showed that increasing the processing temperature of the CH reaction increased the final conversion of the polyesters. This result was expected as the increased temperature will facilitate water removal whilst also reducing the viscosity of the reaction mix (this made it easier for condensate to travel through and away from the reaction mixture). This shows that by processing at a higher temperature a better product can be produced in identical timeframes. However, comparing the MWH results at 200 °C to the CH at 225 °C case showed that there was no difference in the polyester product as very similar MWt values were achieved. Although it should be noted that the PDI was lower for the MWH reaction at both temperatures.

However, there is also little difference in the materials made in the MWH reaction at both 200 and 225 °C, even though the latter was processed for 2/3 of the time as the 200 °C reaction. Therefore, to deduce whether a reduction in temperature is beneficial overall, a cost benefit analysis is needed to assess whether the time saving of high temperature processing negates the increased energy costs and heat-up/cool-down time elongation of higher temperatures. But, as MWH is accepted as a highly efficient heating method and an instant on/off energy switch, the processing time saving will likely outweigh the energy costs due to the possibility of higher throughput. [16,17]

The thermal properties of these polyesters are displayed below in Table 4-10.

Table 4-10. Comparison of polyester thermal properties after processing at different temperatures.

Heating method	Processing Temp. (°C)	[a] Final Conv. (%)	[b] T_g (°C)
CH	200	94	53.1
	225	95	59.4
MWH	[c] 200	94	55.8
	[d] 225	96	60.0

[a] Calculated using polymer to monomer peak ratio in ^{1}H NMR. [b] Calculated using TA-Q2000 DSC and Universal analysis software by TA. [c] Reaction processed for 180 mins. [d] Reaction processed for 120 mins.

Table 4-10 shows some surprising results when cross-referencing with Table 4-9. From the MWt data, it was expected that the T_g values would be similar, due to the similar MWt of the products. Therefore, there was another phenomenon influencing the T_g values. This was likely the plasticising nature of monomers on a polymeric system.[18] This was hypothesised as the polymers processed at 225 °C had higher final conversions and a smaller PDIs than at 200 °C. Therefore, it was proposed that residual monomer/oligomers plasticised the polyester and lowered the T_g, with a lower conversion and broader PDI

supporting this hypothesis. This plasticisation occurs because the smaller monomeric molecules will migrate in between the polymeric chains and increase the free volume between them. This allows the polymer chains to slide past each other more easily, creating a more pliable product. To test this hypothesis, DSC experiments were conducted of the higher T_g products but with the addition of a small amount of mono/di/trimer from previous kinetic samples, shown below in Table 4-11.

Table 4-11. Thermal properties of isophthalic acid, neopentyl glycol polyester with addition of mono/di/trimeric kinetic sample.

Heating method	[a] T_g before monomer addition (°C)	[a] T_g after monomer addition (°C)	T_g Reduction (°C)
CH	59.4	57.5	1.9
MWH	60.0	58.9	1.1

[a] Calculated using TA-Q2000 DSC and Universal analysis software by TA.

Table 4-11 above demonstrated that there was a plasticisation effect due to the presence of low MWt species in the material, thus supporting this as the root cause of the lowered T_g values exhibited by the polyesters processed at 200 °C compared to at 225 °C. This was demonstrated by a drop in T_g value by ~1.5 °C in both samples when monomer/oligomer was added. However, this drop was surprisingly low, most likely due to the lack of purification on the final polymer sample. Therefore, there will already be some monomer present, even in the highly converted samples.

Because of this increase in polyester T_g and therefore increase in polymer stability, it was concluded that the future reactions were to be carried out at 225 °C. This was because the product synthesised needed to be as thermally stable as possible and implementing the higher temperature helped achieve this. But, if lower T_g polyesters are needed for other applications, reduced heat has been

shown to be a viable option for this. Especially if MWH was applied to reduce cycle times.

4.2.1.2.4 Addition of Vacuum Effects on Polyesterification Between Conventional and Microwave heating at 225 °C

As discussed in chapters 2 and 3, vacuum is applied in industrial polycondensation processes to aid in driving the reaction towards 100 % conversion and increase the MWt of the final polyester product. Therefore, vacuum was added to a typical CH and MWH polyesterification following the methods used in this study and the product was assessed for final properties to determine if there was any differences between the heating methods. The conversion with time achieved in this reaction is detailed below in Figure 4-16.

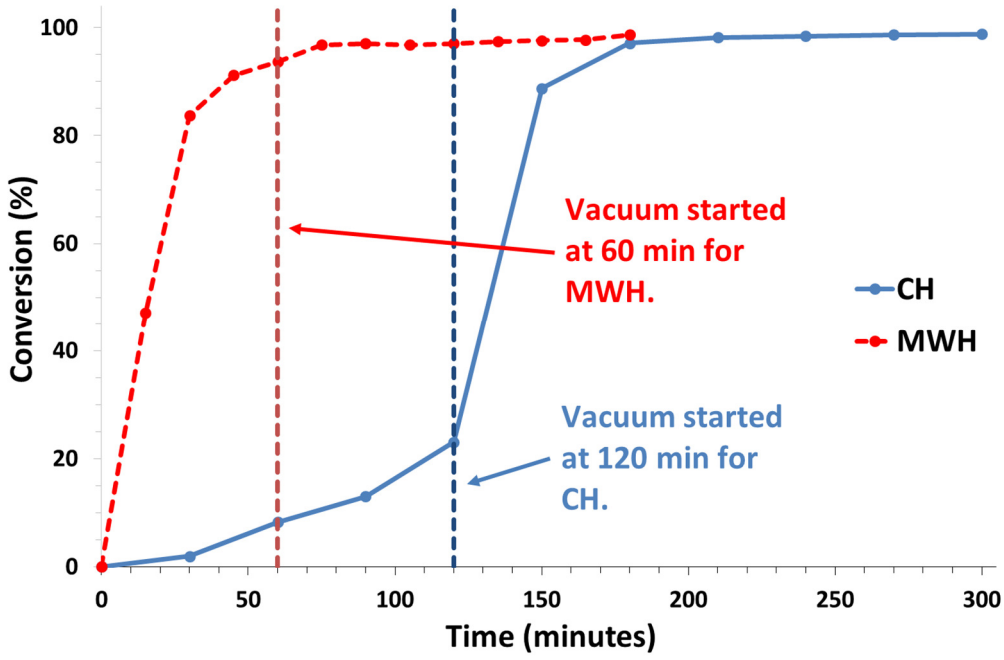


Figure 4-16. Conversion versus. time plot for isophthalic acid, neopentyl glycol polycondensation at 225 °C with 400 mbar vacuum addition after 120 mins in CH and 60 mins in MWH.

Note: Vacuum was added at 60 minutes in MWH due to product clarity (no diacid particles visibly remained) and 120 minutes in CH due to the twice as long reaction time in CH reactions shown in Figure 4-13.

In Figure 4-16, as in previous reactions, the reaction rate when implementing MWH was greatly increased when compared to CH. Again, this can be explained by the increased efficiency of heat transfer into the bulk solution, shown by the heat-up times in Figure 4-17.

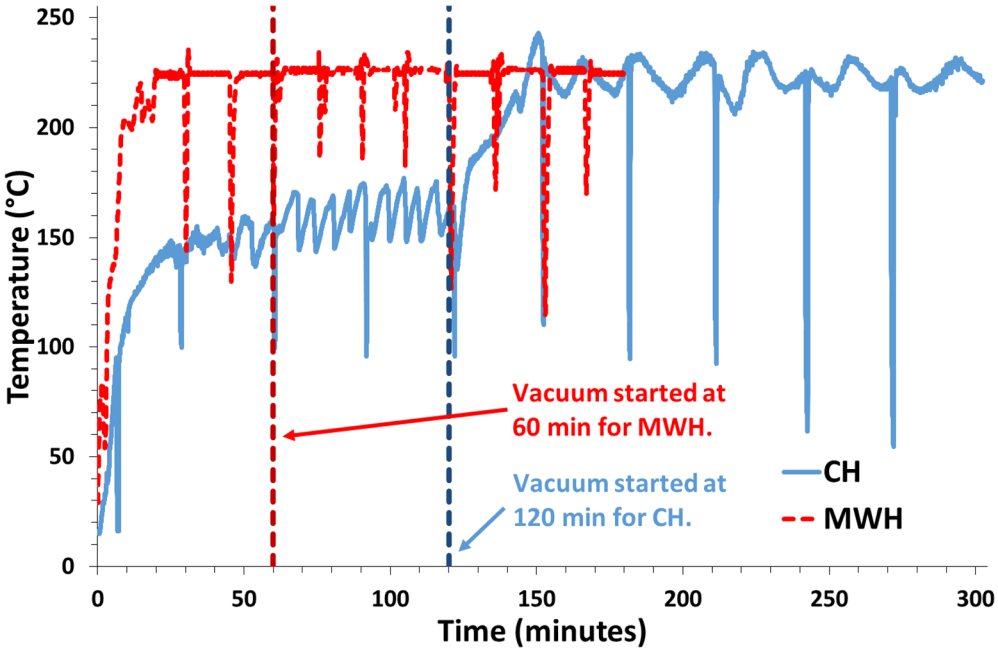


Figure 4-17. Heat-up times of isophthalic acid, neopentyl glycol polycondensation to 225 °C reaction temperature. Lines have been added to show at what point the 400 mbar vacuum was added.

When considering the CH reaction in Figure 4-16, there was a reaction rate increase after application of vacuum, shown by the large jump in conversion between 120 mins (23 % conversion) and 150 minutes (89 % conversion). This large rate increase was corroborated by the quick increase in temperature detailed in Figure 4-17. Before the vacuum was applied, the reaction temperature was consistently between 150 - 170 °C (the area observed in previous reactions were large amounts of condensate was created). But, once

the vacuum was applied there was a temperature jump to 225 °C within 30 minutes. This result showed that the application of the vacuum was related to an increase in temperature, due to the removal of water from the reaction head-space. This stopped the condensate refluxing and cooling the mixture.

MWt and thermal analysis was then conducted on the products and is detailed below in Table 4-12 with the GPC traces in Figure 4-18.

Table 4-12. GPC data for isophthalic acid, neopentyl glycol polycondensation with addition of 400 mbar vacuum.

Heating Method	[a] Final Conv. (%)	[b] M_n^{GPC} (g.mol^{-1})	[b] M_w^{GPC} (g.mol^{-1})	[b] M_p^{GPC} (g.mol^{-1})	[b] Đ
CH	99	1,540	4,420	5,400	2.87
MWH	99	2,120	8,890	8,900	3.38

[a] Calculated using polymer to monomer peak ratio in ^{1}H NMR. [b] Calculated using THF GPC and ASTRA processing software relative to a polystyrene standard.

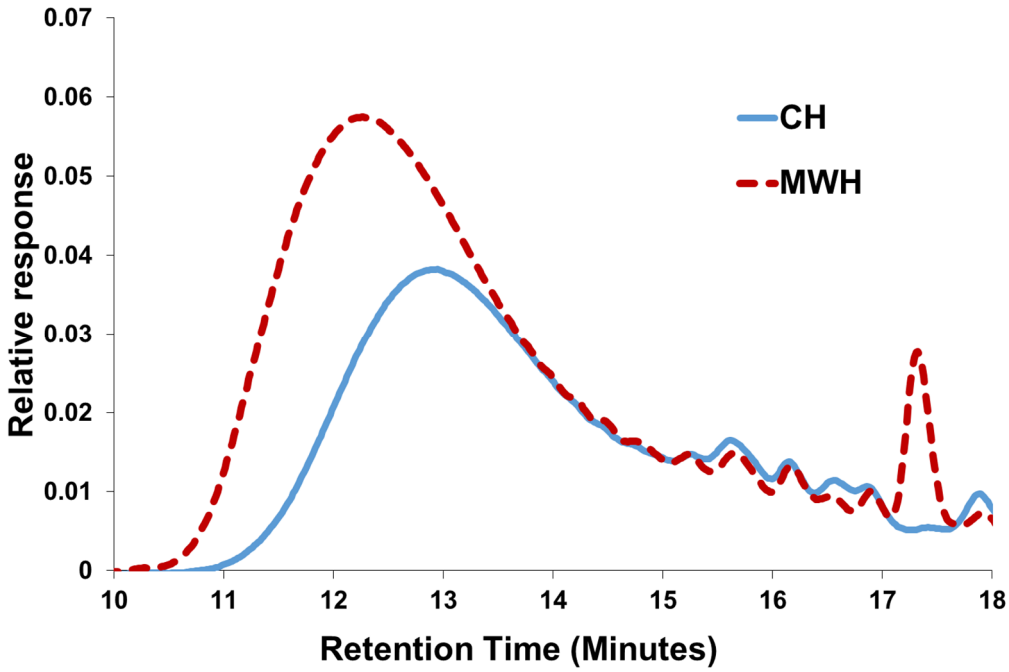


Figure 4-18. GPC traces for an isophthalic acid, neopentyl glycol polycondensation at 225 °C using different heating methods and vacuum addition.

Table 4-12 displays that the MWt data for the two products were significantly different. Although both heating methods were shown to achieve final conversions of 99 %, there was a M_n^{GPC} difference of ~600 g.mol$_{-1}$. This suggested a larger chain by ~3 repeating units in the MWH version. There was also a clear difference in PDI between the two heating methods, with MWH having a significantly increased value compared to CH. This is most likely because of the reduced MWt's achieved in CH compared to MWH because a large percentage of the monomeric diols were stripped off by using the vacuum at such a low conversion levels. This led to minimal higher MWt chains being formed in the CH synthesis, whereas these species where able to be made when processing with MWH. The PDI in the MWH reactions was also significantly higher than the previous non-vacuum reactions because the vacuum promoted the higher MWt chains to combine and increase the MWt. This increase in high MWt species was shown by the large M_p^{GPC} value in the vacuum MWH reactions (~8,000 g.mol^{-1}) compared to the non-vacuum reaction (~5,000 g.mol^{-1}).

When comparing the data in Table 4-12 for the vacuum reactions to the non-vacuum reactions in Table 4-8, there are some surprising differences, shown below in Table 4-13.

Table 4-13. MWt comparison between isophthalic acid, neopentyl glycol polycondensation with and without addition of vacuum.

Heating method	[a] M_n^{GPC} without vacuum (g.mol^{-1})	[a] M_n^{GPC} with vacuum (g.mol^{-1})	[a] M_p^{GPC} without vacuum (g.mol^{-1})	[a] M_p^{GPC} with vacuum (g.mol^{-1})
CH	2,020	1,540	5,470	5,400
MWH	2,430	2,120	5,040	8,900

[a] Calculated using THF GPC and ASTRA processing software relative to a polystyrene standard.

Table 4-13 details that the non-vacuumed samples have significantly larger M_n^{GPC} values compared to the vacuumed samples. Therefore, this data suggested that the addition of a vacuum produced shorter chained polyesters than when no vacuum was applied. Hence, these findings contradict what is commonly assumed for polycondensation reactions. But, this difference was attributed to loss of unreacted monomeric species from the reaction.

When applying vacuum the aim was to extract the condensate from the vessel head-space. But, the vacuum was applied too early and facilitated removal of the more volatile monomer, NPG. In the CH reactions the vacuum was applied at ~25 % conversion, leading to a significant amount of monomeric species still being present in the reaction bulk which were prone to evaporation *via* vacuum. Therefore, this early addition of vacuum led to a significant amount of NPG loss from the system. In the case of the MWH reactions the vacuum was applied at ~85 % conversion. Therefore, there wasn't as much monomeric NPG to be evaporated from the system as in CH, which explained the higher MWt data at identical conversions. But, there was still some NPG losses observed due to the reduction in MWt when compared to the non-vacuum reactions.

However, when considering the MpGPC values there is a clear difference between the heating methods. In the CH reactions there is minimal difference, again suggesting that although the values are similar, vacuum is negatively effecting the reaction by aiding diol evaporation. In the case of MWH there is a clear increase in M_p^{GPC} between the non-vacuum and vacuum samples. This therefore suggests that although there are some diol losses, highlighted by the reduction in MnGPC, there are larger MWt chains being formed. This is most likely die to the vacuum, being applied at a higher conversion level, which allowed significantly more monomeric diol to react than in the CH case before application of the vacuum.

Therefore, this data showed that application of vacuum can drive the reactions towards high conversion levels and can create high MWt species. However, care must be taken in ensuring there is minimal monomeric species left in the reaction bulk to minimise the monomer loss. For polyester resin manufacturing in industry this is accomplished *via* a “clarity test”. This is a visual check on the product to confirm that the bulk solution is clear and without white powder inside (unreacted diacid monomer). The lack of diacid monomer is an indication that there has been full conversion of monomer to at least dimeric species and therefore no/minimal monomer will be lost with addition of a vacuum.

4.2.1.3 Isophthalic Acid, Neopentyl Glycol Polycondensation Conclusions

Overall, the polycondensation of crystalline monomers has been shown to proceed most efficiently by the inclusion of the tin catalysts compared to non-organometallic alternatives. For the tin reactions it was shown that the MWH reactions proceed at significantly faster reaction rates than CH. Whereas, the non-organometallic catalysts react more slowly with application of MWH energy than CH. This was attributed to the difference in heat-up times between the heating methods and the selective heating for both sets of catalysts. The tin catalysts heat-up times were vastly reduced in MWH. But, for the non-organometallic catalysts the CH system produced faster heat-up times. This was attributed to the significantly high dielectric values of the catalyst of the non-organometallic catalysts, which will absorb the majority of the EM energy leading increased degradation and therefore the reaction will not be as efficiently catalysed when compared to the tin catalysts. Whereas in the CH scenario for the non-organometallic catalysts the heat will be going straight into

heating the reagents which will led to faster reaction heating. This, coupled with the slow reaction rate due to the poor catalysts and therefore lack of cooling condensate is why the CH reaction achieved reaction temperature faster than the MWH reaction when using the non-organometallic catalysts.

When the tin catalysts were compared it was shown that the reaction proceeded most efficiently using DHBTC in both CH and MWH reactions, attributed to this catalysts increased stability over $Sn(Oct)_2$ at high temperatures. For the DHBTC reactions, when comparing CH to MWH, there was a large difference in the heat-up times and therefore reaction cycle times. By implementing MWH into the system, the heat-up times were up to 10 times faster, which equated to ~2 hours when compared to CH. This meant that to achieve similar levels of conversion and MWt, the MWH samples were processed for half the time of the CH polyesters. This time saving was at 50 mL scale and therefore when increasing the monomer mass, this time saving is hypothesised to increase.

When processing the polyesters by pre-heating a water/diol mix there were significant differences in the polyester heat-up time between heating methods. Considering the CH reactions at 200 °C there was an increase in heat-up times of ~66 % from non-pre-heated to pre-heated. This increase in heat-up time was due to the extra water in the system (added at the start) which led to an increase in water reflux and therefore cooling effect when compared to the non-pre-heated reaction. Implementing MWH at 200 °C produced opposite results with pre-heating the water/diol mix decreasing the heat-up time by ~70 %. This was because the MWH efficiently coupled with the extra water added and this increased the bulk temperature rapidly. This efficient heating by using MWH led to the water evaporating quickly at 100 – 130 °C and minimal condensate cooling the reaction.

Vacuum has been shown to increase the final conversion of the polyesters when applied. But, this conversion increase was due to the loss of monomeric diol from the reaction *via* evaporation from the system. This was shown by the reduction in M_n^{GPC} between no vacuum addition and vacuum addition products. However, some higher MWt species were achieved when applying the vacuum after a high conversion level was achieved, shown by the significant increase in M_p^{GPC} between non-vacuum and vacuum in the MWH reactions. Therefore, this highlights that in future polycondensations, care must be taken when implementing vacuum in the industrial process to minimise diol losses by waiting for full monomer conversion to oligomers.

4.2.2 Industrial Resin Process

After the initial study of the NPG, IPA polycondensation, the actual industrial process was then investigated. This involved the addition of a triol, TMP, shown in Figure 4-19, into the diol/water preheat.

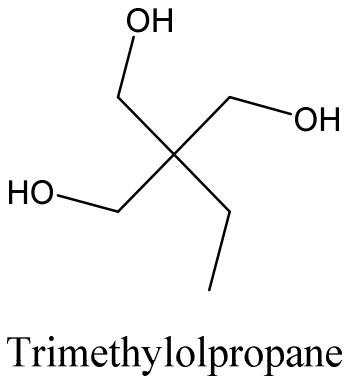


Figure 4-19. Structure of trimethylolpropane.

As discussed previously, TMP promotes the branching of polyester chains and so acts as a cross-linking agent. This increases MWt of the polyester and

therefore improves the material properties of the powder coating product when applying to a surface.

From the prior work in section 4.2.1, it has been shown that although a processing temperature of 200 °C produced an acceptable product, a higher temperature was beneficial in terms of building MWt, achieving higher conversions and increasing the thermal properties of the product. Therefore, for the industrial process, a temperature of 225 °C was implemented in both the CH and MWH reactions. This temperature is also similar to the temperatures applied in industry for these polyester resin processes. Also, for these reactions, vacuum was implemented to aide with the water removal and to build MWt.

Below in Figure 4-20, is the kinetic reaction profile for a CH and MWH reaction conducted using this methodology.

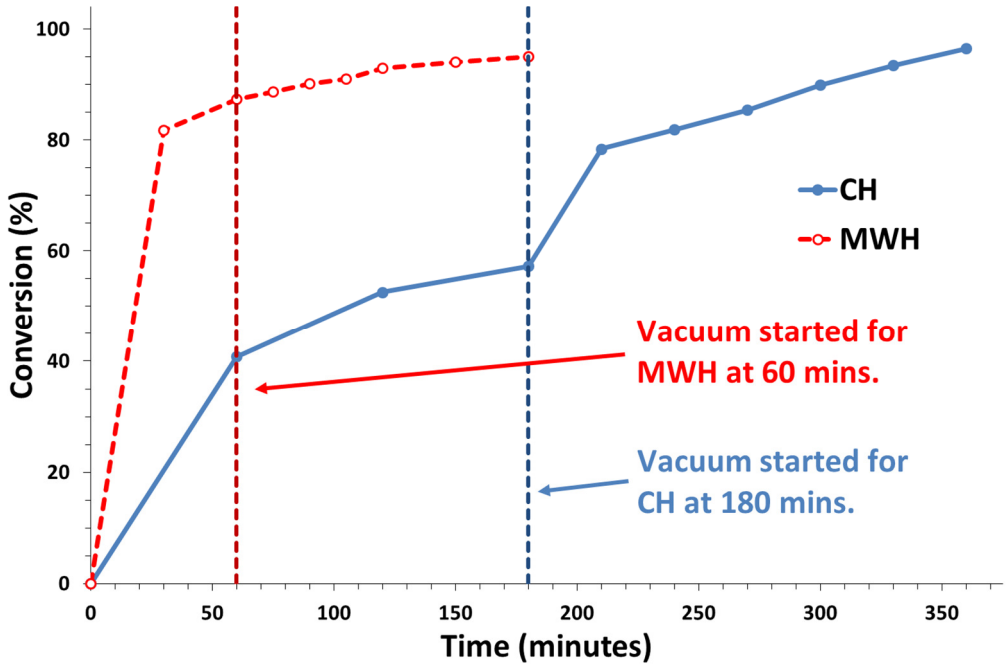


Figure 4-20. Plot of conversion versus time for a CH and MWH reaction for an industrially synthesised polyester resin.

Note: For the CH reaction, the vacuum was left off 60 minutes longer than in the NPG, IPA process as it was found to negatively aid evaporation of the monomeric species if applied too early. Also, only low levels of vacuum were used (~950 – 600 mbar).

As in previous results, Figure 4-20 indicates that by implementing MWH there was a significant increase in reaction rate than when compared to CH. This can be explained by assessing the reaction heat-up profiles in Figure 4-21.

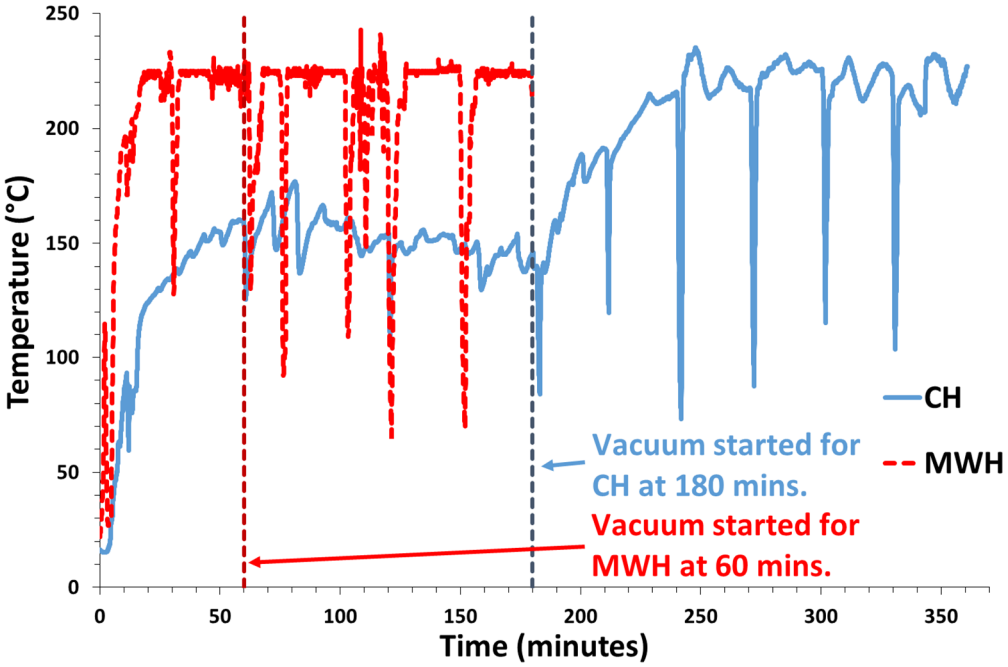


Figure 4-21. Heat-up times of industrial polyester resin process to 225 °C reaction temperature using CH and MWH with indication of vacuum application.

Figure 4-21 explains why the MWH reaction had a significantly increased reaction rate over CH. A heat-up time of ~18 minutes was achieved for MWH compared to ~245 minutes for CH. Therefore, it took over 13 times longer to attain the reaction temperature in CH when compared to MWH. This further indicated that the heat transfer when using MWH was significantly more efficient than when implementing CH. Once the reaction temperature was reached, the two heating methods had the same time (~2 hours) to process, Therefore, if the heating mechsnisms were the same, the product properties should be identical.

Figure 4-21 showed a rapid increase in temperature after application of the vacuum in CH. This suggested the vacuum was again applied too early, as in section 4.2.1.2.4. But, considering the relative jumps in conversion, 30 – 88 %

in section 4.2.1.2.4 and 60 – 78 % in the industrial resin process, showed that there was a reduced effect when the polyester was processed for an extra hour before vacuum application. Therefore, if the polyester MWt was affected, it should be to a lesser extent than in the previous work.

Assessment of the polyester MWt and thermal properties is discussed below in Table 4-14 with the GPC traces shown in Figure 4-22.

Table 4-14. GPC and DSC data for the industrial polyester resin synthesis at 225 °C using CH and MWH.

Heating Method	[a] Final Conv. (%)	[b] M_n^{GPC} (g.mol^{-1})	[b] M_w^{GPC} (g.mol^{-1})	[b] M_p^{GPC} (g.mol^{-1})	[b] Đ	[c] T_g (°C)
CH	97	2,290	12,040	27,000	5.26	54.1
MWH	94	3,210	13,400	56,200	4.18	48.8

[a] Calculated using polymer to monomer peak ratio in ^{1}H NMR. [b] Calculated using THF GPC and ASTRA processing software relative to a polystyrene standard. [c] Calculated using TA-Q2000 DSC and Universal analysis software by TA.

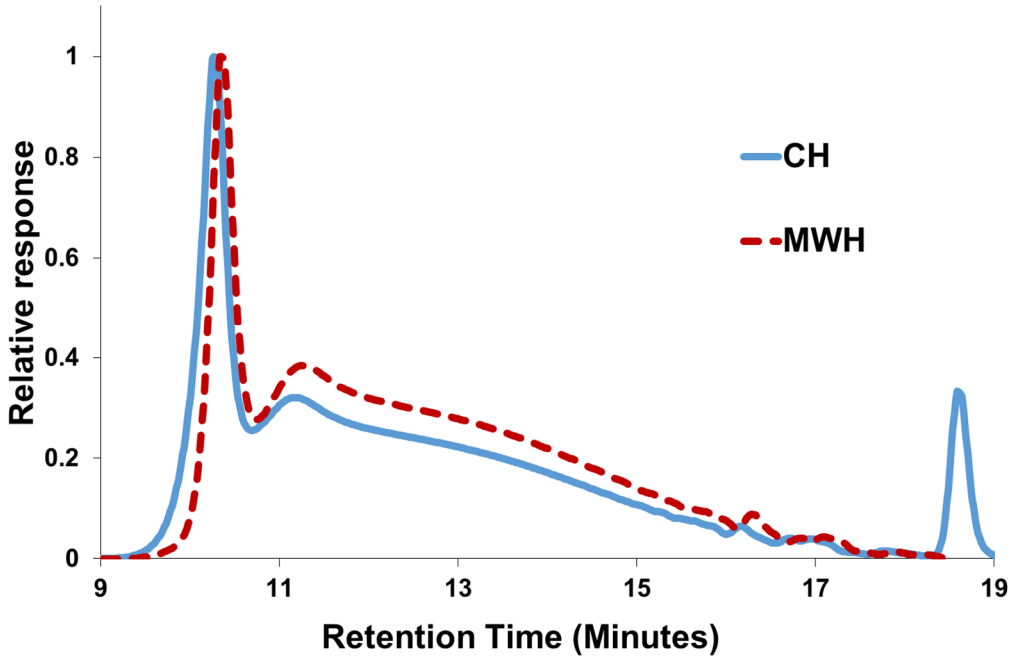


Figure 4-22. GPC traces of an isophthalic acid, neopentyl glycol, trimethylolpropane polycondensation at 225 °C implementing different heating methods.

Table 4-14 indicates that the two polyesters synthesised reached similar conversion levels of 97 and 94 % for CH and MWH respectively. This was a positive result as the MWH system was processed for 2 hours less than the CH system, explained earlier by the heat-up times.

Assessing the M_n^{GPC} values in Table 4-14 suggests a vast difference in MWt's. When processing with MWH there was an increase in M_n^{GPC} of ~900 $g.mol^{-1}$ compared to CH. This was equivalent to an increase in chain length by ~3.3 repeating units or an overall chain mass increase of ~40 %. This suggested a significant increase in the MWt and cannot be entirely explained by monomer losses, as was the case of the IPA, NPG system. However, considering the traces in Figure 4-22 disagrees with these numbers. This is because a peak at a shorter retention time would suggest a higher M_n due to the larger molecules spending less time in the GPC column. Therefore, the traces would suggest that the CH polyester has produced a larger polyester, supported by the increased T_m of the CH sample in Table 4-14. This reported increase in MWt for the MWH polymer is likely due to the increased area under the MWH sample when compared to the CH sample skewing the values. Therefore, it cannot be categorically stated that the MWH sample has a higher MWt than the CH sample and further experiments are needed to assess this.

The Đ values reported in Table 4-14 were considerably higher than the previously reported values for the AA, HD and NPG, IPA polyester resins. This was because of the addition of triol which branched the polyester chain. It is well known that branched and hyperbranched polymers have increased Đ's compared to linear polymers. [19-21] But, the MWH Đ was significantly lower than the CH reaction. This was likely because the polyester produced were of lower conversion than the CH counte4rparts. This would mean that less of the

branching triol will have reacted and this in turn has lowered the Đ. However, there could be other reasons this occurred which include:

a) The plasticising nature of the mono/di/trimers, as discussed previously in 4.2.1.2.3. This showed that even though the MWH reaction has higher MWt values, the T_g was lowered due to the lower conversion levels which left residual lower MWt species in the polyester. This can be negated by processing the reaction for slightly longer or with purification of the final product.

b) An increase in branching for the MWH system, which lowers the T_g. This occurred in the MWH reactions as MWH selectively heated the chain ends of the triol, overcoming the steric barriers encountered in branching polymers when using CH.

These two hypotheses are suggested due to the previous results in this chapter and would need further experiments to assess.

4.2.2.1 Increasing Vacuum in Polyester Resin Synthesis – The Weissenberg Effect

Due to the success of the previous experiments using a relatively low level of vacuum addition, experiments were performed but with higher level of vacuum applied. The aim of these experiments were to increase the removal of water and build MWt as quickly as possible. Therefore, experiments were conducted with the maximum vacuum level achievable on the system (~30 mbar).

These high vacuums were observed to increase the evaporation of the water from the reaction head space but also started to cause foaming. After 30 minutes of vacuum application, the sample started to climb/wrap around the

stirring shaft for both heating methods. This phenomenon is known as the Weissenberg Effect, first reported in 1946 by Garner and Nissan [22] and expanded on in 1947 by K. Weissenberg. [23]

This phenomenon can occur in polyester resin synthesis when:

a) A polyester becomes gelled or is in a near-gelled state.
b) High molecular weights are achieved, leading to highly entangled chains.

Hence, a dissolution test was conducted to assess which phenomenon occurred. This would indicate whether the polyester had gelled as a gelled polyester would not dissolve whereas a highly entangled network would.

In THF (the usual solvent for dissolving this polyester), at room temperature, both the CH and MWH products didn't dissolve and it was therefore assumed that the samples cross-linked into a gelled network. This occurred due to the vacuum being applied too high which removed significant amounts of diol from the system to create a 1:1 stoichiometry of diacid:diol. This created a highly/fully cross-linked network at conversions approaching 100 %, in which all the polyester chains combined into one large molecule.

Due to the products not dissolving in solvent, only thermal property analysis was performed. The data attained is shown below in Table 4-15.

Table 4-15. DSC data for industrial polyester resin processed at 225 °C using CH and MWH and maximum vacuum settings.

Heating Method	[a] T_g (°C)
CH	61.0
MWH	61.9

[a] Calculated using TA-Q2000 DSC and Universal analysis software by TA.

The values of T_g reported in Table 4-15 are 6 - 10 °C higher than the values previously presented in Table 4-14. This confirms that a large polyester/cross-linked network was created by processing at high vacuum levels.

Therefore, when processing at larger scales, care must be taken to ensure that the vacuum is added at the correct point and to the correct level to minimise the chances of gelling/high entanglement. This is because having a ≥5 kg batch of polyester resin cross-linking and becoming insoluble would potentially cause large problems in the reaction vessel, such as; stirrer shaft problems (e.g. shearing due to high torque of polyester wrapping round shaft) and difficulties in cleaning out the reactor which would affect future experiments.

4.3 Conclusions

It was shown that the tin catalysts provided significantly increased reaction rates than the non-organometallic catalysts, independent of heating method. This was explained by the non-organometallic catalysts decomposition occurring at the 200 °C processing temperature implemented with these polyesterifications. This was especially true in the case of PPA, which, it has been hypothesised, can be readily hydrolysed into the PA monomer at high temperatures. Interestingly, between the organometallic and non-organometallic catalysts, there was a difference in reaction rates between heating methods. This was demonstrated by the heating profiles, in which the non-organometallic catalysts achieved processing temperature quicker when using CH, whereas the tin catalysts achieved processing temperature quicker when implementing MWH. This was explained by the high dielectric properties of the non-organometallic catalysts absorbing the bulk of the EM energy in their reactions, leading to localised

heating around these species and poor energy transfer into the main reaction bulk and increased degradation of the catalyst. Whereas, when implementing a tin catalyst the diol monomer had higher dielectric properties than the catalysts, leading to a high proportion of the EM energy being input into the sample bulk, heating a larger proportion of the reaction mix and creating faster heat-up times. But, overall it was demonstrated that the DHBTC catalyst was the only catalyst to create a resin-like polyester with significant MWt's over the allotted cycle time. Therefore, further research only included this catalyst.

In industry, a pre-heating step is implemented where diol is dissolved in water at ~90 °C. Therefore, a brief investigation was conducted to investigate how this affected polyester processing in both CH and MWH. It was discovered that the heat-up times between these two methods varied depending on heating method. In the CH system, it was the non-pre-heated reactions which achieved processing temperature quicker than the pre-heated ones. This was explained by the 30% increase in water needing to be evaporated from the reaction to attain 100 % conversion. This led to an increased quantity of water refluxing and cooling the bulk. Furthermore, as CH is an ineffective method of heat transfer, this extra water substantially affected the heat-up times due to inefficient transportation away from the bulk. Whereas, in the MWH reactions it was the pre-heated reactions which had faster heat-up times. This was because the EM current readily coupled with the excess water, which was quickly evaporated. Also, an overall advantage to the pre-melt was dissolving the NPG in water initially allowed easier homogenisation/solvation of the diacids when added. Therefore, the reaction had better processing conditions than in the non-pre-heated system, hence why it is implemented on an industrial scale.

An investigation into the difference in polyester properties between the two heating methods was conducted to assess if using MWH effected the inherent

properties of the molecule. This was completed by heating the reactions to reaction temperature and processing for similar periods of time. This allowed identical conversion percentages to be reached (94 %) and therefore a fair method of comparison. These polyesters were subjected to MWt and thermal analysis. This deduced that the MWH reactions consistently had higher M_n^{GPC} values than their CH counterparts, with the difference equating to ~400 $g.mol^{-1}$ (DP of ~1.5 units). This MWt increase was supported by an increase in T_g of ~2.5 °C with the MWH products compared to the CH products. This increase was due to the fact that by implementing MWH a selective heating effect occurs, this excited the chain ends and/or catalyst in the polyesters to help build higher MWt chains, unlike the thermal heating effect of CH.

Changing the stoichiometry of the system to increase the molar proportion of diol was shown to have specific effects on the polyester. When increasing the NPG ratio it was found that the conversion rate dropped for both CH and MWH (with a larger difference in CH). This was hypothesised to be because the increased NPG ratio effected the ^1H NMR analysis as there was more NPG monomer in the system and therefore the proportion of diol to polymer peaks increased, lowering conversion. But, when assessing the MWt's, it was shown that a mole ratio of 1.1:1 NPG:IPA produced a higher MWt polyester when compared to the other stoichiometries. This suggested that having a slight excess of diol was favourable in the reaction to build MWt, but a large excess had a negative effect. This was demonstrated by the 1.2:1 system producing the lowest MWt polyesters. Also, it was reported that increasing the stoichiometry ratio, decreased the Đ. This was explained by the excess of NPG creating mainly hydroxyl functional polyesters and therefore reducing the amount of acid groups in the system. This would reduce the reaction rate and create smaller molecules in a more controlled environment.

As a prelude to the industrial resin synthesis, the temperature in the NPG, IPA polycondensation was increased to 225 °C. This made the difference between the heat-up times in CH and MWH increase, with MWH attaining processing temperature ~13 times faster than CH. Once the reaction temperatures were reached the reaction was left to process for similar time periods to probe the potential differences on the product between heating methods. The analysis showed that employing MWH created an almost identical product to the CH process, but the reaction was processed for 40 % of the cycle time. This proved that significant time savings can be achieved by heating *via* EM energy.

Comparing the 200 and 225°C products produced some interesting differences between the final products. Between the CH products, it was shown that increasing the temperature increased the MWt over a similar processing period, with an increase of ~200 $g.mol^{-1}$ observed between 200 and 225 °C. However, this was a minimal increase for a large jump in temperature. Comparing the MWH reactions showed that the polyesters produced formed almost identical products, but the reaction at 225 °C was processed for 67% of the time as the one at 200 °C. Between the two temperatures there was a significant difference in T_g's, with the polyesters processed at 225 °C achieving values ~5 °C higher than at 200 °C. This was hypothesised to be because of the increased mono/di/trimer content in the 200 °C samples (lower conversions) plasticising the polymer. Therefore, thermal analysis was conducted on the 225 °C samples with the addition of a small amount of oligomeric sample to examine this theory. It was shown that addition of oligomeric material lowered the T_g by ~1.5 °C, indicating that plasticisation occurred.

Following this, addition of a vacuum to the polycondensations was assessed for MWt increases and to evaluate if there was a difference between heating

methods. As the MWH reaction proceeds at a significantly faster rate than the CH reaction the vacuum was added 1 hour earlier, which equated to a conversion difference of ~60 %. Adding the vacuum this early (23 % conversion) in the CH reaction proved to create problems with the final product *i.e.* low M_n^{GPC} values for high conversion percentages. Therefore, addition of the vacuum at this reduced conversion led to significant amounts of monomeric diol evaporating from the system. This was shown by the sharp increase in conversion and temperature after vacuum addition. Therefore, although the reactions were processed at 225 °C for similar time periods, there was a difference in M_n^{GPC} of ~600 g.mol^{-1}, which was a significant amount at these smaller MWt's. However, comparing the M_p^{GPC} indicated that the vacuum addition was assisting the formation of higher MWt polyesters in the MWH system. This was because the vacuum added species had an increased M_p^{GPC} of 3,000 g.mol^{-1} compared to the non-vacuum sample. Therefore in this case the vacuum was helping remove the condensate from the reaction and increasing MWt. This was present in the MWh sample and not the CH sample because the vacuum was added at a high conversion level (+80 %) in the MWH reaction and therefore the evaporation of monomer was reduced (but still present), whereas in the CH case too many diol monomers had been evaporated from the system for the vacuum to assist the MWt elongation. Hence, this indicated that when processing the industrial resin system, care must be taken to apply the vacuum once the majority of the conversion has elapsed to minimise the loss of diol from the system.

For the industrial resin process, implementing MWH was shown to significantly increase reaction rates. Reactions using MWH were processed for half the time of CH and the final product was shown to be significantly higher MWt. To reach processing temperature in the CH system it took ~13 times longer than in the

MWH system which equated to ~3 hours of processing time. The difference in M_n^{GPC} of ~900 g.mol^{-1} showed a significant difference between heating methods. This confirmed that implementing MWH can positively affect the MWt of polyesters by promoting chain elongation. However evaluation of the GPC traces suggested that the larger area under the MWH peak may have skewed the results in favour of a higher value. This was because the peak retention time in the CH polyester was at a shorter time than MWH, suggesting a higher MWt. Đ was also shown to be lowered in the MWH reaction, however this was likely to be because of the reduced conversion in the MWH. This could suggest that implementing MWH assisted polyesterification control. However, a significant decrease in T_g was observed for the MWH sample, even though the MWt data suggested a larger molecule. This was attributed to either an increase in oligomer content, due to the lower conversion percentage achieved, or an increase in branching. An increase in branching is possible as the MWH energy will selectively heat the chain ends of the triol monomer which will help overcome the steric barrier to branching and therefore promote this more than the CH reaction. This potential increase in branching could have led to reduced inter-polyester chain interactions and therefore lowered the T_g. However, these theories would need further research to prove or disprove.

Vacuum addition to the industrial resin system is a vital part in building high MWt polyesters. But, the addition of a very strong vacuum for prolonged periods of time negatively affected the polyester product. This was shown by the polyesters foaming and climbing the stirrer due to the creation highly entangled/gelled networks which didn't dissolve in solvent, which is known as the Weissenberg effect. Therefore, this polyester could not be post-functionalised with acid groups to create the powder coating product. As such,

when scaling up, care must be taken with vacuum strength, timing and application period to stop gelling on a large scale.

4.4 References

1 Dholakiya, B. *Unsaturated Polyester Resin for Specialty Applications*. (InTech, 2012).

2 Subramanian, R. Typical ingredients of weather-resistant powder coatings. *Metal Finishing* 101, 21-25, doi:http://dx.doi.org/10.1016/S0026-0576(03)90104-8 (2003).

3 Okamoto, S. Resin composition for electrical equipment insulation. Japan patent JP2002294057 (2001).

4 Weissermel, K. & Arpe, H. J. *Industrial Organic Chemistry*. (Wiley-VCH, 2003).

5 Eastman™. Eastman ™ polyester resin intermediates for powder coatings. (2009).

6 Chanda, M. & Roy, S. K. *Plastics Technology Handbook*. Fourth edn, (CRC Press, 2006).

7 Merck, Y., Maetens, D., Moens, L. & Buysens, K. Flexible super-durable polyester based powder coatings. *European Coatings Journal* (1999).

8 Stevenson, T., Subramanian, R., Starcher, R., Smedley, L. & Dove, H. Flexible, super durable powder coating composition. US20060079650 (2006).

9 Streitberger, H. J. & Dossel, K. F. *Automotive Paints and Coatings*. 225-230 (Wiley, 2008).

10 Smith, O. W., Thames, S. F., Zhou, L., Forschner, T. C. & Boon, W. H. Carboxyl-functional polyester epoxy resin powder coatings based on 1,3-propanediol. WO2001070893 (2001).

11 Gavish, N. & Promislow, K. Dependence of the dielectric constant of electrolyte solutions on ionic concentration: A microfield approach. *Physical Review E* 94, 012611 (2016).

12 Adlington, K. *et al.* Mechanistic Investigation into the Accelerated Synthesis of Methacrylate Oligomers via the Application of Catalytic Chain Transfer Polymerization and Selective Microwave Heating. *Macromolecules* 46, 3922-3930, doi:10.1021/ma400022y (2013).

13 Moore, T. C., Griffith, S. S., Thompson, D. E., Kluesener, N. R. & Honeycutt, J. R. Methods for Making Polyester Resins in Falling Film Melt Polycondensation Reactors. US 20090093600 (2009).

14 Wiley-VCH. *Ullmann's Polymers and Plastics, 4 Volume Set: Products and Processes*. Vol. 2 783-785 (Wiley, 2016).

15 Schumann, H. D. & Thiele, U. Process for the acceleration of the polycondensation of polyester. US5744572 (1998).

16 Metaxas, A. C. & Meredith, R. J. *Industrial Microwave Heating*. (P. Peregrinus, 1983).

17 Meredith, R. J. & Engineers, I. o. E. *Engineers' Handbook of Industrial Microwave Heating*. (Institution of Electrical Engineers, 1998).

18 Thomas, S. & Zaikov, G. *Recent Advances in Polymer Nanocomposites: Synthesis and Characterisation*. (CRC Press, 2010).

19 Satoh, T. Synthesis of Hyperbranched Polymer Using Slow Monomer Addition Method. *International Journal of Polymer Science* 2012, doi:10.1155/2012/816163 (2012).

20 Hawker, C. J., Lee, R. & Frechet, J. M. J. One-step synthesis of hyperbranched dendritic polyesters. *J. Am. Chem. Soc.* 113, 4583-4588, doi:10.1021/ja00012a030 (1991).

21 Hölter, D., Burgath, A. & Frey, H. Degree of branching in hyperbranched polymers. *Acta Polym.* 48, 30-35, doi:10.1002/actp.1997.010480105 (1997).

22 Garner, F. H. & Nissan, A. H. Rheological properties of high-viscosity solutions of long molecules. *Nature* 158, 634-635 (1946).

23 Weissenberg, K. A continuum theory of rhelogical phenomena. *Nature* 159, 310 (1947).

5 Pulsed Microwave and Scale-up Experiments

5.1 Overview

Chapter 5 focuses on the application of pulsed microwaves on a melt polycondensation system and also discusses the preliminary results when reactions were scaled up to a 5 L load in a bespoke conventional (CH) and microwave heated (MWH) hybrid vessel.

Initially, the pulsed microwave application system was investigated with the adipic acid (AA) and 1,6-hexanedio (HD) melt polycondensation system, which was discussed previously in chapter 3. An investigation was conducted into assessing if the pulse frequency (how often the microwave pulses switch on and off per second) effected the polymerisation kinetics and products. This was done with a constant duty cycle/factor (percentage of time the microwave pulses were switched on).[1] This showed that more efficient energy application occurred when pulses were used compared to a continuous wave (CW) experiment due to an increase in average absorbed power. This led to higher conversions and molecular weights (MWt) being achieved in identical processing times.

Pulsed microwaves were then assessed using the industrial resin monomers. It was again shown that when compared to a CW experiment, there was a decrease in heat-up time and therefore an increased reaction rate. However, assessing the power and temperature profiles it was observed that there were long periods where the power was not applied due to the efficient heating of the high powered pulses. Therefore, an investigation into matching the duty cycle with the internal temperature was investigated to deduce if the constant

application of a high powered pulse was beneficial over the intermittent use. These experiments proposed that matching the duty cycle with the internal temperature could potentially lead to higher MWts, likely due to the constant application of the high power selectively heating the catalyst and/or monomers more consistently than the intermittent use, pushing the forward polyester reaction.

The scale up of the process is then discussed, with the AA, HD system being presented initially. Between the heating methods a slower heat-up time was produced by implementing MWH and therefore a lower conversion was achieved. But, it was shown that by implementing MWH, higher MWts and thermal properties were produced. This further suggested a specific microwave effect on the system which was amplified due to the size of the reaction load.

Finally, the two stage industrial resin system is discussed. It was shown that the 5 L vessel could be used to create a product which was similar to the specification of the industrial sponsors. When comparing the MWH and CH products, it was shown that by implementing MWH there was a reduction in glycol losses of 45 % from the first stage, attributed to the selective heating of the chain ends/catalyst which promoted reactions over evaporation of the diol monomer. It is also discussed that the MWH reaction created a product with increased MWts when compared to the CH sample. But, the difference in heating profile is the potential cause of this and more research was needed to critically assess these claims.

5.2 Results and Discussion

5.2.1 Pulsed Microwaves

For this section of work, implementing a pulsed microwave heating method was briefly evaluated. The theory behind implementing a pulsed microwave over the usual CW is that to achieve an identical average power (P_{av}), higher "bursts" of power can be implemented in a pulsed regime. This is because instead of the power being turned on continuously, it is switched on and off rapidly over a certain time period. This is known as the pulse frequency or "ripple frequency" and is different to the operating frequency of the microwave (2.45 GHz). The pulse frequency describes the amount of times the microwave energy is switched from on to off within a second and is measured in Hertz (Hz). This frequency does not affect the overall P_{av} as the same amount of power goes into the experiment overall, it's just the way it is delivered which changes. The pulse frequency is described schematically below in Figure 5-1.

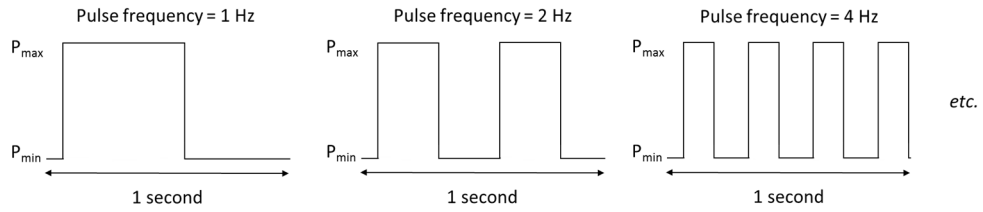


Figure 5-1. Schematic of pulse frequency.

Where P_{min} and P_{max} represent the minimum and maximum power applied respectively.

These pulses also allow a low average power to be applied while applying large amounts of maximum power (P_{max}) for short periods of time. Therefore, if an input power of 100 W is being targeted there are many different combinations of P_{max} and pulse frequencies which can be used e.g. 200 W P_{max} for 50 % of

the time, 1,000 W P_{max} for 10 % of the time *etc.* This creates what is known as a rectified signal *i.e.* instant on/off application of microwaves over a period of time. Therefore, when performing pulsed microwave experiments there are many different parameters which can be altered. Examples of the different parameters for an identical P_{av} experiments are described below in Table 5-1. These experiments will thermodynamically apply the same amount of power (same P_{av}) and therefore the heat-up times of the reactions would be identical. Therefore, any differences in final product properties would suggest that the method of high power application is essential to optimising microwave application.

Table 5-1. Example of different experiments to input identical average powers but changing how the microwave power is applied.

P_{max} (W)	% of Time Microwave Power is ON	P_{av} (W)	Pulse Freq. (Hz)
2,000	10	200	1,000
2,000	10	200	10
1,000	20	200	1,000
400	50	200	1,000
400	50	200	100

The pulsing method of microwave application is of specific interest due to previously reported success in pulsing reported by Costa *et al.* [2] and Cheng *et al.* [3] who both suggested a non-thermal microwave effect when pulsing which was beneficial towards the reaction rates. However, these non-thermal effects are not expected in this polymeric system and there is no ability to measure the temperature at this microscopic scale to prove their existence. Therefore, the pulsing experiments were used to maximise the selective heating which has been suggested in the previous chapters of this thesis and was investigated to

assess if applying higher levels of power in short bursts effected the polymerisation in terms of final polymer composition/properties.

5.2.1.1 Adipic acid, 1,6-Hexanediol Polycondensation – Assessing Pulse Frequency

To assess the use of pulsed microwave heating in polycondensation reactions versus CW, a set of AA, HD polymerisations were conducted using the dihydroxybutyl tinchloride (DHBTC) catalyst in the new apparatus set-up, described in chapter 2 section 2.2.2.2. These new experiments are shown below in Figure 5-2 and detail a pulsed experiment at 50 Hz (with 10 % of the microwave pulse) and 1,000 Hz (with 14 % of the microwave pulse) with a comparison to the CW experiment. These two percentages of pulse application were used to make sure P_{av} for each reaction were identical as applying 10 % at each pulse frequency lead to differences in P_{av} due to the lead time (time for microwaves to switch on) of the pulsed equipment.

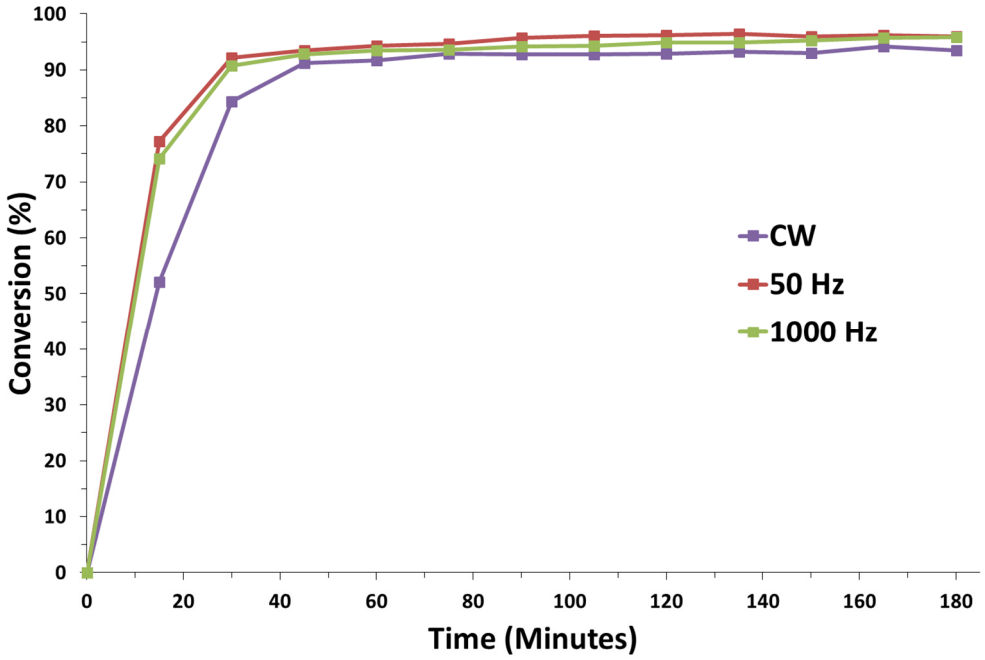


Figure 5-2. Comparison between pulsed microwave at differing frequencies and continuous wave microwave heating for an adipic acid, hexanediol polycondensation at 185 °C.

Figure 5-2 demonstrates that when implementing pulsed microwave heating, there was minimal difference between a low pulse frequency (50 Hz) and a high pulse frequency (1,000 Hz) if the average absorbed powers are identical. But, when comparing this to the CW experiment, there was a clear difference in conversion rate. CW was shown to convert at a reduced rate, with 80 % conversion achieved after 28 mins, compared to 20 using pulsed microwaves.

The differences between the pulsed and CW experiments can be investigated by assessing the heating profiles for the reaction, detailed in Figure 5-3.

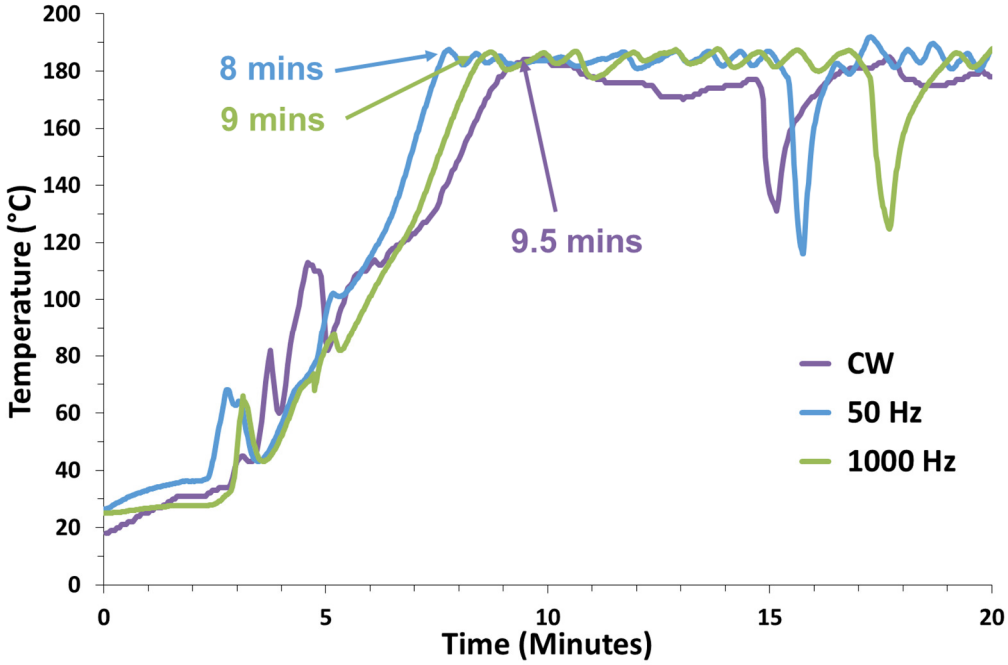


Figure 5-3. Initial heating profile comparison for an adipic acid, hexanediol polycondensation between a CW and pulsed microwave reactions at 50 Hz for 10 % and 1,000 Hz for 14 % of the time to achieve an average absorbed power of 150 W.

Figure 5-3 demonstrates that when considering the initial heat up of the AA, HD reactions to 185 °C between the two microwave input methods, there was an almost identical heat-up time, within the expected variation amount of ±5 minutes. This was shown by a difference in less than two minutes between the three reactions. Therefore, the heat-up time cannot explain why there was an obvious difference between the initial conversion of the pulse and CW experiments. Considering the average absorbed power for the averaged pulse reactions and the CW reaction produces the following plot in Figure 5-4.

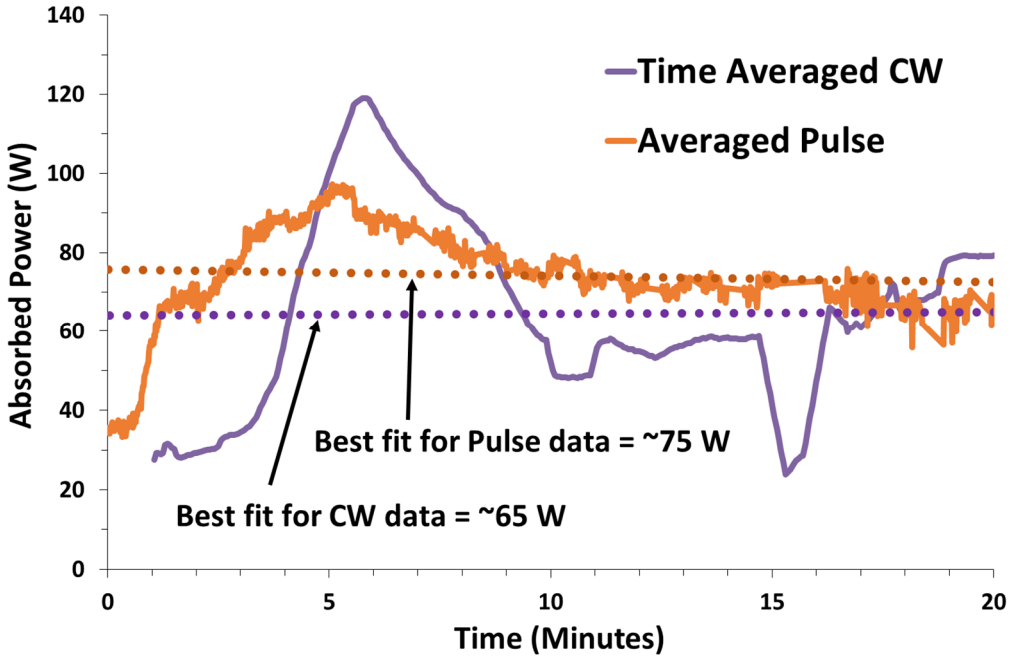


Figure 5-4. Averaged absorbed power for CW and Pulsed microwave application reactions. Note. The CW data is time averaged and therefore cannot start from time = 0 minutes.

Figure 5-4 displays the difference in initial absorbed power profiles between CW and pulsed microwave application experiments. It shows that although the CW power application has more spikes and troughs, the average absorbed power over the initial period was similar, but not identical. With pulsed and CW methods starting at 75 and 65 W respectively and becoming separated by only 5 W towards the end of the initial 20 minute period. This plot therefore shows that although there was an increase in the absorbed power of 5 – 10 W in pulsed reactions this does not greatly affect the heat-up times of the reactions significantly and does not explain why there was an increase in initial conversion of 25 % (50 % for CW and 75% for the pulsed reactions after 15 minutes). Therefore, there must be another, non-kinetic factor as to why there was a significantly increased heat-up time in the pulsed reactions. This could potentially be an example of how applying a high power in short bursts can selectively excite the chain ends/catalyst and lead to increased conversion

rates. The high power applied will have selectively heated the chain ends/catalyst to a higher degree than the bulk, increasing the localised temperature at these sites and promoting polyester formation. Although this can happen in the CW synthesis, the high powers used in the pulsed experiments will increase the localised heating effects. Consequently creating higher temperatures at the reactive sites in these experiments and therefore increase polymerisation rates.

The polyesters synthesised from the pulse and CW reactions were then analysed for MWt and thermal data to assess if there was a difference between these methods. The data is shown below in Table 5-2 with the GPC traces in Figure 5-5.

Table 5-2. MWt data for the adipic acid, hexanediol polyesterifications conducted on the pulse microwave rig.

Microwave Freq. (Hz)	Conv. (%)	[b] M_n^{GPC} (g.mol^{-1})	[b] M_w^{GPC} (g.mol^{-1})	[b] M_p^{GPC} (g.mol^{-1})	[b] Đ	[c] T_m (°C)
CW	93	2,456	6,384	6,980	2.59	52.0
50	96	3,060	8,050	9,240	2.63	54.2
1,000	96	2,810	8,000	9,240	2.85	54.8

[a] Calculated using polymer to monomer peak ratio in ^{1}H NMR. [b] Calculated using THF GPC and ASTRA processing software relative to a polystyrene standard. [c] Calculated using TA-Q2000 DSC and Universal analysis software by TA.

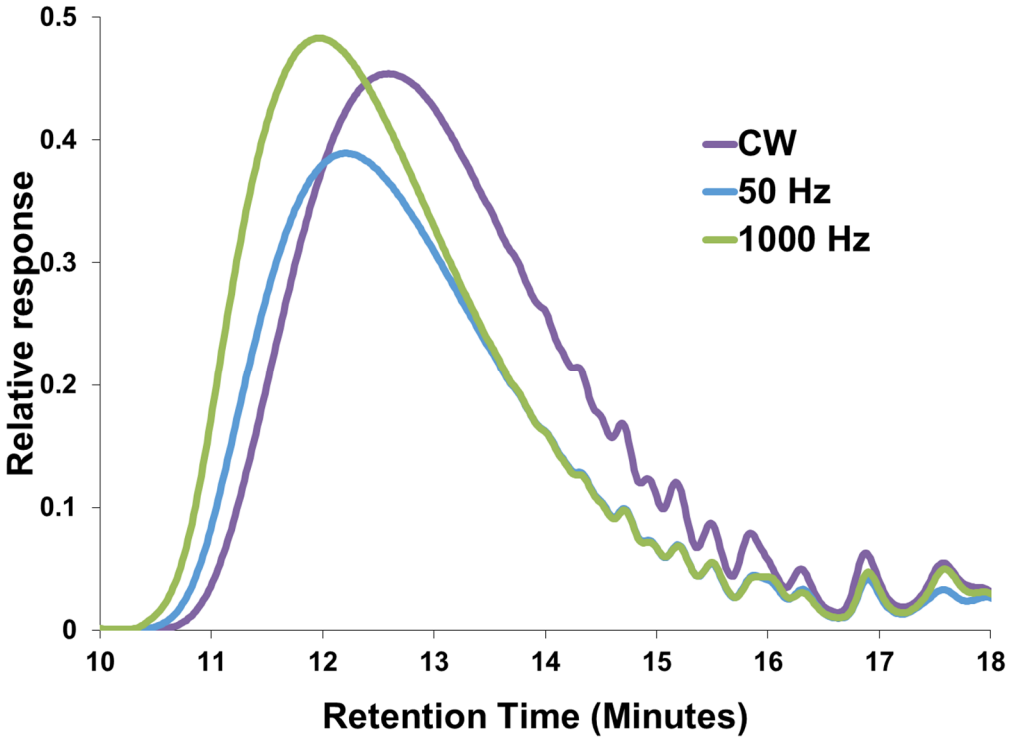


Figure 5-5. GPC traces for the adipic acid, hexanediol polyesterification using CW and pulsed microwave power input.

Table 5-2 details that there was a difference in final properties between inputting microwaves *via* pulse or CW in the polycondensation of AA and HD. The main difference observed was the reduced final conversion when implementing CW, also shown by the plot in Figure 5-2. This led to an increase in the MWts and thermal data for the pulsed products compared to the CW product. This, along with Figure 5-4, suggested that pulsing a high power into the system meant that the energy was being absorbed more efficiently than in the CW system. This increased the power being used by the system for chemical reactions and therefore increased the final conversion, MWts and thermal properties or, the high powers excited the reactive parts of the polymerisation to a higher degree than in the lower power CW reaction, leading to a higher temperature at these parts of the system and therefore increased reactions.

Comparing the two pulse frequencies, 50 and 1,000 Hz, showed that there was minimal difference in the MWt and thermal properties. There was a slight increase in M_n^{GPC} for the 50 Hz product compared to the 1,000, but the increased Đ of the 1,000 Hz product shows that this may be due to a larger spread of MWts in this product. This is also confirmed by an increased T_m, which suggested that there are some higher MWt species in the 1,000 Hz product compared to the 50 Hz product. Also, assessing the identical M_p^{GPC} values showed that the peak MWt was the same for both samples. This suggested that they can be treated as almost identical products. Overall, the product properties and final conversions suggested that changing the frequency of the pulses did not have a significant effect on the chain building mechanism of the polyesterification. It was just the average absorbed power which was key to defining chemical differences.

Therefore, when applying MWH, there was some minor differences between using a CW and pulsed microwave for the AA, HD system. By implementing pulsed microwaves there was a faster heat-up rate, attributed to the high powers used exciting the molecules to a higher degree and therefore leading to a larger amount of power being absorbed at the reaction outset. This amplified the initial rapid heating effect, but was only marginal. However, once processing temperature was achieved, the high powers potentially had a positive effect on the mechanism used in the polyesterification. This is because there was an increased final conversion of 3 % between the CW and pulsed reactions, which cannot be accounted for by a decrease in heat-up time of 1 minute. This suggested that the high powers selectively heated the chain ends/catalyst to promote polymer formation to a greater extent than the lower powered CW reaction, confirmed by the increased MWts achieved in identical cycle periods. Between the pulsing frequencies it was displayed that there was almost no

differences. The heat-up times between 50 and 1000 Hz were almost identical as were the conversion profiles. When considering the final product qualities it was shown that the 50 Hz product had a higher M_n^{GPC}, suggesting a higher MWt product. But, this was cannot be confirmed as there was a higher Đ observed in the 1,000 Hz sample and the products had identical M_p^{GPC} values.

5.2.1.2 Isophthalic Acid, Neopentyl Glycol Polycondensation

The previous work conducted in section 5.2.1.1, showed that the pulse/ripple frequency makes minimal difference on the polyester product. Hence, the experiments in this section will focus on one frequency, 50 Hz. Initially, the monomer system was tested using 1,500 W applied for 10 % of the time (i.e. duty cycle = 10%) at 50 Hz, with a processing temperature of 200 °C and the DHBTC catalyst. This reaction proceeded and the conversion data is shown in Figure 5-6.

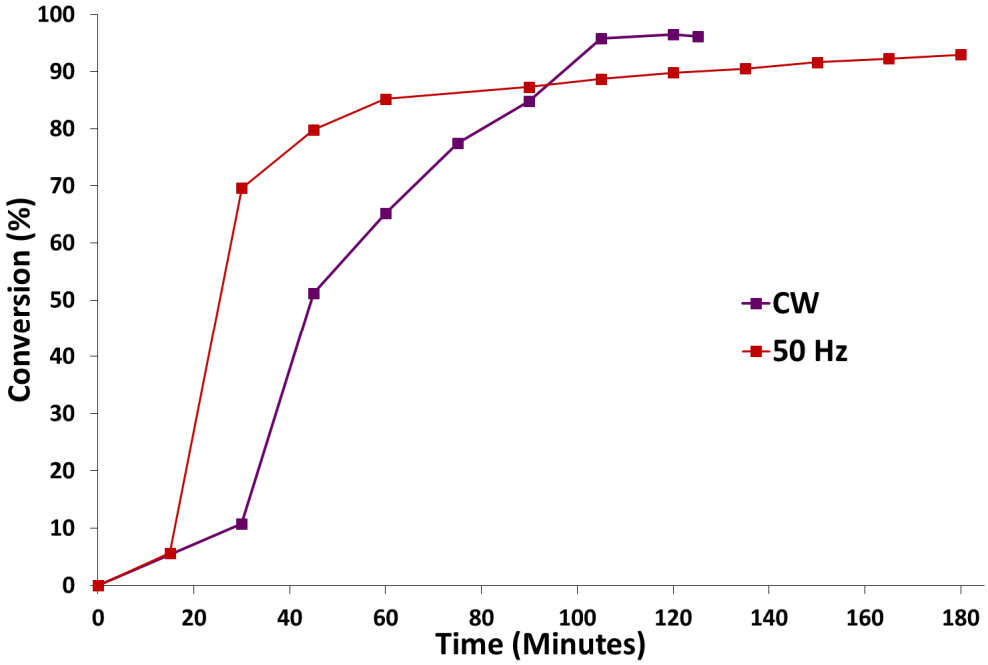


Figure 5-6. Conversion versus time for a neopentyl glycol, isophthalic acid polycondensation at 200 °C reaction using pulsed microwaves at 50 Hz with 1,500 W at 10 % of the time compared to a CW reaction.

Figure 5-6 demonstrated that using a pulsed heating method can produce a highly converted polyester in a short amount of time when compared to a CW method. The slow conversion observed from 0 to 15 minutes occurred due to the monomers starting to melt and reach reaction temperature, but compared to the CW reaction this time was reduced by 50 %. This was possibly because the high power of the pulsed reactions was heating the monomers at a faster rate than the CW reaction. The high power input for a short period of time highly excited the monomers and this led to an increase in the rapid heating effect observed with MWH, as was observed previously in section 5.2.1.1. This is shown by the heating and energy input profile in Figure 5-7.

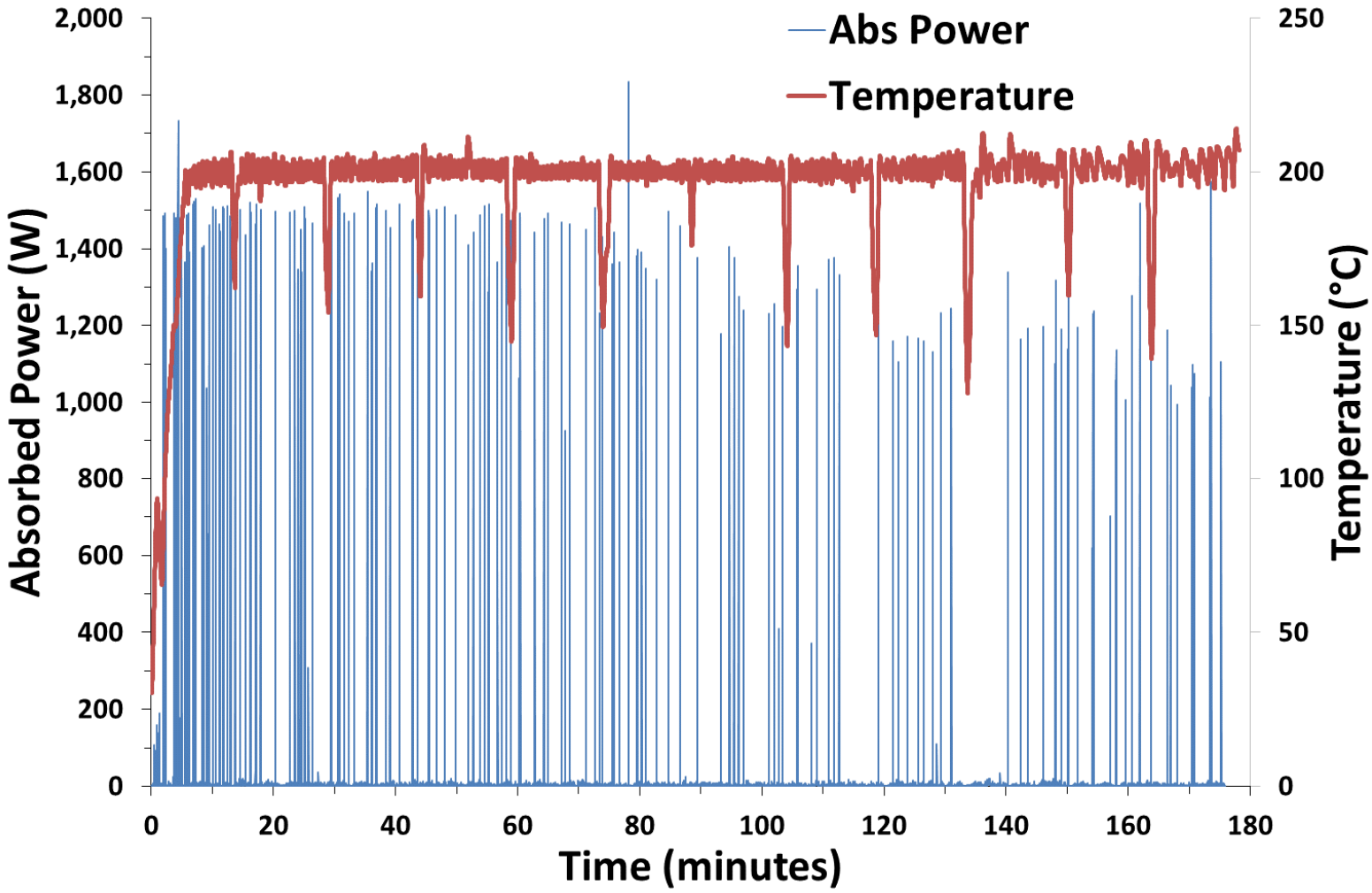


Figure 5-7. Absorbed power and temperature profile for an isophthalic acid, neopentyl glycol polycondensation at 200 °C using 1,500 W of pulsed microwaves 10 % of the time

Figure 5-7 shows the spikes in power input (blue line) from 0 W to 1,500 W. At the beginning of the reaction (0 – 15 mins) there was little to no gaps in the absorbed power data, showing that the microwaves needed to be applied consistently to heat the reaction up to processing temperature. But, once the temperature was achieved (~10 mins) the microwaves started to turn off for elongated periods of time, with large gaps being prominent towards completion of the cycle time. This meant that the average absorbed power throughout the reaction was not 150 W, but considerably lower. This can be shown by adding an average power trend line to the absorbed power data, shown in Figure 5-8.

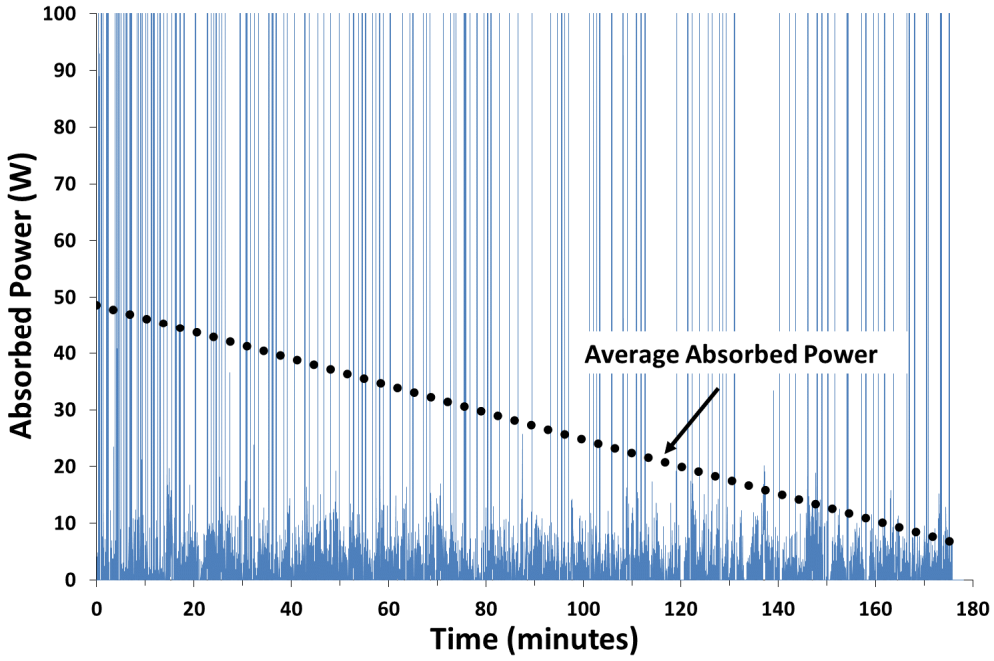


Figure 5-8. Time averaged absorbed power for pulsed isophthalic acid, neopentyl glycol polyesterification at 200 °C using a 10 % duty cycle and with P_{max} = 1,500 W.

Figure 5-8 shows that the average absorbed power started at ~50 W and decreased over the reaction cycle to ~10 W by completion. This was due to the large periods of time in which the microwaves are off due to the reaction being at temperature and needing no power input. As a result, an investigation into evaluating the effects on the polyesterification if high powered pulse

microwaves are on throughout the reaction was undertaken. This was achieved by keeping the peak power and pulse frequency identical (P_{max} = 1,500 W and pulse frequency = 50 Hz), but reducing the duty cycle to match the processing temperature. Therefore, at the beginning the duty cycle was set to 10 %, to achieve an average power input of 150W, but once the processing temperature was reached, this was lowered to keep the power application in line with a constant reaction temperature. This reaction was repeated and the conversion profiles are shown below in Figure 5-9.

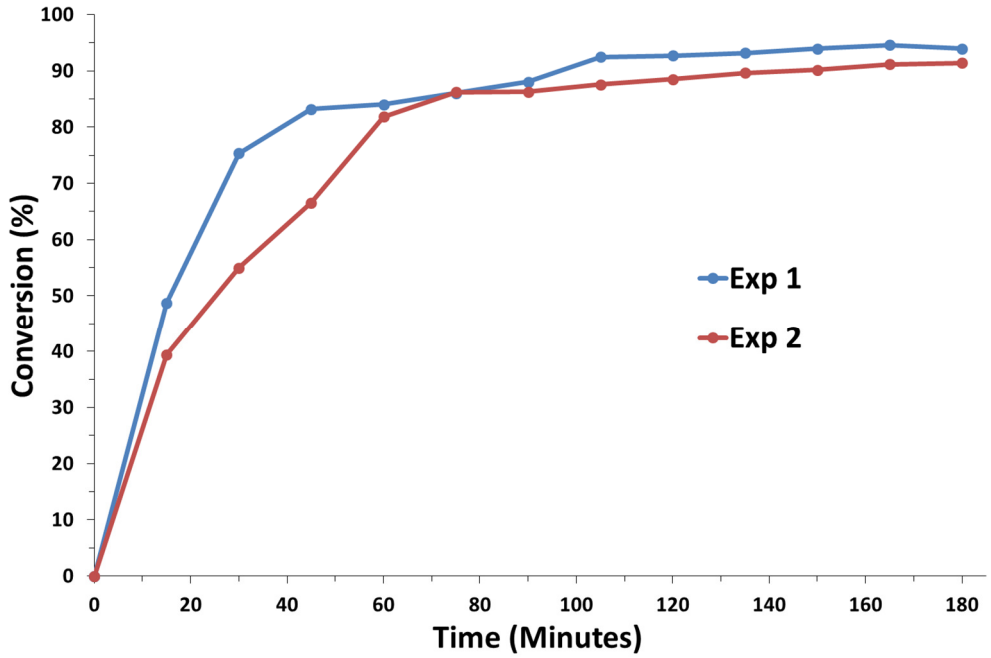


Figure 5-9. Conversion versus time for a polycondensation of isophthalic acid with neopentyl glycol using pulsed microwaves at P_{max} = 1,500 W and pulse frequency = 50 Hz with duty cycle matching to an internal temperature of 200 °C.

Figure 5-9 demonstrated that the initial reaction rate and final conversion percentage of the repeats were very similar. There was a slight disparity between the conversion of the products between 15 and 60 minutes, but this was likely due to the stirring problems occurred when using a magnetic stirrer for these viscous products. If the stirrer was stirring the bulk efficiently, as in experiment 1, there was a faster conversion. Whereas, in experiment 2, there

was a large agglomeration of IPA after addition and stirring was effected, reducing its initial homogenisation and therefore reaction with NPG. But, after an hour of processing, the reactions become comparable in conversions.

To assess the differences between the two reactions the power and temperature profiles for the repeats are detailed below in Figure 5-10.

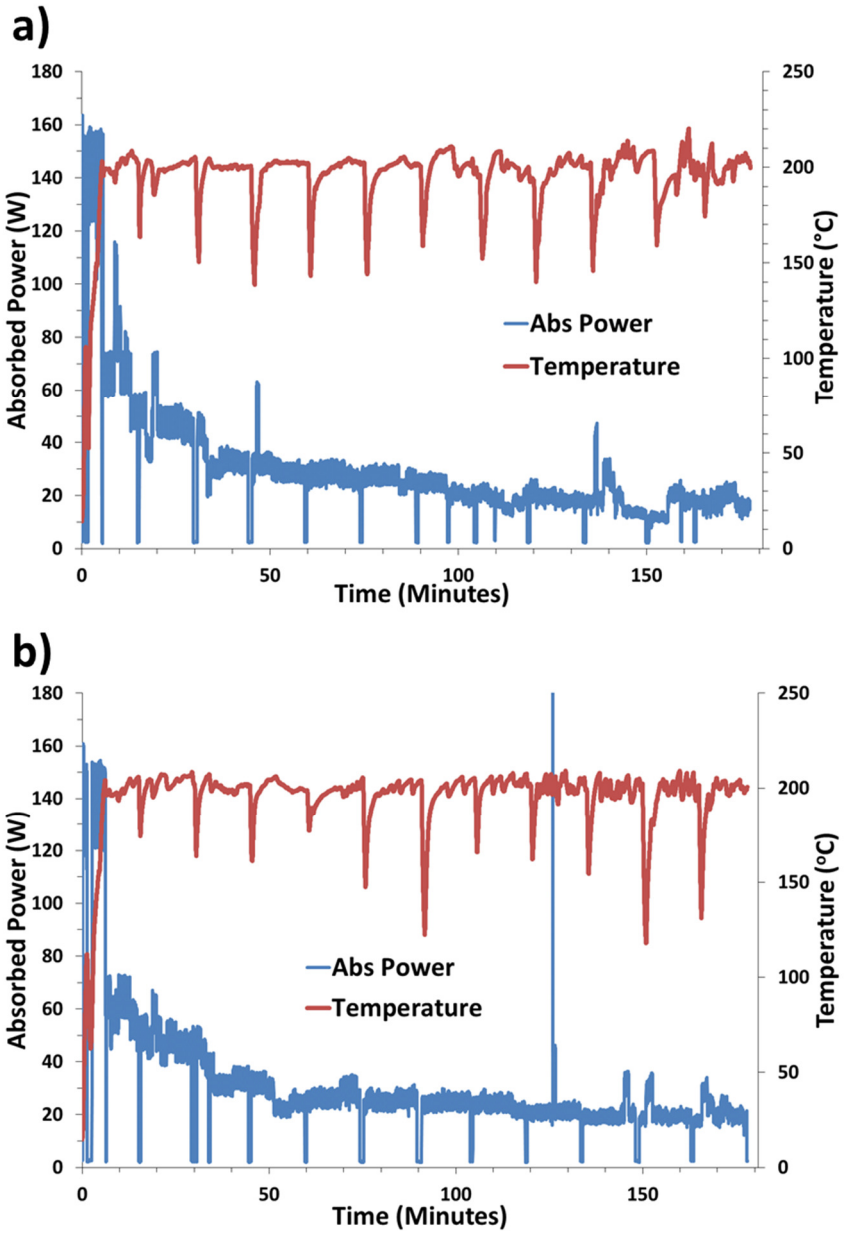


Figure 5-10. Absorbed power and temperature profiles for the polycondensation of isophthalic acid with neopentyl glycol using pulsed microwave power at a maximum powers of 1,500 W, matching duty cycle to an internal temperature of 200 °C. a) Experiment 1, b) Experiment 2.

Figure 5-10 shows that the period of higher power input was only required for the initial heat-up of the reaction. Once a temperature of 200 °C was achieved, the input power was lowered from 150 W to ~70 W in both experiments. This showed that once the initial energy barrier was crossed with high levels of condensation, a low amount of power was needed to keep the reaction at 200 °C, as expected by thermodynamics. As the reaction proceeded, the power required to keep a steady temperature decreased, until it plateaued at 20 – 30 W in both experiments. This displayed that once at temperature, a very low amount of power was needed to sustain these MWH reactions. If the average percentage of power input into the reactions (duty cycle) was evaluated over the whole cycle, the flowing values in Table 5-3 were found.

Table 5-3. Average power percentage and therefore overall average absorbed power for the power matching pulse reactions.

Experiment Number	Average Power Percentage (%)	Average Absorbed Power (W)
1	2.75	41.28
2	2.76	41.38

The values presented in Table 5-3 showed that even though the pulsed microwaves input a power of 1,500 W when on, they were on average only required for ~2.75 % of the time to keep the reaction at 200 °C. This averaged at 41.33 W between the two experiments. This was a low amount of power required and further demonstrates that MWH was an efficient source of heating for chemical reactions.

To assess if there was a difference between the 10 % duty cycle and the duty cycle to temperature matching experiments, the polyester products were assessed for MWt and thermal properties. The details of these results are shown below in Table 5-4 with the GPC traces in Figure 5-11.

Table 5-4. Molecular weight and thermal properties of isophthalic acid, neopentyl glycol polyesters synthesised using continuous microwave pulsing and matching the temperature to pulse duration at 200 °C

Pulse Input Type	[a] Conv. (%)	[b] M_n^{GPC} (g.mol^{-1})	[b] M_w^{GPC} (g.mol^{-1})	[b] M_p^{GPC} (g.mol^{-1})	[b] Đ	[c] T_g (°C)
10 % Duty Cycle	93	1,830	4,010	4,240	2.24	54.15
Temperature Matching	94	2,310	4,910	5,160	2.13	57.27
Duty Cycle	91	1,830	3,900	3,790	2.13	52.17

[a] Calculated using polymer to monomer peak ratio in ^{1}H NMR. [b] Calculated using THF GPC and ASTRA software. [c] Calculated using TA-Q2000 DSC and Universal analysis software by TA.

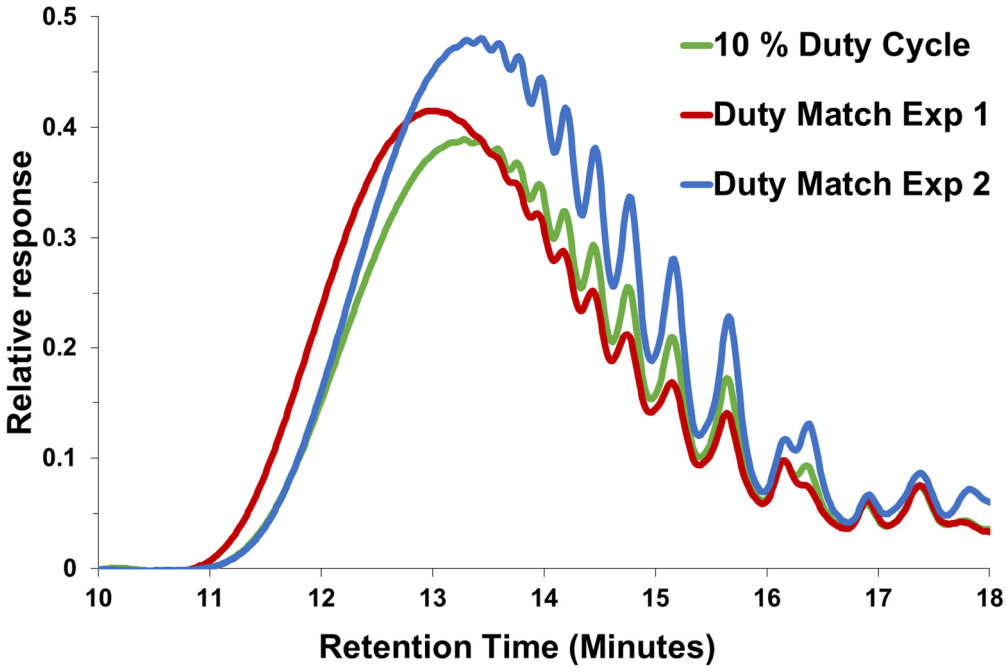


Figure 5-11. GPC traces of isophthalic acid, neopentyl glycol polyesters synthesised using continuous microwave pulsing and matching the temperature to pulse duration at 200 °C.

Table 5-4 details that there was a slight difference between the two techniques. The duty cycle to temperature matching produced polymers with MWt values which were higher at specific conversions (similar MWts seen between 10 % duty cycle at 93 % conversion and duty cycle matching at 91 % conversion).

This potentially suggested that continuous use of high power pulsing can increase MWt when compared to its intermittent use. This occurred due to the selective heating of the end groups/catalysts when implementing MWH. The more continuous application of the duty cycle matching led to the selective heating of the molecules to occur at a more constant rate, building MWt to a higher degree than in the intermittent microwave application.

Table 5-4 also showed that by matching the duty cycle to reaction temperature there was tighter control over the reaction, with both reactions having lower Đ values than the 10 % duty cycle product. This was because the continuous use of the pulsing microwaves will regularly excite the reacting molecules, leading to regular, controlled chain extension. Whereas, the intermittent use of the pulses negated this effect by having long periods with no heating applied, leading to larger fluctuations in reactive group energy/temperature and more irregular chain elongations and therefore a higher Đ.

Again, as observed in chapter 4 section 4.2.1.2.3, there was shown to be a lower T_g value for the polyester with a lower conversion, even though the MWt values were similar. This can again be explained by the increase amount of lower MWt moieties in the reaction mix plasticising the samples.

5.2.2 5 L Scale-Up Hybrid Heating Rig

Due to the success with product processing times and product quality in the previous chapters when using MWH, there was sufficient evidence to progress with scaling up the reaction to the 5 L scale. This scale was selected as it is the load commonly used by the sponsoring industrial company when researching new polymer formulations for coatings. It therefore gives an accurate indication

of how scalable a process is and allows for work to be commenced towards industrial implementation.

The following section discusses the design criteria, and initial polyesterifications using the vessel.

5.2.2.1 5 L Hybrid Heating Vessel Design Criteria

Initially, a design criteria for the equipment was discussed between the sponsoring company and the university. This was accomplished to make sure all the future ambitions for both parties were fulfilled with the creation of the apparatus. The main attributes which must be included into the design were:

- The ability to process with CH, MWH or both.
- Have suitable safety protocols for operation *i.e.* High temperature safety protocol, microwave leakage detection, E-stop, torque cut out, electromagnetically inert stirrer.
- Create comparable products to the current apparatus used at the sponsoring company site.

Therefore, the original vessel design used in the 5 L apparatus at the sponsoring company was used as base for the MWH vessel. This vessel geometry was subject to electromagnetic simulations by Dr Angeliki Sklavounou of the Microwave Process Engineering (MPE) research group at the University of Nottingham and it was found that the vessel could be used as a microwave cavity with the addition of microwaves through the lid. Therefore, this allowed the use of a CH oil jacket around the vessel walls, accomplishing the hybrid heating criteria.

For microwaves to be applied through the lid, a microwave transparent material was selected (PTFE, tanδ = 0.0015 at 3 GHz). [4] This PTFE lid was designed to allow one half for charging, temperature and distillation ports, while leaving the other half for the microwaves to penetrate through. The angle at which the waveguide interacted with the lid was investigated through the electromagnetic simulations but it was found that the angle did not drastically affect the heating patterns. Therefore, the waveguide was left at 90° to the lid.

As PTFE is microwave transparent an over-lid was needed to seal the vessel from leakages. This over-lid was crafted from stainless steel, identical to the main vessel with dimensions to fit tightly over the PTFE lid. The over lid was then clamped to the main vessel to create an airtight seal between the lids and vessel. This led to no microwave leakage and allowed vacuum addition to the reaction mix. A schematic of the apparatus is described below in Figure 5-12.

The vessel was designed and built in collaboration with Asynt who produced the stainless steel vessel and the CH apparatus. Dr Adam Buttress of the University of Nottingham then headed the team which collated all the required parts and tested the vessel to the required safety specification to be used at the university. More information on the vessel can be found in chapter 2 section 2.2.3

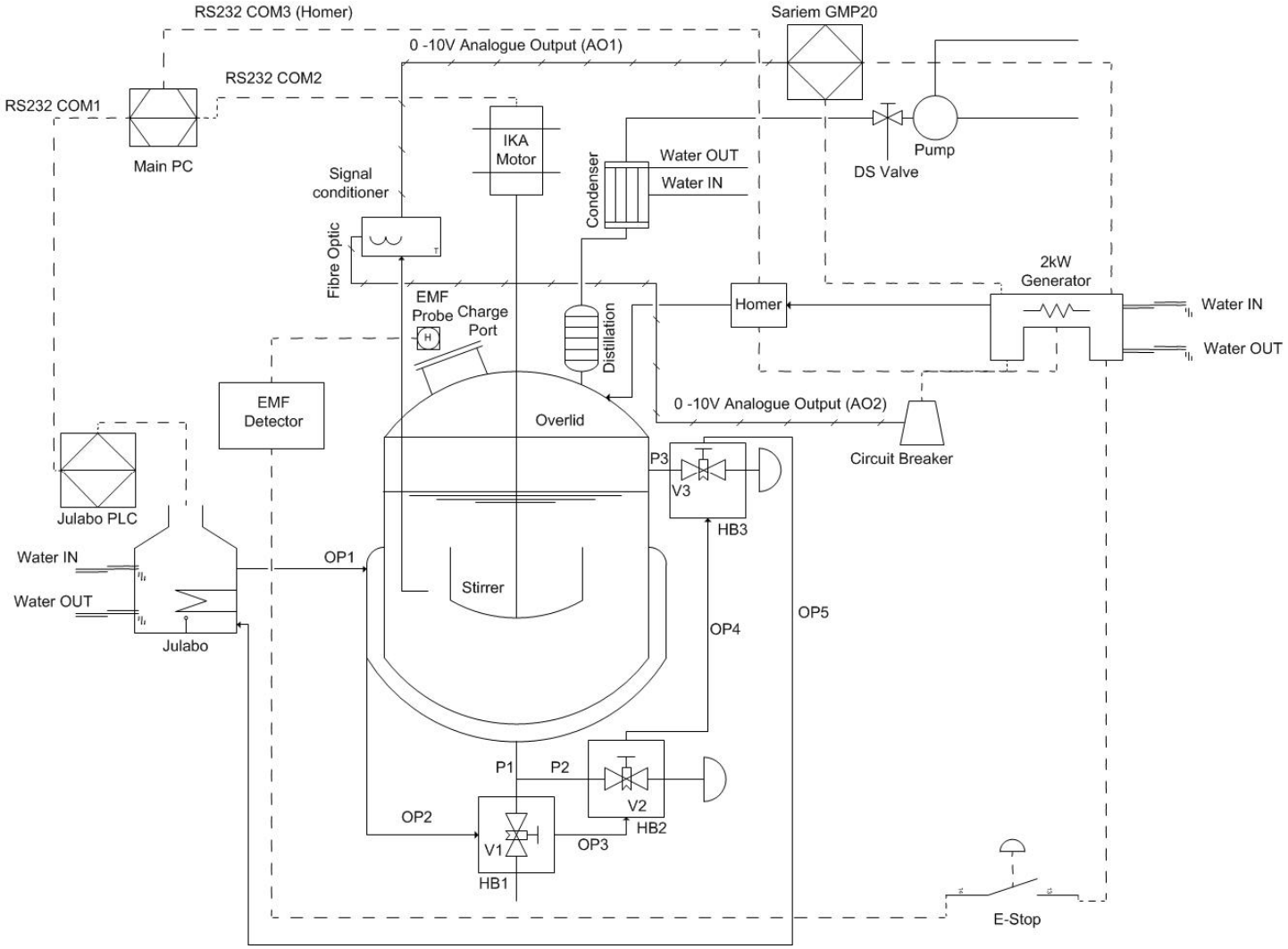


Figure 5-12. Schematic of 5 L vessel.

5.2.2.2 Adipic Acid, Hexanediol Polycondensation at 185 °C - 5 L Scale

Tests involving the AA, HD polyesterification at 185 °C were first performed with the 5 L vessel to fully assess the equipment and to continue the work discussed in chapter 3. As stated before, the AA, HD system was significantly less viscous and reaction times vastly reduced when compared to the industrial resin process. Therefore, if any problems arose from the testing, it was safer to test using this system. For these experiments CH and MWH were evaluated and the conversion profiles are described below in Figure 5-13.

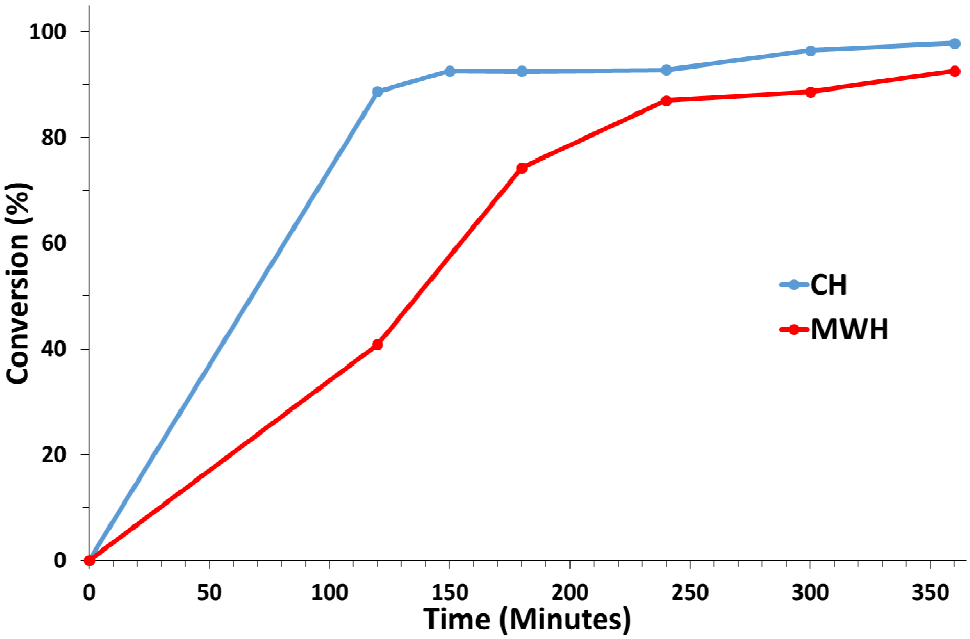


Figure 5-13. Comparison of heating method conversion over time for a 5 L scale adipic acid, hexanediol polycondensation at 185 °C.

Figure 5-13 shows that in contrast to the results at a 50 mL scale, an increased reaction rate was observed in CH compared to MWH, with 80 % conversion being achieved in less than 110 and 200 mins for CH and MWH respectively. Therefore, CH was almost twice as fast to reach this conversion as MWH. CH was also shown to achieve a higher final conversion of 98 % when compared to the 93 % of MWH.

These results can be explained due to the low application of the microwave power. It was the goal to match the heating rate/profile of the CH reaction when using MWH, but this was not achieved and too low amounts of power were input. This was because caution was used with the microwave application as it was the first time the equipment was being used for a large scale MWH reaction. This experiment was not repeated due to the time constraints imposed on the research in this project. Therefore, these initial results will be discussed but future work iss needed to assess the conclusions.

Assessing the heating profiles confirms that the MWH reaction took longer to reach reaction temperature than the CH reaction, shown in Figure 5-14.

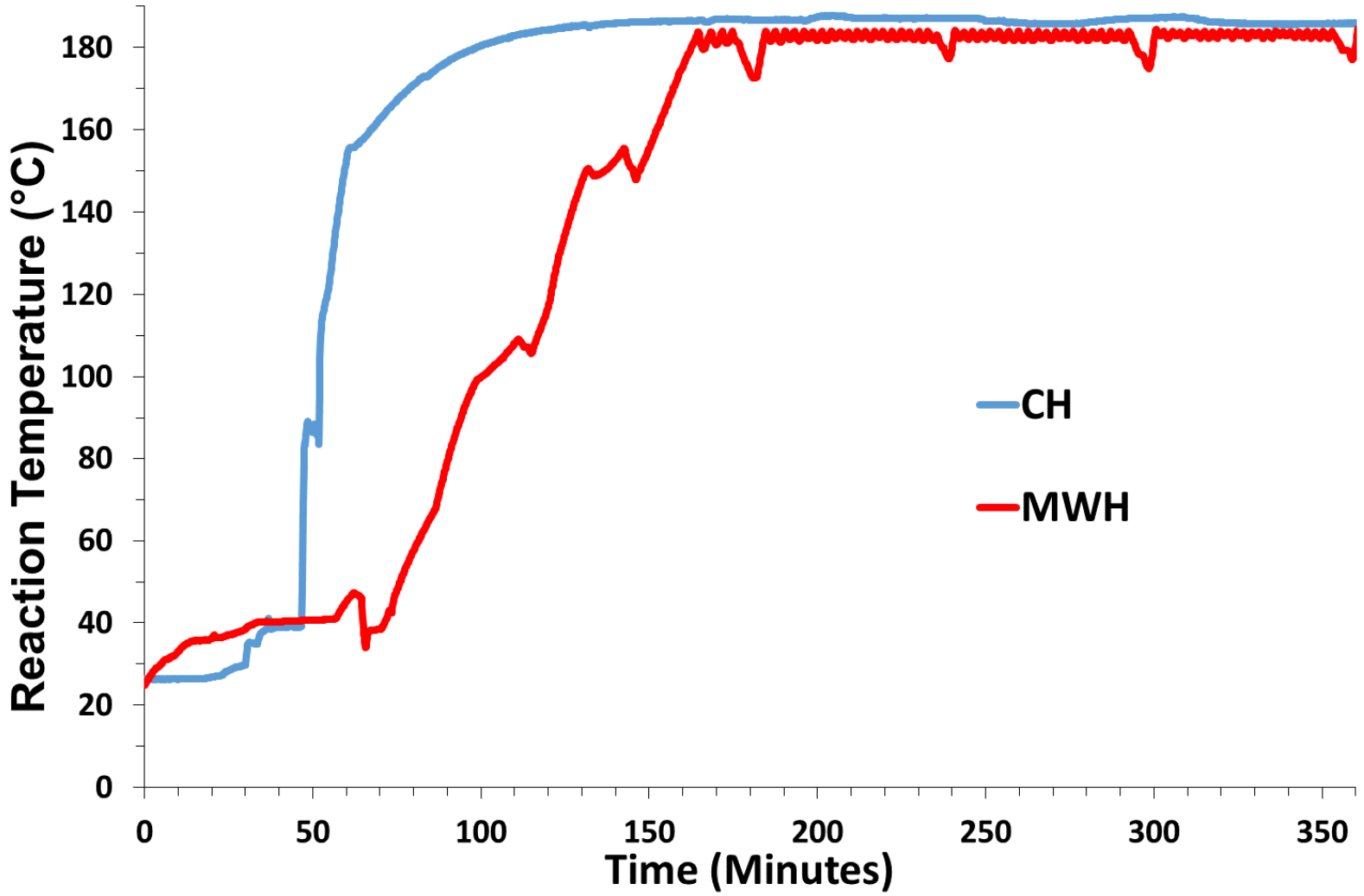


Figure 5-14. Temperature profiles for the CH and MWH reaction of adipic acid, hexanediol at a 5 L scale at 185 °C.

Figure 5-14 describes the difference in heating rate for the two heating methods. CH was shown to achieve a significantly faster heating rate than MWH, reaching reaction temperature in 120 mins whereas MWH achieved this in 160 minutes. This was due to the aforementioned low amount of power being input into the reaction for the MWH experiments to make sure the equipment was safe. Figure 5-14 also describes how the temperature ramp in the CH reaction was far shorter than in the MWH reactions. This was also due to the low power initially being input to the system, leading to a comparatively slow heating time. Whereas, the oil temperature was set to increase to reaction temperature after the addition of the diacid and catalyst, leading to a quick ramp. Once the low powers were tested and deemed safe, the power was increased throughout the initial heat-up period, shown by the absorbed power profile in Figure 5-15.

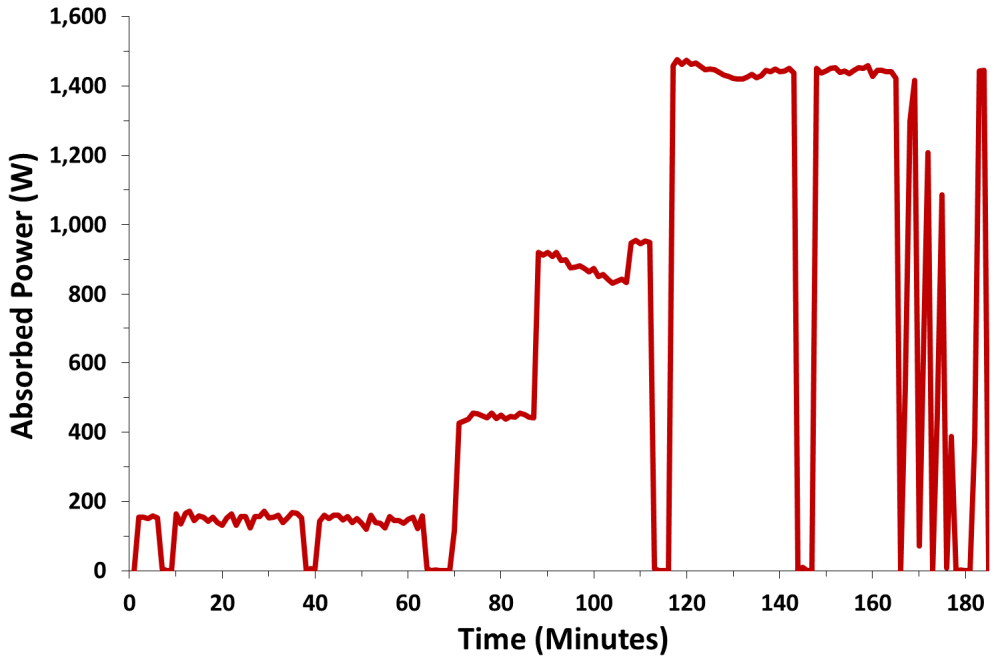


Figure 5-15. Absorbed power for the heat-up period of the adipic acid, hexanediol polycondensation at 185 °C.

Figure 5-15 demonstrated the low amounts of power initially being input into the system (200 W for first hour) which was why there was a comparatively low

heating and conversion rate. This was then increased to a P_{max} of 1,500 W as the reaction was not proceeding. Once the internal bulk temperature reached reaction temperature, (~160 mins) the absorbed power was shown to decrease dramatically to keep the reaction at processing temperature.

For completion of the polymerisation, a 300 mbar vacuum was added at the end of each reaction. This was from 4 - 6 hours in CH and 4.5 - 6 hours in MWH. The difference in application lengths between the heating methods was due to the increased heat-up period of the MWH reaction. Therefore, the vacuum was applied later to reduce unreacted monomer losses, as described in chapter 4.

The polyesters synthesised were subject to MWt analysis, with the GPC traces reported in Figure 5-16.

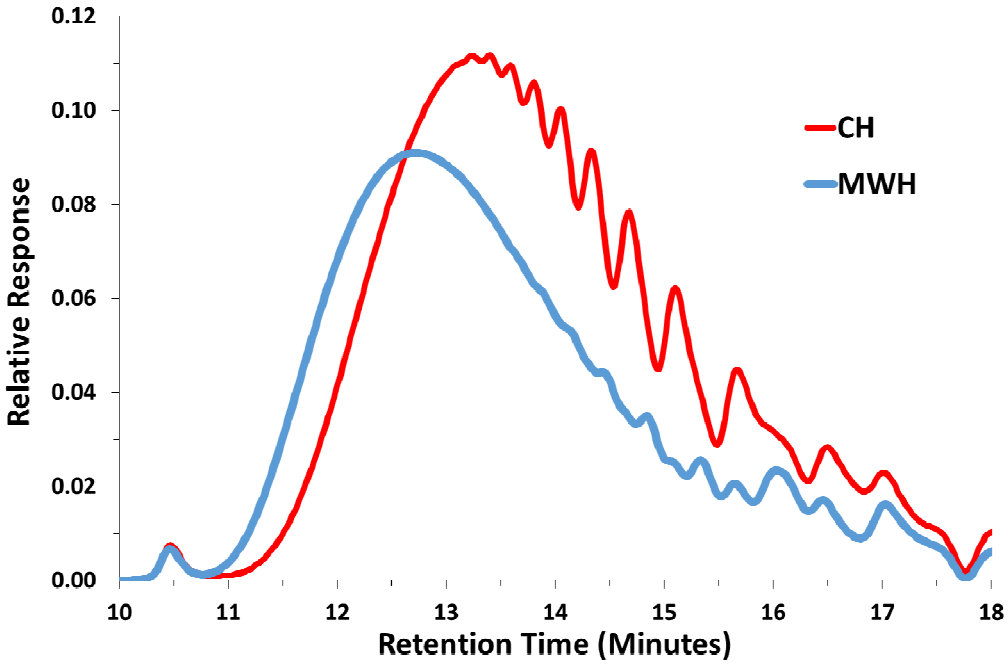


Figure 5-16. GPC traces for the AA, HD polyesterification using DHBTC catalyst at 185 °C at 5 L scale.

Figure 5-16 shows that the GPC traces are similar to those expected at small scale, with the characteristic "long tail", described in chapter 3 section 3.4.1.2.1. Interestingly, Figure 5-16 details that the polyester processed *via* a MWH

method produces a product with a larger MWt. This was shown by its peak retention time being lower than the CH processed product. The numeric values from the GPC analysis are detailed in Table 5-5 with the accompanying thermal property data.

Table 5-5. Molecular weight and thermal properties data for the 5 L scale adipic acid, hexanediol polycondensations at 185 °C.

Heating Method	[a] Final Conv. (%)	[b] M_n^{GPC} (g.mol^{-1})	[b] M_w^{GPC} (g.mol^{-1})	[b] M_p^{GPC} (g.mol^{-1})	[b] Đ	[c] T_m (°C)
CH	98	1,780	4,780	4,490	2.68	49.4
MWH	93	2,360	6,620	7,240	2.79	51.2

[a] Calculated using polymer to monomer peak ratio in ^{1}H NMR. [b] Calculated using THF GPC and ASTRA processing software relative to a polystyrene standard. [c] Calculated using TA-Q2000 DSC and Universal analysis software by TA.

Table 5-5 confirms the increased MWt results for the product processed using MWH, with corroboration from increased thermal data. This was surprising as it was expected that the CH reaction would produce a polyester with a significantly increased MWt and T_m due to the decreased heat-up period, extended time at processing temperature and the increased vacuum addition period. However, Table 5-5 displayed that the M_n^{GPC} of the MWH sample was ~ 600 g.mol^{-1} higher than that of the CH sample. This increase in MWt was supported by an increase in T_m of ~2 °C. Therefore, these results suggested that by applying MWH the polymerisation was positively affected, producing longer chained polymers when compared to the CH reaction. This was likely due to the selective heating effect experienced with MWH. As reported in the 50 mL reactions, the microwaves were penetrating into the bulk and selectively heating certain aspects of the polymerisation, most likely the monomer chain ends or catalyst. This therefore heated a specific molecule/part of the molecule to an increased temperature than the bulk and promoted longer chain growth compared to CH,

which heats *via* conduction from the hot vessel walls and convection throughout the system. Consequently, although the processes were not identical in terms of conversion and heating profile, obtaining a product with an increased MWt and T_m at a lower conversion, strongly suggested that there was a specific microwave heating effect on this system.

Considering the PDI values from Table 5-5 showed that there was a slight difference between the two values, with CH obtaining a narrower distribution. But due to the MWts being smaller, this was expected. Therefore, currently there was not enough evidence to suggest that there was a difference in control of the reaction between the two heating methods.

5.2.2.3 Industrial Polyester Synthesis at 5 L Research Scale

5.2.2.3.1 Overview

After the commissioning and testing using the AA, HD polycondensation the industrial resin synthesis was commenced. At this scale, the synthesis is a 2 stage process, which differs from the reactions at 50 mL which focused on only stage 1. Below the two stages of the reaction are outlined.

Stage 1 focused on building short polyester chains. This was achieved by mixing an excess of diol with diacid and catalyst and slowly ramping the temperature (approx. 6/8 °C/hour) to reaction temperature (>220 °C) until a colourless product was produced *i.e.* no monomeric particles present, known as achieving “clarity”. A slow ramp was used to minimise glycol evaporation as the glycols boiling point is below the processing temperature needed to react/homogenise the highly crystalline diacids. Glycol losses are needed to be

minimised to help with MWt growth as well as reducing the amount of raw product lost from the system. Reducing the glycol losses, coupled with the excess added at the start creates a OH terminated polyester as the end product for this stage. The product then undergoes acid value (AV) and hydroxyl value (OHV) titrations, to compare to pre-determined values, reported in Table 5-6. If the values are met, stage 2 follows, if they are not, an acid or hydroxyl correction was added following Equation 5-1 and Equation 5-2.

Diol correction:

$$\boldsymbol{Mass_{NPG}} = \frac{(\boldsymbol{OHV_{theo}} - \boldsymbol{OHV_{exp}}) \times (\boldsymbol{yeild\ S1} - \boldsymbol{mass\ sample}) \times \boldsymbol{Mn_{NPG}}}{\boldsymbol{Functionality} \times \boldsymbol{56,100}} \qquad \textit{Equation 5-1}$$

Diacid correction:

$$Mass_{IPA} = \frac{(OHV_{theo} - OHV_{exp}) \times (yield\ S1 - mass\ sample) \times Mn_{IPA}}{Functionality \times 56{,}100} \qquad \textit{Equation 5-2}$$

Where OHV_{theo} and OHV_{exp} are the theoretical and experimental hydroxyl value in mgKOH/g, yield S1 is the overall yield of the stage 1 reactants in grams, mass sample is the mass of the sample withdrawn for analysis in grams, functionality is 2 and 56,100 is the mg/mol of KOH.

OHV_{theo} was calculated below using Equation 5-3.

$$OHV_{theo} = \frac{moles\ OH\ func - moles\ acid\ func}{total\ weight - water\ evolved} \times mg\ of\ KOH \qquad \textit{Equation 5-3}$$

Stage 2 focussed on building the MWt of the polyester chains and changing from a OH to COOH terminated polyester. MWt was increased by processing the material for elongated periods of time at high temperatures (leading to an undesirable yellowing of the product) and was also promoted by the addition of vacuum. Following a colourless product being formed the polyester was again subject to AV and OHV testing to meet the required specification in Table 5-6.

If this was not met the product was left to react further or a correction was added, if it was met then the product was discharged.

This process is outlined in a flow chart below, Figure 5-17.

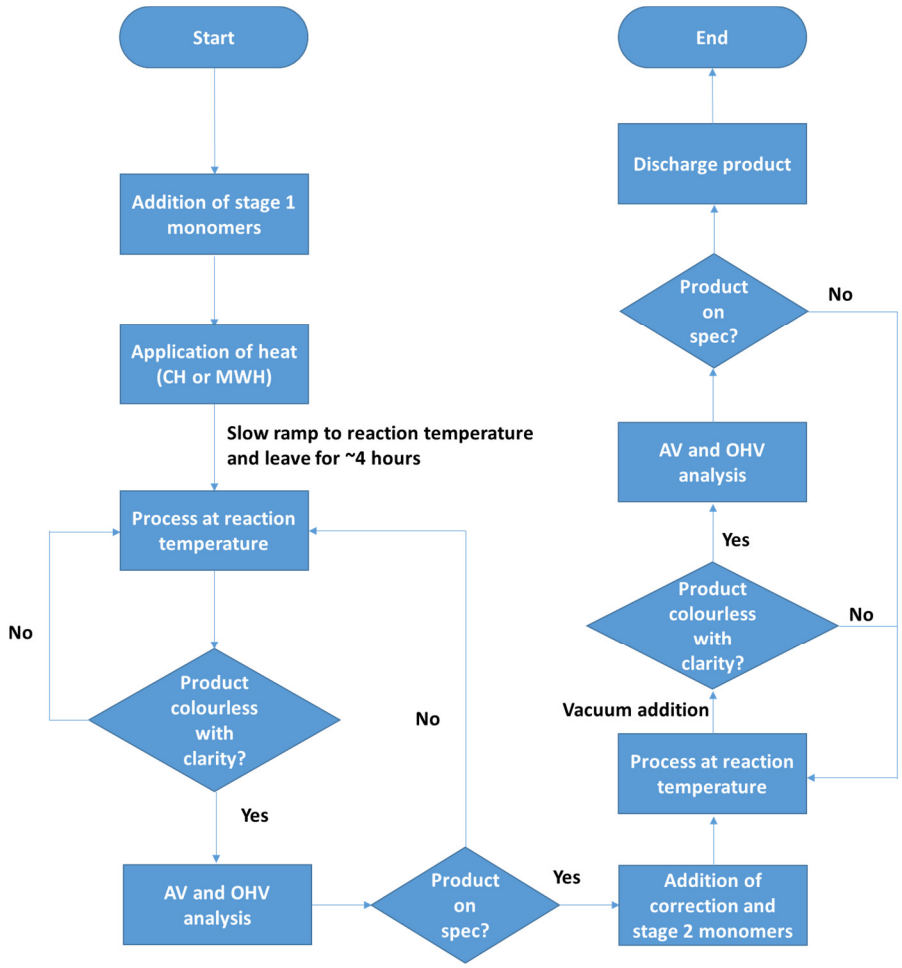


Figure 5-17. Flow chart for industrial resin production.

For the industrial synthesis an exact method was supplied by the industrial sponsor. This led to exact specifications of AV and OHV being targeted, shown below in Table 5-6. AV and OHV are used as analysis methods for the polyesters synthesised in industry due to their ease of use and reproducibility.

Table 5-6. Targeted acid and hydroxyl values for an isophthalic acid, trimethylolpropane, neopentyl glycol and adipic acid industrial resin to meet industrial specification.

Stage	End of stage AV set point (mgKOH/g)	End of stage OHV set point (mgKOH/g)
1	<15	50.47
2	24 - 26	-20.50

For both stages it was important to achieve the OHVs stated above to within ±0.5 units to confirm the polymer produced was to the right specification. If these values were not met then the polyester synthesised was not to the correct specification and the corrections discussed earlier in Equation 5-1 and Equation 5-2 (OHV_{theo}) were employed. Commonly, it was a diol correction which was needed due to the aforementioned evaporation of the NPG (glycol losses) because of the high temperatures and vacuum used in the reaction.

5.2.2.3.2 Conventional and Microwave Heated Reactions

5.2.2.3.2.1 Conventional Heated Polycondensation of the Industrial Resin System at 5 L

Initially, a CH reaction was conducted to assess if a product could be produced within the specification limits set by the sponsoring company. This was to prove that the new equipment worked identically to the current equipment employed at the sponsoring company's research facilities. It also allowed the temperature and condensate profiles to be assessed to give targets for the MWH process, shown below in Figure 5-18.

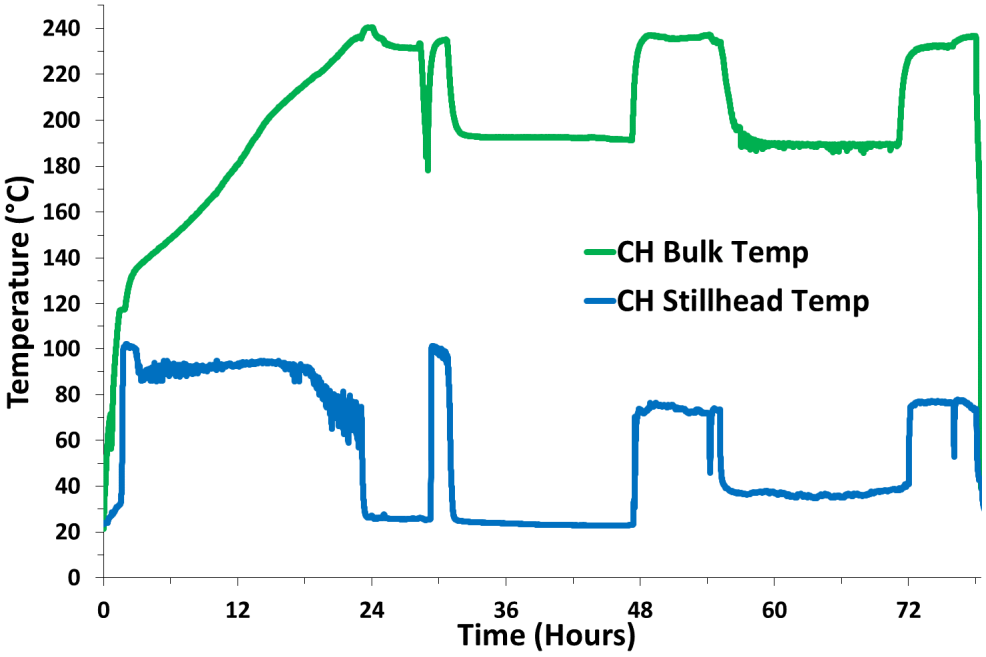


Figure 5-18. Bulk and stillhead temperature profiles for an industrial polyester resin synthesis at 5 L scale implementing CH.

Note. The condensate temperature was important as this indicated the extent at which the diol was evaporating from the system. This is because the stillhead temperature should be at 100 °C (for water), if the temperature was above this it indicated that the diol was being evaporated.

Figure 5-18 details the temperature profile for the industrial resin synthesis using CH. It shows the slow, 6 - 8 °C/minute temperature ramp achieved for the first 24 hours of the reaction, implemented to reduce glycol losses. This was demonstrated by assessing the stillhead temperature profile for this period. It was shown that this temperature did not rise above the 100 °C targeted set point. It also demonstrated that there was a clear correlation between the bulk temperature and the stillhead temperature. This was because towards reaction temperature (235 °C) there were condensation reaction occurring and therefore water was evolved, raising the temperature of the stillhead. When the temperature was lowered to 180 °C for the overnight sections the stillhead's temperature reduced, detailing that minimal reactions were occurring at this lowered temperature. The temperature of the reaction was lowered overnight

due to safety concerns (very high and unattended temperatures, reaction progressing too far overnight leading to cross-linking) whereas, an industrial size batch (50 tonnes) would be processed continuously.

A note from the profile in Figure 5-18 was that the decrease in temperature around 30 hours was due to the second stage reactants being added. Prior to the addition of the monomers, the reaction bulk temperature was dropped because of the addition of diol, which has a lower boiling point than the processing temperature. This drop in bulk temperature meant that the added diol would not instantaneously evaporate out of the system.

As stated previously, the reaction was followed using AV and OHV. OHV was assessed at the end of stage 1 and after clarity formed in stage 2. AV was used on every sample as towards the end of the reaction it was used to determine if the polymers have achieved the required MWt. Therefore, throughout the polycondensation, 5 samples were taken. The AV and OHV data for these sample are shown below in Table 5-7.

Table 5-7. Evolution of acid and hydroxyl value over time in an industrial polyester resin synthesis using CH.

Sample	[a] AV	[a] OHV
1	13.95	44.37
2	45.65	-20.42
3	29.65	[c] Not tested
4	29.21	[c] Not tested
5	27.55	[c] Not tested
Final Product	29.23	[c] Not tested

[a] Calculated using gravimetric titration against 0.1 M KOH methanolic solution. [b] Calculated using auto-titration against 0.6 M KOH methanolic solution. [c] Samples not tested for OHV as this is not needed for the COOH terminated polyester product.

Table 5-7 demonstrates how the AV and OHV changed over time in the polyester resin synthesis. The details from the first sample at the end of stage 1 describe that the polymer was processed to a high enough chain length (known by the AV being below 15) but, the OHV was 6.10 OHV units lower than targeted (44.37 compared to 50.47). This indicated that some diol was lost *via* evaporation during the reaction. This meant a correction of diol was needed to be added, which was calculated using the previously described Equation 5-1.

This led to a 22.02 g correction being required, which was added with the stage 2 reactants. This amount of correction was comparable to the amount expected, which is commonly between 5 and 15 units.

Sample 2 demonstrates that after the addition of the stage 2 acids a COOH terminated polyester was created due to the negative OHV value. The product produced an OHV of -20.42 which was within the ±0.5 error of the -20.50 target, meaning further correction was not required. The AV of the first sample was high at 45.65, but this was expected due to the slow nature of high MWts being achieved in step-growth polymerisations (related to mass transfer problems). This led to vacuum addition to the reaction to accelerate mass transfer, as discussed in chapter 4, and the reaction being left for extended periods until the AV had reduced to within 2 units of the targeted zone (24 – 26). This occurred on the fifth sample with an AV of 27.55. Although this was outside the targeted values, advice from the sponsoring company suggested that the resin continued to react once discharged and therefore the AV would drop a further 2 units. But, when the final products AV was calculated an increase in AV was witnessed. This was due to either an erroneous result in the 5th sample's calculation, or was due to residual monomer being present in the final sample. Therefore, sample 5 and the final sample were re-evaluated with similar results. This suggested that residual monomer in the final sample was the likely reason for this. This

monomer was likely to be from the small amount present in the discharge valve and the vessel walls.

The samples from this synthesis were evaluated for MWt, shown in Figure 5-19 and thermal properties. The data is compared in Table 5-8.

Table 5-8. Molecular weight and thermal properties data for the samples taken throughout the industrial resin polyesterification using CH.

Sample	[a] M_n^{GPC} (g.mol^{-1})	[a] M_w^{GPC} (g.mol^{-1})	[a] M_p^{GPC} (g.mol^{-1})	[a] Đ	[b] T_g (°C)
1	1,790	4,600	4,810	2.57	51.4
2	1,890	4,730	4,490	2.50	54.1
3	2,630	8,600	9,620	3.27	59.8
4	2,810	9,060	10,150	3.23	62.5
5	2,890	9,400	10,300	3.25	61.4
Final Product	2,810	10,000	11,800	3.56	61.5

[a] Calculated using THF GPC and ASTRA processing software relative to a polystyrene standard. [b] Calculated using TA-Q2000 DSC and Universal analysis software by TA.

Table 5-8 shows how the MWt of the polyester product increased over time. This increase in M_n^{GPC} was also supported by a rise in T_g. Large MWt and T_g increases were shown between samples 2 and 3, this occurred because the full monomer load was added by this point and the vacuum was in effect. This vacuum addition led to increased mass transfer of the remaining condensate and therefore accelerated polyester formation.

There was a decrease in M_n^{GPC} between the 5th and final samples in Table 5-8. This was because of the residual monomer, discussed earlier in relation to the AV. This therefore decreased the M_n^{GPC} value but not the M_p^{GPC} value, which increased. Therefore, it can be hypothesised that the chain length has increased

between the samples and it was only a small contamination of monomer which has affected this value.

Figure 5-19 demonstrates the increase of polyester MWt from the initial sample to the end sample as the retention time of the polyester increases. This corroborated with the actual values presented in Table 5-8. An interesting property observed from the later polyester samples (sample 3, 4, 5 and final) is the appearance of a shoulder at the shorter retention times. This shoulder is due to the formation of more high MWt species which is also corroborated by the M_p^{GPC} and M_w^{GPC} increases observed in Table 5-8.

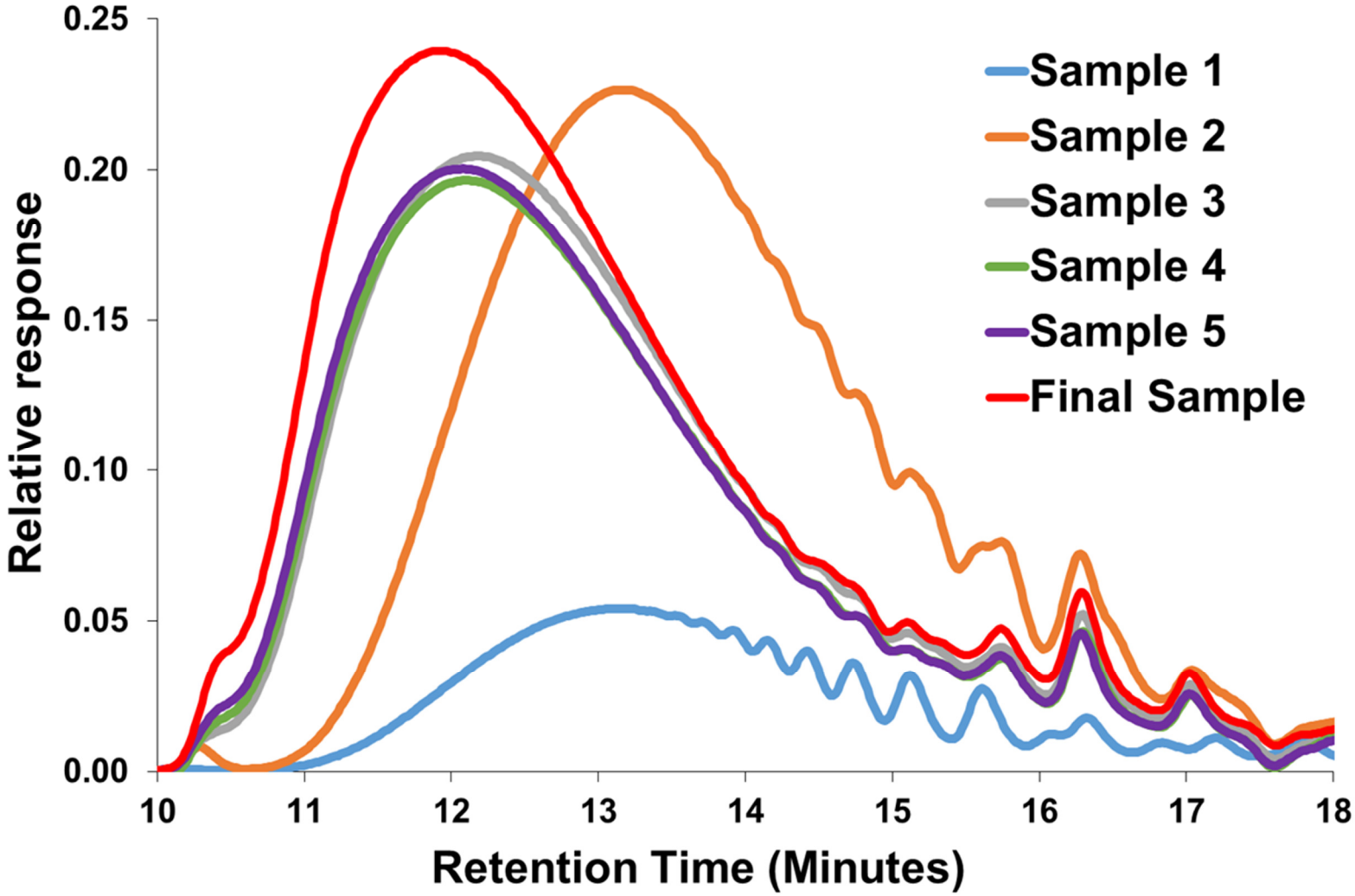


Figure 5-19. GPC traces for the samples and final product of the industrial polyester resin using conventional heating at a 5 L scale.

5.2.2.3.2.2 Microwave Heated Polycondensation of the Industrial Resin System at 5 L

After the polyester resin synthesis was shown to be achievable by implementing CH, MWH was tested. For this reaction, the main aim was to re-produce the heating profile of the CH reaction, but by only using a MWH source. This allowed a direct comparison between the two methods in terms of diol losses, AV, OHV, MWt and thermal properties. Therefore, a reaction was conducted and the heating profile is detailed below in Figure 5-20, with a direct comparison of CH included.

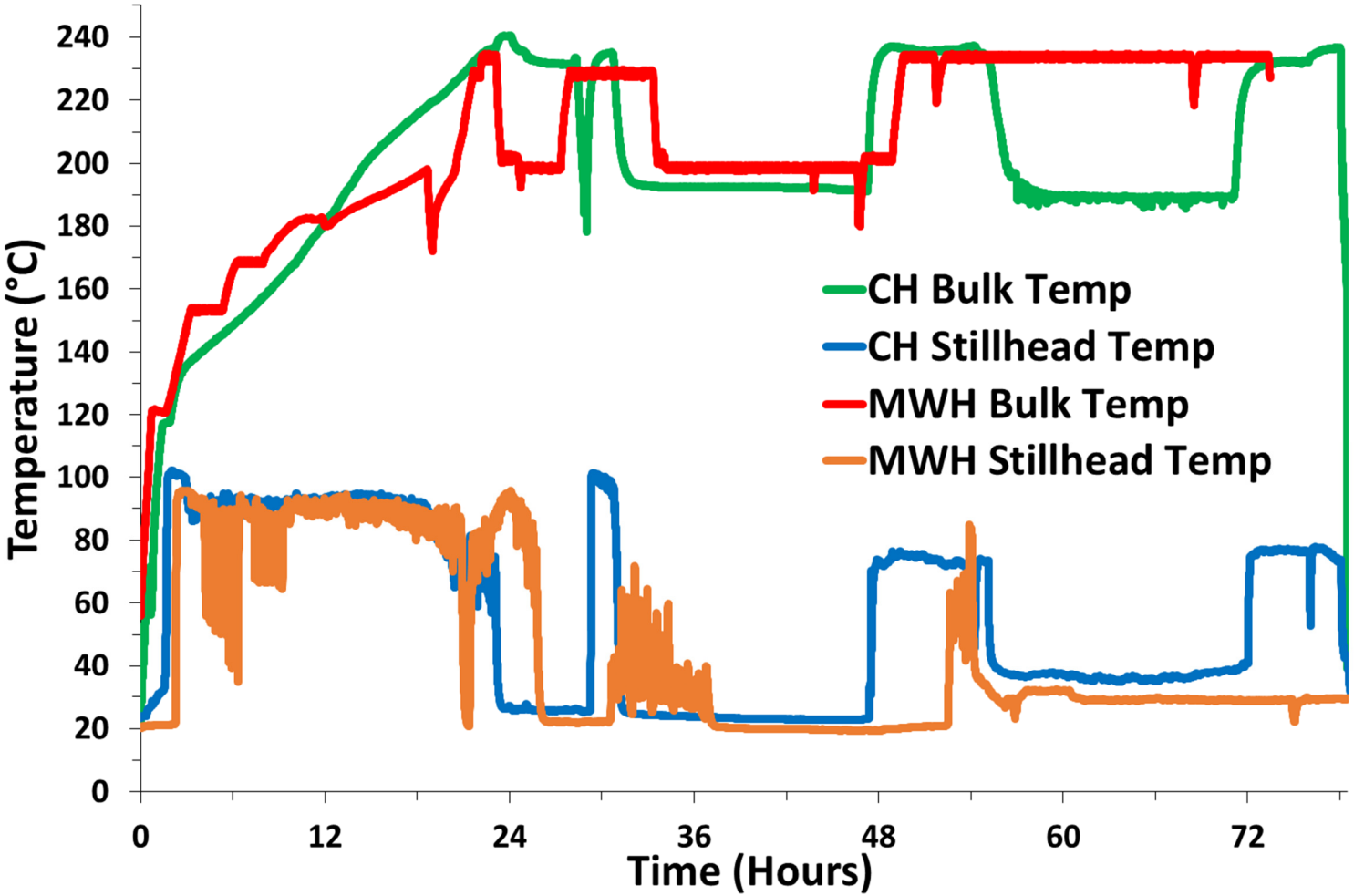


Figure 5-20. Comparison of bulk and stillhead temperature profiles for an industrial polyester resin synthesis at 5 L scale implementing CH and MWH.

Figure 5-20 shows the comparison for the heating profile between the CH and MWH 5 L polycondensations. It demonstrates that the CH reactions initial heat-up was considerably smoother than the MWH, due to step setting needed in the microwave heating unit and thermal lag of the cold oil encountered when implementing MWH. The other significant difference between the heating methods was that the MWH reaction was left at reaction temperature overnight between ~54 and 72 hours, but this was needed to achieve a polyester which was on specification within the allotted reaction timeframe.

Considering the stillhead temperature profiles confirms that it was at the beginning of the reaction which produces the most condensate, with temperatures being consistently around 100 °C. Comparing the MWH profile to the CH showed that there was a significantly higher amount of fluctuation in the temperature in the MWH process than in CH. This was explained by the MWH being constantly switched on and off throughout the reaction to keep the bulk temperature at 235 °C. This therefore significantly affected the rate of condensation and led to quick fluctuations of increased amount of condensate when MWH was switched on, to decreased amounts when switched off.

For the MWH reaction, the average power which was needed to keep the bulk at reaction temperature throughout the process is described in the power profile below in Figure 5-21.

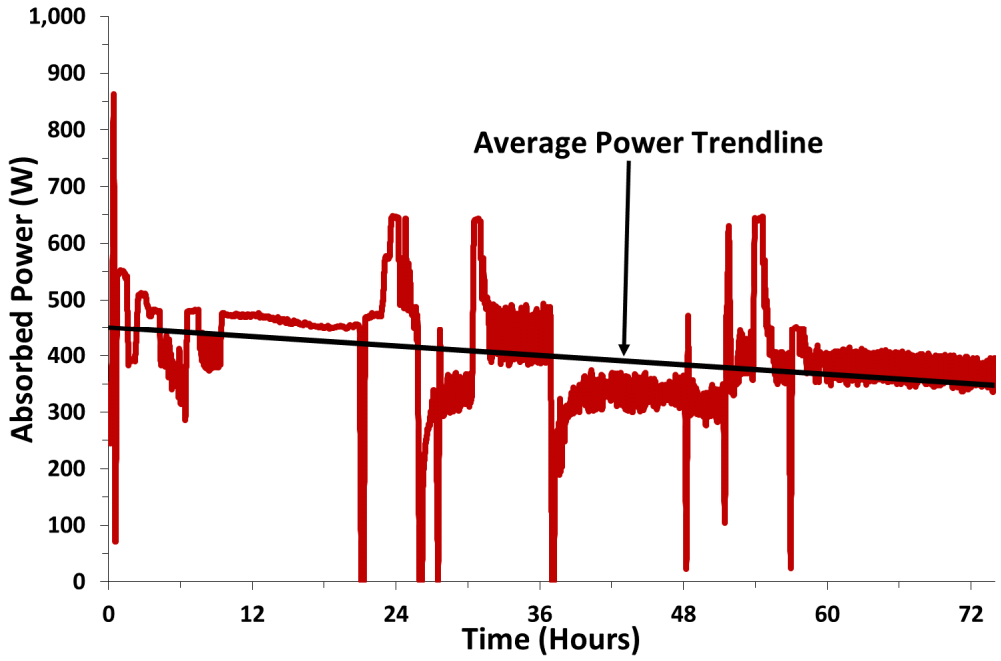


Figure 5-21. Time averaged absorbed power for the 5 L microwave polycondensation of an industrial resin system.

Figure 5-21 describes the time averaged absorbed power profile for the MWH polyesterification reaction. The average absorbed power trend line describes that the average amount of power required to keep the reaction at processing temperature diminished over time. This suggested that towards the end of the reaction a lower amount of power was needed for the reaction to proceed compared to the amount required at the start. This was expected as the reaction was already at temperature at this point, meaning only enough power to keep it at temperature was needed, whereas, at the beginning of the reaction enough power was needed to heat up the reagents to reaction temperature from RT.

Initially, Figure 5-21 shows that ~1 kW of power was needed to be input to melt/dissolve the diols. But once this was achieved the amount of absorbed power was reduced to ~500 W to slowly heat the reaction mixture at the desired rate. But, at 24 hours, after the addition of the stage 2 monomers, the temperature settled at ~200 °C, therefore an increase in power to ~700 W was

needed to heat up the MWH reaction back to processing temperature. Therefore, in future MWH reactions, a higher power is needed to keep the MWH profile similar to the CH reaction when starting stage 2 of the reaction. But, once the processing temperature was reached, the amount of power required to keep the reaction at 235 °C was ~400 W.

As in the CH reaction, the samples were tested for AV and OHV to assess the extent of the reaction and if the product was on specification. The AV and OHV data collated for each sample is shown below in Table 5-9, with the CH results added for ease of comparison.

Table 5-9. Evolution of acid and hydroxyl value over time in an industrial polyester resin synthesis using MWH.

Sample	[a] MWH AV	[a] CH AV	[b] MWH OHV	[a] CH OHV
1	11.86	13.95	47.03	44.37
2	45.50	45.65	-20.79	-20.42
3	26.70	29.65	[c] Not tested	[c] Not tested
4	26.16	29.21	[c] Not tested	[c] Not tested
5	Not taken	27.55	Not taken	[c] Not tested
Final Product	30.75	29.23	[c] Not tested	[c] Not tested

[a] Calculated using gravimetric titration against 0.1 M KOH methanolic solution. [b] Calculated using auto-titration against 0.6 M KOH methanolic solution. [c] Samples not tested for OHV as this is not needed for the COOH terminated polyester product.

Table 5-9 shows that the polyester was sufficiently processed for chain length with the first sample (AV <15) but, as in the CH reaction, glycol was lost. The MWH reaction produced an OHV 3.44 units lower than targeted (47.03 produced, 50.47 targeted) which equated to a correction of 12.41 g of NPG. This led to a reduction in the correction needed of ~45 % when compared to the CH reaction (6.10 in CH to 3.44 in MWH). Therefore, this suggested that by

implementing MWH the selective heating of the microwaves promoted the reaction of the diol over its evaporation.

The stage 2 OHV of -20.79 was within ±0.5 of the targeted -20.50 and therefore no correction was required. Compared to the CH reaction (-20.42), this was a slightly lower number, which suggested that slightly more of the polymers had reacted to form OH functionalised end groups. This further suggested that by implementing MWH there was a selective heating mechanism occurring which promoted the reaction of the NPG monomer over its evaporation. At this stage a high vacuum was added to help with building chain length, shown by the diminishing value of AV over the following samples until sample 4 yielded an AV just above the 24 – 26 target range.

As in the CH sample, Table 5-9 demonstrated an increase in the AV between the 4th and final sample. Again, this was likely due to the residual monomer on the vessel walls and in the discharge port. Therefore, to offset this problem, future reactions will have a small amount of resin (~200 g) initially discharged into a separate container to extract the unreacted monomers. This small amount of product will then be discarded and the remaining product will be discharged.

As in CH, the samples and product were evaluated for MWt, with the GPC traces shown in

Figure 5-22 and thermal properties. This data is compared below in Table 5-10.

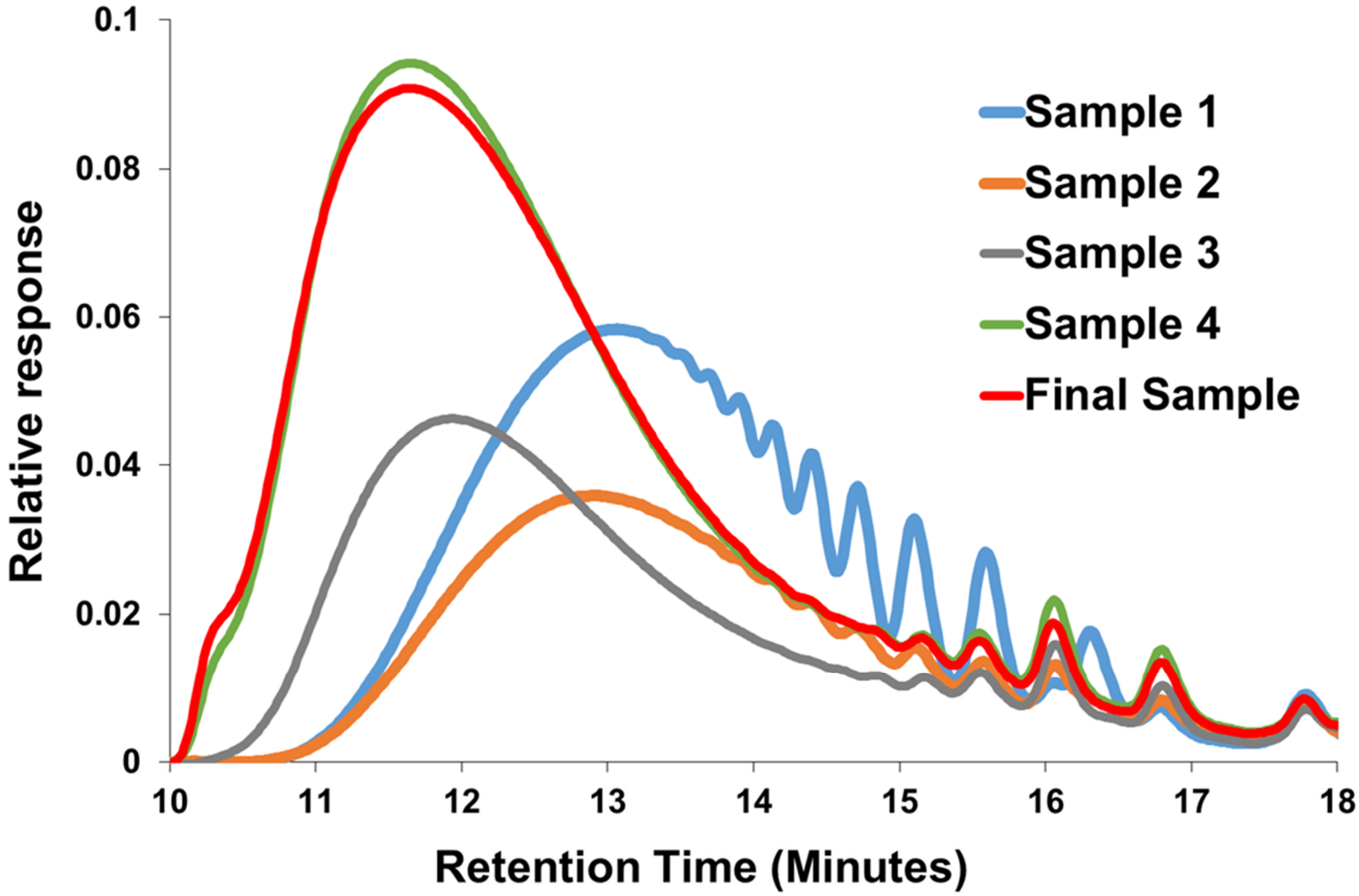


Figure 5-22. GPC traces for the samples and final product of the industrial polyester resin using microwave heating at a 5 L scale.

Table 5-10. Molecular weight and thermal properties data for the samples taken throughout the industrial resin polyesterification using MWH.

Sample	[a] M_n^{GPC} (g.mol^{-1})	[a] M_w^{GPC} (g.mol^{-1})	[a] M_p^{GPC} (g.mol^{-1})	[a] Đ	[b] T_g (°C)
1	2,070	4,990	4,980	2.41	51.3
2	1,820	5,120	5,600	2.81	56.0
3	2,320	8,760	11,800	3.78	64.8
4	2,970	11,800	14,800	3.96	61.7
Final Product	3,210	12,200	15,000	3.79	62.8

[a] Calculated using THF GPC and ASTRA processing software relative to a polystyrene standard. [b] Calculated using TA-Q2000 DSC and Universal analysis software by TA.

Table 5-10 details the build in MWt and T_g as the polyester resin synthesis proceeds *via* MWH. Interestingly, between sample 1 and 2 there was a reduction in M_n^{GPC}. This was most likely due to the addition of the diacid monomers not being fully incorporated, leaving some monomeric residue behind in the sample. This was shown by the increased M_w^{GPC}, M_p^{GPC}, Đ and T_g. A large T_g increase was shown between samples 2 and 3, suggesting the full incorporation of the acids added. All other result agree with what was expected during the polyesterification process.

Figure 5-22 again showed the increase in MWt as the reaction progresses due to the decreased retention times, as was described in Table 5-10. Again, in sample 4 and the final product there was a shoulder peak towards the lower retention times. This is an indication, as in the CH experiments, that higher MWt species are being produced at these parts of the reaction.

A comparison of the MWt and T_g of the final products between CH and MWH is shown below in Table 5-11.

Table 5-11. Comparison of the final product between implementing CH and MWH at 5 L scale for an industrial resin synthesis.

Heating Method	[a] M_n^{GPC} (g.mol^{-1})	[a] M_w^{GPC} (g.mol^{-1})	[a] M_p^{GPC} (g.mol^{-1})	[a] Đ	[b] T_g (°C)
CH	2,810	10,000	11,800	3.56	61.5
MWH	3,210	12,200	15,000	3.79	62.8

[a] Calculated using THF GPC and ASTRA processing software relative to a polystyrene standard. [b] Calculated using TA-Q2000 DSC and Universal analysis software by TA.

Table 5-11 indicated that there was increased MWt and thermal data values observed in the MWH product compared to the CH product. CH produced a polyester with an M_n^{GPC} of 2,810 g.mol^{-1} and T_g of 61.5 °C, compared to 3,210 g.mol^{-1} and 62.8 °C in the MWH sample. This was an increase of 400 g.mol^{-1} between the heating methods, which equated to ~2 DP with a corroborating increase of ~1.3 °C in the T_g. Therefore, by implementing MWH a product was produced which had an increased MWt and therefore an increased thermal stability. This was similar to the result observed in the 50 mL reactions and could be a result of a selective heating effect on the monomer chain ends or catalyst due to the electromagnetic energy, promoting increased chain growth. But, due to the slight differences in the heating profiles and AVs/OHVs of the 2 reactions, this cannot be fully confirmed at this point. As such, more reactions need to be conducted at this large scale with identical heating profiles, AVs and OHVs to confirm if MWH can positively affect MWt elongation at the 5 L scale.

5.3 Conclusions

Pulsed microwave apparatus was assembled including a 2 kW magnetron to evaluate the application of a high maximum power through short, intermittent pulses. This was to assess if the way in which the same average amount of energy was applied over a period of time had any effect on final polyester composition. This meant that a P_{max} of 1,500 W could be input with each pulse, but on average, 150 W was being applied to the bulk over the reaction cycle.

With the data logging and input powers defined, the pulse system was implemented into the AA, HD polycondensation at 185 °C. Two different pulse frequencies of 50 and 1,000 Hz were applied into the system to investigate the difference between a high and low pulse frequency. It was established that by implementing a pulsed MWH system, heat-up times were slightly shortened when compared to CW heating, but this was most likely due to the 5 – 10 W increase in absorbed power in the pulsed system. This suggested that for this system that applying intermittent amounts of high power increased the amount of power which was being absorbed, on average, into the system. This was potentially due to the high powers “superheating” the monomers, allowing for faster melting and therefore a faster increase in dielectric properties. This led to higher conversions, MWts and thermal properties being achieved in identical timeframes for the pulsed systems. For the pulsed reactions it was shown that implementing the lower frequency of 50 Hz produced a polyester with a higher M_n^{GPC} when compared to the 1,000 Hz product. This difference was minimal when assessing all MWt values. However, this observation can be explained by the lead time (time it takes for microwave to switch on) of the microwave generator effecting the quicker 1,000 Hz pulses, leading to a decreased amount of time at the high powers and therefore negating the positive effects of

implementing the pulsed system. However, it cannot be conclusively proved that a lower frequency was preferable to a high frequency at this point and more research is needed to be conducted.

Pulsed microwaves were then implemented into the IPA, NPG system to assess if the high powers had an effect on this polyesterification. Only a frequency of 50 Hz was studied for this system after this frequency was shown to potentially create a larger polyester than at 1,000 Hz in the AA, HD system. It was shown that by inputting 1,500 W for a 10 % cycle time at a pulse frequency of 50 Hz reduced the time to start polymerisation by 50 % and processed the polyester to 80 % conversion in half the time of CW. However, the microwaves in the process were shown to be deactivated for long periods of time in the reaction, due to the 10 % cycle time overheating the reaction bulk if left on. This meant that for elongated periods of the reaction, no power was being input. Therefore, duty cycle to temperature matching reactions were conducted where once the reaction temperature of 200 °C was reached, the duty cycle was lowered to an amount which kept the temperature stable. This proved to be difficult due to the changing dielectric properties of the material, as well as the depleting amount of condensation to cool the reaction mix. Repeats were conducted and the reaction was shown to proceed, but at differing reaction rates. This difference was attributed to the difference in agglomeration of IPA which affected the stirring in the system. But, overall this did not drastically effect the polyester product as similar end conversions were achieved. The power profiles for both duty cycle to temperature matching reactions displayed the higher power required to rapidly heat the bulk to processing temperature, but once at temperature, this diminished to 20 – 30 W to keep the temperature constant. As explained earlier, this reduction in power application was expected due to the reaction only needing enough power to keep it at temperature and

not to heat-up, but it highlights how little power was needed to keep a reaction at high temperatures. The overall power profile equated to the 1,500 W of power being applied for 2.75 % of the reaction cycle. By implementing this duty cycle to temperature matching process a polyester with higher MWt values and tighter MWt control (Đ) was produced when compared to the intermittent use of the 10 % duty cycle pulsed microwave power. This suggested that a more continuous application of high powered pulses was beneficial over intermittent application due to the constant application of a large amount of energy, allowing constant selective heating of the reactive parts of the system.

A 5 L vessel which allowed implementation of both CH and MWH was constructed and commissioned by the University of Nottingham to allow polyesterifications to be performed at large scale. This load size meant that polyesters could be synthesised using MWH at a meaningful scale for the industrial sponsors and enabled full testing of a microwave system on an industrial, 2 stage polyester resin process.

Initial experiments were conducted on the AA, HD polyester system. This was due to the lower temperature (185 compared to +230 °C) needed for processing and the lower viscosity of the process when compared to the industrial polyester resin. Different heating rates were achieved in the polyester synthesis between CH and MWH, leading to a significantly longer heat-up time in MWH due to the input of low amounts of microwave power to test the magnetron. This led to the CH reaction being processed at reaction temperature for an hour longer (~16%) when compared to the MWH system. This also meant that the vacuum addition was for a longer time period (2 hours) when compared to the MWH system (1.5 hours). Both of these factors led to a higher final conversion being achieved in the CH product compared to the MWH product. Yet, when the MWt and thermal properties of the polyesters were compared, MWH was shown to create a

polyester with an increased M_n^{GPC} of ~600 g.mol^{-1} (~3 DP) and T_g of ~2 °C. This was surprising due to the lower conversions achieved when applying MWH, less time at 185 °C and reduced time under vacuum when compared to the CH reaction. This phenomenon potentially occurred due to the microwaves penetrating into the bulk of the reaction and selectively heating the monomer chain ends and/or catalyst, promoting polyester chain elongation. This was in contrast to CH which heated *via* convection and conduction currents from the hot oil in the vessels walls.

Finally, the 2 stage industrial resin process was performed at 5 L scale implementing CH and MWH. Initially a CH experiment was conducted to gain heating rates and profiles for the industrial process. This data was then used to attempt to closely match the temperature ramps in the MWH system, targeting a process and product which was comparable. This proved difficult due to the large amount of reagents needing to be heated, as well as the large amounts of condensation generated when the reaction started. Both heating methods were shown to create a polyester resin which achieved AV and OHVs close to the industrially targeted regions due to the AVs increasing upon discharge. This was attributed to the residual monomer in the vessel discharge valve and can be easily rectified in future polyesterifications.

Comparing the products suggested that implementing MWH produced an end of stage 1 polyester with minimised diol losses (45 % reduction) when compared to CH. This suggested that by implementing MWH there was promotion of the NPG monomer reacting with the acids over evaporation. Also, when comparing the final product MWts, the MWH reaction was shown to create a polyester with an M_n^{GPC} which was ~400 g.mol^{-1} higher than the CH product. This was potentially because, as previously discussed, MWH selectively heated the chain ends and/or catalysts which resulted in an increase in MWt. However, this

cannot be proven at the 5 L scale because the MWH reaction was left at reaction temperature for a slightly longer period than the CH reaction. Therefore, even though the AV and OHVs were similar, this could have allowed further reactions to take place.

Overall, MWH was shown to reduce side evaporations from the process, while also having potential to enhance final polyester properties when compared to CH over identical reaction cycle times. MWH was also shown to have scaling potential in polyesterifications and therefore could be applied into a large, industrial scale process.

5.4 References

1. R. T. Hitchcock and A. I. H. A. N.-i. R. Committee, *Radio-frequency and Microwave Radiation*, American Industrial Hygiene Association, 2004.
2. C. Costa, A. F. Santos, M. Fortuny, P. H. H. Araújo and C. Sayer, *Materials Science and Engineering: C*, 2009, 29, 415-419.
3. Z. Cheng, X. Zhu, G. Chen, W. Xu and J. Lu, *Journal of Polymer Science Part A: Polymer Chemistry*, 2002, 40, 3823-3834.
4. *Agilent Technologies: Loss Tangent*, http://cp.literature.agilent.com/litweb/pdf/genesys200801/reference.htm#elements/substrate_tables/tablelosstan.htm, Accessed 10th January 2017.

6 Conclusions and Future Work

6.1 Overview

This chapter summarises the conclusions drawn from the polyesterifications investigated in this thesis. It also outlines further areas of interest for each section of work; this is intended to promote development of the understanding of the topics discussed.

6.2 Chapter 3: Adipic Acid, 1,6-Hexanediol Polycondensation Reaction

6.2.1 Conclusions

This chapter discussed work which investigated the linear polyesterification of adipic acid (AA) with hexanediol (HD) using both conventional heating (CH) and microwave heating (MWH). Stringent temperature monitoring/control and identical reaction geometries were employed to allow direct comparisons between the heating techniques. The optimal processing time was initially evaluated as well as the effects of stirring and applying vacuum. It was concluded that because of the homogeneous state of the reaction, stirring did not have an effect on the overall rate of the process. Vacuum was shown to increase the final conversions of the polyester, with a higher vacuum consistently creating polyesters with larger molecular weights (MWts).

Investigation into efficacy of two tin catalysts (Tin(II) 2-ethylhexanoate ($Sn(Oct)_2$) and dihydroxybutyl tinchloride (DHBTC)) was conducted, with

temperature of reaction and heating method proving to be key factors in the polyesterifications. As expected, at 185 °C there were increased reaction rates than at 150 °C. More interestingly, at both temperatures, a catalyst efficiency switch was observed between CH and MWH. In the CH experiment it was DHBTC which reacted at the fastest rate, whereas, when using MWH it was $Sn(Oct)_2$. This was attributed to the mechanistic pathway by which the polyesterification occurs. $Sn(Oct)_2$ is in fact a pre-catalyst and the mechanism was proposed to proceed *via* an in-situ formation step to form the true catalyst (previously shown to increase in reaction rate using microwaves), {Adlington, 2013 #1663} whilst the propagation stage proceeded *via* coordinative interactions with the carboxyl moiety. By comparison, the DHBTC catalysts proceeds *via* insertion of the tin complex into the growing polyester chain, creating formal bonds with the chain. The coordinative mechanism involved when using $Sn(Oct)_2$ was shown to increase reaction rate under MWH more so than the insertion mechanism of DHBTC. This was attributed to the fact microwave heating is non-ionising in nature so is unlikely to cleave the more formal bonds at the core of the DHBTC mechanism. Meanwhile, in the $Sn(Oct)_2$ mechanism, associative bonds are exclusively involved which have been shown to be very receptive to an electromagnetic (EM) field.

To investigate this observation further, the reaction rate efficiency between a number of organometallic catalysts was investigated at 185 °C and these demonstrated a range of efficiencies. These efficiency differences exhibited by these different catalytic species were ascribed to the differing dielectric properties of the catalysts, with higher tanδ values leading to more efficient heating in the EM field and therefore an increased reaction rate.

Additional observations with specific catalysts were the following: Implementing Bi triflate as a catalyst was shown to create no high MWt

polyester species with either heating method, this was attributed to a mixture of thermal instability of the complex and the condensate hydrolysing Bi and denaturing the catalyst. Zinc triflate was shown to favour a carboxyl terminated polyester, differing from the racemic termination found using the other catalysts and this was independent of heating method used.

Investigating the polyesterification using organometallic catalysts at 150 °C demonstrated the catalyst efficiency differed between heating methods. These observation were also related to whether the catalytic mechanism contained mainly associative or “formal” bonds. Those possessing the former being shown to be more accelerated with MWH. Unlike at 185 °C, the reaction rates when using MWH did not follow the tanδ of the catalyst. This was attributed to the catalysts generally being less active at these lower temperatures. Furthermore, processing the polyester with a Bi triflate catalyst was shown to create higher MWt polyesters at this temperature, suggesting that the lower temperature reduced hydrolysis/catalyst decomposition. Additionally, it was demonstrated that MWH has a positive effect on final product colour, with no products having higher discolouration using this heating method at this temperature. It was suggested by MALDI analysis that the terminal groups of the polyesters were predominantly COOH. But, this suggestion did not correlate with acid value (AV) titrations and therefore cannot be confirmed. The MWt and thermal properties of the 150 °C polymers were shown to demonstrate a much closer correlation with conversion than at 185 °C, suggesting that by processing at this lower temperature tighter MWt control is achieved.

Non-organometallic catalysts were also investigated at 185 and 150 °C to evaluate the use of a more environmentally friendly catalyst in the system. It was again shown that implementing MWH can increase the reaction rate when compared to CH, due to the efficient heat transfer. Between the non-

organometallic catalysts investigated (phosphoric acid (PA) and pyrophosphoric acid (PPA)), there was minimal difference in reaction rate, likely due to the dimer species degrading into the monomer species at high temperatures. However, there was a clear increase in MWt between CH and MWT for PA, and none for PPA. This suggested that there was a difference in mechanistic pathway/catalyst availability between heating methods. But, this needed further investigation to define the root cause.

For the conversions achieved, higher than expected MWts were formed when using PA and PPA at both temperatures. This was because of the high dielectric properties and labile nature of the H^+ ions involved in the polyesterification mechanism with these catalysts. No discolouration was observed in the polyesters synthesised using either heating method, demonstrating the benefits of using a non-organometallic catalyst. Racemic functionalisation was found at both temperatures with normal thermal properties.

6.2.2 Future Work

The main area of future work from this chapter will involve further investigation into the effect MWH has on different mechanistic approaches to polyesterifications. Examining more catalysts, which proceed *via* predominantly coordinate or formal bonds is a key area. Comparing the rate increases between CH and MWH will need to be examined to confirm that a predominantly coordinate mechanism route is favoured when implementing MWH. During this, studies using catalysts with similar dielectric properties would be beneficial as it would specifically highlight the potential differences between the mechanism routes. However, further investigations into collecting the dielectric properties

of organometallic species will be required as there is a level of uncertainty about the relative figures that are produced using the current cavity perturbation methods. This would involve measuring the dielectric properties of reaction mixtures instead of separate component as the intermolecular interactions will greatly affect the dielectric properties of each species.

6.3 Chapter 4: Crystalline Polymerisation of Isophthalic acid (IPA), Neopentyl glycol (NPG) and Trimethylolpropane (TMP) – Working Towards an Industrial Resin Process

6.3.1 Conclusions

Tin and non-organometallic catalysts were investigated for the processing of crystalline monomer polyesterification studies (neopentyl glycol with isophthalic acid). It was shown that the tin catalysts proceed at significantly higher reaction rates than the non-organometallic alternatives. This was due to the high processing temperatures needed, which led to the non-organometallic catalysts reaching their decomposition temperature. From the comparison of the catalyst types studied, there was a processing difference observed in regards to which heating method led to a faster heat-up time for this reaction medium. With CH the system heat up time noted to be faster with the non-organometallic catalysts, whilst the target temperatures were more rapidly attained for the tin catalysts with MWH. This was explained by the high tanδ of the non-organometallic catalysts. It was therefore proposed that these catalysts absorbed a much more significant proportion of the EM energy input into the system, leading to only a small portion of the reaction mix being heated and selective “overheating” of the catalyst. This resulted in processes which led to

the decomposition/degradation of the non-organometallic catalysts dominating, not polyesterifications. Whereas, using the tin catalysts led to the diol having the highest tanδ, therefore a larger proportion of the mix was being heated compared to the non-organometallic reactions and the tin catalysts also have much greater thermal stability thus are not deactivated by these higher temperature rather these activity is enhanced. This led to quicker heat transfer throughout the mixture and therefore a quicker heat-up time with MWH. Overall, comparing the MWt and thermal properties of the polyesters showed that the DHBTC catalyst was the only catalyst which produced a polymeric product, leading to future reactions only involving this catalyst.

Pre-heating of the reaction mixture demonstrated that the heating profiles between the heating methods differed. Using CH led to the non-pre-heated reactions reaching processing temperature faster, explained by the smaller amount of water refluxing when compared to the pre-heated reactions. Whereas, it was the pre-heated reaction which had the fastest heat-up time when implementing MWH. This was explained by MWH being a very efficient heater of the excess water, negating the extra energy needed to remove it from the system. While the pre-heat allowed quicker and more efficient homogenisation of the diacid monomer, leading to quicker heating using MWH. As pre-heating was commonly applied in industry, it was the method used for any further reactions.

Investigations between the heating methods provided evidence to suggest that implementing MWH led to a higher MWt of final polyester product when compared to those made using CH techniques. By processing the reactions for identical time periods at reaction temperature the MWt of the MWH samples increased by ~400 $g.mol^{-1}$, with a T_g increase of ~2.5 °C. This further suggested

the occurrence of a selective heating effect towards the molecules when implementing MWH in this polyesterification.

A study into what effect stoichiometry had on the polymerisation with both heating methods was conducted. This showed that there was an optimal ratio between the diol and diacid of 1.1:1 in terms of achieving the highest MWt possible, and this observation was heating method independent. Increasing the stoichiometry was also shown to reduce the Đ of the reactions, suggesting closer control of the polymerisation. This was explained by the excess diol capping the polymer chains, making chain elongation less likely. This led to slower reactions and therefore more controlled growth.

An increased reaction temperature was shown to emphasise the benefits of implementing MWH for heat-up times with temperature being achieved ~13 times quicker than when applying CH. This meant to achieve similar conversions and MWts the MWH samples were processed for 40 % of the time that a CH sample was. Vacuum application showed that it was important to apply the vacuum after the bulk of the monomeric species had reacted. This was because early addition led to significant monomer losses through evaporation and therefore a reduced MWt.

For the full industrial resin process with branching triol, it was again demonstrated that implementing MWH can decrease the heat-up time of the system significantly. It was shown that by implementing MWH processing temperature was achieved ~13 times faster than CH, meaning the overall processing time was halved. It was also described that leaving the products at reaction temperature for the same periods of time led to an increase in MWt of ~900 $g.mol^{-1}$ for the MWH sample. However, when analysing the GPC traces this increase in MWt was not conclusive due to the CH polymer having a shorter peak retention time than the MWH sample. Some of this was attributed to diol

losses after vacuum addition, but this did not describe the full MWt increase. Therefore, it was again suggested that there is a selective heating effect which promoted chain elongation in MWH processing. However, these theories would need further research to prove or disprove.

When vacuum was added to the samples at maximum power a Weissenberg effect was observed. This led to gelling of the polyester, showing that when processing at large scale care must be taken with vacuum addition to stop this from happening.

6.3.2 Future Work

Further experiments need to be performed to investigate the differences in MWt observed between the two heating methods. Therefore, an extended set of repeats of both the NPG, IPA polycondensation and the full industrial resin system reactions are required. This would involve processing for identical times at reaction temperature to achieve identical conversions and comparing MWt and thermal data.

It would be also be of interest to develop a system which can implement mechanical stirring safely and effectively at these small scale reactions. This is because the viscous nature of the product meant that in most cases, there was non-optimal mixing throughout the reaction vessel. Although mechanical stirring experiments were conducted in some cases, it proved to be difficult to consistently repeat them safely due to the minimal space afforded down the long necked vessel coupled with the need to have internal temperature monitoring. Some suggestions for future vessel geometries are detailed below in Figure 6-1.

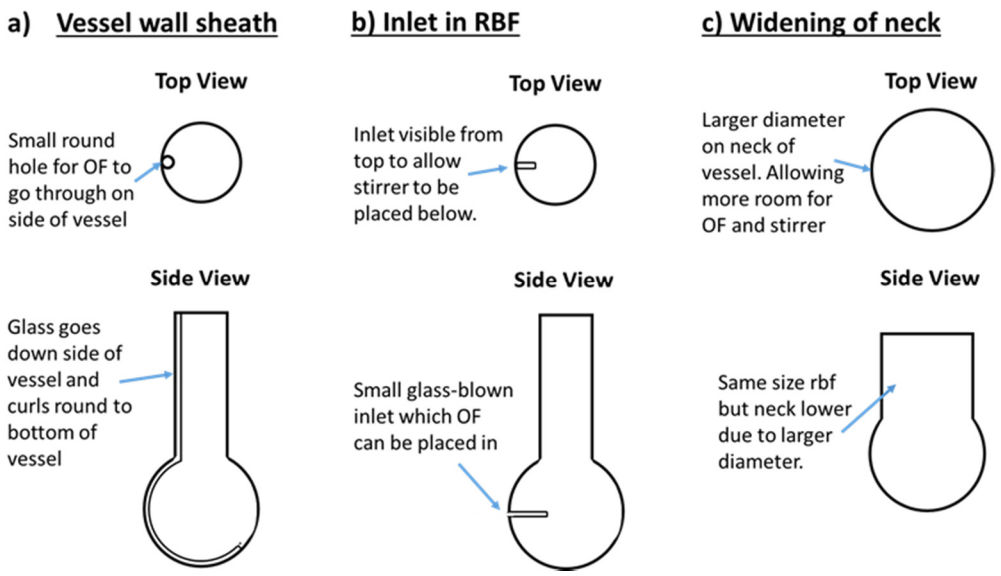
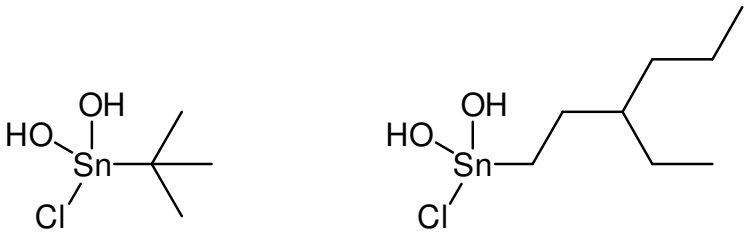


Figure 6-1. Designs for 50 mL vessel to allow mechanical stirring in current microwave cavities.

An investigation into different tin catalysts would also be beneficial. The most interesting avenue for investigation for the MWH system would be to source a catalyst with similar characteristic to DHBTC but which is liquid at room temperature. This could be done by elongating the butyl chain and/or creating branching points e.g. a t-butyl chain or 3-Ethylhexane chain (to make the structure similar to tin octanoate), these structures are shown below in Figure 6-2.



t-butyl adduct 3-ethylhexane adduct

Figure 6-2. Chemical structures of proposed lower b.p. polyesterification catalysts.

A longer chain would lower the molecules intermolecular interaction/packing and increased the degrees of freedom in the side chain, hence lowering the boiling point (b.p.). Having a liquid catalyst at RT would increase its dielectric properties and, if it is similar to the catalyst employed in this chapters investigations, would show that having any catalyst with higher dielectric properties than the monomers is detrimental to heat-up times of the system.

6.4 Chapter 5: Pulsed Microwave and Scale-up Experiments

6.4.1 Conclusions

For the AA, HD system it was detailed that implementing pulsed microwaves decreased the heat-up times and therefore created polyesters with higher conversions, MWts and thermal properties in identical timeframes. Between the two pulse frequencies investigated, a lower frequency was shown to achieve faster reaction rates and create a higher MWt polyester. But, these differences were negligible and were not categorically proven.

For the IPA, NPG system it was shown that implementing pulsed microwaves created comparable heat-up and reaction rates to the continuous wave (CW) system. But, there were long periods where the power was fully off due to the efficient nature of inputting high powered pulses. Therefore, studies were undertaken to match the power input percentage (duty cycle) with the temperature. This led to the power needing to be at 1,500 W for 2.75 % of the time to keep the reaction at processing temperature and it was shown that the MWts and thermal properties obtained from these polymers were increased from the higher duty cycle experiments. But, as in the previous chapter there

was problems with stirring of reagents due to the mixtures high viscosity and the use of magnetic stirring.

Development and commissioning for a 5 L conventional and microwave heating hybrid vessel was completed. This allowed larger scale experiments to be conducted for these polyester products.

For the AA, HD system, different heat-up times were achieved due to attempting to match the MWH experiment to the CH. This occurred due to extreme care taken with power matching because it was the first MWH experiment of the newly commissioned vessel. Therefore, the CH reaction was processed for 20 % longer at reaction temperature than the MWH reaction. But, when analysis of the polyester product was conducted it was shown that the MWts and thermal properties of the MWH sample were higher than that of the CH sample. Therefore, this again suggested a selective microwave heating effect was promoting chain elongation in the polyester synthesis.

For the industrial polyester resin synthesis, similar processing conditions and temperature profiles were achieved, but the results were still not identical. Both heating methods were shown to create a polyester which initially matched the analysis specifications targeted. However, problems were encountered with monomeric material in the discharge port and future reactions will be needed to define routes to negate this problem. The MWH reaction was shown to create a polyester with a higher MWt compared to the CH reaction, but this cannot be confirmed to be because of the heating mechanism due to the polyester being processed at reaction temperature for a longer period than the CH sample.

Overall, with the MWH synthesis it was shown that a low power level was needed to keep the reaction at processing temperature, showing the potential energy efficiency benefits of a MWH system.

6.4.2 Future Work

The pulsed work showed that applying high pulses power for elongated periods of time may be beneficial for polyester synthesis. Therefore, more research will need to be conducted into this. It would be interesting to also implement this into a CW system as well. This would show that a low power may infact be chemically beneficial over a high one. It would also show if consistent use of MWH is beneficial for polyesterifications when compared to the sporadic application currently used to keep reactions at processing temperatures.

As in chapter 4, investigations into altering the vessel geometry at the 50 mL scale would be beneficial for future work. This would involve the sample examples described in Figure 6-1.

For the 5 L reactions more repeats need to be conducted to gain an accurate method for matching the CH and MWH heating profiles for both AA, HD and the industrial resin process. This would allow more accurate comparisons to be made between the two heating methods. For the industrial polyester resin process an important factor when processing is the loss of diol. Therefore, it would be beneficial to investigate if MWH can reduce this and/or create a more reproducible value for this. This is because industrially the diol losses are not constant between product batches and therefore hydroxyl value analysis needs to be conducted at the end of stage 1. If this step can be negated due to the reproducibility of MWH then this would be a significant time saving (~10 - 20 %). This would involve conducting a plethora of stage 1 polyester syntheses at different heating rates with CH and MWH and comparing the diol losses between them.

Another interesting area of investigation would be to follow the reaction using dielectric analysis. This technique has been previously shown to track

polymerisation conversion by Kamaruddin et al. and Santos et al. [2,3] This would involve conducting dielectric analysis on the resin at different points in the reaction and assess how the dielectric properties change over time. If these values can then be correlated with acid and hydroxyl values, conversions and MWts this would allow instant product analysis and lead to significant process optimisation.

6.5 References

1 Adlington, K. *et al.* Mechanistic Investigation into the Accelerated Synthesis of Methacrylate Oligomers via the Application of Catalytic Chain Transfer Polymerization and Selective Microwave Heating. *Macromolecules* 46, 3922-3930, doi:10.1021/ma400022y (2013).

2 Kamaruddin, M. J. *et al.* Continuous direct on-line reaction monitoring of a controlled polymerisation via dielectric measurement. *Green Chemistry* 13, 1147-1151, doi:10.1039/c1gc15102a (2011).

3 Santos, A. F. *et al.* Inline Dielectric Monitoring of MMA/BuA Copolymerization Reactions. *Polymer Reaction Engineering* 55, 251-253 (2001).